ISSN: 0128-7680

Pertanika Journal of

SCIENCE & TECHNOLOGY

VOLUME 12 NO.1
JANUARY 2004

A scientific journal published by Universiti Putra Malaysia Press

Pertanika Journal of Science & Technology

About the Journal

Pertanika, the pioneer journal of UPM, began publication in 1978. Since then, it has established itself as one of the leading multidisciplinary journals in the tropics. In 1992, a decision was made to streamline Pertanika into three journals to meet the need for specialised journals in areas of study aligned with the strengths of the university. These are **(i) Pertanika Journal of Tropical Agricultural Science (ii) Pertanika Journal of Science & Technology (iii) Pertanika Journal of Social Science & Humanities.**

Aims and Scope

Pertanika Journal of Science & Technology welcomes full papers and short communications in English or Bahasa Melayu in the fields of chemistry, physics, mathematics, and statistics, engineering, environmental control and management, ecology and computer science. It is published twice a year in January and July.

Articles must be reports of research not previously or simultaneously published in other scientific or technical journals.

Communications are notes of a significant finding intended spaced typewritten pages and must be accompanied by a letter from the author justifiying its publication as a communication.

Reviews are critical appraisals of literature in areas that are of interest to a board specturm of scientist and researchers. Review papers will be published upon invitation.

Submission of Manuscript

Three complete clear copies of the manuscript are to be submitted to

The Chief Editor
Pertanika Journal of Science & Technology
Universiti Putra Malaysia
43400 UPM, Serdang, Selangor Darul Ehsan
MALAYSIA
Tel: 03-89468854; Fax: 03-89416172

Proofs and Offprints

Page proofs, illustration proofs and the copy-edited manuscript will be sent to the author. Proofs must be checked very carefully within the specified time as they will not be proofread by the Press editors.

Authors will receive 20 offprints of each article and a copy of the journal. Additional copies can be ordered from the Secretary of the Editorial Board.

EDITORIAL BOARD

Prof. Ir. Abang Abdullah Abang Ali- *Chief Editor*
Faculty of Engineering

Assoc. Prof. Ir. Dr. Norman Mariun
Faculty of Engineering

Assoc. Prof. Ir. Dr. Mohd. Saleh Jaafar
Faculty of Engineering

Assoc. Prof. Dr. Gwendoline Ee Cheng Lian
Faculty of Science & Environmental Studies

Prof. Dr. Abu Bakar Salleh
Faculty of Science & Environmental Studies

Prof. Dr. W. Mahmood Mat Yunus
Faculty of Science & Environmental Studies

Assoc. Prof. Dr. Noor Akma Ibrahim
Faculty of Science & Environmental Studies

Assoc. Prof. Dr. Hamidah Ibrahim
Faculty of Information Technology & Science Computer

Rosta Harun
Faculty of Science & Environmental Studies

Sumangala Pillai - *Secretary*
Universiti Putra Malaysia Press

Published by Universiti Putra Malaysia Press
ISSN No. 0128-7680

INTERNATIONAL PANEL MEMBERS

Prof. D.J Evans
Parallel Algorithms Research Centre

Prof. F. Halsall
University College of Swansea

Prof. S.B Palmer
University of Warmick

Prof. Dr. Jerry L. Mc Laughlin
Purdue University

Prof. Dr. John Loxton
MaxQuarie University

Prof. U.A Th. Brinkman
Vrije Universiteit

Prof. A.P. Cracknell
University of Dundee

Prof. A.J. Saul
University of Sheffield

Prof. Robert M. Peat
University of Florida

Prof. J.N Bell
Imperial College of Science, Technology and Medicine

Prof. Yadolah Dodge
University De Neuchatel

Prof. W.E Jones
University of Windsor

Prof. A.K. Kochar
UMIST

DR. NAYAN DEEP S. KANWAL
EXECUTIVE EDITOR
Pertanika Journals
Research Management Centre (RMC)
Universiti Putra Malaysia
43400 Serdang, Selangor, Malaysia
Tel: +603 8947 1622, +6016 217 4050
E-mail: ndeeps@admin.upm.edu.my

Pertanika Journal of Science & Technology

Volume 12 No. 1, 2004

Contents

ISSN: 0128-7680
Pertanika J. Sci. & Technol. 12(1): 1 - 9 (2004) © Universiti Putra Malaysia Press

On Robust Environmental Quality Indices

[1]Azme Khamis & [2]Mokhtar Abdullah

[1]Pusat Pengajian Sains, Kolej Universiti Teknologi Tun Hussein Onn
[2]Pusat Pengajian Sains Matematik, Fakulti Sains & Teknologi
Universiti Kebangsaan Malaysia,
43600 UKM, Bangi, Selangor, Malaysia

Received: 8 December 1998

ABSTRAK

Kajian ini membincangkan rumus baru indeks kualiti alam sekitar yang boleh digunakan untuk memantau parameter udara dan juga parameter kaji cuaca yang lain. Perumusan indeks ini berasaskan kepada analisis komponen utama konvensional dan analisis komponen utama teguh yang dapat memberikan gabungan linear terbaik bagi parameter alam sekitar. Perbandingan telah dilakukan di antara indeks daripada analisis komponen utama konvensional (PCA) dan indeks analisis komponen utama teguh (RPCA). Keputusan menunjukkan bahawa RPCA dapat memberikan satu alternatif gabungan linear yang lebih baik. Contoh berangka mengenai kualiti udara telah dilakukan untuk menunjukkan penggunaan indeks kualiti alam sekitar teguh.

ABSTRACT

This paper discusses a formulation of new environmental quality indices, which can be used for monitoring environmental as well as meteorological parameters. The formulation of the indices is based on conventional and robust principal component analysis, which gives the linear combination of environmental parameters. Comparisons are made between the conventional principal component analysis (PCA) indices and robust principal component analysis (RPCA) indices. The results show that the RPCA gave a better alternative linear combination. A numerical example on air quality was used to illustrate the application of the robust environmental indices.

Keywords: Conventional principal component analysis, robust principal component analysis, quality indices, MLT-estimator, CMB-estimator

INTRODUCTION

Indices or indicators are useful means of observing trends, analysing programs, policy making and informing the public of important concepts in a simple understandable manner. An index is defined as a scheme that transforms the (weighted) values of individual pollutant-related parameters (for example, carbon monoxide concentration or visibility) into a single numbers, or set of number and the result is a set of rules (for example, an equation) that translates parameter values by means of a numerical manipulation into a more parsimonious form (Ott and Thom 1976). Pikul (1974) defined an index, which is a mathematical combination of two or more parameters, which can have utility at least, in an interpretive sense.

In an environmental context, environmental indices are used to give insight into environmental conditions. They should serve as a means to examine the changes in climate, to highlight specific environmental conditions and to help

governmental decision-makers evaluate the effectiveness of regulatory programs. The best measurement of selected parameters, which are reported in a timely and effective manner merely provides the policy maker with large amounts of data. To be useful for evaluation and assessment, these data must be aggregated in a meaningful way to show the right magnitudes and trends.

In discussing environmental aspects, there is more than one parameter that needs to be analyzed. Normally, traditional approaches are used in multivariate data, such as factor analysis, principal component analysis, discriminant analysis, biplot analysis and multidimensional scaling. This paper discusses the implementation of the robust PCA in developing environmental indices.

METHODOLOGY

A principal component analysis (PCA) is concerned with explaining the variance covariance structure through a few linear combinations of original variables. Its general objectives are data reduction and data interpretation. Although p components are required to reproduce the total system variability, often a small number, k, of the principal components, can account for much of this variability. If so, there is as much information in the k components as there is in the original p variables. The original data, consisting of n measurement on p variables, is reduced to one consisting of n measurements on k principal components.

Algebraically, principal components are particular linear combinations of the p random variables $X_1, X_2,..., X_p$. Geometrically, these linear combinations represent the election of a new coordinate system obtained by rotating the original system with $x_1, x_2,..., x_p$ as the coordinate axes. The new axes represent the directions with maximum variability and provide a simpler and parsimonious description of the covariance structure.

The method of principal components is based on a key result from matrix algebra: A $p \times p$ symmetric, nonsingular matrix, such as the covariance matrix Σ, may be reduced to a diagonal matrix L by premultiplying and postmultiplying it by a particular orthonormal Matrix U such that $U'\Sigma U = L$. The diagonal elements of L, $l_1, l_2,..., l_p$ are called the characteristic roots, latent roots or eigenvalues of Σ. The columns of U, $u_1, u_2,..., u_p$ are called the characteristic vectors or eigenvactors of Σ. The characteristic roots may be obtained from the solution of the characteristic equation $|\Sigma - l\, I| = 0$, where I is the identity matrix. This equation produces a p^{th} degree polynomial in l from which the values $l_1, l_2,..., l_p$ are obtained.

If the covariances are not equal to zero, it indicates that a linear relationship exists between these two variables, the strength of that relationship being represented by the correlation coefficient. The principal axis will transform p correlated variables $x_1, x_2,..., x_p$ into p new uncorrelated variables $z_1, z_2,..., z_p$. The coordinate axis of these new variables are described by the characteristic vectors u_i which make up the matrix U of direction cosines used in the transform $z = U'[x - \Sigma]$. The transformed variables are called the principal components of x and the covariance matrix of Z is $\text{cov}(Z) = \text{tr}\ (\lambda_1, \lambda_2, \lambda_3,..., \lambda_p)$.

The majority of techniques have assumed that the data with which we are working are basically 'good'. A number of problems may occur. First, the assumptions regarding the underlying distribution used. Second, there are assumptions of independence of the sample observation. Third, 'outliers' observations. It is possible that outliers can affect the roots and vectors themselves and for that, robust estimation procedures will be required. There are four classes of robust estimators; namely the adaptive estimator, the L-estimator, the M-estimator and the rank test estimator. Let $x_1, x_2, ..., x_n$ be a random sample from a distribution with a probability density function $f(x_i-\theta)$, where θ is the location parameter. Then, the log likelihood function can be written as

$$\ln L(\theta) = \sum_{i=1}^{n} ln\, f(x_i-\theta)$$

$$= -\sum_{i=1}^{n} \eta(x_i-\theta), \quad \text{where } \eta(x) = -\ln f(x)$$

Thus,

$$\frac{d \ln L(\theta)}{d\theta} = -\sum_{i=1}^{n} \frac{f'(x_i-\theta)}{f(x_i-\theta)} = \sum_{i=1}^{n} \eta(x_i-\theta)$$

where $\eta'(x) = \tau(x)$. The solution, $\hat{\theta}$, of $\sum_{i=1}^{n} \tau(x_i-\theta) = 0$ maximise $L(\theta)$ and $\hat{\theta}$ is called the maximum likelihood estimator of θ.

Marrona (1976) introd uced M-estimator for the location vector, μ, and covariance matrix, Σ, for the solution of the system

$$(1/n)\sum_{i=1}^{n} w_1(d_i)(x_i-\mu) = 0$$

and

$$(1/n)\sum_{i=1}^{n} w_2(d_i^2)(x_i-\mu)(x_i-\mu)' = \Sigma$$

where $d_i = [(x_i - \mu)'\Sigma^{-1} (x_i - \mu)]^{1/2}$ is the Mahalanobis distance function and w_1 and w_2 are functions of the technique involved.

The M-estimator

An iteration procedure is needed to calculate the robust value of d_i^2 where $d_i=[(x_i - m^*) S^{*-1} (x_i - m^*)]^{1/2}$, i = 1, 2, ..., n. where m^* and S^* are the new estimators of μ and Σ. Generally, the M-estimators of μ and Σ are given by

$$m^* = \sum_{i=1}^{n} w_1(d_i)x_i \Big/ \sum_{i=1}^{n} w_1(d_i) \text{ and } S^* = \frac{\sum_{i=1}^{n} w_2(d_i^2)(x_i - m^*)(x_i - m^*)'}{f\left[w_2(d_i^2)\right]}$$

where $w_1(d_i)$ and $f[w_2(d_i^2)]$ are some suitable weight functions.

(i) The MLT-estimator

Marrona (1976) suggested the weight functions of w_1 and w_2 as follows. Let

$$w_1(d_i) = \frac{(p+v)}{(v+d_i^2)} = w_2(d_i^2)$$

where v is the degree of freedom associated with the multiple t-distribution. Generally, v is set to 1, the Cauchy distribution. This is the value used by Devlin *et al.* (1981) and $f\{w_2(d_i)\} = 1/n$. So, the likelihood maximum t-estimator (MLT) of mean μ, and covariance matrix Σ, are:

$$m_{MLT} = \frac{\sum_{i=1}^{n} w_1(d_i)x_i}{\sum_{i=1}^{n} w_1(d_i)} \text{ and } S_{MLT} = (1/n)\sum_{i=1}^{n} w_2(d_i^2)(x_i - m^*)(x_i - m^*)'$$

where $w_1(d_i) = (1+p)/(1+d_i^2) = w_2(d_i^2)$, refer to Jackson (1991) for details.

(ii) The CMB-estimator

Campbell (1980) suggested a phi-function ψ, redeclines in $w(d_i) = \psi(d_i)/d_i$ where

$$w(d_i) = \begin{cases} 1 & \text{if } d_i \le \xi \\ \dfrac{\xi}{d_i} exp\left\{\dfrac{-(d_i - \xi)^2}{2c_2^2}\right\} & \text{if } d_i > \xi \end{cases}$$

if $w_2(d_i^2) = [w_1(d_i)]^2$ and $\xi = \sqrt{p} + c_1/\sqrt{2}$. Then $w_1(d_i) = [w_1(d_i)]/d_i$;

$w_2(d_i^2) = [w_1(d_i)]^2$ and $f[w_2(d_i)] = \sum_{i=1}^{n} [w_2(d_i)]^2 - 1$

the c_1 and c_2 are the robust scale estimators to ensure w has robust characteristics. When normality assumption is considered, square root of Fisher transformation

for Chi-square distribution will give d_i approximates to normal distribution with mean $\sqrt{p}$ and variance $1/\sqrt{2}$. Campbell also suggested that $c_1 = 2$ and $c_2 = 1.25$ to produce the robust characteristics which have been suggested by Hampel (1973). This procedure produced weights that decrease at a faster rate than other procedures.

The mean and covariance matrix estimator are

$$m_{M;B} = \frac{\sum_{i=1}^{n} w_1(d_i)x_i}{\sum_{i=1}^{n} w_1(d_i)} \quad and \quad S_{C;MB} = \frac{\left\{\sum_{i=1}^{n} w_2(d_i^2)(x_i - m^*)(x_i - m^*)'\right\}}{\left\{\sum_{i=1}^{n} [w_2(d_i)]^2 - 1\right\}}$$

All of the multivariate procedures are sensitive to starting values and usually work best with robust estimates at the beginning. For the starting values in the iteration, the sample mean, $\bar{x}$ and sample covariance matrix, S, are used. If there are extreme values, the robust median estimator, x_m and matrix $S_m = \frac{\sum_{i=1}^{n}(x_i - x_m)(x_i - x_m)'}{n-1}$ are used for $\bar{x}$ and S, respectively. The procedure is repeated until the correlation matrix converges.

The methods discussed earlier produced robust estimates of the mean and variance while the characteristic roots and vectors were obtained from them by conventional PCA. These results are called robust PCA because the starting matrices were robust.

The Development of the Robust Indices

The air quality index introduced by Pikul (1974), is defined as

$$Q_I = 1 - P_I \qquad (1)$$

where P_I is an index of air pollution. The air pollutant index is defined without regard to synergistic effects, which occur as a result of reactions between two or more pollutants. The keys to determining P_I are the index standard for each pollutant, which need not correspond to legal standards. Let

S_{i1} be the standards concentration at 50th percentile (median) for pollutant i
S_{i2} be the standards concentration at 85th percentile (1σ) for pollutant i
S_{i3} be the standards concentration at 95th percentile (2σ) for pollutant i

Then, the standards pollution index from the first principal component, $S_{z1(ik)}$ can be written as $S_{z1(ik)} = \Sigma\omega_{ik} S_{ik}$ where $k = 1, 2, 3$; $i = 1, 2, 3, 4, 5$; and ω_{ik}

the coefficient or weight from the first principal component. The air quality index includes five pollutants, namely ozone (O_3), nitrogen dioxide (NO_2), sulfur dioxide (SO_2), carbon monoxide (CO) and suspended particulate matter (SPM).

Let M_{ik}, k =1, 2, 3, correspond to the measured concentration values of pollutant i for the k-th percentile index and let $M_{z1(ik)}$ be the pollutants indices from the first principal components, Z. So we can get the pollutant indices which correspond to the measured concentration values of pollutant i for the k^{th} percentile index; $M_{z1(ik)} = \Sigma\omega_{ik} M_{ik}$ k=1, 2, 3; i = 1, 2, 3, 4, 5; and ω_{ik} are the coefficients and weights from the first principal component.

Then the pollution index is computed as

$$P_I = \frac{1}{M}\left(\sum_{k=1}^{3} \upsilon_{ik} \frac{M_{z1(ik)}}{S_{z1(ik)}}\right) \qquad (2)$$

where the υ_{ik} is the relative weights assigned to each percentile value ($\Sigma\upsilon_{ik} = 1$) and M is a factor that ensures that P_I does not exceed unity.

RESULT AND DISCUSSION

The CPCA Indices

Standard indices have been used for the five primary pollutants shown in Table 1. The standard indices are based on the MAQI (Malaysian Air Quality Index) and RMG (Recommended Malaysian Guideline).

TABLE 1
Standard index based on the RMG and MAQI

Pollutants	Standard index		
	S_{i1}	S_{i2}	S_{i3}
Ozone, O_3 (ppm)	0.1000	0.3270	0.5541
Nitrogen Dioxide, NO_2 (ppm)	0.0600	0.2795	0.4989
Sulphur Dioxide, SO_2 (ppm)	0.0400	0.1265	0.2130
Carbon Monoxide, CO (mg/m^3)	9.0000	24.2634	39.5269
Suspended Particulate Matter, SPM (µg/m3)	150.000	314.9889	479.9777

For this study, the data from 1st to 31st July 1995 from the Kuala Lumpur environmental station were used. To get the standard pollutant index $S_{z1(ik)}$, the coefficient derived from the conventional and robust PCA are multiplied with the pollutant value for each percentile.

Table 2 shows the correlation value (from conventional correlation matrix) between pollutants and it is found that the pollutants have a positive relationship except for O_3 and CO and O_3 and SPM respectively. However, the correlation values are small -0.1205 and -0.2639, respectively.

TABLE 2
The correlation matrix based on conventional PCA

Pollutants	O_3	NO_2	SO_2	CO	SPM
O_3	1.0000				
NO_2	0.4231	1.0000			
SO_2	0.3147	0.4239	1.0000		
CO	-0.1205	0.2135	0.6427	1.0000	
SPM	-0.2639	0.1169	0.9237	0.5428	1.0000

The first eigen value from the correlation matrix is 2.5380 and it explains 50.7% of the variation in the data. As mentioned before, the quality index is calculated based on the first principal component. The pollution index equation is

$$P_I = 0.2797*NO_2 + 0.0440*O_3 + 0.5848*CO + 0.5245*SO_2 + 0.5501*SPM.$$

Pollutant index, $M_{z1(ik)}$ can be derived by multiplying each M_{ik} with the coefficient (which is derived from the conventional and robust PCA) and then totalled. The air quality index would be computed from equation (1) by substitution from equation (2).

The quality indices throughout July 1995 are displayed in Table 3.

TABLE 3
Indices derived from the first day to the 31st with the conventional PCA

Day	QI	Day	QI
1	0.97120	17	0.95986
2	0.97063	18	0.96771
3	0.97282	19	0.97701
4	0.97855	20	0.96706
5	0.96860	21	0.97477
6	0.96476	22	0.97918
7	0.96188	23	0.97743
8	0.96588	24	0.98261
9	0.97005	25	0.97232
19	0.96570	26	0.97881
11	0.96065	27	0.98127
12	0.95916	28	0.97928
13	0.96007	29	0.96015
14	0.95881	30	0.95901
15	0.95614	31	0.96566
16	0.96288		

This method shows that the air quality in Kuala Lumpur is in good condition.

The RPCA Indices

The calculation of RPCA index is still the same as in CPCA, the only difference is the coefficient former index is derived from a robust estimator. Table 4 shows that *CO* and *SPM* are highly correlated with correlation value of 0.9318 whereas *CO* and SO_2 have a correlation value of 0:6060.

TABLE 4
The correlation matrix based on the robust PCA

Pollutants	O_3	NO_2	SO_2	*CO*	*SPM*
O_3	1.0000				
NO_2	0.5769	1.0000			
SO_2	0.5626	0.5616	1.0000		
CO	0.1678	0.4046	0.6060	1.0000	
SPM	0.0358	0.2960	0.9318	0.4924	1.0000

The first eigen value is 2.8963 and it explains 57.9% of the variation in the data. This means the RPCA can explain more variation than the conventional counterpart. The pollution index equation is

$$P_I = 0.4272*NO_2 + 0.3319*O_3 + 0.5023*CO + 0.5024*SO_2 + 0.4502*SPM$$

Finally, the quality indices throughout July 1995 are displayed in Table 5.

TABLE 5
Indices derived from the first day to the 31st with the robust PCA

Day	QI	Day	QI
1	0.97656	17	0.95472
2	0.97023	18	0.97019
3	0.97038	19	0.97954
4	0.99989	20	0.96483
5	0.96882	21	0.97765
6	0.96748	22	0.97486
7	0.96241	23	0.97612
8	0.96346	24	0.98723
9	0.96918	25	0.97232
19	0.96623	26	0.99940
11	0.95920	27	0.98339
12	0.95271	28	0.99724
13	0.96256	29	0.96609
14	0.95923	30	0.96018
15	0.95928	31	0.96357
16	0.96254		

This method also shows that the air quality in Kuala Lumpur is in good condition.

CONCLUSIONS

The PCA structure can be a better alternative to explain the combination environmental parameters in developing environmental indices. The largest weight in pollution index equation indicates the most influencing factor in air pollution phenomenon. From the pollution index equation, the contribution of each parameter in air pollution can be determined. The results show that the robust estimators are more successful in giving a better alternative result. The CPCA explains only 50.7% of the variation in the data, while RPCA explains 57.97%. However, the CPCA and RPCA give the same caution signals regarding the air condition, but the values of indices are relatively different.

From the structure of the new quality indices, it shows that it gives a better alternative to monitor the level of air quality. Furthermore, the indices are easy to understand, easy to calculate and more comprehensive. This method (RPCA) is very flexible and it can be adapted to any type of environmental parameters, such as water quality, noise pollution, quality of life, etc. If the indices are plotted on the graph, the trends of environmental parameters can be detected and can be used for forecasting purposes.

REFERENCES

AZME KHAMIS. 1996. Pembinaan indeks kualiti udara teguh. MSc. thesis, Universiti Kebangsaan Malaysia.

CAMPBELL, N. A. 1980. Robust procedures in multivariate analysis I: robust covariance estimation. *Applied Statistics* **29:** 231–237.

DEVLIN, S. J. R. GNANADESIKAN and J. R. KETTENRING. 1981. Robust estimation of dispersion matrices and principal components. *Journal of the American Statistical Association* **76:** 354–362.

HAMPEL, F. R. 1973. Robust estimation a condensed partial survey. *Z. Wahr.verw. Geb.* **27:** 87–104.

JACKSON, J. E. 1991. *A User's Guide to Principal Components.* John Wiley & Sons Inc.

JOHNSON, R. A. and D. W. WICHERN. 1988. *Applied Multivariate Statistical Analysis.* Second edition. Prentice Hall International, Inc.

MARRONA, R. A. 1976. Robust M-estimators of multivariate location and scatter. *Annals of Statistics* **1:** 51–67.

OTT, W. R and G. C. THOM. 1976. *Air Pollution Indices: A Compendium and Assessment of Indices Used in United States and Canada.* Michigan: Ann Arbor Science.

PIKUL, R. 1974. Development of environmental indices. In *Statistical and Mathematical Aspects of Pollution Problems,* ed. J. W. Pratt.

ISSN: 0128-7680
Pertanika J. Sci. & Technol. 12(1): 11 - 20 (2004) © Universiti Putra Malaysia Press

Comparison of Lung Functions Among Asthmatic Children in Malaysia

[1]Zailina Hashim, [1]Juliana Jalaluddin & [2]Jamal H. Hashim

[1]Environmental and Occupational Health Unit,
Faculty of Medicine and Health Sciences, Universiti Putra Malaysia,
43400 UPM, Serdang, Selangor, Malaysia
[2]Department of Community Health, Faculty of Medicine,
Universiti Kebangsaan Malaysia Hospital, Bandar Tun Razak, Cheras
56000 Kuala Lumpur, Malaysia

Received: 24 January 2000

ABSTRAK

Satu kajian perbandingan telah dijalankan ke atas 163 kanak-kanak asma di Kuala Lumpur (tercemar) dan 38 orang di Terengganu (kurang tercemar) telah dipilih dalam kajian. Objektif kajian adalah untuk membandingkan fungsi paru-paru kanak-kanak asma mengikut jantina dan kawasan kajian. Borang soal selidik dan kad diari digunakan untuk mengumpul maklumat latar belakang dan kekerapan serangan asma di kalangan responden. Alat "spirometer" digunakan untuk mengukur fungsi paru-paru. Hasil kajian mendapati perbezaan yang signifikan bagi nilai FEV_1 % jangkaan (p=0.002), FEV_1/FVC % jangkaan (p=0.001) dan %FEV_1/FVC (p=0.002) antara kanak-kanak lelaki di kedua-dua kawasan. Walau bagaimanapun, perbezaan yang signifikan hanya terdapat antara FEV_1% jangkaan di kalangan kanak-kanak perempuan di kedua-dua kawasan. Korelasi yang signifikan juga didapati antara kekerapan serangan asma dengan FEV_1% jangkaan (p=0.008) FEV_1/FVC % jangkaan (p=0.001) dan % FEV_1/FVC (p=0.001) di kalangan kanak-kanak asma di Kuala Lumpur tetapi tiada korelasi yang signifikan didapati di kalangan kanak-kanak asma di Terengganu.

ABSTRACT

A comparative study was conducted on 163 asthmatic children from Kuala Lumpur (polluted area) and 38 asthmatic children from Terengganu (less polluted area). The objective of this study was to compare the lung functions of the asthmatic children between the 2 sexes and study areas. Questionnaires and diary cards were used to obtain background information and frequency of asthma attacks. A spirometer was used to measure lung functions of the asthmatic children. Findings showed that there was a significant difference in the FEV_1% predicted (p=0.002), FEV_1/FVC % predicted (p =0.001) and the %FEV_1/FVC (p=0.002) between male children in the two areas. However, only the FEV_1% predicted (p=0.011) was significantly different between the female children in the two areas. Significant correlation was also found between the frequency of asthma attacks with FEV_1% predicted (p=0.008), FEV_1/FVC % predicted (p=0.001) and % FEV_1/FVC (p=0.001) among the asthmatic children Kuala Lumpur but no significant correlation was found among the asthmatic children in Terengganu.

Keywords: Asthmatic children, lung functions, asthmatic attacks

INTRODUCTION

A study on asthmatic school children was conducted in Kuala Lumpur and Terengganu. Lung function measurements such as the Forced Vital Capacity (FVC), Forced Expiratory Volume in One Second (FEV_1) and $\%FEV_1/FVC$ are essential indicators for identifying the obstructive problems in the respiratory system due to diseases such as asthma, bronchitis or emphysema. If the FEV_1 is less than 80% of the expected percent, then the patient is categorized as having obstructive effects. The FEV_1/FVC % predicted is the most important index in evaluating the severity of asthma among patients (Murray 1979). If the FEV_1/ FVC % predicted is less than 75%, then the patients have serious asthma problems and need attention (Miller 1978). The objective of this study was to assess and compare lung function measurements of asthmatic children in K. Lumpur and Terengganu.

METHODOLOGY

Four primary schools in Kuala Lumpur and 2 schools in Terengganu were selected. The schools in K. Lumpur are located in the city center on a main road where the traffic is busy. The schools in Kemaman and Setiu in Terengganu are located away from the main road.

Due to the fact that the prevalence of asthmatic cases in Terengganu is lower, only 38 children were selected while in Kuala Lumpur, a total of 163 asthmatic children were selected. Information on the socio-economics, history and severity of asthma attacks, type of medicine used, hospital visits and treatment were obtained through questionnaire interviews on the children and their guardians.

Lung functions of the children were carried out to determine their lung volume and flow (volume per unit of time). A "Pony Cosmed Spirometer" which met the American Thoracic Society (1987) specifications was used in this study. The spirometer was calibrated each day before measurements. The procedure was explained and demonstrated to each child in which he or she was asked to inhale deeply in the standing position and blow rapidly and completely into a calibrated spirometer. Three acceptable and at least two reproducible curves were obtained in each subject. The highest values of forced vital capacity (FVC) and forced expiratory volume in the 1st second (FEV_1) were selected. Age was recorded to the nearest year, height was measured to the nearest 0.5 cm (with the subject standing without shoes), and weight was recorded to the nearest 0.5 kg. All readings were recorded at ambient temperature and pressure saturated (ATPS). FVC and FEV_1 measurements were adjusted to body temperature and pressure saturated (BTPS).

For comparative purposes, only the Malay respondents from the K. Lumpur school were studied because the asthmatic children selected in the Terengganu schools were made up of only ethnic Malays. At the same time, the prediction equations were based on sex and racial ethnicity. Therefore, other ethnic groups had to be excluded.

RESULTS AND DISCUSSIONS

Respondents' Background Information

The background and socioeconomic information of the asthmatic children are shown in Tables 1, 2 and 3. The mean age between the 2 groups of asthmatic children were about the same. The 163 children in Kuala Lumpur, were made up of 143 Malays, 10 Chinese and 10 Indians. There were 98 male children and 103 female children in both areas and the numbers were almost equal.

The household income in Table 2 shows that the children in K. Lumpur (RM1170.40) were in the lower middle class socioeconomic group while the children in Terengganu (RM586.80) were in the lower class socioeconomic group. About half of the families in K. Lumpur had household incomes of more than RM1000 while in Terengganu, all of the families have household incomes of less than RM1000. The difference in their total incomes was statistically significant (Table 3). In K. Lumpur, the fathers were mostly businessmen (34.4%), officers or office assistants (8.3%) and technicians (8.3%). In Terengganu, the majority of the fathers work as drivers (18.4%), businessmen (13.2%), labourers (13.2%) and fishermen (13.2%). The mothers in K. Lumpur (47.2%) and in Terengganu (81.6%) are mostly housewives.

TABLE 1
Respondents' background information

Location	Total (n)	Sex		Mean age	Race	(n)
		Boys	Girls			
K. Lumpur	163	81	82	10 yrs 2 mth	Malay	143
					Chinese	10
					Indian	10
Terengganu	38	17	21	10 yrs 1 mth	Malay	38

TABLE 2
Comparison of respondents' socioeconomic background in the study areas

	Kuala Lumpur (mean±s.d)	Terengganu (mean±s.d)	p-value (t-test)
Household income(RM)	1170.37 ± 755.44	586.84 ± 194.41	0.001
Length of residency (mth)	98.34 ± 33.94	103.89 ± 32.93	0.356
Length of stay in school (mth)	48.36 ± 10.20	50.52 ± 11.31	0.282

s.d = standard deviation
mth =month

TABLE 3
Household income of respondents in the study areas

Household income	Kuala Lumpur[a] Total (%)	Terengganu[b] Total (%)
< RM500	6 (3.7)	12 (31.6)
RM500 - RM1000	84 (51.5)	26 (68.4)
RM1001 - RM1500	37 (22.6)	-
RM1501 - RM2000	23 (14.1)	-
> RM2000	13 (8.1)	-

a: n=163
b: n=38

The children in K. Lumpur have resided in the area for an average length of 98.34 months (~8.16 years) and have been attending the school for an average period of 48.36 months (~4. 03 years). The children in Terengganu have resided and attended the school for an average period slightly longer than the children in K. Lumpur (Table 2).

Only about half of the K. Lumpur (49.1%) and Terengganu (44.7%) children have a family history of asthma (Table 4). They inherited the disease from their parents, grandparents or siblings. However, the other half of these children must have contracted the disease by other means. This type of asthma is called extrinsic asthma. It can be caused by several factors such as food, emotional stress, cigarette smoke, dust, medicine and physical exhaustion (Rahmat 1992). According to Azizi (1994), environmental pollutants in the atmosphere can trigger asthmatic attacks.

The asthmatic children in K. Lumpur usually get treatment from hospitals and clinics (73.6%). Their asthmatic conditions are probably more severe than the Terengganu children because they were prescribed with Becotide® and Ventoline® (33.2%) which are bronchodilater medications (Table 4). Asthmatic attacks are a great concern for parents in K. Lumpur due to the frequency and severity of the attacks on the children. The percentage who seek treatment at clinics or hospitals is also higher in K. Lumpur (73.6%) than in Terengganu (5.8%). Table 4 also shows how parents perceive their children's asthmatic attacks. It seems that the attacks among the K. Lumpur children are more severe than those among Terengganu children.

The Lung Functions

Figs. 1 to *4* show the distribution of FEV_1% predicted and %FEV_1/FVC among the asthmatic children in both areas according to their sex. The classification was based on Miller *et al.* (1978). The mean FEV_1% predicted among the asthmatic children in Kuala Lumpur (87.66) was lower than the asthmatic children in Terengganu (100.01).

TABLE 4
Comparisons of medical history, medication and severity of asthma attacks of children in the study areas

	Total (%)		
	K. Lumpur [a]	Terengganu [b]	p-value (Chi-square)
Family history of asthma	81 (49.7)	17 (44.7)	0.778
Medication (Becotide® (Glaxo) & Ventoline® (Glaxo))	54 (33.2)	-	-
Percentage who seek clinic or hospital treatment	120 (73.6)	2 (5.79)	0.001
Severity of asthma attacks			
-Very severe	5 (3.1)	-	0.597
-Severe	14 (8.6)	-	
-Moderate	102 (62.6)	29 (76.3)	
-Mild	42 (25.8)	9 (23.7)	

a: n=163
b: n=38

Table 5 shows the difference in the means of FEV_1% predicted between the 2 groups with regard to sex. The mean FEV_1% predicted value for the males (75.19) and females (83.03) in K. Lumpur was lower than the males (91.73) and females (100.24) in Terengganu. Statistics showed that there was a significant difference in the mean FEV_1% predicted value between both groups. Asthmatic children in Terengganu have better expiratory air flow from the lungs compared to the K. Lumpur children.

The measurements of $\%FEV_1/FVC$, were also carried out according to sex as shown in Table 6. The mean $\%FEV_1/FVC$ for the males (75.70) and females (84.81) in K. Lumpur was lower than that of the males (94.91) and females (92.21) in Terengganu. However, the difference was only significant for the males ($p = 0.002$).

As for the mean FEV_1/FVC% predicted, the mean for male children (82.76) and female (91.41) in K. Lumpur was also lower than the Terengganu male (102.67) and female (100.39) respectively (Table 6). However, similar to the $\%FEV_1/FVC$, a significant difference in FEV_1/FVC% predicted was found only among the male children. This implies that the lung obstructiveness in the male K. Lumpur children was more severe than that of Terengganu.

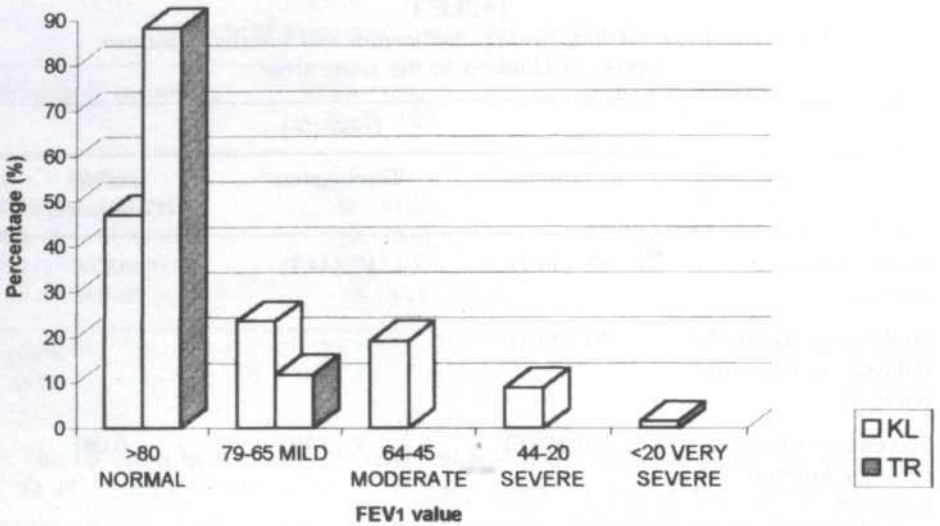

Fig. 1: Distribution of FEV_1% predicted among asthmatic boys in the study areas

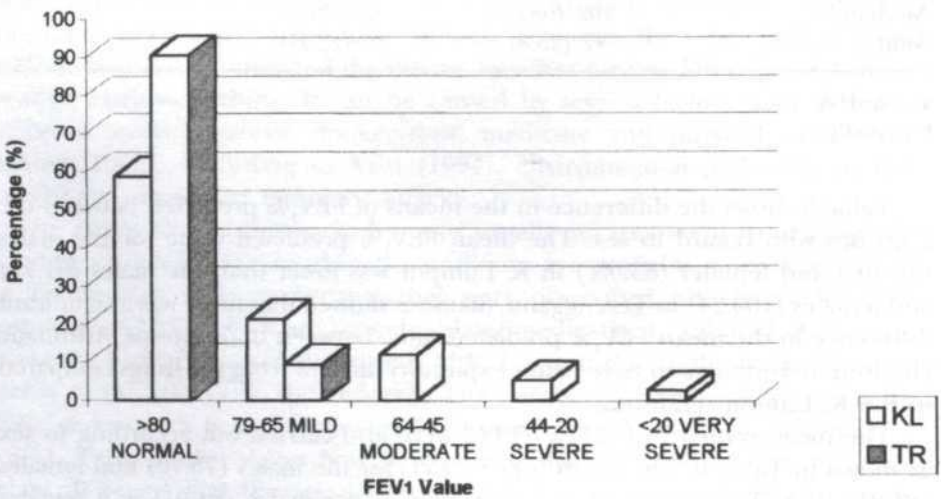

Fig. 2: Distribution of FEV_1% predicted among asthmatic girls in the study areas

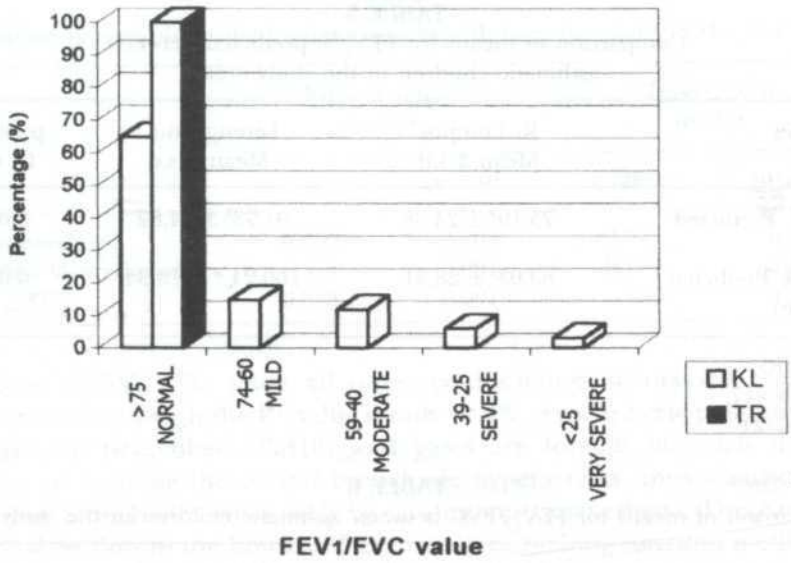

Fig. 3: Distribution of FEV_1/FVC% predicted among asthmatic boys in the study areas

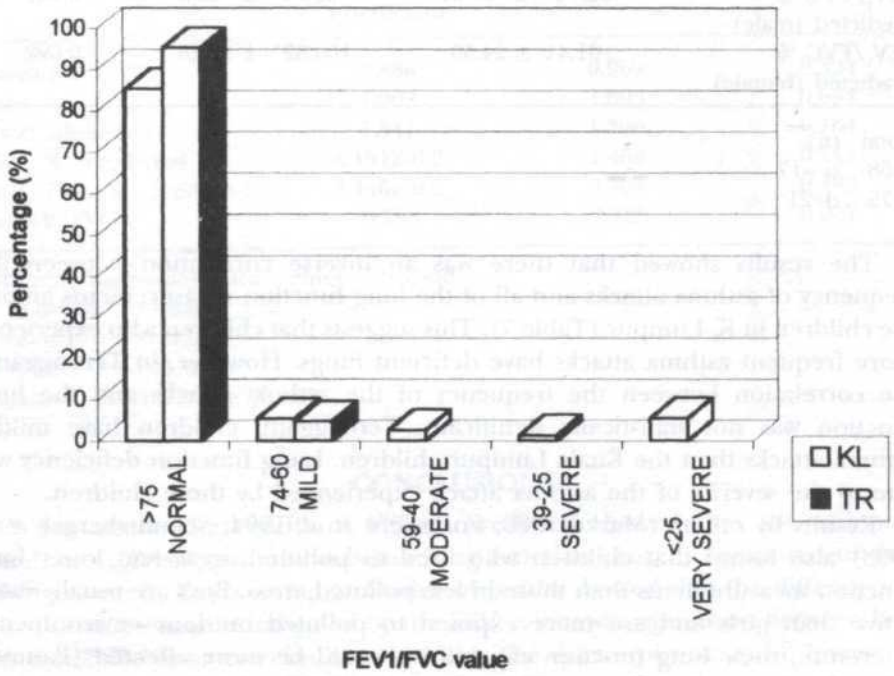

Fig. 4: Distribution of FEV_1/FVC% predicted among asthmatic girls in the study areas

TABLE 5
Comparison of means for FEV_1 % predicted between asthmatic children in the study areas

Variables	K. Lumpur Mean ± s.d	Terengganu Mean ± s.d	p value (t- test)
FEV_1 % Predicted (Male)	$75.19^a \pm 24.38$	$91.73^b \pm 14.82$	0.002
FEV_1 % Predicted (Female)	$83.03^c \pm 28.31$	$100.24^d \pm 18.34$	0.011

Total (n)
a=68 b =17
c=75 d=21

TABLE 6
Comparison of means for FEV_1 /FVC between asthmatic children in the study areas

Variables	K.L Mean ± s.d	TR Mean ±s.d	p (t-test)
$\%FEV_1/FVC$ (male)	$75.70^a \pm 23.27$	$94.91^b \pm 7.19$	0.002
$\%FEV_1/FVC$ (female)	$84.81^c \pm 22.50$	$92.21^d \pm 5.51$	0.126
FEV_1/FVC % Predicted (male)	$82.76^a \pm 23.97$	$102.67^b \pm 8.05$	0.001
FEV_1/FVC % Predicted (female)	$91.41^c \pm 24.55$	$100.39^d \pm 10.28$	0.092

Total (n)
a=68 b =17
c=75 d=21

The results showed that there was an inverse correlation between the frequency of asthma attacks and all of the lung function measurements among the children in K. Lumpur (Table 7). This suggests that children who experience more frequent asthma attacks have deficient lungs. However, in Terengganu, the correlation between the frequency of the asthma attacks and the lung function was not statistically significant. Terengganu children have milder asthma attacks than the Kuala Lumpur children. Lung function deficiency was due to the severity of the asthma attack experienced by these children.

Results by others (Marko 1980; Forestiere *et al.* 1994; Schmitzberger *et al.* 1993) also found that children who lived in polluted areas had lower lung function measurements than those in less polluted areas. Boys are usually more active than girls and are more exposed to polluted outdoor environments. Therefore, their lung function capabilities would be more affected (Paumels 1986).

The Multiple Regression "enter" method conducted on the individual asthmatic attacks for all the children have a statistically significant relationship

TABLE 7
Correlation between individual asthma attacks with lung functions in the study areas

	Kuala Lumpur (n=163)		Terengganu (n=38)	
	r value	p value	r value	p value
FEV_1 % predicted	-0.206	0.008	0.048	0.775
FEV_1/FVC % predicted	-0.317	0.001	0.139	0.405
% FEV_1/FVC	-0.343	0.001	-0.246	0.136

with only %FEV_1/FVC when all other confounding factors are controlled (Table 8), even though the R^2. value is only 12.4%. Atmospheric pollutants such as respirable particulate (PM10) and gases are foreign materials that can promote or increase the overall bronchiole hyperactivity, thus obstructing or restricting bronchioles repetitively by causing mucuosal edema. This can cause abnormal air flow in the lungs and as a result, cause lung function inefficiency.

TABLE 8
Relationship between individual asthma attacks with selected variables

Independent variable	Regression Coefficient	t value	p value
Constant	3.856	0.969	0.334
Sex	1.902	1.693	0.092
Food tabulation	1.541	1.396	0.164
FEV_1 % Predicted	4.191E-0.2	1.463	0.145
FEV_1/FVC % Predicted	4.146E-0.2	0.704	0.482
% FEV/FVC	-0.193	-2.728	0.007

'Multiple Regression' for 'enter' method
F statistics = 5.698
p value = 0.01
R value = 0.387
adjusted R^2 value = 0.124

CONCLUSIONS

On the whole, the results of FEV_1% predicted showed that the asthmatic children in Terengganu have better lung function capacity compared to their counterparts in Kuala Lumpur. Statistical results showed that the difference in the obstructiveness as indicated by the FEV_1 values was significant between both the males and females in both study areas. The degree of severity of the asthma attacks as shown by the %FEV_1/FVC also differ significantly among the male children in both areas. The K. Lumpur asthmatic children have poorer lung

capacity and functions and experience more severe asthma attacks than Terengganu children as indicated by the $\%FEV_1/FVC$.

Atmospheric pollutants influence the lung function efficiency of these children. Even though the medical facilities are better in Kuala Lumpur, the children are more exposed to these pollutants. The children in Kuala Lumpur are experiencing more serious asthmatic problems than in Terengganu due to the high industrial and traffic activities in these urban areas which contribute to air pollution.

REFERENCES

American Thoracic Society. 1978. *Health Effects of Air Pollution.* p.1–25. American Lung Association, 1740 Broadway, New York.

Azizi B.H.O. and R. L. Henry. 1994. Ethnic differerences in normal spirometric lung function of Malaysian children. *Respiratory Medicine* **88:** 349–356.

Forestiere F., M. G. Corbo, R. Pistelli., M. Paola, N. Agabati, B. Ciappi and A. G. Perucci. 1994. Bronchial responsiveness pollution levels. *Archives of Environmental Health* **63(5):** 113–120. Washington, D.C.

Marko, S., F. Mirka and H. Omer. 1980. Effect of urban air pollution on school age children. *Achives of Environmental Health* **36(3):** 101–107.

Miller, W. F., R. Scacci and L. R. Gast. 1978. *Laboratory Evaluation Pulmonary Function.* Phidadelphia: J.B. Uppincott. Company.

Murray, A. D. 1979. The physiological basis of pulmonary function testing. *Clinical Symposia* **31(2):** 1–30.

Paumels R., P. D. Snaishall and C. H. Bowker. 1986. *A Practical Approach to Asthma.* CBA Publishing Services on Behalf of Fison Pic. 2–30.

Rahmat, H. 1992. *Asma.* p.15–20. Petaling Jaya: Fajar Bakti Sdn. Bhd.

Schmitzberger R., B. K. Rhomberg, R. Puchegger, N. D. Schmitzberger, G. Kemmler and N. Panosh. 1993. Effects of air pollution on the respiratory tract of children. *Pediatric Pulmonology* **1592:** 68–74.

ISSN: 0128-7680
Pertanika J. Sci. & Technol. **12(1)**: 21 - 32 (2004) © Universiti Putra Malaysia Press

Urban Forestry Planning Using Remote Sensing/GIS Technique

Mohd. Hasmadi Ismail & *Kamaruzaman Jusoff
Department of Forest Production
Faculty of Forestry,
Universiti Putra Malaysia
43400 UPM, Serdang, Selangor, Malaysia
E-mail: kjusoff@aeroscan.biz

Received: 2 March 2001

ABSTRAK

Perhutanan bandar kini menjadi semakin penting bukan sahaja kepada nilai estetiknya tetapi juga kepada keberkesanannya dalam mengawal persekitaran. Potensi untuk membangunkan hutan bandaran di Malaysia adalah amat besar kerana Malaysia kaya dengan kepelbagaian tumbuhan. Kemajuan teknologi penderiaan jauh dan sistem maklumat geografi (GIS) bukan sahaja berguna untuk pemantauan perubahan persekitaran tetapi juga amat berguna untuk perancangan dan pengurusan hutan bandaran. Objektif kajian ini ialah untuk menilai kemampuan data penderiaan jauh dan GIS untuk memberi maklumat bagi menentukan kawasan yang berpotensi untuk perhutanan bandar di sekitar Lapangan Terbang Antarabangsa Kuala Lumpur. Imej Landsat TM 126/58 (jalur/baris) berbentuk pita komputer padat diproses dan dianalisis secara digital menggunakan perisian PCI EASIPACE versi 6.2. Data sokongan seperti peta topografi, peta guna tanah dan siri tanah digunakan untuk membantu penganalisisan imej satelit. Integrasi kawasan untuk pelandskapan hutan bandar. Kajian akan datang adalah disarankan agar menggunakan data beresolusi tinggi untuk mendapatkan pemetaan yang lebih tepat bagi tujuan proses pelandskapan.

ABSTRACT

Urban forestry has become an important value, not only for the aesthetic but also their effeetiveness in the environmental control and health. There is a potential to plan and develop urban forest landscape in Malaysian cities due to her richness in plant biodiversity. The advances in remote sensing technology and geographic information system (GIS) technique have provided an effective tool not just for monitoring the change of environment but also very useful for planning, managing and developing of urban forest landscaping. This study was undertaken to assess the capability of integrating remote sensing and GIS to provide information for urban forest potential sites surrounding Kuala Lumpur International Airport (KLIA) and its vicinity. Landsat TM imagery scene 126.58 (path/row) in the form of computer compatible tape (CCT) taken in May 1996 was digitally processed and analysed using a PC-based PCI EASIPACE software system version 6.2. Ancillary data such as topographical map, land use map and soil series map were used to support the satellite data.

* Correspondence Author

Integrating satellite data and GIS produced a map showing the potential site for urban forest landscaping at KLIA. Future studies should attempt to utilize airborne hyperspectral high-resolution data for more accurate mapping and landscape planning process.

Keywords: Urban forestry, planning, remote sensing/GIS technique

INTRODUCTION

The Malaysian Government under the Ministry of Local Government and Housing introduced the National Landscape Guideline in 1995. Malaysia is committed to build a beautiful country with green space with systematic and professional task (Anonymous 1995). At the launching of the National Tree Planting Campaign, the government's vision is to turn Malaysia into Garden Nation by the year 2005. The landscape has to be carefully designed and must be properly maintained according to the right technique. This guideline was launched under the impression of rapid landscape destruction on regulated consumption of natural resources.

Urban forestry is a practice of raising and scientifically managing suitable types of woody plants within the environment of all populated places that are used and influenced by urban development and urban population for their sustained environmental, physical, sociological, recreational and economic benefit. Land evaluation is needed to assess the performance of land use for specific purposes. Recently, remote sensing and the GIS technique have become important tools for forestry conservation and management purposes. Space remote sensing is one of the processes of obtaining information about the earth from instruments mounted on satellite (Anonymous 1991). Many studies (Makoto *et al.* 1997; Mazlan and Norhan 1997; Honda *et al.* 1997) have proved that the integration of remote sensing and GIS can be reliable and fast information with affordable cost and workforce for decision-making in forest resource planning and landscaping.

The general objective of this study is to assess the applicability and usefulness of integrating remote sensing satellite data and GIS for urban forest landscape mapping. The specific objectives are (i) to classify and map the different land cover types that are found in the KLIA and surrounding areas and, (ii) to identify, monitor and map the potential areas for urban forest landscapes.

MATERIALS AND METHODS

Description of Study Area

The Kuala Lumpur International Airport (KLIA) is located in the south of Kuala Lumpur city in the District of Sepang, Selangor within latitude 101° 40'E to 101° 47'E and longitude 02° 44'N to 02° 50'N, cover an area of approximately 50 km by 50 km. KLIA is being developed as the vehicle for information technology (IT) application for airport management services. The distance of KLIA to Kuala Lumpur city is approximately 50 km. *Fig. 1* shows the location map of the study area.

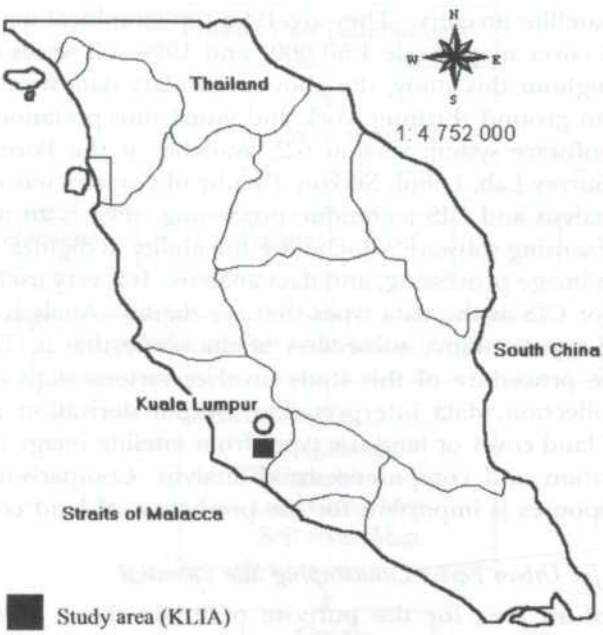

Fig. 1: A map of P. Malaysia showing the location of the study site

The climate of the study area is typically humid tropical and is characterized by year-round high temperature and seasonal heavy rain especially in October or November to February or March. The average rainfall is about 2375 mm per annum with a maximum of 2500 mm and minimum of 2250 mm. The mean annual temperature ranges from 22°C to 32°C. The relative humidity is always high, and ranges from 60% to 97%, with a daily mean of 82.5%. The study area is mainly covered by agricultural crop, mostly rubber, oil palm with occasional patches of forest. In addition, some grassland, shrubs and paddy can be found at the valley area of 70 m to 300 m wide. The topograhpy of this region is generally characterized by hilly and dissected sediment with altitude ranging from 10 m to 120 m. In the lower part of the hill area, slope ranges from 5° to 8°, while in the upper part, slope ranges from 12° to 15°. The main geological content of this region is shales with sandstones and conglomerates (Lawrence 1978).

METHODS

Sources of Data and Image Processing Techniques

The Landsat TM digital spectral data was taken in May 1996 for path/row 126/58 and acquired with spatial resolution of 30 m in the form of computer compatible tape (CCT). The image has been corrected from geometric distortion and atmospheric problem. Satellite imagery was obtained from Malaysia Centre for Remote Sensing (MACRES) in Kuala Lumpur. Secondary data are acquired

to support the satellite imagery. They are 1992 topographical map (Scale 1:50 000), 1992 land cover map (Scale 1:50 000) and 1996 soil series map (Scale1: 253 444). Throughout this study, the above secondary data were also used as reference map in ground thruting work and visual interpretation stage. The PC-based PC1 software system version 6.2, available at the Forest Geospatial Information & Survey Lab, Lebuh Silikon, Faculty of Forestry was used for both digital image analysis and GIS technique processing. PCI is an integration of GIS and remote sensing software, which have the ability to digitize image as well as map, perform image processing, and data analysis. It is very useful and is one of the sources for GIS as the data types that are digital. Analysis was initiated by selecting the representative subsection of the scene that is covered in the study area. The procedure of this study involves various steps of processing such as data collection, data interpretation, output derivation and (*Fig. 2*). Classification of land cover or land use types from satellite image involved both visual interpretation and computer-assisted analysis. Comparison of spectral signature or responses is important for the prediction of land cover features.

Physical Criteria for Urban Forest Landscaping Site Potential

The selection of an area for the purpose of urban forest landscaping was focused on developed and undeveloped areas surrounding the KLIA. The approach was to take an assessment and evaluation according to several factors or parameter, which were shown in Table 1. All parameters consisting of

TABLE 1
Physical criteria for urban forest landscaping site potential

Factor	Criteria/rank		
	1 (Most potential)	2 (Moderately potential)	1 (Least potential)
Slope	Level, gently sloping (0%-8%)	Gently, sloping, moderate steep (9%-18%)	Moderately steep, steep, very steep (19%-35%)
Soil texture	Fine loamy to moderate, clay loam, deeply developed soil with detectable accumulation of organic material	Sandy, silty and clayey alluvial soil. Recent soil development	Sandy soil, silty, clayey alluvial and graveled alluvial deposits
Drainage	Good drainage, good aquifer, surface water and infiltration zone. Infiltration rates of 3.75 to 18.75 cm/hr.	Moderate drainage, interfloor water and spring zone. Infiltration rates of 4.7 to 9.38 cm/hr.	Excessively drained, high runoff. Infiltration rates of 0.75 to 4.69/hr.
Spatial area	> 50 m wide	30 m-50-m wide	< 30 m wide
Availability of natural resources	Dense forest, pond lake, and river, etc.	Secondary forest, stream, plantation,	Shrub, grassland, bare land, swampy,
Vicinity to urban area	< 1 km from urban area	1 km-2 km from urban area	> 3 km from urban area

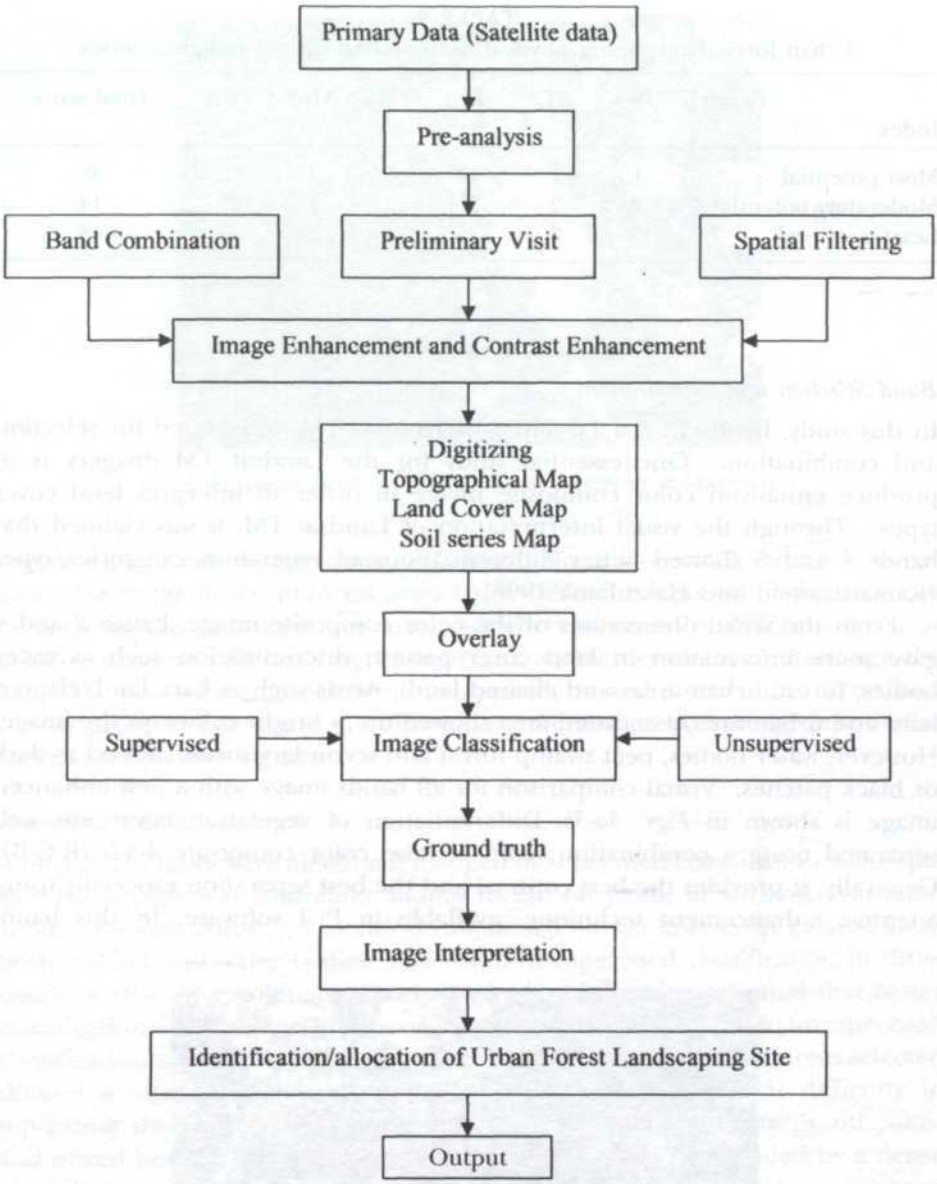

Fig. 2: The flow chart of the study procedure

physical criteria were given rank 1,2 and 3 indication most least potential for urban forest landscaping and development. Meanwhile, the standard range of site potential category is summarized in Table 2, where range from 6-13 (most potential), 14-17 (moderately potential) and 18 and above is least potential, respectively. The lowest score obtained implies that a particular site has the most potential for urban forest landscaping in KLIA and its vicinity.

TABLE 2
Urban forest landscaping physical factors-based on site potential index

Factor / Index	S	ST	D	SA	ANR	VUA	Total score
Most potential	1	1	1	1	1	1	6
Moderately potential	2	2	2	2	2	2	14
Least potential	3	3	3	3	3	3	18

RESULTS AND DISCUSSION

Band Selection and Combination

In this study, bands 1,2,3,4,5,6 and 7 of Landsat TM were tested for selection and combination. One essential study for the Landsat TM imagery is to produce enhanced color composite image in order to interpret land cover types. Through the visual interpretation of Landsat TM, it was claimed that bands 4 and 5 showed better differentiations of vegetation categories/types (Kamaruzaman and Haszuliana 1996).

From the visual observation of the color composite image, bands 2 and 4 gave more information in land cover pattern discrimination such as water bodies, forest, urban areas and cleared land. Areas such as bare land/cleared land and urban area/associated area showed up as bright colors on the image. However, water bodies, peat swamp forest and secondary forest showed as dark or black patches. Visual comparison for all bands image with a new enhanced image is shown in *Figs. 3a-3b.* Differentiation of vegetation cover was well separated using a combination band of false color composite 4-3-5 (R-G-B). Generally, it provides the best contrast and the best separation especially using adaptive enhancement technique, available in PCI software. In this band,

Fig. 3a: Image band 4-5-3 (R-G-B) with adaptive enhancement

Fig. 3b: Image band 5-4-2 (R-G-B) with adaptive enhancement

vegetation appears in red tones. However, there is a small variation in red tones due to the different forest cover types. Different degrees of brightness can be seen in the non-vegetative areas, which represent the different types or urban areas especially building, cleared land and settlement area. Although the adaptive enhancement technique is applied, mixed horticulture crop and rubber plantation areas are still difficult to differentiate because of their similar spectral reflectance signature.

Supervised Classification

A total of 10 classes were identified/mapped by supervised classification technique as follows: peat and freshwater swamp forest, oil palm, urban and associated areas, secondary forest, grassland/shrub, mixed horticulture crop, cleared land, bush, rubber and water bodies. The result of supervised classification in three bands of (R-G-B) combination is shown in *Fig. 4*. Results indicated that better classification was obtained in supervised classification compared to unsupervised classification approaches. The mean spectral value of the training areas selected showed a satisfactory separation of land cover types. There is difficulty in separating the small urban and settlement areas from rubber trees, oil palms and mixed horticulture crops because the study area is surrounded by a dense plantation and homestead garden. Certain settlement areas (e.g. worker's house in rubber estate) are confused with other classes such as cleared land due to their similar spectral response.

Ground Truth

A total of 25 training areas were selected and visited with the support of satellite imagery and ancillary data. The ground truth work was conducted for two days from 16 to 18 February 1998. For each site, photographs were taken and major types of land cover observed and recorded in the form.

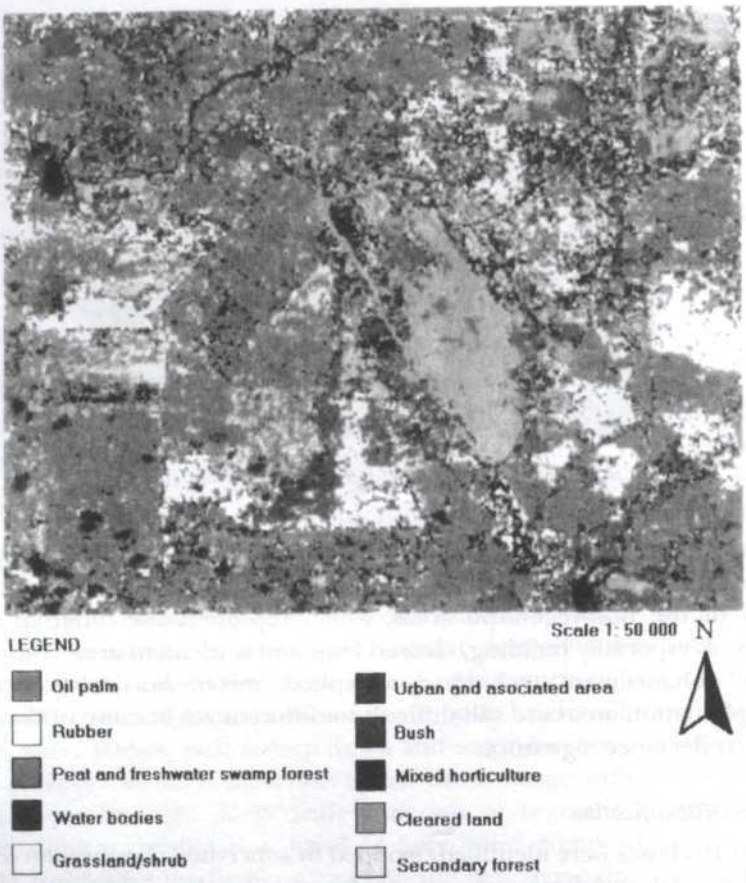

Fig. 4: Supervised classification of KLIA

Accuracy Assessment

The result of confusion matrix was expressed in tabular form and shown in Table 3. The percentage listed in the table represents the accuracy of classification of 10 classes of land cover. From this classification, it is found that the accuracy ranges from 40% for class 7 (secondary forest) to 88% for class 10 (water bodies). The mean overall classification accuracy obtained was 61%. Among them, water bodies showed the highest accuracy since only 12 pixels were confused with peat and freshwater swamp forest. However, secondary forest gave the lowest accuracy because it was confused with rubber, mixed horticulture crop and peat swamp forest.

Allocation of Potential Urban Forest Landscaping Site

The potential site for the urban forest landscaping map was produced after digitizing and overlaying the soil series, land cover and topographical map *(Figs. 5a-5c)*. Sites indicating most, moderate and least potential were finally mapped

TABLE 3
Analysis of confusion matrix for 10 classes of land covers

Referred Data	Total Number of Pixels										Total Pixel	Accuracy (%)
	1	2	3	4	5	6	7	8	9	10		
1	472	-	20	-	67	101	-	9	-	-	669	70
2	-	106	24	232	-	-	-	14	2	-	378	61
3	7	11	201	76	-	-	-	-	72	-	367	54
4	122	-	-	328	6	-	-	-	-	-	456	71
5	-	-	-	-	237	2	101	98	-	-	438	54
6	203	-	78	-	8	587	2	-	-	-	878	66
7	10	-	-	-	52	7	76	43	-	-	188	40
8	-	-	-	-	17	-	-	32	-	-	49	65
9	-	-	-	-	18	-	-	-	98	-	116	84
10	12	-	-	-	-	-	2	-	-	112	126	88
TOTAL	826	117	323	636	405	697	196	196	172	112	3665	

1 - Peat and freshwater swamp forest
2 - Urban and associated area
3 - Grassland/shrub
4 - Cleared land
5 - Rubber
6 - Oil palm
7 - Secondary forest
8 - Mixed horticulture
9 - Bush
10 - Water bodies

Mean overall accuracy (%):

$$\frac{472 + 106 + 201 + 328 + 237 + 587 + 76 + 32 + 98 + 112}{3665}$$

= 61%

as illustrated in *Fig. 6.* The most potential site for urban forest landscaping, which was indicted in green has the least score range (6-12) with the fine loamy to moderate soil and with the existence of various natural resources such as river, pond, forest, rubber tree and oil palm plantation. Moderately potential site with a score of 14-17 (yellow color) was mainly focused at the south and northwest of KLIA center and small patches in the north. These gentle slope (9%-15%) sites are appropriate for a 'moderate landscape' area due to the presence of secondary forest, rubber tree and oil palm plantation. Least potential sites, which were indicated in purple, are located at the west of KLIA because the soil is poor with least availability of natural resources. In addition, the area was a little bit far away (about 2 km) from KLIA center.

The Planning and Development of Urban Forest Landscaping in KLIA

The landscape concept at KLIA and its surroundings has been designed to be an airport within a 'forest'. In addition, better planning could be achieved with satellite imagery for urban forestry landscape concept surrounding KLIA. Based on this study, there are still lots of potential for such planning and development in the KLIA vicinity. There is still plenty of 'green cover' in the KLIA surrounding with suitable soil if forest planting needs to be carried out. The gently sloping to rolling terrain features of the forest landscape around KLIA should provide a better 'green cover' with a great scenic view to the tourists upon arrival at the KLIA.

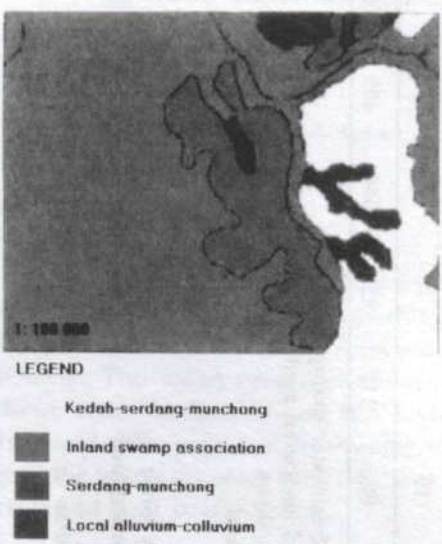

Fig. 5a: Soil series map of KLIA and its vicinity

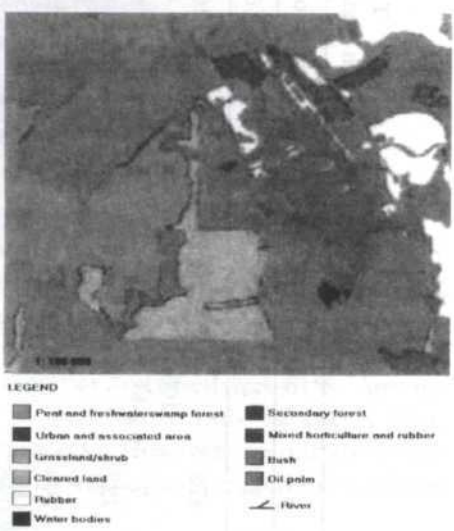

Fig. 5b: Land cover map of KLIA and its vicinity

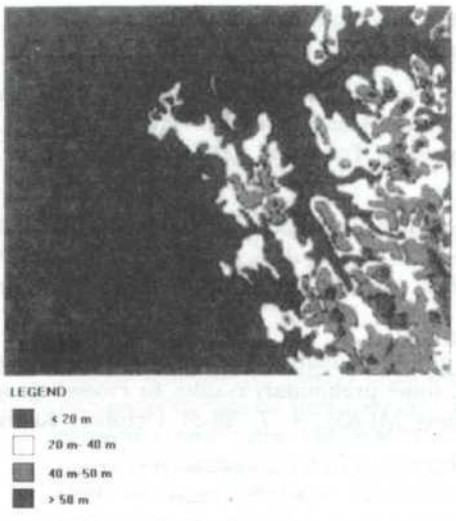

Fig. 5c: Topographical map of KLIA and its vicinity

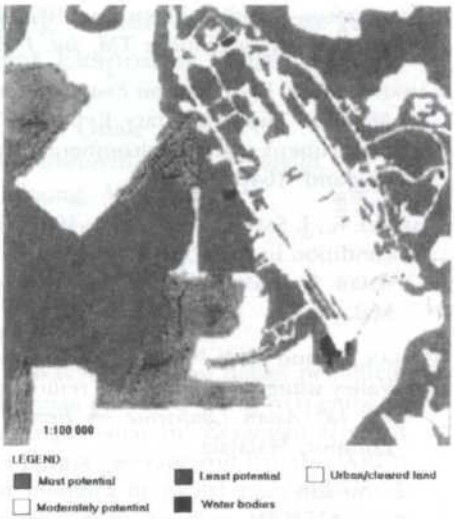

Fig. 6: The urban forest landscape potential map for KLIA

CONCLUSION

Several conclusions can be derived from this study as follows:

1. Integration of remote sensing and GIS technique is a powerful tool for generating base map in order to identify the potential areas for landscape purposes at KLIA and its surroundings.
2. Landsat TM with false color composite (FCC) of band 4-5-3 (R-G-B) using a PCI software processing system has the capability to classify the different 'green cover' types in KLI and surrounding areas with an accuracy of 61%.
3. Supporting information such as soil series, land cover and topographical maps are very useful to aid identification and allocation of potential site for urban forest landscaping.
4. In order to provide a detailed and better landscape planning, additional information such as meteorological and geological data are important to support the GIS to map the potential landscape area using remotely sensed data.

REFERENCES

ANONYMOUS. 1991. *Satellite Remote Sensing.* p.17. ISRO headquarter, Bangalore, India.

ANONYMOUS. 1995. *National Landscape Guideline.* 181p. Dept. of Urban and Countryside Planning, Peninsular Malaysia, Kuala Lumpur.

HONDA, K., S. LERTHUM and S. MURAI. 1997. Forest monitoring framework at regional level using multi-resolution satellite data with combination of optical and thermal bands. In *Proceedings of the 18th Asian Conference on Remote Sensing (ACRS)*, p. 9, 20-24 October, Kuala Lumpur, Malaysia.

KAMARUZAMAN, J. and H. HASZULINA. 1996. Forest recreation planning in Langkawi Island, Malaysia using Landsat TM. *Int. J. Remote Sensing* **17(18)**: 3599-3613.

LAWRENCE, C. J. 1978. *Terrain Evaluation in West Malaysia-Part 2: Land System of Sounthwest Malaysia.* Supplementary Report 378. Transport and Road Research Laboratory, Department of the Environment, Department of Transport, Crowthorne, Berkshire, England. 164p.

MAKOTO, K., J. SAVATH and T. YUJI. 1997. Comparison of urbanization and environmental condition in Asian cities using satellite remote sensing data. In *Proceedings of the 18th Asian Conference on Remote Sensing (ACRS)*, p. 6, 20-24 October, Kuala Lumpur Malaysia.

MAZLAN, H. and M. Y. NORHAN. 1997. Change detection analysis of urban forest in Klang Valley using multi-temporal remote data: some preliminary results. In *Proceedings of the 18th Asian Conference on Remote Sensing (ACRS)*, p. 7, 20-24 October, Kuala Lumpur, Malaysia.

ISSN: 0128-7680
Pertanika J. Sci. & Technol. 12(1): 33 - 43 (2004) © Universiti Putra Malaysia Press

Pengiraan Persentil Taburan Panjang Larian bagi Carta Kawalan Purata Bergerak Berpemberat Eksponen Multivariat

[1]B.C. Khoo & [2]S.H. Quah
Pusat Pengajian Sains Matematik, Universiti Sains Malaysia, 11800 USM, Pulau Pinang, Malaysia
E-mel: [1]mkbc@usm.my & [2]shquah@cs.usm.my

Diterima: 16 Januari 2001

ABSTRAK

Prabhu dan Runger (1997) telah mengemukakan cadangan dalam pemilihan parameter-parameter untuk skema carta kawalan purata bergerak berpemberat eksponen multivariat (MEWMA). Walau bagaimanapun, cadangan tersebut hanya berdasarkan prestasi panjang larian purata (average run length – ARL). Oleh itu, dalam makalah ini, kami akan mengira nilai-nilai persentil untuk taburan panjang larian bagi pelbagai skema carta kawalan MEWMA yang dikemukakan oleh Prabhu dan Runger (1997). Persentil-persentil yang dikira akan membekalkan maklumat tambahan seperti kekerapan isyarat luar kawalan palsu yang awal (early false out of control signals), panjang larian median (median run length – MRL) dan kepencongan taburan panjang larian untuk sesuatu skema tertentu. Maklumat-maklumat tambahan ini mungkin berguna dalam membekalkan jurutera kawalan mutu pengetahuan mendalam dan lengkap tentang sesuatu skema carta kawalan MEWMA yang dipilih berdasarkan cadangan Prabhu dan Runger (1997).

ABSTRACT

Prabhu and Runger (1997) provided recommendations for the selection of parameters of the MEWMA control chart schemes. However, the recommendations are only based on the average run length (ARL) performance. Therefore, in this work, we will compute the percentiles of the run length distribution for the various MEWMA control chart schemes of Prabhu and Runger (1997). The computed percentiles will provide extra information such as the frequency of early false out-of-control signals, the median run length (MRL) and the skewness of the run length distribution of a particular scheme. This extra information may be useful in providing quality control engineers with further knowledge of a particular MEWMA control chart scheme selected based on the recommendations of Prabhu and Runger (1997).

Kata kunci: Taburan panjang larian, panjang larian, MEWMA, ARL, MRL, parameter tak memusat

PENGENALAN

Penilaian prestasi skema-skema carta kawalan dengan hanya berdasarkan nilai ARL semakin menerima kritikan meluas. Sebaliknya, penggunaan nilai-nilai persentil untuk taburan panjang larian kian digalakkan (Barnard 1959; Bissell 1969; Klein 1996). Dalam Bahagian 4, kami akan membincangkan penggunaan nilai-nilai persentil untuk taburan panjang larian termasuk MRL sebagai

tambahan kepada ARL dalam penilaian prestasi skema carta kawalan MEWMA. Nilai-nilai persentil yang berlainan untuk semua skema carta kawalan MEWMA telah dikira dengan menggunakan SAS, versi 6.12.

CARTA KAWALAN MEWMA

Biarkan X_1, X_2, ..., X_t, ..., sebagai turutan cerapan-cerapan multivariat yang tertabur secara secaman dan tak bersandar (i.i.d.) antara satu sama lain dengan taburan normal multivariat N_p (μ_X, Σ_X) di mana μ_X dan Σ_X ialah masing-masing vektor min dan matriks kovarians untuk turutan vektor X. Statistik-statistik untuk carta kawalan MEWMA diberikan dalam persamaan berikut (Prabhu dan Runger 1997):

$$W_t = rX_t + (1\text{-}r)W_{t-1} \tag{1}$$

Untuk persamaan (1) di atas, W_0 ialah vektor sifar dengan dimensi-p dan r ($0 < r \leq 1$) merupakan parameter yang mengawal magnitud pelicinan. Carta kawalan MEWMA memberikan isyarat luar kawalan jika

$$Q_t = W_t' \Sigma_W^{-1} W_t > H \tag{2}$$

iaitu $H > 0$ merupakan had kawalan atas yang dipilih untuk memberikan nilai ARL dalam kawalan (ARL_0) yang diingini. Dalam kajian simulasi untuk mengira nilai-nilai persentil untuk taburan panjang larian bagi skema carta kawalan MEWMA, kami telah menggunakan nilai asimptot bagi matriks kovarians seperti berikut:

$$\Sigma_W = \left(\frac{r}{2-r}\right)\Sigma_X \tag{3}$$

PENGIRAAN NILAI-NILAI PERSENTIL

Lowry, Woodall, Champ dan Rigdon (1992) serta Montgomery (2001) telah menunjukkan bahawa prestasi carta kawalan MEWMA bergantung kepada μ hanya melalui punca kuasa dua nilai parameter tak memusat (noncentrality parameter),

$$\lambda^2 = (\mu - \mu_X)' \Sigma_X^{-1} (\mu - \mu_X) \tag{4}$$

iaitu μ_X dan μ ialah masing-masing vektor min yang nominal dan yang berubah untuk turutan cerapan-cerapan multivariat X_1, X_2, ..., X_t, ...,. Untuk kajian simulasi yang dijalankan, dengan SAS, versi 6.12, vektor min nominal yang digunakan ialah vektor sifar, $\mu_X = (0, 0, ..., 0)'$, manakala matriks kovarians yang digunakan ialah matriks identiti, $\Sigma_X = I$, dengan pekali korelasi, $\rho = 0$. Min

vektor di luar sasaran yang dipertimbangkan ialah $\mu = (\delta, 0, \ldots, 0)'$. Oleh sebab prestasi carta MEWMA hanya bergantung pada magnitud perubahan vektor min dari μ_X kepada μ, iaitu λ, maka nilai ρ, μ dan Σ_X yang lain tidak dipertimbangkan. Dalam kajian simulasi yang dijalankan, pelbagai nilai λ yang berlainan dipertimbangkan.

Kami telah mengira nilai-nilai persentil untuk taburan panjang larian bagi skema carta kawalan MEWMA dengan dimensi $p = 2$, 4 dan 10 dan $\lambda = 0.0$, 0.2, 0.5, 1.0, 1.5, 2.0, 2.5 dan 3.0. Nilai-nilai persentil yang dikira termasuk persentil ke-0.1, 1, 5, 10, 20, 30, 40, 50, 60, 70, 80 dan 90. Persentil ke-50 juga dikenali sebagai MRL. Nilai-nilai persentil yang dikira diberikan dalam Jadual 1, 2 dan 3 (sila lihat Lampiran) untuk $p = 2$, 4 dan 10 masing-masing.

PERBINCANGAN

ARL dalam kawalan untuk semua skema carta kawalan MEWMA mempunyai nilai yang serupa iaitu kira-kira 200. Ini dicapai dengan memilih had kawalan atas (H) yang sesuai untuk setiap skema.

Perhatikan bahawa MRL dalam kawalan untuk semua skema carta kawalan MEWMA bagi $p = 2$, 4 dan 10 adalah kurang daripada ARL dalam kawalan masing-masing. Misalnya, untuk $p = 2$ dan $r = 0.2$, MRL dalam kawalan menunjukkan bahawa setengah daripada semua panjang larian (run lengths) adalah kurang daripada atau sama dengan 139 walaupun ARL dalam kawalan memberikan nilai kira-kira 200. Untuk skema tersebut peratusan panjang larian yang kurang daripada atau sama dengan 200 terletak di antara 60 hingga 70 peratus. Sebenarnya, nilai MRL sentiasa kurang daripada nilai ARL bagi semua nilai λ untuk semua skema dalam Jadual 1, 2 dan 3. Walau bagaimanapun, perbezaan di antara MRL dan ARL semakin menyusut apabila nilai λ meningkat. Ini bermakna bahawa kepencongan taburan panjang larian semakin berkurangan apabila nilai λ meningkat. Oleh itu, tafsiran berdasarkan MRL adalah lebih bererti berbanding ARL kerana taburan panjang larian terutamanya untuk nilai-nilai λ yang kecil adalah pencong. Palm (1990) telah menunjukkan bahawa untuk taburan panjang larian yang pencong, median adalah lebih berguna berbanding purata sebagai ukuran memusat.

Pengiraan nilai-nilai persentil untuk taburan panjang larian bagi skema carta kawalan MEWMA juga membolehkan analisis kebarangkalian untuk isyarat luar kawalan palsu yang awal dijalankan sebaik sahaja sesuatu skema dipilih berdasarkan prestasi ARL. Isyarat luar kawalan palsu yang awal merupakan isyarat yang berhubung dengan panjang larian dalam kawalan yang kurang daripada ARL dalam kawalan. Kekerapan berlakunya isyarat luar kawalan palsu yang awal diberikan oleh nilai-nilai persentil dalam kawalan yang kecil. Sebagai contoh, untuk persentil ke-10, nilai panjang larian dengan $\lambda = 0.0$ dan $p = 2$ untuk $r = 0.05$ dan 0.8 ialah masing-masing 33 dan 21. Jelaslah bahawa dari segi isyarat luar kawalan palsu yang awal, skema dengan $r = 0.05$ adalah lebih baik daripada skema dengan $r = 0.8$ sebab nilai persentil ke-10 yang lebih tinggi menunjukkan bahawa kebarangkalian untuk skema dengan $r = 0.05$ memberikan

isyarat luar kawalan palsu yang awal adalah lebih rendah daripada skema dengan $r = 0.8$.

Sekarang pertimbangkan kes untuk persentil ke-5 dengan dimensi $p = 4$ bagi proses yang stabil, iaitu, $\lambda = 0$. Untuk situasi ini, nilai panjang larian semakin menyusut apabila nilai r kian bertambah besar. Misalnya, untuk $r \in \{0.05, 0.1, 0.2, 0.3, 0.4, 0.5, 0.6, 0.8, 1\}$, nilai-nilai panjang larian yang sepadan ialah 24, 18, 14, 14, 13, 13, 12, 11 dan 11 masing-masing, di mana nilai-nilai ini menunjukkan tren yang menurun. Oleh itu, jelaslah bahawa $r = 0.05$ memberikan perlindungan tertinggi terhadap ralat Jenis-I. Sebaliknya, $r = 1$ menyebabkan ralat Jenis-I yang tertinggi. Keputusan yang dipaparkan dalam Jadual 3 untuk dimensi $p = 10$ juga menunjukkan tren yang sama.

Sebenarnya, untuk sesuatu skema yang dipilih adalah diingini agar nilai semua panjang larian dalam kawalan melebihi atau sama dengan ARL dalam kawalan. Disebabkan ini merupakan sesuatu yang mustahil, maka matlamat yang berikutnya adalah supaya panjang larian dalam kawalan yang pendek berada sedekat yang mungkin dengan ARL dalam kawalan. Tujuannya adalah supaya kekerapan berlakunya isyarat luar kawalan palsu yang awal dapat dikurangkan untuk jangka masa yang panjang bagi sesuatu skema yang dipilih.

Skema carta kawalan MEWMA akan menjadi skema carta kawalan χ^2 Hotelling apabila nilai parameter pelicinan $r = 1$. Berdasarkan Jadual 1, 2 dan 3, sungguhpun semua skema mempunyai ARL dalam kawalan yang sama tetapi taburan panjang larian untuk skema carta kawalan MEWMA agak berbeza dengan skema carta kawalan χ^2 Hotelling terutamanya untuk nilai-nilai r yang kecil.

KESIMPULAN

Makalah ini telah menunjukkan kepentingan menggunakan nilai-nilai persentil untuk taburan panjang larian sebagai kriteria tambahan dalam penilaian prestasi sesuatu skema carta kawalan MEWMA yang dipilih berdasarkan prestasi ARL. Antara kepentingan kriteria tambahan ini ialah memberikan maklumat tambahan tentang kebarangkalian sesuatu proses mempunyai panjang larian yang kurang daripada suatu nilai tertentu bagi gabungan nilai λ, r dan p yang berlainan di samping menjelaskan kepada jurutera kawalan kualiti tentang kelemahan ARL dalam penilaian prestasi carta kawalan MEWMA. Makalah ini juga bertujuan untuk menggalakkan jurutera kualiti menggunakan MRL dalam menilai prestasi carta MEWMA dan meyakinkan mereka tentang kelebihan MRL. Satu lagi kepentingan yang perlu dinyatakan ialah kaedah yang dicadangkan membolehkan analisis kebarangkalian isyarat luar kawalan palsu yang awal dijalankan untuk suatu skema carta MEWMA yang dipilih. Perbincangan tambahan tentang penggunaan nilai-nilai persentil dalam penilaian prestasi carta-carta kawalan diberikan oleh Barnard (1959), Bissell (1969) dan Klein (1996).

RUJUKAN

BARNARD, G. A. 1959. Control charts and stochastic processes. *Journal of the Royal Statistical Society* **21(B):** 239–271.

BISSELL, A. F. 1969. CUSUM techniques for quality control. *Applied Statistics* **18:** 1–30.

KLEIN, M. 1996. Composite Shewhart-EWMA statistical control schemes. *IIE Transactions* **28:** 475–481.

LOWRY, C. A., W. H. WOODALL, C. W. CHAMP and S. E. RIGDON. 1992. Multivariate exponentially weighted moving average control chart. *Technometrics* **34:** 46–53.

MONTGOMERY, D. C. 2001. *Introduction to Statistical Quality Control.* 4th ed. New York: John Wiley & Sons.

PALM, A. C. 1990. Tables of run length percentiles for determining the sensitivity of shewhart control charts for averages with supplementary runs rules. *Journal of Quality Technology* **22:** 289–298.

PRABHU, S. S. and G. C. RUNGER. 1997. Designing a multivariate EWMA control chart. *Journal of Quality Technology* **29(1):** 8–15.

LAMPIRAN

JADUAL 1

ARL dan nilai-nilai persentil untuk taburan panjang larian bagi skema-skema carta kawalan MEWMA dengan $p = 2$

λ	r	H	ARL	0.001	0.01	0.05	0.1	0.2	0.3	0.4	0.5	0.6	0.7	0.8	0.9
0.0	0.05	7.37	200.19	8	13	23	33	55	80	109	144	183	238	312	446.5
	0.10	8.64	200.17	5	8	17	28	51	76	105	141	185	239.5	321	454.5
	0.20	9.64	200.36	3	6	15	25	48	74	105	139	183	241	321	459
	0.30	10.08	199.78	2	5	13	24	48	74	104	140	184	242	318	456
	0.40	10.33	200.48	2	4	13	24	47	73	103	138	184	240	318	454
	0.50	10.45	200.23	2	4	12	23	46	74	105	140	184	239.5	318	455
	0.60	10.53	200.03	1	3	12	22.5	46	74	105	141	183	239	320	453
	0.80	10.57	199.66	1	3	11	21	44	71	102	138	181	239.5	320	460
	1.00	10.61	199.89	1	3	11	22	45	70	101	139	184	242	326	458
0.2	0.05	7.37	85.52	7	10	16	21	31	41	52	65	80	101	130	176
	0.10	8.64	98.44	4	7	13	18	29	42	56	72	92	117	153	211
	0.20	9.64	118.11	3	5	11	16	30	45	63	84	109	143	186	265
	0.30	10.08	133.24	2	4	10	17	32	50	71	95	123	160	212	301
	0.40	10.33	147.29	2	3	10	17	35	55	78	104	133	176	236	334.5
	0.50	10.45	154.34	2	3	10	18	36	57	81	108	140	184	250	353.5
	0.60	10.53	161.84	1	3	10	18	38	59	84	114	147	192	261	372
	0.80	10.57	169.38	1	3	9	18	38	61	89	119	156	203	276	388
	1.00	10.61	180.38	1	2	9	19	39	63	92	125	166	218	293	412
0.5	0.05	7.37	26.76	5	7	10	12	14	17	20	23	27	31	37	47
	0.10	8.64	27.99	4	5	8	9	13	16	19	23	27	33	40	53
	0.20	9.64	34.65	2	4	6	8	12	16	21	26	33	41	53	73
	0.30	10.08	43.72	2	3	6	8	13	18	24	32	41	52	69	96
	0.40	10.33	53.56	2	3	5	8	14	21	29	38	49	65	86	120
	0.50	10.45	63.96	1	2	5	9	16	24	34	46	59	77	103	144
	0.60	10.53	74.33	1	2	5	9	18	28	40	54	69	89	119	165
	0.80	10.57	94.38	1	2	5	11	22	35	50	67	87	115	149	216
	1.00	10.61	116.16	1	2	6	12	26	42	60	81	106	140	187	267
1.0	0.05	7.37	11.30	4	5	6	7	8	9	10	11	12	13	14	17
	0.10	8.64	10.21	3	4	5	5	6	7	8	9	10	12	13	16
	0.20	9.64	10.28	2	3	4	4	5	6	7	9	10	12	14	18
	0.30	10.08	11.36	2	2	3	4	5	6	8	9	11	13	17	22
	0.40	10.33	13.27	1	2	3	4	5	7	8	10	13	16	20	27
	0.50	10.45	15.77	1	2	3	3	5	7	9	12	15	19	24	34
	0.60	10.53	19.12	1	1	2.5	4	6	8	11	14	18	23	30	42
	0.80	10.57	28.13	1	1	2	4	7	11	15	20	26	34	45	64
	1.00	10.61	42.06	1	1	3	5	10	15	21	29	39	51	68	96

Jadual 1 - *Sambungan*

λ	r	H	ARL	0.001	0.01	0.05	0.1	0.2	0.3	0.4	0.5	0.6	0.7	0.8	0.9
1.5	0.05	7.37	7.16	3	4	4	5	5	6	6	7	7	8	9	10
	0.10	8.64	6.10	2	3	3	4	4	5	5	6	6	7	8	9
	0.20	9.64	5.49	2	2	3	3	4	4	4	5	6	6	7	9
	0.30	10.08	5.48	1	2	2	3	3	4	4	5	5	6	7	9
	0.40	10.33	5.77	1	1	2	2	3	4	4	5	6	7	8	10
	0.50	10.45	6.38	1	1	2	2	3	4	4	5	6	7	9	12
	0.60	10.53	7.22	1	1	2	2	3	4	5	6	7	8	11	15
	0.80	10.57	10.21	1	1	1	2	3	4	6	7	9	12	16	22
	1.00	10.61	15.81	1	1	1	2	4	6	8	11	15	19	26	36
2.0	0.05	7.37	5.29	3	3	4	4	4	5	5	5	5	6	6	7
	0.10	8.64	4.42	2	2	3	3	3	4	4	4	5	5	5	6
	0.20	9.64	3.76	1	2	2	2	3	3	3	4	4	4	5	5
	0.30	10.08	3.54	1	1	2	2	2	3	3	3	4	4	5	5
	0.40	10.33	3.53	1	1	2	2	2	2	3	3	4	4	5	6
	0.50	10.45	3.60	1	1	1	2	2	2	3	3	4	4	5	6
	0.60	10.53	3.83	1	1	1	2	2	2	3	3	4	4	5	7
	0.80	10.57	4.69	1	1	1	1	2	2	3	4	4	5	7	10
	1.00	10.61	6.85	1	1	1	1	2	3	4	5	6	8	11	15
2.5	0.05	7.37	4.23	2	3	3	3	3	4	4	4	4	5	5	5
	0.10	8.64	3.50	2	2	2	3	3	3	3	3	4	4	4	5
	0.20	9.64	2.92	1	2	2	2	2	2	3	3	3	3	4	4
	0.30	10.08	2.67	1	1	2	2	2	2	2	2	3	3	3	4
	0.40	10.33	2.56	1	1	1	2	2	2	2	2	3	3	3	4
	0.50	10.45	2.50	1	1	1	1	2	2	2	2	2.5	3	3	4
	0.60	10.53	2.51	1	1	1	1	2	2	2	2	2	3	3	4
	0.80	10.57	2.75	1	1	1	1	1	2	2	2	3	3	4	5
	1.00	10.61	3.51	1	1	1	1	1	2	2	3	3	4	5	7
3.0	0.05	7.37	3.55	2	2	3	3	3	3	3	3	4	4	4	4
	0.10	8.64	2.92	2	2	2	2	2	3	3	3	3	3	3	4
	0.20	9.64	2.41	1	1	2	2	2	2	2	2	2	3	3	3
	0.30	10.08	2.19	1	1	1	2	2	2	2	2	2	2	3	3
	0.40	10.33	2.05	1	1	1	1	2	2	2	2	2	2	2	3
	0.50	10.45	1.95	1	1	1	1	1	2	2	2	2	2	2	3
	0.60	10.53	1.90	1	1	1	1	1	1	2	2	2	2	2	3
	0.80	10.57	1.90	1	1	1	1	1	1	1	2	2	2	3	3
	1.00	10.61	2.14	1	1	1	1	1	1	1	2	2	2	3	4

JADUAL 2
ARL dan nilai-nilai persentil untuk taburan panjang larian bagi skema-skema carta kawalan MEWMA dengan $p = 4$

λ	r	H	ARL	0.001	0.01	0.05	0.1	0.2	0.3	0.4	0.5	0.6	0.7	0.8	0.9
0.0	0.05	11.26	199.85	9	14	24	35	56	81	109	144	184	237	311	439
	0.10	12.79	200.10	6	9	18	28	51	77	106	140	183	238	318	447
	0.20	13.89	200.24	4	6	14	25	48	74.5	104	139	183	243	322.5	460
	0.30	14.35	199.85	3	5	14	25	47	73	103	140	183	244	322.5	457
	0.40	14.59	199.99	2	4	13	24	48	75	105	140	183	241	320	461
	0.50	14.71	199.89	2	4	13	24	47	74	106	140	183	240	319	459.5
	0.60	14.80	199.89	1	4	12	23	48	74	105	140	185	241	319	459
	0.80	14.85	200.05	1	3	11	22	47	74	105	142	186	243	321	453
	1.00	14.86	200.74	1	2	11	22	47	73.5	103	139	183.5	239	323	459
0.2	0.05	11.26	100.96	8.5	12	19	25	36	48	61	76	93	118	152	212
	0.10	12.79	117.56	5	8.5	14	21	34	48	65	85	108	139	184	258
	0.20	13.89	139.38	3	5	11	19	35	52	73	97	126	165	224	318
	0.30	14.35	153.81	3	5	11	18	36	57	80	109	140	186	247	349
	0.40	14.59	164.87	2	4	11	19	39	61	86	117	151	198	261	373
	0.50	14.71	169.87	1	4	11	20	40	63	89	121	155	204	269	387
	0.60	14.80	176.30	1	3	11	20	41	65.5	92	124	162	214	283	399
	0.80	14.85	184.82	1	3	10.5	21	42	67	95	129	173	224	294	421
	1.00	14.86	189.68	1	2	11	21	43	69	97	133	174	228	302	433.5
0.5	0.05	11.26	32.14	7	9	12	14	18	21	24	28	32	37	44	56
	0.10	12.79	35.12	5	6	9	11	16	19	23	28	34	41	51	68
	0.20	13.89	46.17	3	4	7	10	15	20	27	34	43	55	71	98
	0.30	14.35	59.04	2	4	7	10	17	24	32	42	54	70	92	129
	0.40	14.59	72.89	2	3	6	10	19	28	39	51	67	88	115	164
	0.50	14.71	85.93	1	3	7	11	21	32	45	60	79	103	136	195
	0.60	14.80	97.71	1	3	7	12	23	36	50	67	89	117	155	224
	0.80	14.85	119.58	1	2	7	14	27	43	62	84	110	144	192	274
	1.00	14.86	139.94	1	2	8	15	32	51	73	98	129	170	225	320
1.0	0.05	11.26	13.49	5	6	7	8	10	11	12	13	14	15	17	20
	0.10	12.79	12.23	3	4	6	7	8	9	10	11	12	14	16	20
	0.20	13.89	12.67	2	3	4	5	7	8	9	11	12	15	18	23
	0.30	14.35	14.72	2	3	4	5	6	8	10	12	14	17	22	29
	0.40	14.59	17.99	2	2	3	4	6	8	11	14	17	21	27	38
	0.50	14.71	22.20	1	2	3	4	7	9	13	16	20	26	34	48
	0.60	14.80	28.06	1	2	3	5	8	11	15	20	26	33	44	63
	0.80	14.85	42.61	1	1	3	6	11	16	23	30	40	51	67	96
	1.00	14.86	61.67	1	1	4	7	15	22	32	42	56	74	99	142

Jadual 2 - *Sambungan*

λ	r	H	ARL	0.001	0.01	0.05	0.1	0.2	0.3	0.4	0.5	0.6	0.7	0.8	0.9
1.5	0.05	11.26	8.57	4	5	5	6	7	7	8	8	9	9	10	12
	0.10	12.79	7.26	3	3	4	5	5	6	6	7	7	8	9	10
	0.20	13.89	6.57	2	2	3	4	4	5	5	6	7	7	9	10
	0.30	14.35	6.68	2	2	3	3	4	4	5	6	7	8	9	11
	0.40	14.59	7.33	1	2	2	3	4	4	5	6	7	8	10	14
	0.50	14.71	8.38	1	2	2	3	4	4	5	7	8	10	12	16
	0.60	14.80	10.11	1	1	2	3	4	5	6	8	9	12	15	21
	0.80	14.85	15.18	1	1	2	3	4	6	8	11	14	18	24	34
	1.00	14.86	24.49	1	1	2	3	6	9	13	17	23	30	39	55
2.0	0.05	11.26	6.33	3	4	4	5	5	6	6	6	7	7	7	8
	0.10	12.79	5.21	2	3	3	4	4	4	5	5	5	6	6	7
	0.20	13.89	4.43	2	2	3	3	3	3	4	4	4	5	6	6
	0.30	14.35	4.20	1	2	2	2	3	3	3	4	4	5	5	6
	0.40	14.59	4.24	1	1	2	2	3	3	3	4	4	5	6	7
	0.50	14.71	4.50	1	1	2	2	2	3	3	4	4	5	6	8
	0.60	14.80	4.95	1	1	2	2	2	3	3	4	5	6	7	9
	0.80	14.85	6.73	1	1	1	2	2	3	4	5	6	8	10	14
	1.00	14.86	10.60	1	1	1	2	3	4	6	8	10	13	17	24
2.5	0.05	11.26	5.06	3	3	4	4	4	4	5	5	5	5	6	6
	0.10	12.79	4.11	2	2	3	3	3	4	4	4	4	4	5	5
	0.20	13.89	3.38	2	2	2	2	3	3	3	3	3	4	4	5
	0.30	14.35	3.11	1	2	2	2	2	2	3	3	3	3	4	4
	0.40	14.59	3.00	1	1	2	2	2	2	2	3	3	3	4	5
	0.50	14.71	2.99	1	1	1	2	2	2	2	3	3	3	4	5
	0.60	14.80	3.09	1	1	1	1	2	2	2	3	3	3	4	5
	0.80	14.85	3.67	1	1	1	1	2	2	2	3	3	4	5	7
	1.00	14.86	5.26	1	1	1	1	2	2	3	4	5	6	8	11
3.0	0.05	11.26	4.24	3	3	3	3	4	4	4	4	4	5	5	5
	0.10	12.79	3.42	2	2	2	3	3	3	3	3	4	4	4	4
	0.20	13.89	2.77	1	2	2	2	2	2	3	3	3	3	3	4
	0.30	14.35	2.49	1	1	2	2	2	2	2	2	3	3	3	3
	0.40	14.59	2.34	1	1	1	2	2	2	2	2	2	3	3	3
	0.50	14.71	2.26	1	1	1	1	2	2	2	2	2	3	3	3
	0.60	14.80	2.22	1	1	1	1	1	2	2	2	2	3	3	4
	0.80	14.85	2.34	1	1	1	1	1	1	2	2	2	3	3	4
	1.00	14.86	2.94	1	1	1	1	1	1	2	2	3	3	4	6

JADUAL 3
ARL dan nilai-nilai persentil untuk taburan panjang larian bagi skema-skema carta kawalan MEWMA dengan $p = 10$

λ	r	H	ARL	0.001	0.01	0.05	0.1	0.2	0.3	0.4	0.5	0.6	0.7	0.8	0.9
0.0	0.05	20.72	200.45	11.5	17	28	39	61	85	113	145	185	239	308	436
	0.10	22.68	200.27	7	11	20	31	54	81	107	141	183	238	317	453
	0.20	24.06	200.27	4	7	15	25.5	50	77	106	140	183	239	320	458
	0.30	24.57	199.84	3	6	14	25	49	75	105	139	181	238	320	465
	0.40	24.87	199.74	2	5	13	24	47	74	104	139	181	240	320	464.5
	0.50	25.03	200.25	2	4	12	23	45	72	103	140	183	241	319	464
	0.60	25.11	200.13	1	4	12	22	44	71	103	139	183	241	317.5	462.5
	0.80	25.18	199.76	1	3	11	21	44	69	100	137	181	237	320	460
	1.00	25.20	200.20	1	3	11	22	45.5	71	101	138	182	238	318	461
0.2	0.05	20.72	123.00	11	16	24	30	45	59	75	94	115	144	184	257
	0.10	22.68	139.78	6	10	18	25	41	58	78	101	130	164	218	305
	0.20	24.06	161.39	4	7	13	22	42	63	86	113	147	191	256	369
	0.30	24.57	169.64	3	5	12	22	42	64	89	118	154	204	272	385.5
	0.40	24.87	176.99	2	4	11	21	41	65	91.5	123	160	211	283.5	412
	0.50	25.03	182.90	2	4	11	21	41	67	94	127	167	218	292	422
	0.60	25.11	186.32	1.5	3	10	21	41	66	95	129	170	222	299	431
	0.80	25.18	189.41	1	3	10	20	41	66	95	130	173	226	303	437
	1.00	25.20	193.40	1	3	11	21	44	69	99	135	177	233	310	443
0.5	0.05	20.72	42.62	9	12	16	19	23	27	32	36	42	49	58	75
	0.10	22.68	48.72	6	8	12	15	20	26	31	38	46	57	72	97
	0.20	24.06	67.68	3.5	6	9	13	20	28	38	49	63	81	105	148
	0.30	24.57	85.25	3	4	8	13	22	33	46	61	79	102	135	188
	0.40	24.87	101.45	2	4	8	13	25	37	53	71	93	122	161	230
	0.50	25.03	114.27	2	3	8	14	27	41	59	80	105	137	181	258
	0.60	25.11	126.24	1	3	8	14	28	45	65	87	115	152	201	289
	0.80	25.18	146.74	1	2	8	16	33	52	75	101	134	175	235	340
	1.00	25.20	161.95	1	2	9	17	36	58	84	113.5	147	192	259	380
1.0	0.05	20.72	17.52	6.5	8	10	11	13	14	15	16	18	20	22	25
	0.10	22.68	16.08	4	6	7	9	10	11	13	14	16	18	21	26
	0.20	24.06	18.00	3	4	5	7	9	10.5	12	15	17	21	26	34
	0.30	24.57	22.65	2	3	5	6	8	11	14	17	22	27	34	46
	0.40	24.87	29.11	2	3	4	6	9	12	16	21	27	35	45	62
	0.50	25.03	37.33	2	2	4	6	10	15	20	26	34	44	58	83
	0.60	25.11	46.75	1	2	4	6	12	18	25	33	42	56	74.5	106
	0.80	25.18	68.77	1	2	5	8	16	25	35	48	63	83	110	155
	1.00	25.20	92.53	1	1	5	10.5	21	34	48	65	86	111	149	211

Jadual 3 - *Sambungan*

λ	r	H	ARL	0.001	0.01	0.05	0.1	0.2	0.3	0.4	0.5	0.6	0.7	0.8	0.9
1.5	0.05	20.72	11.08	5	6	7	8	9	9	10	11	11	12	13	15
	0.10	22.68	9.28	4	4.5	5	6	7	7	8	9	9	10	12	13
	0.20	24.06	8.62	2	3	4	5	5	6	7	8	9	10	11	14
	0.30	24.57	9.31	2	3	3	4	5	6	7	8	9	11	13	17
	0.40	24.87	10.89	2	2	3	4	5	6	7	9	10	13	16	21
	0.50	25.03	13.47	1	2	3	4	5	6	8	10	13	16	20	28
	0.60	25.11	17.15	1	2	3	4	5	7	10	12	16	20	27	37
	0.80	25.18	27.83	1	1	2	4	7	10	15	20	25	33	44	63
	1.00	25.20	44.75	1	1	3	5	10	16	23	31	41	54	72	104
2.0	0.05	20.72	8.17	5	5	6	6	7	7	8	8	8	9	9	10
	0.10	22.68	6.58	3	4	4	5	5	6	6	6	7	7	8	9
	0.20	24.06	5.58	2	3	3	3	4	4	5	5	6	6	7	8
	0.30	24.57	5.44	2	2	3	3	3	4	4	5	5	6	7	9
	0.40	24.87	5.75	1	2	2	3	3	4	4	5	6	7	8	10
	0.50	25.03	6.49	1	2	2	3	3	4	5	5	6	7	9	12
	0.60	25.11	7.65	1	1	2	2	3	4	5	6	7	9	11	15
	0.80	25.18	11.94	1	1	2	2	4	5	7	9	11	14	18	26
	1.00	25.20	20.55	1	1	1	3	5	7	11	14	19	24	33	47
2.5	0.05	20.72	6.52	4	4	5	5	6	6	6	6	7	7	7	8
	0.10	22.68	5.16	3	3	4	4	4	5	5	5	5	6	6	7
	0.20	24.06	4.21	2	2	3	3	3	4	4	4	4	5	5	6
	0.30	24.57	3.89	2	2	2	2	3	3	3	4	4	4	5	6
	0.40	24.87	3.82	1	2	2	2	3	3	3	3	4	4	5	6
	0.50	25.03	3.99	1	1	2	2	2	3	3	3	4	5	5	7
	0.60	25.11	4.35	1	1	2	2	2	3	3	4	4	5	6	8
	0.80	25.18	5.99	1	1	1	2	2	3	4	5	6	7	9	12
	1.00	25.20	9.93	1	1	1	2	3	4	5	7	9	12	16	22
3.0	0.05	20.72	5.45	3	4	4	4	5	5	5	5	6	6	6	7
	0.10	22.68	4.28	3	3	3	3	4	4	4	4	4	5	5	5
	0.20	24.06	3.41	2	2	2	2	3	3	3	3	3	4	4	4
	0.30	24.57	3.06	2	2	2	2	2	3	3	3	3	3	4	4
	0.40	24.87	2.92	1	1	2	2	2	2	3	3	3	3	4	4
	0.50	25.03	2.89	1	1	2	2	2	2	2	3	3	3	4	4
	0.60	25.11	2.96	1	1	1	2	2	2	2	3	3	3	4	5
	0.80	25.18	3.49	1	1	1	1	2	2	2	3	3	4	5	7
	1.00	25.20	5.19	1	1	1	1	2	2	3	4	5	6	8	11

ISSN: 0128-7680
Pertanika J. Sci. & Technol. 12(1): 45 - 50 (2004) © Universiti Putra Malaysia Press

Preliminary Test Estimation in the Rayleigh Distribution Using Minimax Regret Significance Levels

Ayman Baklizi
Department of Statistics
Yarmouk University
Irbid – Jordan
E-mail: baklizi1@hotmail.com

Received: 3 July 2001

ABSTRAK

Memberikan ramalan awal tentang parameter yang tidak diketahui, penganggar ujian awal yang biasa berdasarkan penganggar kebolehjadian maksimum untuk parameter skala Rayleigh dibangunkan. Tahap signifikan optimum berdasarkan kriteria kesal minimaks dan nilai kritikal sepadan diperoleh secara berangka.

ABSTRACT

Given a prior guess of the unknown parameter, the usual preliminary test estimator based on the maximum likelihood estimator for the Rayleigh scale parameter is developed. The optimal significance levels based on the minimax regret criterion and the corresponding critical values are numerically obtained.

Keywords: Maximum likelihood estimator, minimax regret criterion, preliminary test estimator, optimum significance levels, Rayleigh distribution

INTRODUCTION

The Rayleigh distribution has been used in a variety of fields. It is used in life testing and reliability theory to model products with linearly increasing hazard rate. It has applications in the field of acoustics, spatial statistics and random walks (Johnson *et al.* 1994). An account of the history and properties of the distribution is given by Hirano (1986). The probability density function of the Rayliegh distribution is given by (Cohen and Whitten 1988);

$$f(x)=\frac{2^{-(k-1/2)}}{\sigma\Gamma(k/2)}\left(\frac{x}{\sigma}\right)^{(k-1)} e^{-\frac{1}{2}\left(\frac{x}{\sigma}\right)^2} \quad x,\ \sigma>0.\ k \text{ is a known integer.} \qquad (1)$$

where σ is a scale parameter. Various estimation methods for the parameter σ of the Rayleigh distribution have been discussed in the literature. The best linear unbiased estimator (BLUE) has been discussed by various authors (David 1981; Balakrishnan and Cohen 1991; Adatia 1994) among others. Maximum likelihood estimation is discussed in Cohen and Whitten (1988), Lee *et al.* (1980), and Tiku *et al.* (1986). Bayesian estimation is discussed by Sinha and Howlader (1983).

In some applications, the experimenter possesses some knowledge about the parameter σ. This knowledge may be obtained from past experience, or from the aquaintance with similar situations. Thus he is in a position to make an educated guess or prior estimate σ_0. This prior information may be incorporated in the estimation process using a preliminary test estimator (Ohtani and Toyoda 1978; Toyoda and Wallace 1975; Sawa and Hiromatsu 1973), thus improving the estimation process. In this paper we present a preliminary test estimator for the parameter of the Rayleigh distribution . The procedure for obtaining the optimum values of the significance levels using the minimax regret criterion of Brook (1976) is developed in Section 2. The results are given in the final section.

Preliminary Test Estimation

Consider a random sample X_1, ..., X_n from the Rayleigh distribution. The maximum likelihood estimator of σ is given by (Cohen and Whitten 1988) as

$$\hat{\sigma} = \left(\sum_{i=1}^{n} x_i^2 / nk \right)^{1/2}. \tag{2}$$

It can be shown (Cohen and Whitten 1988) that $nk\hat{\sigma}^2/\sigma^2 \sim \chi^2_{nk}$. Assume that σ_0 is a prior guess of σ. Consider testing $H_0 : \sigma = \sigma_0$ against $H_1: \sigma \neq \sigma_0$; the likelihood ratio test rejects H_0 when $\frac{nk\hat{\sigma}^2}{\sigma_0^2} > c_1$ or $\frac{nk\hat{\sigma}^2}{\sigma_0^2} > c_2$. A preliminary test estimator $\tilde{\sigma}$ of σ may be obtained as follows

$$\tilde{\sigma} = \begin{cases} \sigma_0, c_1 < \dfrac{nk\hat{\sigma}^2}{\sigma_0^2} < c_2 \\ \hat{\sigma}, \quad \text{Otherwise} \end{cases} \tag{3}$$

where c_1 and c_2 are such that $p_{\sigma_0}(W < c_1) = p_{\sigma_0}(W > c_2) = \frac{\alpha}{2}$ and $W \sim \chi^2_{nk}$. Our aim is to find the optimum values of α, according to the minimax regret criterion. The mean of $\tilde{\sigma}$ is given by

$$E(\tilde{\sigma}) = \sigma_0 E\left[I\left(\delta_1 < \frac{nk\hat{\sigma}^2}{\sigma^2} \right) \right] + E\left[\hat{\sigma} \left\{ 1 - I\left(\delta_1 < \frac{nk\hat{\sigma}^2}{\sigma^2} < \delta_2 \right) \right\} \right], \tag{4}$$

where $\delta_1 = \frac{c_1\sigma_0^2}{\sigma^2}, \delta_2 = \frac{c_2\sigma_0^2}{\sigma^2}$ and $I(.)$ is the indicator function. Notice that $nk\hat{\sigma}^2/\sigma^2 \sim \chi^2_{nk}$, so that

$$E\left[I\left(\delta_1 < \frac{nk\hat{\sigma}^2}{\sigma^2} < \delta^2\right)\right] = p\left(\delta_1 < \frac{nk\hat{\sigma}^2}{\sigma^2} < \delta_2\right) = \int_{\delta_1}^{\delta_2} g(w)dw$$ where $g(w)$ is the pdf of a chi-squared random variable with degrees of freedom, also

$$E\left[\hat{\sigma}\left\{1 - I\left(\delta_1 < \frac{nk\hat{\sigma}^2}{\sigma^2} < \delta_2\right)\right\}\right] E(\hat{\sigma}) - E\left(\hat{\sigma} I\left(\delta_1 < \frac{nk\hat{\sigma}^2}{\sigma^2} < \delta_2\right)\right).$$

Now, $E(\hat{\sigma}) = \frac{\sigma}{\sqrt{nk}} E\left(\frac{\sqrt{nk\hat{\sigma}}}{\sigma}\right) = \frac{\sigma}{\sqrt{nk}} E\left(\sqrt{W}\right) = \frac{\sigma}{k}\sqrt{2}\frac{\Gamma(nk+1/2)}{\Gamma(nk/2)}$.

And so $E\left(\hat{\sigma} I\left(\delta_1 < \frac{nk\hat{\sigma}^2}{\sigma^2} < \delta_2\right)\right) = \frac{\sigma}{\sqrt{nk}} E\left(\frac{\sqrt{nk}\hat{\sigma}}{\sigma} I\left(\delta_1 < \frac{nk\hat{\sigma}^2}{\sigma^2} < \delta_2\right)\right)$

$$= \frac{\sigma}{\sqrt{np}} E\left(\sqrt{W}\, I(\delta_1 < W < \delta_2)\right) = \frac{\sigma}{\sqrt{np}} \int_{\delta_1}^{\delta_2} \sqrt{w} g(w)dw.$$

Thus

$$E(\hat{\sigma}) = \sigma_0 \int_{\delta_1}^{\delta_2} g(w)dw + \frac{\sigma}{\sqrt{nk}}\sqrt{2}\frac{\Gamma(nk+1/2)}{\Gamma(nk/2)} - \frac{\sigma}{\sqrt{nk}} \int_{\delta_1}^{\delta_2} \sqrt{w} g(w)dw. \quad (5)$$

Similarly the second moment of $\tilde{\sigma}$ is given by

$$E(\tilde{\sigma}^2) = \sigma_0^2 \int_{\delta_1}^{\delta_2} g(w)dw + \sigma^2 - \frac{\sigma^2}{nk} \int_{\delta_1}^{\delta_2} w g(w)dw \quad (6)$$

The mean squared error of $\tilde{\sigma}$ is given by

$MSE(\tilde{\sigma}) = E(\tilde{\sigma}^2) - (E(\tilde{\sigma}))^2 + (E(\tilde{\sigma}) - \sigma)^2 = E(\tilde{\sigma}^2) - 2\sigma E(\tilde{\sigma}) + \sigma^2$

Thus

$$MSE(\tilde{\sigma}) = \sigma_0^2 \int_{\delta_1}^{\delta_2} g(w)dw + \sigma^2 - \frac{\sigma^2}{nk} \int_{\delta_1}^{\delta_2} w g(w)dw -$$

$$2\sigma\left(\sigma_0 \int_{\delta_1}^{\delta_2} g(w)dw + \frac{\sigma}{\sqrt{nk}}\sqrt{2}\frac{\Gamma(nk+1/2)}{\Gamma(nk/2)} - \frac{\sigma}{\sqrt{nk}} \int_{\delta_1}^{\delta_2} \sqrt{w} g(w)dw\right) + \sigma^2 \quad (7)$$

Now, the quantity $\frac{MSE(\sigma)}{\sigma^2}$ can be considered as a risk function. Let $\psi = \frac{\sigma_0}{\sigma}$ and notice that $\delta_1 = \frac{c_1\sigma_0^2}{\sigma^2}$ and $\delta_2 = \frac{c_2\sigma_0^2}{\sigma^2}$ we get

$$RIS(\psi,\alpha) = \psi^2 \int_{c_1\psi^2}^{c_2\psi^2} g(w)dw + 1 - \frac{1}{np}\int_{c_1\psi_2}^{c_2\psi^2} wg(w)dw -$$

$$2\left(\psi \int_{c_1\psi^2}^{c_2\psi^2} g(w)dw + \frac{1}{k}\sqrt{2}\,\frac{\Gamma(nk+1/2)}{\Gamma nk/2} - \frac{1}{\sqrt{nk}}\int_{c_1\psi^2}^{c_2\psi^2}\sqrt{w}g(w)dw\right) + 1. \qquad (8)$$

Notice that the risk function depends on through which are determined such that $p_{\sigma_0}(W < c_1) = p_{\sigma_0}(W > c_2) = \frac{\alpha}{2}$, where $W \sim c^2_{nk}$.

If $\psi \to 0$ or ∞, then $RIS(\psi, \alpha)$ tends to $RIS(\psi,1)$ which is the risk of the maximum likelihood estimator $\hat{\sigma}$. Chiou (1988) gives us the general shapes of $RIS(\psi, \alpha)$. An optimal value of α is $\alpha = 1$ if $\psi \le \psi_1$ or $\psi \ge \psi_2$ and $\alpha = 0$ otherwise, where ψ_1 and ψ_2 are the intersections of $RIS(\psi, \alpha) = (\psi - 1)^2$ with $RIS(\psi,1) = 2\left(1 - \sqrt{\frac{2}{np}}\,\frac{\Gamma(nk+1/2)}{\Gamma(nk/2)}\right)$.

The points of intersection are $\psi_1 = 1 - (2(1 - (2/nk)^{1/2}(\Gamma(nk + 1/2)/\Gamma(nk/2))$ and $\psi_2 = 1 + (2(1 - (2/nk)^{1/2}(\Gamma(nk + 1/2)/\Gamma(nk/2))$. Since ψ is unknown we seek an optimal value $\alpha = \alpha^*$ which gives a reasonable risk for all values of α. Going along the lines of Sawa and Hiromatsu (1973), the regret function is $REG(\psi,\alpha) = RIS(\psi,\alpha) - \inf_{\alpha} RIS(\psi,\alpha)$, where

$$\inf_{\alpha} RIS(\psi,\alpha) = \begin{cases} RIS(\psi,1), & \psi \le \psi_1 \text{ or } \psi \ge \psi_2 \\ RIS(\psi,0), & \text{otherwise.} \end{cases} \qquad (9)$$

For $\psi \le \psi_2$ $REG(\psi,\alpha)$ takes a maximum value at $\psi_{l'}$. For $\psi > \psi_2$, takes a maximum value at $\psi_{l'}$ (Chiou 1988). Thus the minimax regret criterion determines α^* such that $REG(\psi_{l'},\alpha^*) = REG(\psi_{l'},\alpha^*)$. $REG(\psi_{l'},\alpha^*) = REG(\psi_{l'},\alpha^*)$ A preliminary test estimator for σ that uses the minimax regret significance levels now can be defined as

$$\tilde{\sigma} = \begin{cases} \sigma_0, & c_1 < \frac{nk\hat{\sigma}^2}{\sigma_0^2} < c_2 \\ \hat{\sigma}, & \text{otherwise.} \end{cases} \qquad (10)$$

where c_1 and c_2 are such that $p_{\sigma_0}(W < c_1) = p_{\sigma_0}(W > c_2) = \frac{\alpha^*}{2}$ where $W \sim \chi^2_{nk}$.

RESULTS

We found numerically the optimum significance levels α^* and the corresponding critical values for n=2,3,...,15, and k = 1,2,3. The results are given in Table 1. To illustrate the use of the results in this table assume, for example, that the sp. Rayleigh distribution from which the data came has (k=2) and the sample size is n=10. Using the results in the table, the preliminary test estimator for σ (with prior estimate σ_0) is

$$\tilde{\sigma} = \begin{cases} \sigma_0, & 13.247 < \dfrac{2\sum_{i=1}^{n} x_i^2}{\sigma_0^2} < 27.065 \\ \left(\sum_{i=1}^{n} x_i^2 / 2n\right)^{1/2} & \text{Otherwise.} \end{cases}$$

TABLE 1
Optimum significance levels and the corresponding critical values

	k=1			k=2			k=3		
n	α^*	c_1	c_2	α^*	c_1	c_2	α^*	c_1	c_2
2	0.568	0.669	2.516	0.426	1.722	5.817	0.369	2.946	8.812
4	0.426	1.166	4.218	0.337	2.946	8.812	0.301	4.964	13.000
3	0.478	1.722	5.817	0.369	4.273	11.633	0.325	7.118	16.981
5	0.393	2.318	7.342	0.316	5.670	14.345	0.285	9.364	20.833
6	0.369	2.946	8.812	0.301	7.118	16.981	0.273	11.676	24.595
7	0.351	3.600	10.239	0.289	8.607	19.561	0.264	14.040	28.290
8	0.337	4.273	11.633	0.280	10.128	22.096	0.257	16.445	31.933
9	0.325	4.964	13.000	0.273	11.676	24.596	0.252	18.885	35.535
10	0.316	5.670	14.345	0.267	13.247	27.065	0.247	21.353	39.101
11	0.308	6.389	15.671	0.262	14.837	29.510	0.243	23.847	42.638
12	0.301	7.118	16.981	0.257	16.445	31.933	0.240	26.362	46.149
13	0.295	7.858	18.277	0.253	18.068	34.338	0.237	28.896	49.639
14	0.289	8.606	19.561	0.250	19.705	36.727	0.234	31.448	53.109
15	0.285	9.364	20.833	0.247	21.353	39.101	0.231	34.014	56.562

ACKNOWLEDGEMENTS

The author is thankful to the editor and the referees for their constructive comments and suggestions that improved the paper.

REFERENCES

ADATIA, A. 1994. Best linear unbiased estimator of the Rayleigh scale parameter based on fairly large censored samples. *IEEE Trans. on Reliability.*

BALAKRISHNAN, N. and A. C. COHEN. 1991. *Order Statistics and Inference: Estimation Methods.* San Diego: Academic Press.

BROOK, R. J. 1976. On the use of a regret function to set significance points in prior tests of estimation. *J. Amer. Statistical Assoc.* **71:** 26–131.

CHIOU, P. 1988. Shrinkage estimation of scale parameter of the extreme value distribution. *IEEE Trans. Reliability* **37(4):** 370–374.

CHIOU, P. and C. P. HAN. 1989. Shrinkage estimation of threshold parameter of the exponential distribution. *IEEE Trans. Reliability* **38(4):** 449–453.

COHEN, A. C. and B. J. WHITTEN. 1988. *Parameter Estimation in Reliability and Life Span Models.* Marcel Dekker: New York.

DAVID, H. A. 1981. *Order Statistics.* Second edition. New York: Wiley.

HIRANO, K. 1986. Rayleigh distribution. In *Encyclopedia of Statistical Sciences,* ed. S. Kotz, N.L. Johnson and C.B. Read, **7:** 647-649. New York: Wiley.

JOHNSON, N. L., S. KOTZ and BALAKRISHNAN. 1994. *Continuous Univariate Distributions.* **1**. New York: Wiley.

OHTANI, K. and T. TOYODA. 1978. Minimax regret critical values for a preliminary test in pooling variances. *J. Japan Statistical Soc.* **8:** 15-20.

SAWA, H. and T. HIROMATSU. 1973. Minimax regret significance points for a preliminary test in regression analysis. *Econometrica* **41:** 1093–1101.

SINHA, S. K. and H. A. HOWLADER. 1983. Credible and HPD intervals of the parameter and reliability of Rayleigh distribution. *IEEE Trans. on Reliability* **32:** 217-220.

TIKU, M.L., W.Y. TAN and N. BALAKRISHNAN. 1986. *Robust Inference.* New York: Marcel Dekker.

TOYODA, T. and D. WALLACE. 1975. Estimation of variance after a preliminary test of homogeneity and optimum levels of significance for the pre-test. *J. Econometrics* **3:** 395–404.

ISSN: 0128-7680
Pertanika J. Sci. & Technol. 12(1): 51 - 67 (2004) © Universiti Putra Malaysia Press

Improving the Quality of Solutions by Automated Database Design Systems with the Provision of Real World Knowledge – An Evaluation

[1]Shahrul Azman Noah & [2]Michael Williams

[1]Faculty of Information Science and Technology, National University of Malaysia, 43600 UKM, Bangi, Selangor, Malaysia
E-mail: samn@ftsm.ukm.my

[2]School of Computing, University of Glamorgan, Pontypridd, CF3 1DL, UK
E-mail: m.d.william@swansea.ac.uk

Received: 20 September 2001

ABSTRAK

Sistem pengautomasian reka bentuk pangkalan data berkemampuan untuk membantu pereka bentuk dalam proses analisis dan reka bentuk sebuah sistem pangkalan data. Walau bagaimanapun, kemampuan sistem seumpama ini menjanakan model yang berkualiti setanding dengan pakar pangkalan data masih lagi menjadi persoalan. Sehubungan dengan itu, beberapa sistem yang bukan sahaja berpengetahuan dalam proses reka bentuk pangkalan data tetapi juga berkemampuan untuk menggunakan pengetahuan tentang dunia sebenar telah dibangunkan. Sungguhpun begitu, penggunaan pengetahuan dunia sebenar dikatakan mampu untuk meningkatkan kualiti model pangkalan data, satu kajian tentang keberkesanan kaedah ini masih lagi belum dilakukan. Kertas kerja ini membincangkan penilaian tiga pendekatan dalam perwakilan pengetahaun yang dicadangkan untuk pengetahuan dunia sebenar iaitu *dictionary, thesaurus,* dan *knowledge reconciliation.* Hasil kajian menunjukkan bahawa sistem yang dilengkapkan dengan pengetahuan dunia sebenar mampu menjanakan model reka bentuk yang lebih berkualiti berbanding sistem yang tidak dilengkapkan dengan pengetahuan dunia sebenar. Walau bagaimanapun, bagi sistem yang dilengkapkan dengan pengetahuan sebenar untuk mencapai kualiti reka bentuk yang setanding dengan reka bentuk yang dihasilkan oleh pakar pereka bentuk pangkalan data masih lagi belum terjawab melalui kajian ini.

ABSTRACT

Automated database design systems have the capability of assisting human designers in the process of database analysis and design. However, the capacity of these systems to produce quality solutions which are similar to expert human designers remains largely unresolved. Therefore, in recent years there have been a number of attempts to develop systems that are not only "knowledgeable" about database design process but also have the capability of exploiting knowledge of the real world. Although such use of real world knowledge was claimed capable of increasing the quality of design models, there is currently little, if any, formal evaluation that this claim has taken place. This paper presents such an evaluation of three existing approaches proposed to facilitate system-storage and exploitation of real world knowledge; the dictionary approach, the thesaurus approach, and the knowledge reconciliation approach. Results obtained have indicated that some of the approaches under examination in

this study are capable of producing higher quality design models compared to when no such knowledge is in use. However, the ability of such representations of real world knowledge to achieve the standard quality of human generated design models remains unanswered.

Keywords: Database design, automated database design, system evaluation, artificial intelligence

INTRODUCTION

Automated database design systems are mainly concerned in assisting novice human designers in producing high quality of data models (Vessey and Sravanapudi 1995). This aspect was claimed to be achieved from the capability of such systems to provide intelligent assistance in the form of advice, suggesting alternative solutions, helping to investigate the consequences of design decisions, and maintaining the availability of the design knowledge by providing information should a decision be questioned or require explanation in retrospect (Lloyd-Williams 1994). However, it was realised that expert human designers contribute far more than database design expertise to the design process (Storey *et al.* 1993). Expert human designers, even when working in an unfamiliar domain, are able to make use of their knowledge of the real world in order to interact with users, make helpful suggestions and inferences, and identify potential errors and inconsistencies (Storey 1992; Storey and Goldstein 1993). This situation has resulted in numerous calls for the representation of real world knowledge within such systems, coupled with the ability to reason with and make use of this knowledge.

Although it has been claimed that the use and exploitation of real world knowledge is capable of improving the quality of designs produced by an automated database design system, little or no attention has been directed to provide decisive evidence regarding this claim. This fundamental issue has not yet been fully explored possibly due to the lack of a rigorous and unified framework and methodology in providing such evidence. This paper presents the testing and evaluation of three approaches proposed to facilitate the system-storage and exploitation of real world knowledge; the dictionary approach (Kawaguchi *et al.* 1986), the thesaurus approach (Lloyd-Williams 1994, 1997), and the knowledge reconciliation approach (Storey *et al.* 1993; Storey *et al.* 1997), the intention being to initiate the gathering of evidence to support the claim previously stated or otherwise.

This paper is organised into the following topics. In the next section we provide a brief overview of the existing approaches to representing real-world knowledge. We then discuss the research methodology employed in this evaluative experiment, and present the results of our empirical investigation. Finally we present the conclusions that may be drawn from our work.

Brief Overview of Existing Approaches to Representing Real-World Knowledge

The following provides a brief overview of the methods of knowledge representation employed by the dictionary, thesaurus and knowledge reconciliation approaches. Those interested in detailed discussions of each approach, along with the claimed benefits associated with their use, are referred to the relevant source literature (Lloyd-Williams 1994; Storey *et al.* 1993; Kawaguchi *et al.* 1986).

The dictionary approach to representing and exploiting real-world knowledge by an automated database design system is illustrated by the Intelligent Interview System (I^2S) of Kawaguchi *et al.* (1986). The I^2S approach organises the encapsulated real-world knowledge into a series of domain specific dictionaries, each dictionary comprising verb information with both past and present forms of each verb being presented. During a design session, I^2S makes use of the dictionary in an attempt to "interview" the user, extracting a series of simple queries that the eventual database will be expected to satisfy. These queries are analysed by the system and used in the generation of a logical structure representing the target database.

The thesaurus approach is illustrated by the Object Design Assistant (ODA) system of Lloyd-Williams (1993). Knowledge is represented within the thesaurus structure by making use of series of concepts and associated synonyms, linked together via abstraction mechanisms, categorised according to those recognised by the system (aggregation, association and generalisation). During a design session, the ODA system attempts to make use of the thesaurus in order to obviate the need to ask what may be viewed as being trivial questions of the user.

The knowledge reconciliation approach is illustrated by the Common Sense Business Reasoner (CSBR) system of Storey *et al.* (1993, 1997). The approach is similar to the thesaurus in that it organises domain knowledge into a collection of domain specific concepts and relationships between these concepts. Synonyms, however, are not represented by this approach. During a design session the system attempts to reason with this knowledge in order to reconcile it with the user-specified application domain, the intention being to provide the user with meaningful suggestions of concepts and relationships missing from the evolving database design, and to augment the contents of the domain knowledge after the completion of each design session.

MATERIAL AND METHODS

In order to conduct the evaluative experiments on the use of the dictionary, thesaurus and knowledge reconciliation approaches, a prototype automated database design system, the *Intelligent Object Analyser* (IOA), was developed. IOA provides support for the conceptual design of databases. As IOA was used as a research vehicle to this study, it has the capability of operating in four different modes; either using real-world knowledge provided by the thesaurus, dictionary or knowledge reconciliation approaches (throughout this paper, processing

associated with these approaches are respectively referred to as the thesaurus mode, the dictionary mode and the knowledge reconciliation mode) or without the use of real-world knowledge (basic mode). In each real-world knowledge assisted modes of processing, the information provided is exploited throughout the design process wherever possible in order to improve the completeness and consistency of the evolving design model. A brief outline of the method and process employed by the system is discussed in the following subsection to facilitate the understanding on how the real-world knowledge may be represented and exploited during design processing.

The Intelligent Object Analyser

As illustrated in *Fig.1*, the structure of IOA comprises three main components: the user interface, the inference engine and the knowledge bases, plus a plugable component, consisting of real world knowledge structures respectively represented using the dictionary, thesaurus and knowledge reconciliation approaches.

The *user interface* is a medium for communication between the user and the IOA. The IOA system employs an interactive window system interface which includes the use of pull down menus and a natural language interface. The system contains multiple menus for controlling a design session, viewing an evolving design model and saving and loading a design model.

The inference engine of the IOA system acts as a controller that controls the interaction between the user and the system. It directs any part of the user input to the correct processor for processing and decides which rules to trigger. The domain selection engine, which is part of the inference engine, is used to control the use of selected domain representation structures. The domain selection engine was specifically incorporated in IOA to assist during the course of testing and evaluation of the three approaches in representing real world knowledge structures.

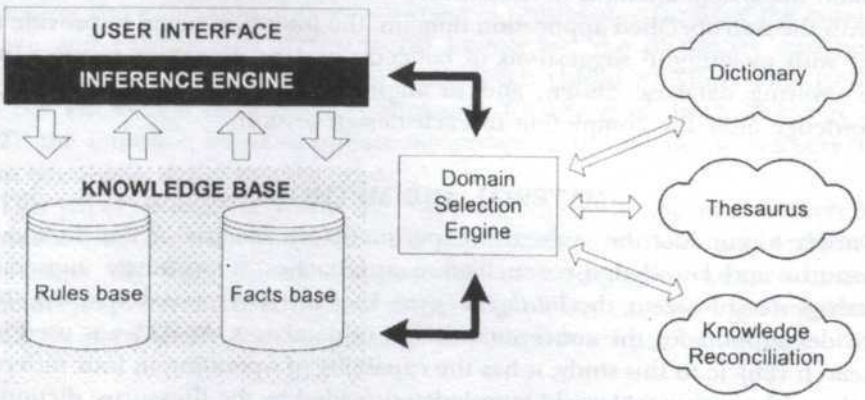

Fig. 1: The IOA architecture

The IOA knowledge-base contains a mixture of rules and facts. Rules correspond to knowledge of how to perform the design task (the order in which design activities take place), detecting and resolving ambiguities, redundancies and inconsistencies within an evolving design, and handling the gradual augmentation of an evolving design as a design session progresses. Facts are used to represent two views of the application domain; an initial representation (the problem domain model) as provided by the user, and the object-oriented design generated from this initial representation. During a design session, IOA follows a two-step procedure.

- The first step involves creating an initial representation of the application domain (known as the problem domain model) and the subsequent refinement of this model.
- The second step involves the refinement of the problem domain model by detecting and resolving any inconsistencies that may exist, and the transformation of the model into object-oriented form.

The first stage of processing requires a set of declarative statements that describe the application domain to be submitted to IOA. These statements are a variation of the method of interactive schema specification described by Baldiserra *et al.* (1979), being based upon the binary model described by Bracchi *et al.* (1976). Each statement links together two concepts (taking the form *A verb-phrase B*), and falls into one of three classes of construct, corresponding directly to the structural abstractions of association, generalization, and aggregation. The statements are used to construct a problem domain model representing the application domain. Once constructed, IOA attempts to confirm its *understanding* of the semantic aspects of the problem domain model; that is, whether each structure within the model represents generalization, aggregation or association.

Once constructed, the problem domain model is submitted to a series of refinement procedures in order to detect and resolve any inconsistencies (such as redundancies that may be present within generalization hierarchies) that may exist. These procedures are performed both with and without the requirement of user input (sometimes referred to as *external* and *internal* validation respectively). Once such inconsistencies have been resolved, IOA makes use of the problem domain model in order to generate a conceptual model.

Although the basic approach represented by the IOA is seen capable of producing reliable design solutions, there are avenues whereby relying on the basic approach alone fails to produce high quality design solutions. For example, the basic approach is incapable of providing suggestions to the user of any important elements found missing from the design model since the system does not have any forms of domain knowledge. The IOA system's inability to identify inconsistencies arises as a result of synonyms and verbs represented by different forms of tenses. Therefore, the provision of real world knowledge as represented by the thesaurus, dictionary and knowledge

reconciliation approaches is seen by many as one of the solutions to overcome this ineffectiveness. It is however beyond the scope of this paper to discuss the technical details of how such representations are being exploited within the IOA system. Interested readers may want to refer to the following articles for further details (Noah and Lloyd-Williams 1998a; 1998b; Noah and Williams 2000; 2001). For instance Noah & Lloyd-Williams (1998a) have discussed in detail the potentiality of the dictionary approach to improve the quality of design solutions particularly within the aspects of design consistency. Noah and Williams (2000 and 2001), on the other hand, have discussed in great detail the exploration of the thesaurus and the knowledge reconciliation approaches in improving the performance of automated database design systems.

Testing and Evaluation Framework

The testing and evaluation framework designed for this study consists of the following aspects.

- Setting up the performance-related criteria, and particularly the accepted level of performance, i.e. the level of performance that the system must perform or produce.
- Conducting the testing activity involving the generation and execution of a series of test cases in various modes of system processing under a prototype automated database design system.
- Analysing the observed results produced from the execution of test cases in (2), in order to assess the achievement of the accepted performance level previously set up in (1).

The aforementioned framework is now being discussed.

Setting up an Accepted Level of System's Performance

In any artificial intelligence (AI) based systems, the performance is usually judged from the ability of the systems to perform at levels equivalent to human expertise or any simulated models (such as the regression model) (Moody and Shanks 1994). For example, diagnosis made by an expert cardiac diagnostic system should be similar or comparable to the diagnosis made by a cardiologist. Therefore in the case of this study, the model produced as an output by an automated database design system should be comparable to the quality of design models produced by human experts.

Although elements that relate to the quality of data models have always been a subjective issue, many researchers agree that they can be judged from the aspects of completeness and consistency. This indication was derived from the opinions of (Moody and Shanks 1994; Kesh 1995; Teuw and Van Den Berg 1997; Moody 1998) that a good quality conceptual model must be complete and consistent (free from any redundancy and inconsistency). According to Moody (1998) completeness relates to whether a data model contains all information required to meet user requirements. If a model is incomplete, the resulting database system will not satisfy users. Consistency, on the other hand,

refers to whether a data model contains any forms of redundancies and incorrectness in data modelling conforming to a set of rules. Inconsistent models may result in the database system being developed containing redundant information, and aspects of information anomalies.

In this study, as our intention was to ascertain whether the use and exploitation of real world knowledge make a significant contribution towards enhancing the quality of designs solution, the acceptable level of performance being set-up are twofold. The design solutions provided by the knowledge-assisted modes of processing should be: 1) comparable and equivalent to those of human design solutions (either actual or simulated); and 2) of higher quality as compared to those design solutions produced when no such knowledge was in use.

In the case where actual human outputs are not easily available, simulated human output can be used (O'Keefe and O'Leary 1993).

Testing Activity

This stage involved generating a representative set of test cases and the subsequent execution of these test cases. These intentionally synthesised test cases were generated from a set of design problems which were primarily extracted from the available literature. The advantage is that the accompanying solution could be used as a benchmark and compared to the system-suggested solution in order to confirm the appropriateness or otherwise of the designs produced. Although actual test cases are ideal sources in performing this test, such test cases that guaranteed to expose all the aspects required under the prescribed input domain considered in this study are very difficult to find (Chandrasekaran 1983). As a result, intentionally synthesised test cases are generally acceptable (O'Keefe and O'Leary 1993).

To assess whether the use and exploitation of the dictionary, thesaurus and knowledge reconciliation approaches can achieve the required performance level previously described in terms of its completeness and consistency, two types of tests have been implemented. The first test involved the generation and execution of a set of test cases with varying degrees of complexity (Test A), whereas the second test involved the execution of a set of test cases with a different number and combination of type of errors (Test B).

In Test A, each of the initial design problems (extracted from the available literature) was systematically altered by dividing them into multiple test cases with varying degrees of complexity as illustrated in *Fig. 2.* The intention is to assess whether the information and reasoning associated with the use of real-world knowledge are capable of increasing the completeness (measured in terms of the number of missing elements) of the designs produced up to an acceptable performance range specified.

During the execution of these test cases, in certain instances the user may be provided with a number of suggestive design elements which were previously detected by IOA as being missing from the test case. The decision for the inclusion of such design elements refers to the example design problem used

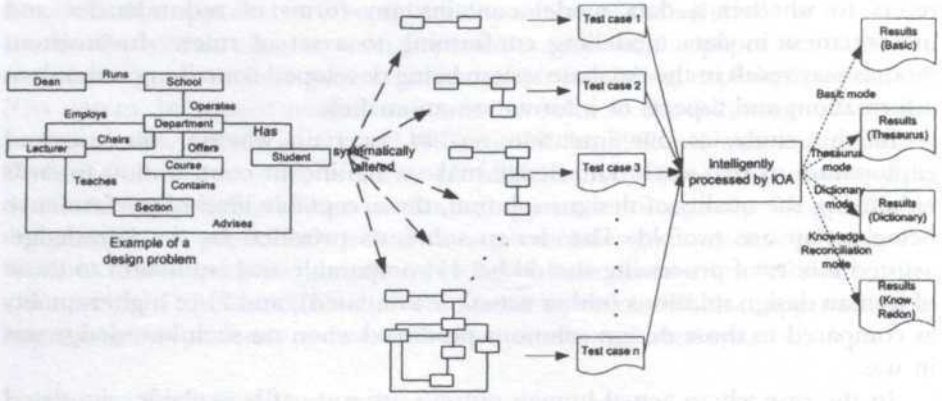

Fig. 2: Approach in case testing of Test A

to generate the test case. The suggested missing design elements are only included in the evolving design model if it is also represented by the design problem in use.

As previously mentioned, Test B involved the generation and execution of a series of test cases with a combination of different types and numbers of synthesised errors. The purpose is to evaluate whether designing using the real-world knowledge-assisted modes of processing are capable of increasing the consistency in the designs produced (measured in terms of the number of errors introduced of the final design output) within the performance range specified. As illustrated in *Fig. 3*, the approach taken firstly requires the production of a number of synthesised errors. The errors introduced included synonymous concept(s), synonymous or related relationship(s) and a combination of both. Secondly, each of these synthesised errors and combination of them were then systematically embedded into the corresponding design problem to generate the set of test cases.

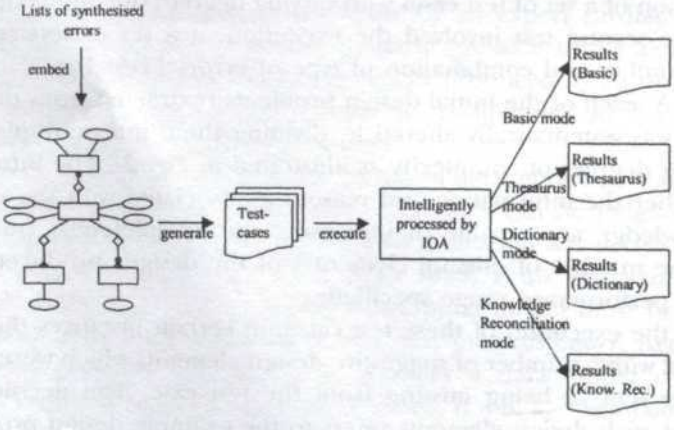

Fig. 3: Approach in case testing of Test B

As illustrated in *Figs. 2* and *3*, both sets of test cases were then executed within the four modes of processing (basic, dictionary, thesaurus and knowledge reconciliation). Results produced from the execution of the dictionary, thesaurus and knowledge reconciliation modes are compared to the solutions provided by the design problem in use and are also compared to those results produced when no such knowledge was in use. As human expert outputs are not easily available, this study assumed that the accompanying solutions associated with each design problem in use act as the human expert solutions. This paper refers to these type of solutions as human-simulated solutions.

Analysis of the Observed Results

As completeness and consistency defined in this study are measured in terms of the number of required missing design elements and the number of errors introduced within the designs output, respectively, the quantitative method of analysis was employed. In this evaluation, the hypothetical test with a 5% significance level was used to compare the differences between the real-world knowledge-assisted modes of processing solutions with those of human-simulated solutions and the basic mode processing solutions.

Although there are several recommended statistical methods available to test such hypotheses, the paired t-test method is highly appropriate in such circumstances as those prevailing in this study (O'Keefe and O'Leary 1993; O'Keefe *et al.* 1987). The paired t-test method is a form of *repeated measures design*, where the same variable (observed criterion) is measured on several occasions (processing modes) for each subject (test case).

RESULTS AND DISCUSSION

The results presented here emanate from a series of tests performed on university domain problem found in the general literature (Rob and Rob 1993; Batini *et al.* 1992; Bowers 1993; Elmasri and Navathe 1989). A total of 24 and 84 test cases were generated from these initial problems for Test A and Test B respectively. The real-world knowledge structure (thesaurus, dictionary and knowledge reconciliation) used was constructed as the result of a series of interviews with researchers, the results of the interviews being integrated in order to form a single representative of the domain. This was a deliberate attempt to minimise any bias that might be introduced by taking the content of the test material into account. It is not claimed that these representations portray the definitive knowledge of the university domain, but it does provide an illustration of the way in which such knowledge may be stored and exploited by an automated database design system. Examples of fragments of the real world knowledge structure constructed according to the three approaches are illustrated in Appendix A.

Completeness (Test A)

The main purpose in this test is to assess whether the real-world knowledge-assisted solutions are comparable (similar) to the expected solutions provided by human designers; and better (improved) to the solutions provided when processing using the basic approach. The hypotheses for these tests are:

H_1: the output produced from the exploitation of the thesaurus, dictionary and knowledge reconciliation approaches are comparable to those of simulated models (there are no significant differences between the two outputs in terms of the number of required missing design elements).

H_1: the output produced from the exploitation of the thesaurus, dictionary and knowledge reconciliation approaches are of higher quality compared to those solutions produced using the basic approach (the output from real-world knowledge assisted modes of processing contains less number of missing design elements compared to the output produced from the basic mode of processing).

The completeness of the design solutions is measured by the number of missing design elements of the design problem in use. This was achieved by comparing the output complexity from the execution of the initial (unaltered) design problem and that from the execution of the generated test-case (altered design problem).

Table 1 illustrates the statistical paired t-test results of this study, whereby n is the degree of freedom, t is the value which is derived from the following equation:

$$t = \frac{d}{S_d / \sqrt{n}}$$

where d is the mean difference, S_d is the standard deviation and n is the degrees of freedom. Using statistical software packages such as the *Statistical Package for Social Science* (SPSS), the values of t and the P value illustrating the probability for accepting the null hypothesis can be obtained. The null hypothesis is rejected and the research hypothesis is accepted if $P <$ significance level (0.05). As the objective of the statistical analysis was to validate whether the approaches taken to representing domain knowledge significantly reduced or increased any of the evaluation criteria, referring to P alone will not provide a sufficient result as it only shows whether there is any significant difference between the observed results. In this case, the value of t can be used (Rees 1995), where a negative t value implies that the observed criterion is significantly reduced by the use of real world knowledge and a positive t value implies otherwise.

As can be seen in Table 1, there have been significant differences between the output produced from the dictionary, thesaurus and knowledge reconciliation approaches compared to those of human-simulated solutions. The corresponding negative t values indicate that exploiting such approaches does not achieve the

required performance level specified in terms of the completeness of the designs produced. In this case, the outputs produced from the real-world knowledge-assisted modes of processing contain a high number of missing design elements as compared to the simulated human output. In other words, the approaches under testing are incapable of suggesting the required missing design elements that will eventually improve the quality of data models (in terms of completeness) as compared to the human simulated models.

The paired t-test results presented in Table 2, however, indicate that, when comparing with the solutions provided using the basic approach, the knowledge reconciliation approach has the capacity of improving the completeness of the designs produced. This conclusion ensued as the result of the significant P value and the corresponding positive t value. The dictionary and thesaurus approaches, however, are incapable of achieving the required performance range specified. In this case, the statistical tests were invalid as the dictionary and thesaurus approaches do not provide suggestions for missing information. Therefore, both approaches result in similar numbers of required missing design elements within the resulting design output.

Consistency (Test B)

In this test, the main concern is to investigate if the solutions provided by the IOA system when using the dictionary, thesaurus and knowledge reconciliation approaches are comparable (similar) to the expected solutions provided by human designers; and better (improved) to the solutions provided when processing using the basic approach. The hypotheses for this test are as follows:

TABLE 1
The paired t-test results between real-world knowledge-assisted solution processing and human simulated solution in terms of completeness

Approaches	*n*	*t*	*P*
Dictionary	23	-5.456	0.000
Thesaurus	23	-5.456	0.000
Knowledge Reconciliation	23	-4.175	0.000

TABLE 2
The paired t-test results between the real-world knowledge-assisted processing solutions and the basic processing solution in terms of completeness

Approaches	*n*	*t*	*P*
Dictionary	N/A	N/A	N/A
Thesaurus	N/A	N/A	N/A
Knowledge Reconciliation	23	6.091	0.000

H_1: the output produced from the exploitation of the thesaurus, dictionary and knowledge reconciliation approaches are comparable to those of simulated models (there are no significant differences between the two outputs in terms of the number of elements of redundancies and inconsistencies).

H_1: the output produced from the exploitation of the thesaurus, dictionary and knowledge reconciliation approaches are of higher quality compared to those solutions produced using the basic approach (the output from real-world knowledge assisted modes of processing contains a lesser number of elements of redundancies and inconsistencies compared to those outputs produced from the basic mode of processing).

Based upon the paired t-test results presented in Table 3, although it is apparent that there are significant differences between the solutions provided by the IOA when using the dictionary, thesaurus and knowledge reconciliation approaches as compared to those of human-simulated solutions; the positive t-values associated with each approach show that the outputs produced from the real world knowledge assisted modes of processing still contain high numbers of redundancies and inconsistencies. Therefore, no real world knowledge-assisted modes of processing are capable of qualifying for the acceptable performance range specified in this study.

The paired t-test results presented in Table 4, on the other hand, suggest that compared to the solutions provided when processing using the basic approach, the solutions provided by IOA when processing using the real world knowledge-assisted modes are more consistent. These conclusions are evidenced by the significant values of P and the corresponding negative t-Values.

TABLE 3
The paired t-test results between real-world knowledge-assisted solutions processing and human simulated solutions in terms of design consistency

Approaches	*n*	*t*	*P*
Dictionary	83	10.674	0.000
Thesaurus	83	8.370	0.000
Knowledge Reconciliation	83	8.433	0.000

TABLE 4
The paired t-test results between the real-world knowledge-assisted processing solutions and the basic processing solution in terms of design consistency

Approaches	*n*	*t*	*P*
Dictionary	83	-4.547	0.000
Thesaurus	83	-9.735	0.000
Knowledge Reconciliation	83	-4.684	0.000

DISCUSSION AND CONCLUSION

Tables 5 and 6 present a summary of conclusions reached for the dictionary, thesaurus and knowledge reconciliation approaches.

TABLE 5
Design completeness – summary

Performance Level	Dictionary	Thesaurus	Knowledge Reconciliation
Solutions are similar to those of human-simulated solutions	No	No	No
Solutions are better than those of basic mode solutions	No	No	Yes

TABLE 6
Design consistency – summary

Performance Level	Dictionary	Thesaurus	Knowledge Reconciliation
Solutions are similar to those of human-simulated solutions	No	No	No
Solutions are better than those of basic mode solutions	Yes	Yes	Yes

Both tables suggest that the possibility of automated database design systems to provide quality solutions similar to those of human experts are far from reach even with the provision of real-world knowledge models. All the approaches proposed to facilitate the use and exploitation of real-world knowledge under investigation in this study are incapable of achieving the required performance range specified neither in the form of design completeness nor design consistency.

However, providing real-world knowledge within automated database design systems at least makes it capable of enhancing the systems' performance compared to when no such knowledge is in use. The knowledge reconciliation approach, for instance, based on its understanding from the reconciliation of knowledge process was seen capable of improving the completeness and consistency of the designs produced compared to the basic approach. Verbs and synonym-related information provided by the dictionaries and the thesaurus-type structure respectively, on the other hand, were seen capable of improving the consistency of the designs output. The incapability of both approaches to increase the completeness of the resulting designs output was due to the fact that both approaches proved incapable of suggesting any missing design element.

Although this evaluation study has produced satisfying results, it is recognised that consideration must be given to a number of practical issues. Firstly, the effectiveness of the system depends greatly on the accuracy and completeness of the system-held real world knowledge, and the results obtained from the testing may be influenced to a certain extent by the variety and coverage of the generated test cases used during the testing.

Secondly, the use and exploitation of the thesaurus, dictionary and knowledge reconciliation approaches to representing real world knowledge rely on the aspects of processing employed by the IOA system, which may be viewed by some as misleading from the original proposal of representation and usage of such approaches. For instance, the VCS system and the I^2S system have dissimilar approaches to design processing as compared with the IOA system. Therefore, the approaches to representing real-world knowledge by both systems might be intended to address other aspects of systems performance criteria and characteristics.

SUMMARY AND IMPLICATIONS FOR FUTURE RESEARCH

This paper has presented the findings of the performance evaluation of the dictionary, thesaurus and knowledge reconciliation approaches to representing and exploiting real world knowledge by an automated database design system. In this evaluation, we specified performance as the quality of solutions provided by the system from exploiting the represented real world knowledge in terms of design completeness and design consistency. We have compared the solutions produced from the real world knowledge modes of processing with the simulated human models (the accompanying solutions of design problem example used) and the solutions from processing using the basic mode.

The results show that although the represented real world knowledge provide significant contribution in enhancing the quality of designs output as compared to the basic mode (particularly within the aspect of design consistency), such representations of real world knowledge are still incapable of meeting the standard quality of human simulated designs output. This may due to the incapability of the automated database design system to cumulatively augment the system-held domain knowledge from one application domain encountered to the next application domain encountered.

Therefore, it is recommended that future research propose a method of how previous design knowledge could be reused for other design sessions. This seems to be a straightforward process. However, a few feasibility studies should be taken into account and the following questions should be answered first (Vanwelkenhuysen 1995):

- How can design knowledge be modified to provide new insights into the problem or to remove undesired contents of the knowledge?
- How should implications of a change in the design knowledge be perceived?
- How can users be persuaded to participate in the augmentation of the design knowledge?

REFERENCES

BALDISERRA, C., S. CERI, G. PELAGATTI and G. BRACCHI. 1979. Interactive specification and formal verification of user's views in database design. In *Proceedings of the 5th International Conference on Very Large Databases*, p. 262-272. Brazil: Rio de Janeiro.

BRACCHI, G., P. PAOLINI and G. PELAGATTI. 1976. Binary logical associations in data modelling. In *Modelling in Data Base Management Systems*, ed. G. M. Nijsen, p. 125-148. Amsterdam: North-Holland.

BATINI, C., S. CERI and S. NAVATHE. 1992. *Conceptual Database Design: An Entity Relationship Approach.* California: Benjamin-Cummings.

BOWERS, D.S. 1993. *From Data to Database.* London: Chapman Hall.

CHANDRASEKARAN, B. 1983. On evaluating AI systems for medical diagnosis. *AI Magazine* **4(2)**: 34-37.

ELMASRI, R. and S.B. NAVATHE. 1989. *Fundamentals of Database Systems.* California: Benjamin Cummings.

KAWAGUCHI, A., N. TAOKA, R. MIZOGUCHI, T. YAMAGUCHI and O. KOKUSHO. 1986. An intelligent interview system for conceptual design of database. In *ECAI '86: The 7th European Conference on Artificial Intelligence*, p. 1-7.

KESH, S. 1995. Evaluating the quality of entity relationship models. *Information and Software Technology* **37(12)**: 681-689.

LLOYD-WILLIAMS, M. 1997. Exploiting domain knowledge during the automated design of object-oriented databases. In *Proceedings of the 16th International Conference on Conceptual Modeling*, ed. D. W. Embley and R. C. Goldstein, p. 16-29.

LLOYD-WILLIAMS, M. 1993. Expert system support for object-oriented database design. *International Journal of Applied Expert Systems* **1(3)**: 197-212.

LLOYD-WILLIAMS, M. 1994. Knowledge-based CASE tools: improving performance using domain specific knowledge. *Software Engineering Journal* **9(4)**: 167-173.

MOODY, D.L. 1998. Metrics for evaluating the quality of entity relationship models. In *Proceedings of the 17th International Conference on Conceptual Modeling*, p. 211-225. Singapore.

MOODY, D. L. and G. G. SHANKS. 1994. What makes a good data model? Evaluating the quality of entity-relationship models. In *Proceedings of the 13th International Conference on the Entity-Relationship Approach*, ed. P. Loucopoulos, p. 94-101.

NOAH, S. A. and M. WILLIAMS. 2000. Exploring and validating the contributions of real-world knowledge to the diagnostic performance of automated database design tools. In *Proceedings of 15th IEEE International Conference on Automated Software Engineering (ASE2000)*, p. 177-186. France: Grenoble.

NOAH, S. A. and M. WILLIAMS. 2001. Reconciliation of knowledge – applications in automated database design diagnosing. *Jurnal Antarabangsa Teknologi Maklumat:* 107-123.

NOAH, S. A. and M. LLOYD-WILLIAMS. 1998a. An evaluation of two approaches to exploiting real-world knowledge by intelligent database design tools. In *Proceedings of the 17th International Conference on Conceptual Modelling*, p. 197-210. Singapore.

NOAH, S. A. and M. LLOYD-WILLIAMS. 1998b. Exploitation of domain knowledge by knowledge-based database design tools: the dictionary approach. In *Proceedings of the 3rd Joint Conference on Knowledge-Based Software Engineering*, p. 250-257. Slovakia: Smolenice.

O'KEEFE, R. M. and A. D. PREECE. 1996. The development, validation and implementation of knowledge-based systems. *European Journal of Operational Research* **92(3)**: 458-473.

O'KEEFE, R. M. and D. E. O'LEARY. 1993. Expert system verification and validation: a survey and tutorial. *Artificial Intelligence Review* **7(1)**: 3-42.

O'KEEFE, R. M., O. BALCI and E. P. SMITH. 1987. Validating expert system performance. *IEEE Expert* **2(4)**: 81-90.

REES, D. G. 1995. *Essential Statistics*. 3rd edition. London: Chapman & Hall.

ROB, P. and C. C. ROB. 1993. *Database Systems: Design, Implementation and Management*. California: Wadsworth Publishing.

STOREY, V. C. 1992. Real world knowledge for databases. *Journal of Database Administration* **3(1)**: 1-19.

STOREY, V. C. and R. C. GOLDSTEIN. 1993. Knowledge-based approach to database design. *Management Information Systems Quarterly* **17(1)**: 25-46.

STOREY, V. C., R. H. L. CHIANG, D. DEY, R. C. GOLDSTEIN, A. SUNDARARAJAN and S. SUNDARESAN. 1997. Database design with common sense reasoning and learning. *ACM Transactions on Database System* **22(4)**: 471-512.

STOREY, V. C., R. C. GOLDSTEIN, R. H. L. CHIANG and D. DEY. 19933. A common-sense reasoning facility based on the entity-relationship model. In *Proceedings of the 12th International Conference on the Entity Relationship Approach*, ed. R. A. Elmasri, V. Kouramajian and B. Thalheim, p. 218-229. Berlin: Springer-Verlag.

TEUW, W.B. and H. VAN DEN BERG. 1997. On the quality of conceptual models. In *Proceedings of the ER'97 Workshop on Behavioural Models and Design Transformations: Issues and Opportunities in Conceptual Modelling*.

VANWELKENHUYSEN, J. 1995. Using DRE to augment generic conceptual design. *IEEE Expert* **10(1)**: 50-56.

VESSEY, I. and A. P. SRAVANAPUDI. 1995. CASE tools as collaborative support technologies. *Communications of the ACM* **37(1)**: 83-102.

APPENDIX A

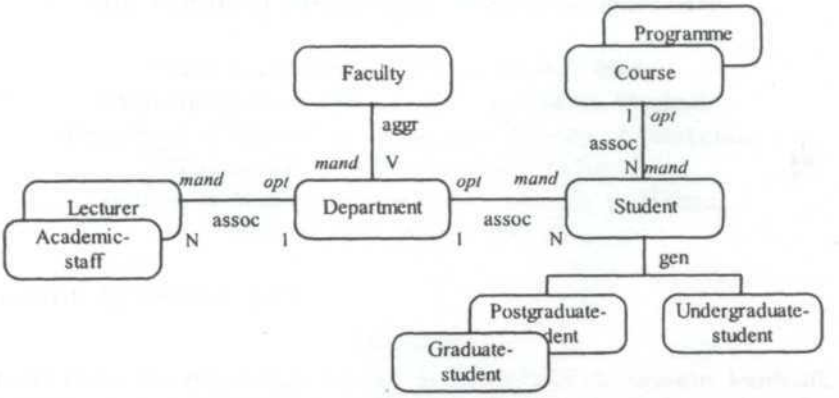

Fragment of real-world knowledge represented as the thesaurus approach

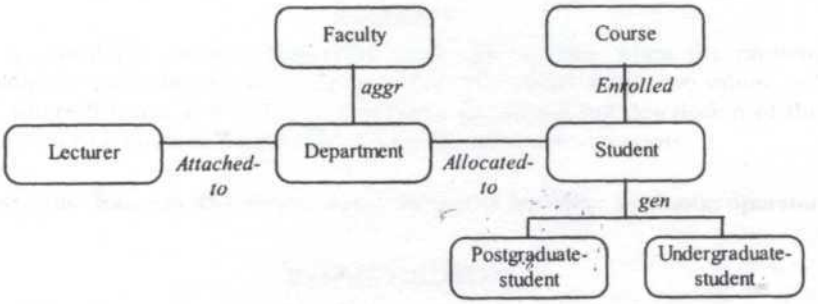

Fragment of real-world knowledge represented as the knowledge reconciliation approach

verb-phrase (enrol, enrolled)
verb-phrase (teach, taught)
verb-phrase (allocate, allocated)
verb-phrase (run, ran)
verb-phrase (supervise, supervised)
. . . . .
. . . . .
. . . . .

Fragment of real-world knowledge represented as the dictionary approach.

ISSN: 0128-7680
Pertanika J. Sci. & Technol. 12(1): 69 - 80 (2004) © Universiti Putra Malaysia Press

Trajectories of Random Quadratic Operators of the Random Mendelian Model of Heredity

[1]Nasir Ganikhodjaev, [2]Noor Hasnah Moin,
[2]Wan Ainun Mior Othman & [2]Nor Aishah Hamzah
[1]Department of Mathematics, National University of Uzbekistan, Vuzgorodok, 700095 Tashkent, Uzbekistan
[2]Institute of Mathematical Sciences, University of Malaya, 50603 Kuala Lumpur, Malaysia

Received: 24 November 2001

ABSTRAK

Model rawak Mendelian bagi keturunan adalah apabila operator kuadratik stokastik yang menakrifkan model ini mengambil dua nilai V_α dan V_β, iaitu $0 \le \alpha \le 1$, $0 \le \beta \le 1$. Kertas ini memberikan keterangan lengkap perilaku trajektori bagi operator kuadratik rawak.

ABSTRACT

It is considered random Mendelian model of heredity, when the random quadratic stochastic operators, which define this model, admit two values and V_β, where $0 \le \alpha \le 1$, $0 \le \beta \le 1$. This paper provides a full description of the behaviour of random trajectories of random quadratic operators.

Keywords: Random Mendelian model, model of heredity, stochastic operator

INTRODUCTION

Genetic Motivation

Before we discuss the mathematics of genetics, we need to acquaint ourselves with some necessary language from biology. A vague, but nevertheless informative definition of a gene is that it is simply a unit of hereditary information. The genetic code of an organism is carried in its chromosomes. Each gene in a chromosome has a different form that it can take. These forms are called alleles. Alleles A of the so-called normal or wild type in a population are most widespread. Any other forms are considered as mutable alleles a. For simplicity, we will assume that there are two forms $\{A,a\}$ of a gene, that is, the mutable allele a is unique.

Let us consider a population of N organisms with a single gene and let N_1 of them have allele A and N_2 of them have allele a, where $N = N_1 + N_2$. Assume that $\frac{N_1}{N} = X_A$ is a fraction of organisms while allele A and $\frac{N_2}{N} = X_a$ is the fraction of the organisms with allele a. Clearly, $X_A \ge 0$, $X_a \ge 0$ and $X_A + X_a = 1$.

Now assume $p_{AA,A}$ is the probability that parents with allele A interbreed to produce organisms with allele A. By simple Mendelian inheritance, we have

$$\begin{aligned} &p_{AA,A}=1 \quad p_{Aa,A}=p_{aA,A}=\frac{1}{2} \quad p_{aa,A}=0 \\ &p_{AA,a}=0 \quad p_{Aa,a}=p_{aA,a}=\frac{1}{2} \quad p_{aa,A}=1 \end{aligned} \tag{1}$$

These numbers are called coefficients of heredity. In random interbreeding (panmixia) the fractions of the organisms with alleles A and a in the next generation are found from the formulae of *complete probability*, i.e. the parent pairs with alleles A and A (respectively A and a, a and a) arise for a fixed state x_A, x_A with probability $x_A x_A = x_A^2$ (respectively $x_A x_a = x_A x_a$ and $x_a x_a = x_a^2$), so

$$\begin{aligned} X_A' &= p_{AA,A}X_A^2 + 2p_{Aa,A}X_A X_a + p_{aa,A}X_a^2 \\ X_a' &= p_{AA,a}X_A^2 + 2p_{Aa,a}X_A X_a + p_{aa,a}X_a^2 \end{aligned} \tag{2}$$

Substituting (1) in (2), we then have

$$\begin{aligned} X_A' &= X_A^2 + X_A X_a = X_A\left(X_A + X_a\right) \\ X_a' &= X_A X_a + X_a^2 = X_a\left(X_A + X_a\right) \end{aligned}$$

that is, under simple Mendelian inheritance, the fractions of organisms with alleles A and a are invariant. The same goes for all new generations.

We will consider the generalised Mendelian model of heredity, which is defined by the following coefficients of heredity:

$$\begin{aligned} &p_{AA,A}=1 \quad p_{Aa,A}=p_{aA,A}=\alpha \quad p_{aa,A}=0 \\ &p_{AA,a}=0 \quad p_{Aa,a}=p_{aA,a}=1-\alpha \quad p_{aa,A}=1 \end{aligned} \tag{3}$$

where $0 \le \alpha \le 1$. If $\alpha = \frac{1}{2}$, the generalised Mendelian model of heredity reduces to simple model (2).

For simplicity, let us enumerate $A \to 1$ and $a \to 2$. The set

$$S^1 = \left\{\left(X_1, X_2\right): X_1 \ge 0, X_2 \ge 0, X_1 + X_2 = 1\right\}$$

is called a one dimensional simplex (see *Fig. 1*).

A transformation $V_\alpha : S^1 \to S^1$ which is defined as follows:

$$\begin{aligned} X_1' &= X_1^2 + 2\alpha\, X_1 X_2 \\ X_2' &= X_2^2 + 2(1-\alpha)\, X_1 X_2 \end{aligned} \tag{4}$$

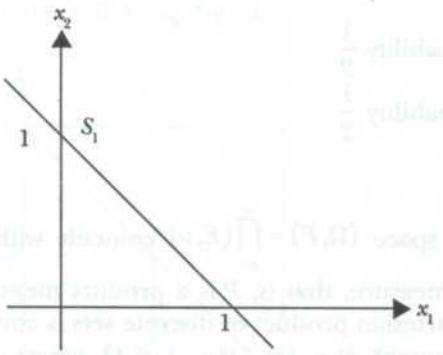

Fig. 1

where $0 \leq \alpha \leq 1$ is called a quadratic stochastic operator (q.s.o), which is determined by the coefficients of heredity (3).

The trajectory of a point $\underline{X}^{(0)} \in S^1$, where $\underline{X}^{(t)} = (X_1^{(t)}, X_1^{(t)})$, $t = 0,1, \ldots, n$, is defined as a sequence of iterations $\underline{X}^{(1)} = V_\alpha \underline{X}^{(0)}$, $\underline{X}^{(2)} = V_\alpha \underline{X}^{(1)}, \ldots, \underline{X}^{(n)} = V_\alpha \underline{X}^{(n-1)}$ for $n > 2$. One of the main problems in mathematical biology involves the study of the asymptotic behaviour of the trajectories of the q.s.o. [1:3]. The fixed points of the q.s.o. are called equilibrium states of the population. From the definition of q.s.o. (4), we obtain the following:

Theorem 1

Let V_α be a q.s.o. on S^1, where $0 \leq \alpha \leq 1$.

(i) If $0 \leq \alpha < \frac{1}{2}$, then (0,1) and (1,0) are fixed points of q.s.o. (4) and for any $\underline{X}^{(0)} \in$ Int S^1, the trajectory of $\underline{X}^{(0)}$ converges to (0,1);

(ii) If $\frac{1}{2} < \alpha \leq 1$, then (0,1) and (1,0) are fixed points of q.s.o. (4) and for any $\underline{X}^{(0)} \in$ Int S^1, the trajectory of $\underline{X}^{(0)}$ converges to (1,0);

(iii) If $\alpha = \frac{1}{2}$, V_α is an identity transformation.

The proof to Theorem 1 is trivial, following from the definition of q.s.o. (4).

The Random Models

Let $T_o = V_\alpha$ and $T_1 = V_\beta$ be two q.s.o. (4). Let us consider the probability space (E, υ) where $E = \{0,1\}$ and $\upsilon(0) = \upsilon(1) = \frac{1}{2}$. A random quadratic stochastic operator T is defined as follows:

$$T=\begin{cases} T_o \text{ with probability } \dfrac{1}{2} \\ T_1 \text{ with probability } \dfrac{1}{2} \end{cases} \tag{5}$$

Let the probabilistic space $(\Omega,P)=\prod_{i=1}^{\infty}(E,\upsilon)$ coincide with segment [0,1) with the usual Lebesque measure, that is, P is a product measure. It is well known that the countable Cartesian product of discrete sets is continuous. In our case, E = {0,1} and an element ω = (ω_1, ω_2,...) $\in \Omega$, where $\omega_n \in$ {0,1}, so every $\omega \in \Omega$ corresponds to the dyadic number 0, ω_1, ω_2,... from [0,1). Then, for an arbitrary ω = (ω_1, ω_2,...) $\in \Omega$, we assume

$$\left\{T_n(\omega)\right\}_0^{\infty}=\left(T_{\omega_0},T_{\omega_1},T_{\omega_2},\ldots\right), \tag{6}$$

where for any i, $\omega_i \in$ {0,1}.

Let $\underline{X}^{(0)} \in S^1$ be any arbitrary initial distribution. The random trajectory of this point is defined in the following way:

$$\underline{X}^{(n+1)} = T_n(\omega)\underline{X}^{(n)} \qquad \text{where } n = 0,1,2,\ldots .$$

Now we give a full description of the random trajectories of the random q.s.o. (5) and (6).

Theorem 2

Let T be a random q.s.o (5) and (6). Then (0,1) and (1,0) are the fixed points of this operator and

(i) if $\alpha+\beta<1$, where $0\le\alpha<\frac{1}{2}$ and $0\le\beta<\frac{1}{2}$, and $0\le\alpha<\frac{1}{2}$ and $\beta=\frac{1}{2}$ or $\alpha=\frac{1}{2}$ and $0\le\beta<\frac{1}{2}$, then for arbitrary initial distribution $\underline{X}^{(0)} \in$ Int S^1, almost all random trajectories of this point converge to (0,1).

(ii) if $\alpha+\beta<1$, $\frac{1}{2}<\alpha\le1$ and $\frac{1}{2}<\beta\le1$, and $\frac{1}{2}<\alpha\le1$ and $\beta=\frac{1}{2}$ or $\alpha=\frac{1}{2}$ and $\frac{1}{2}<\beta\le1$, then for arbitrary initial distribution $\underline{X}^{(0)} \in$ Int S^1, almost all random trajectories of this point converge to (1,0).

(iii) if $\alpha+\beta=1$, where $\alpha=\beta$, then arbitrary initial distribution $\underline{X}^{(0)} \in$ Int S^1, is a fixed point.

Proof: Let us consider the following *Fig. 2.*

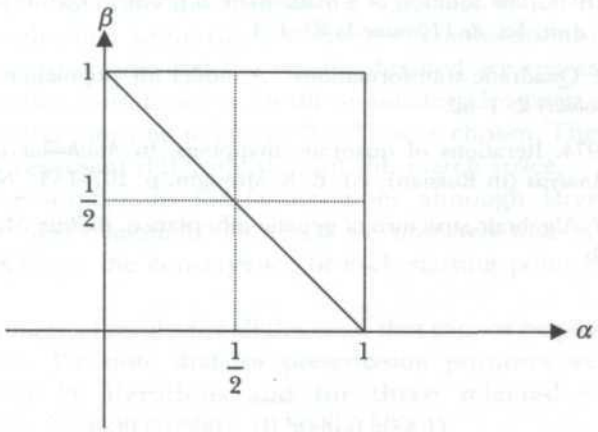

Fig. 2

(i) The proof of Theorem 2(i) follows from Theorem 1.
(ii) The proof of Theorem 2(ii) also follows from Theorem 1.

(iii) The case of $\alpha + \beta = 1$ when $\alpha = \beta = \frac{1}{2}$, is a trivial case.

We have carried out extensive numerical simulations (more than 10000 iterations for each case, please refer to appendix) and we observed that:

(i) the result of Theorem 2(i) also holds for $\left\{(\alpha,\beta): 0 \le \alpha < \frac{1}{2} \text{ and } \frac{1}{2} < \beta \le 1\right\}$,

or $\left\{(\alpha,\beta): \frac{1}{2} < \alpha \le 1 \text{ and } 0 \le \beta < \frac{1}{2}\right\}$.

(ii) the result of Theorem 2(iii) also holds for $\left\{(\alpha,\beta): 0 \le \alpha < \frac{1}{2} \text{ and } \frac{1}{2} < \beta \le 1\right\}$,

or $\left\{(\alpha,\beta): \frac{1}{2} < \alpha \le 1 \text{ and } 0 \le \beta < \frac{1}{2}\right\}$.

(iii) if $\alpha + \beta = 1$, where $\alpha \neq \beta$, then for arbitrary initial distribution $\underline{X}^{(0)} \in \text{Int } S^1$, almost all random trajectories of this point do not converge.

CONCLUSION

In this paper, we have obtained the behaviour of random trajectories of a random q.s.o.. For all (α,β) which are in the neighbourhood of $\alpha + \beta = 1$, we observe that the random trajectories of an arbitrary initial point may either converge very slowly or may not converge at all. A sample of the numerical results for all the cases mentioned above, are shown in the appendix.

REFERENCES

BERNSTEIN, S. N. 1934. The solution of a mathematical problem connected to the theory of heredity. *Ann. Sci. de l'Ukraine* **1:** 83–114.

KESTEN, H. 1980. Quadratic transformations: A model for population growth, I. *Adv. Applied Probability* **2:** 1–62.

LYUBICH, Y. I. 1974. Iterations of quadratic mappings. In *Mathematical Economics and Functional Analysis* (in Russian), ed. B. S. Mityagin, p. 107–133. "Nauka" Moscow.

REED, M. L. 1997. Algebraic structure of genetic inheritance. *Bulletin Mathematical Society* **34**: 107–130.

APPENDIX

The numerical simulations for each of the case mentioned on page 7 were carried out by selecting, arbitrarily, 100 different combinations of the values of α and β. This is to ensure that the results obtained are representative of the search space under consideration. In the simulation, for each combination of α and β, 10 arbitrary starting points $(x_1^{(0)}, x_2^{(0)})$ were chosen. They were selected such that they represent different areas of the search space.

We run the simulations for 50 iterations although larger numbers of iterations were also examined. However, we observed that 50 iterations are sufficient to examine the convergence of each starting point for all the cases considered.

Selected numerical results for all the cases that cannot be proven analytically are given below. We note that for presentation purposes we have run the programme for 20 iterations and for three selected starting points ((0.3000,0.7000), (0.9500,0.0500), (0.5000,0.5000)).

(I) $\alpha + \beta < 1$

(i) $0 \le \alpha < \frac{1}{2};\ \frac{1}{2} < \beta \le 1$

n	$\alpha = 0.4;\ \beta = 0.5$					
	$x_1^{(n)}$	$x_2^{(n)}$	$x_1^{(n)}$	$x_2^{(n)}$	$x_1^{(n)}$	$x_2^{(n)}$
0	0.3000	0.7000	0.9500	0.0500	0.5000	0.5000
1	0.3000	0.7000	0.9500	0.0500	0.5250	0.4750
2	0.2580	0.7420	0.9500	0.0500	0.4751	0.5249
3	0.2580	0.7420	0.9500	0.0500	0.5001	0.4999
4	0.2197	0.7803	0.9500	0.0500	0.4501	0.5499
5	0.2197	0.7803	0.9405	0.0595	0.4006	0.5994
6	0.2197	0.7803	0.9405	0.0595	0.3525	0.6475
7	0.2197	0.7803	0.9293	0.0707	0.3754	0.6246
8	0.1854	0.8146	0.9162	0.0838	0.3988	0.6012
9	0.1552	0.8448	0.9162	0.0838	0.4228	0.5772
10	0.1290	0.8710	0.9162	0.0838	0.4472	0.5528
11	0.1065	0.8935	0.9008	0.0992	0.3977	0.6023
12	0.1065	0.8935	0.8829	0.1171	0.3498	0.6502
13	0.0875	0.9125	0.8829	0.1171	0.3726	0.6274
14	0.0875	0.9125	0.8623	0.1377	0.3960	0.6040
15	0.0715	0.9285	0.8385	0.1615	0.3481	0.6519
16	0.0715	0.9285	0.8385	0.1615	0.3708	0.6292
17	0.0582	0.9418	0.8114	0.1886	0.3942	0.6058
18	0.0582	0.9418	0.7808	0.2192	0.3464	0.6536
19	0.0582	0.9418	0.7466	0.2534	0.3690	0.6310
20	0.0582	0.9418	0.7466	0.2534	0.3225	0.6775

n	$\alpha = 0.1;\ \beta = 0.7$					
	$x_1^{(n)}$	$x_2^{(n)}$	$x_1^{(n)}$	$x_2^{(n)}$	$x_1^{(n)}$	$x_2^{(n)}$
0	0.3000	0.7000	0.9500	0.0500	0.5000	0.5000
1	0.3840	0.6160	0.9690	0.0310	0.6000	0.4000
2	0.1948	0.8052	0.9810	0.0190	0.4080	0.5920
3	0.2575	0.7425	0.9885	0.0115	0.5046	0.4954
4	0.1045	0.8955	0.9930	0.0070	0.3046	0.6954
5	0.1420	0.8580	0.9875	0.0125	0.1352	0.8648
6	0.1907	0.8093	0.9924	0.0076	0.0416	0.9584
7	0.2525	0.7475	0.9864	0.0136	0.0576	0.9424
8	0.1015	0.8985	0.9757	0.0243	0.0793	0.9207
9	0.0285	0.9715	0.9852	0.0148	0.1085	0.8915
10	0.0064	0.9936	0.9910	0.0090	0.1473	0.8527
11	0.0013	0.9987	0.9839	0.0161	0.0468	0.9532
12	0.0018	0.9982	0.9712	0.0288	0.0111	0.9889
13	0.0004	0.9996	0.9824	0.0176	0.0155	0.9845
14	0.0005	0.9995	0.9686	0.0314	0.0216	0.9784
15	0.0001	0.9999	0.9442	0.0558	0.0047	0.9953
16	0.0001	0.9999	0.9653	0.0347	0.0066	0.9934
17	0.0000	1.0000	0.9385	0.0615	0.0092	0.9908
18	0.0000	1.0000	0.8923	0.1077	0.0019	0.9981
19	0.0001	0.9999	0.8155	0.1845	0.0027	0.9973
20	0.0001	0.9999	0.8757	0.1243	0.0005	0.9995

(ii) $\frac{1}{2} < \alpha < 1;\ 0 \le \beta \le \frac{1}{2}$

n	$\alpha = 0.65;\ \beta = 0.3$					
	$x_1^{(n)}$	$x_2^{(n)}$	$x_1^{(n)}$	$x_2^{(n)}$	$x_1^{(n)}$	$x_2^{(n)}$
0	0.3000	0.7000	0.9500	0.0500	0.5000	0.5000
1	0.2160	0.7840	0.9310	0.0690	0.5750	0.4250
2	0.2668	0.7332	0.9503	0.0497	0.6483	0.3517
3	0.3255	0.6745	0.9314	0.0686	0.5571	0.4429
4	0.3914	0.6086	0.9058	0.0942	0.6311	0.3689
5	0.2961	0.7039	0.9314	0.0686	0.5380	0.4620
6	0.3586	0.6414	0.9506	0.0494	0.4386	0.5614
7	0.4276	0.5724	0.9318	0.0682	0.3401	0.6599
8	0.3297	0.6703	0.9063	0.0937	0.2503	0.7497
9	0.2413	0.7587	0.9318	0.0682	0.3066	0.6934
10	0.1681	0.8319	0.9064	0.0936	0.3704	0.6296
11	0.2100	0.7900	0.9318	0.0682	0.4404	0.5596
12	0.2598	0.7402	0.9509	0.0491	0.3418	0.6582
13	0.3175	0.6825	0.9649	0.0351	0.4093	0.5907
14	0.3825	0.6175	0.9751	0.0249	0.3126	0.6874
15	0.4533	0.5467	0.9824	0.0176	0.2266	0.7734
16	0.3542	0.6458	0.9876	0.0124	0.2792	0.7208
17	0.2627	0.7373	0.9826	0.0174	0.1987	0.8013
18	0.1852	0.8148	0.9878	0.0122	0.2465	0.7535
19	0.2305	0.7695	0.9914	0.0086	0.3022	0.6978
20	0.1596	0.8404	0.9880	0.0120	0.2178	0.7822

n	$\alpha = 0.6;\ \beta = 0.1$					
	$x_1^{(n)}$	$x_2^{(n)}$	$x_1^{(n)}$	$x_2^{(n)}$	$x_1^{(n)}$	$x_2^{(n)}$
0	0.3000	0.7000	0.9500	0.0500	0.5000	0.5000
1	0.1320	0.8680	0.9120	0.0880	0.5500	0.4500
2	0.1549	0.8451	0.9281	0.0719	0.5995	0.4005
3	0.1811	0.8189	0.8746	0.1254	0.4074	0.5926
4	0.2108	0.7892	0.7869	0.2131	0.4557	0.5443
5	0.0777	0.9223	0.8204	0.1796	0.2573	0.7427
6	0.0920	0.9080	0.8499	0.1501	0.1044	0.8956
7	0.1087	0.8913	0.7479	0.2521	0.0296	0.9704
8	0.0312	0.9688	0.5970	0.4030	0.0066	0.9934
9	0.0070	0.9930	0.6451	0.3549	0.0079	0.9921
10	0.0014	0.9986	0.4620	0.5380	0.0095	0.9905
11	0.0017	0.9983	0.5117	0.4883	0.0114	0.9886
12	0.0021	0.9979	0.5617	0.4383	0.0024	0.9976
13	0.0025	0.9975	0.6109	0.3891	0.0029	0.9971
14	0.0030	0.9970	0.6584	0.3416	0.0006	0.9994
15	0.0036	0.9964	0.7034	0.2966	0.0001	0.9999
16	0.0007	0.9993	0.7451	0.2549	0.0001	0.9999
17	0.0001	0.9999	0.5932	0.4068	0.0000	1.0000
18	0.0000	1.0000	0.6415	0.3585	0.0000	1.0000
19	0.0000	1.0000	0.6875	0.3125	0.0000	1.0000
20	0.0000	1.0000	0.5156	0.4844	0.0000	1.0000

(II) $\alpha + \beta > 1$

(i) $0 \le \alpha < \frac{1}{2};\ \frac{1}{2} < \beta \le 1$

n	$\alpha = 0.3;\ \beta = 0.75$					
	$x_1^{(n)}$	$x_2^{(n)}$	$x_1^{(n)}$	$x_2^{(n)}$	$x_1^{(n)}$	$x_2^{(n)}$
0	0.3000	0.7000	0.9500	0.0500	0.5000	0.5000
1	0.4050	0.5950	0.9737	0.0262	0.6250	0.3750
2	0.3086	0.6914	0.9865	0.0135	0.5313	0.4688
3	0.4153	0.5847	0.9932	0.0068	0.6558	0.3442
4	0.3182	0.6818	0.9966	0.0034	0.5655	0.4345
5	0.4266	0.5734	0.9952	0.0048	0.4672	0.5328
6	0.5489	0.4511	0.9976	0.0024	0.3676	0.6324
7	0.6727	0.3273	0.9966	0.0034	0.4838	0.5162
8	0.5847	0.4153	0.9953	0.0047	0.6087	0.3913
9	0.4875	0.5125	0.9976	0.0024	0.7278	0.2722
10	0.3876	0.6124	0.9988	0.0012	0.8269	0.1731
11	0.2927	0.7073	0.9983	0.0017	0.7696	0.2304
12	0.3962	0.6038	0.9977	0.0023	0.6987	0.3013
13	0.3005	0.6995	0.9988	0.0012	0.8039	0.1961
14	0.4056	0.5944	0.9984	0.0016	0.8827	0.1173
15	0.3091	0.6909	0.9977	0.0023	0.8413	0.1587
16	0.4159	0.5841	0.9989	0.0011	0.9081	0.0919
17	0.3188	0.6812	0.9984	0.0016	0.9498	0.0502
18	0.4273	0.5727	0.9978	0.0022	0.9308	0.0692
19	0.5497	0.4503	0.9969	0.0031	0.9630	0.0370
20	0.6735	0.3265	0.9984	0.0016	0.9487	0.0513

n	$\alpha = 0.4;\ \beta = 0.8$					
	$x_1^{(n)}$	$x_2^{(n)}$	$x_1^{(n)}$	$x_2^{(n)}$	$x_1^{(n)}$	$x_2^{(n)}$
0	0.3000	0.7000	0.9500	0.0500	0.5000	0.5000
1	0.4260	0.5740	0.9785	0.0215	0.6500	0.3500
2	0.3771	0.6229	0.9911	0.0089	0.6045	0.3955
3	0.5180	0.4820	0.9964	0.0036	0.7479	0.2521
4	0.4681	0.5319	0.9986	0.0014	0.7102	0.2898
5	0.6175	0.3825	0.9983	0.0017	0.6691	0.3309
6	0.7592	0.2408	0.9993	0.0007	0.6248	0.3752
7	0.8689	0.1311	0.9992	0.0008	0.7655	0.2345
8	0.8461	0.1539	0.9990	0.0010	0.8732	0.1268
9	0.8201	0.1799	0.9996	0.0004	0.9396	0.0604
10	0.7906	0.2094	0.9998	0.0002	0.9737	0.0263
11	0.7574	0.2426	0.9998	0.0002	0.9685	0.0315
12	0.8677	0.1323	0.9998	0.0002	0.9624	0.0376
13	0.8447	0.1553	0.9999	0.0001	0.9841	0.0159
14	0.9234	0.0766	0.9999	0.0001	0.9935	0.0065
15	0.9093	0.0907	0.9999	0.0001	0.9922	0.0078
16	0.9588	0.0412	0.9999	0.0001	0.9968	0.0032
17	0.9509	0.0491	0.9999	0.0001	0.9987	0.0013
18	0.9789	0.0211	0.9999	0.0001	0.9985	0.0015
19	0.9913	0.0087	0.9999	0.0001	0.9994	0.0006
20	0.9965	0.0035	1.0000	0.0000	0.9993	0.0007

(ii) $\frac{1}{2} < \alpha < 1;\ 0 \le \beta \le \frac{1}{2}$

n	$\alpha = 0.95;\ \beta = 0.1$					
	$x_1^{(n)}$	$x_2^{(n)}$	$x_1^{(n)}$	$x_2^{(n)}$	$x_1^{(n)}$	$x_2^{(n)}$
0	0.3000	0.7000	0.9500	0.0500	0.5000	0.5000
1	0.1320	0.8680	0.9120	0.0880	0.7250	0.2750
2	0.2351	0.7649	0.9842	0.0158	0.9044	0.0956
3	0.3970	0.6030	0.9718	0.0282	0.8353	0.1647
4	0.6124	0.3876	0.9499	0.0501	0.9591	0.0409
5	0.4225	0.5775	0.9927	0.0073	0.9277	0.0723
6	0.6421	0.3579	0.9992	0.0008	0.8741	0.1259
7	0.8489	0.1511	0.9986	0.0014	0.7861	0.2139
8	0.7464	0.2536	0.9975	0.0025	0.6516	0.3484
9	0.5949	0.4051	0.9997	0.0003	0.8559	0.1441
10	0.4021	0.5979	0.9995	0.0005	0.9669	0.0331
11	0.6185	0.3815	1.0000	0.0000	0.9957	0.0043
12	0.8309	0.1691	1.0000	0.0000	0.9923	0.0077
13	0.9573	0.0427	1.0000	0.0000	0.9992	0.0008
14	0.9941	0.0059	1.0000	0.0000	0.9985	0.0015
15	0.9994	0.0006	1.0000	0.0000	0.9973	0.0027
16	0.9989	0.0011	1.0000	0.0000	0.9997	0.0003
17	0.9980	0.0020	1.0000	0.0000	0.9995	0.0005
18	0.9964	0.0036	1.0000	0.0000	1.0000	0.0000
19	0.9996	0.0004	1.0000	0.0000	1.0000	0.0000
20	0.9993	0.0007	1.0000	0.0000	1.0000	0.0000

n	$\alpha = 0.85;\ \beta = 0.5$					
	$x_1^{(n)}$	$x_2^{(n)}$	$x_1^{(n)}$	$x_2^{(n)}$	$x_1^{(n)}$	$x_2^{(n)}$
0	0.3000	0.7000	0.9500	0.0500	0.5000	0.5000
1	0.3000	0.7000	0.9500	0.0500	0.6750	0.3250
2	0.4470	0.5530	0.9832	0.0167	0.8286	0.1714
3	0.6200	0.3800	0.9832	0.0167	0.8286	0.1714
4	0.7849	0.2151	0.9832	0.0167	0.9280	0.0720
5	0.7849	0.2151	0.9948	0.0052	0.9280	0.0720
6	0.9031	0.0969	0.9984	0.0016	0.9280	0.0720
7	0.9644	0.0356	0.9984	0.0016	0.9280	0.0720
8	0.9644	0.0356	0.9984	0.0016	0.9280	0.0720
9	0.9644	0.0356	0.9995	0.0005	0.9748	0.0252
10	0.9644	0.0356	0.9995	0.0005	0.9920	0.0080
11	0.9884	0.0116	0.9999	0.0001	0.9976	0.0024
12	0.9964	0.0036	1.0000	0.0000	0.9976	0.0024
13	0.9989	0.0011	1.0000	0.0000	0.9993	0.0007
14	0.9997	0.0003	1.0000	0.0000	0.9993	0.0007
15	0.9999	0.0001	1.0000	0.0000	0.9993	0.0007
16	0.9999	0.0001	1.0000	0.0000	0.9998	0.0002
17	0.9999	0.0001	1.0000	0.0000	0.9998	0.0002
18	0.9999	0.0001	1.0000	0.0000	0.9999	0.0001
19	1.0000	0.0000	1.0000	0.0000	1.0000	0.0000
20	1.0000	0.0000	1.0000	0.0000	1.0000	0.0000

(III) $\alpha + \beta = 1; \quad \alpha \neq \beta$

(i) $0 \leq \alpha < \frac{1}{2};\ \frac{1}{2} < \beta \leq 1$

n	$\alpha = 0.3;\ \beta = 0.75$					
	$x_1^{(n)}$	$x_2^{(n)}$	$x_1^{(n)}$	$x_2^{(n)}$	$x_1^{(n)}$	$x_2^{(n)}$
0	0.3000	0.7000	0.9500	0.0500	0.5000	0.5000
1	0.3630	0.6370	0.9642	0.0357	0.5750	0.4250
2	0.2936	0.7064	0.9746	0.0254	0.5017	0.4983
3	0.3559	0.6441	0.9820	0.0180	0.5767	0.4233
4	0.2871	0.7129	0.9873	0.0127	0.5035	0.4965
5	0.3485	0.6515	0.9836	0.0164	0.4285	0.5715
6	0.4166	0.5834	0.9884	0.0116	0.3550	0.6450
7	0.4895	0.5105	0.9850	0.0150	0.4237	0.5763
8	0.4145	0.5855	0.9805	0.0195	0.4969	0.5031
9	0.3417	0.6583	0.9863	0.0137	0.5719	0.4281
10	0.2743	0.7257	0.9903	0.0097	0.6454	0.3546
11	0.2145	0.7855	0.9875	0.0125	0.5767	0.4233
12	0.2651	0.7349	0.9837	0.0163	0.5035	0.4965
13	0.2066	0.7934	0.9885	0.0115	0.5785	0.4215
14	0.2558	0.7442	0.9851	0.0149	0.6516	0.3484
15	0.1987	0.8013	0.9807	0.0193	0.5835	0.4165
16	0.2465	0.7535	0.9864	0.0136	0.6564	0.3436
17	0.1908	0.8092	0.9824	0.0176	0.7241	0.2759
18	0.2371	0.7629	0.9772	0.0228	0.6642	0.3358
19	0.2913	0.7087	0.9705	0.0295	0.7311	0.2689
20	0.3533	0.6467	0.9791	0.0209	0.6721	0.3279

(ii) $\frac{1}{2} < \alpha \leq 1;\ 0 \leq \beta < \frac{1}{2}$

n	$\alpha = 0.85;\ \beta = 0.15$					
	$x_1^{(n)}$	$x_2^{(n)}$	$x_1^{(n)}$	$x_2^{(n)}$	$x_1^{(n)}$	$x_2^{(n)}$
0	0.3000	0.7000	0.9500	0.0500	0.5000	0.5000
1	0.1530	0.8470	0.9167	0.0833	0.6750	0.3250
2	0.2437	0.7563	0.9702	0.0298	0.8286	0.1714
3	0.3727	0.6273	0.9499	0.0501	0.7291	0.2709
4	0.5364	0.4636	0.9166	0.0834	0.8674	0.1326
5	0.3623	0.6377	0.9701	0.0299	0.7869	0.2131
6	0.5241	0.4759	0.9904	0.0096	0.6695	0.3305
7	0.6987	0.3013	0.9838	0.0162	0.5146	0.4854
8	0.5513	0.4487	0.9726	0.0274	0.3397	0.6603
9	0.3781	0.6219	0.9912	0.0088	0.4967	0.5033
10	0.2135	0.7865	0.9852	0.0148	0.6717	0.3283
11	0.3311	0.6689	0.9954	0.0046	0.8261	0.1739
12	0.4861	0.5139	0.9986	0.0014	0.7255	0.2745
13	0.6610	0.3390	0.9996	0.0004	0.8649	0.1351
14	0.8178	0.1822	0.9999	0.0001	0.7831	0.2169
15	0.9221	0.0779	1.0000	0.0000	0.6642	0.3358
16	0.8718	0.1282	1.0000	0.0000	0.8203	0.1797
17	0.7936	0.2064	1.0000	0.0000	0.7172	0.2828
18	0.6790	0.3210	1.0000	0.0000	0.8592	0.1408
19	0.8315	0.1685	1.0000	0.0000	0.9439	0.0561
20	0.7335	0.2665	1.0000	0.0000	0.9068	0.0932

ISSN: 0128-7680
Pertanika J. Sci. & Technol. 12(1): 81 - 92 (2004) © Universiti Putra Malaysia Press

Kadar Pengenapan dan Kepekatan Beberapa Logam Berat pada Permukaan Sedimen di Hutan Paya Bakau Bebar, Pahang

Kamaruzzaman, B. Y., B. S. Hasrizal & B. T. Jamil
Institut Oseanografi,
Kolej Universiti Sains & Teknologi Malaysia,
21030 Kuala Terengganu, Terengganu, Malaysia

Diterima: 22 Julai 2002

ABSTRAK

Sampel permukaan yang dikutip dari 3 transet (54 stesen pensampelan) di hutan paya bakau Bebar telah diukur kadar pemendapan, ciri-ciri sedimen dan kepekatan beberapa logam. Dalam kajian ini, kadar sedimentasi diukur dengan menggunakan kaedah penunjuk tiruan mendatar di mana purata pemendapan sebanyak 0.52 cm.thn^{-1} telah diperoleh. Min saiz partikel sedimen permukaan didapati berjulat di antara dari pasir halus (5.15ϕ) hingga kelodak halus (6.91ϕ). Min saiz partikel menunjukkan hubungan signifikan ($P<0.05$) terhadap perubahan musim dengan penurunan nilainya ketika musim monsun. Bagi logam Cr, Cu, Pb dan Zn didapati menunjukkan perubahan mengikut jarak dengan purata kepekatan yang rendah di kawasan muara dan tinggi secara relatif di kawasan yang lebih jauh dari muara.

ABSTRACT

Surface sediments collected from 3 transects (54 sampling points total) in the Bebar mangrove have been analyzed for their sediment accretion, sediment characteristics and some heavy metals content. The sediment accretion rate in this study was determined using an artificial marker horizon method and an average sedimentation rate of 0.52 cm.yr^{-1} was obtained. Surface sediment mean particle size ranged from fine sand (5.15ϕ) to fine silt (6.91ϕ). There is a significant ($P<0.05$) relationship between the mean particle size with the seasonal changes with a decreasing value occurring during monsoon seasons. The elements Cr, Cu, Pb and Zn, in general, showed considerable spatial variation with a lower average concentration near the estuary and relatively higher concentration at the area away from the estuary.

Keywords: Heavy metals, sediment accretion, sediment characteristics

PENGENALAN

Hutan paya bakau merupakan zon penampan yang terletak di antara persekitaran pantai serta laut dan banyak dipengaruhi oleh paras pasang-surut. Ianya boleh bertindak secara cekap sebagai perangkap sedimen, tetapi bergantung kepada aliran pasang-surut iaitu sama ada membawa masuk atau membawa keluar enapan ke kawasan pantai yang berhampiran (Yeats dan Bewers 1983). Sedimen tadi yang termendap pada kadar konstan dalam satu jangka masa yang lama didapati boleh memberi maklumat masa-masa lampau seperti status pencemaran dan kadar pemendapan (Eisma *et al.* 1989; Nolting dan Helder 1991). Kebelakangan ini, penebusgunaan ekosistem hutan paya bakau bagi tujuan

pertanian, industri, penempatan dan pelbagai bentuk pembangunan didapati telah meningkat dengan mendadak dan secara tidak langsung menyebabkan hakisan di kawasan pantai (Hatcher *et al.* 1989). Kemusnahan hutan paya bakau yang berterusan juga akan meningkatkan kesan antropogenik melalui proses penimbunan bahan yang dibawa dari lautan dan daratan semasa air pasang dan air surut. Di kawasan perbandaran, kepekatan logam dalam sedimen adalah banyak dipengaruhi oleh bahan buangan domestik dan industri (Martin dan Whitfield 1983; Martin *et al.* 1989) yang terdapat banyak di kawasan kajian.

Di Malaysia, kajian berkaitan hutan paya bakau terhadap produktiviti pantai dan perikanan telah banyak didokumentasikan tetapi kebanyakannya lebih tertumpu kepada kajian biologi dan ekologi (Thong dan Sasekumar 1984; Gong dan Ong 1990). Tidak banyak maklumat diketahui tentang peranan alur dan proses pemendapan di hutan paya bakau (Mohd Lokman *et al.* 1994). Ramai berpendapat kewujudan alur hanya sebagai satu ciri morfologi yang bertindak sebagai saluran yang membawa air pasang ke bahagian belakang hutan paya bakau. Tambahan lagi, kajian-kajian geokimia dalam sedimen daripada hutan paya bakau di Malaysia kurang mendapat perhatian dan hanya terhad kepada peranan mereka dalam proses sedimentasi (Kamaruzzaman *et al.* 2000). Berasaskan kepada kepentingan paya bakau daripada pelbagai aspek persekitaran, penyelidikan terhadap kandungan Cr, Cu, Pb dan Zn dan kadar pemendapan dan corak taburan logam dalam sedimen telah dilakukan.

PERALATAN DAN KAEDAH

Lokasi Kajian

Hutan paya bakau Bebar terletak di selatan bandar Kuantan, ibu negeri Pahang (*Rajah 1*). Hutan paya bakau Bebar merupakan kawasan yang unik kerana persekitarannya yang meliputi pelbagai ekosistem seperti muara, paya bakau dan lagun. Selain daripada itu, kawasan ini terletak di zon kawasan yang menerima taburan hujan yang tinggi terutamanya ketika musim monsun iaitu di antara bulan November hingga akhir Januari (*Rajah 2*). Dalam kajian ini, tiga transet (TR1, TR2 dan TR3) telah dipasang di dalam hutan paya bakau dengan jumlah keseluruhan sebanyak 54 stesen pensampelan. TR1 dan TR2 masing-masing menpunyai 15 stesen pensampelan manakala TR3 mempunyai 24 stesen pensampelan. Setiap transet adalah dipilih di kawasan yang tidak terdapat sebarang gangguan biologi ataupun terletak di kawasan yang terdapat banyak aktiviti manusia. Transet 1 terletak berhampiran kawasan muara, manakala transet 2 dan 3 berada lebih jauh daripada pengaruh muara. Setiap stesen pensampelan ditanam dengan sekeping perspek sedalam 0.3 m dan berperanan sebagai penanda untuk pengukuran kadar pemendapan. Sampel permukaan bagi setiap stesen juga diambil bagi tujuan penganalisisan ciri-ciri sedimen dan logam terpilih.

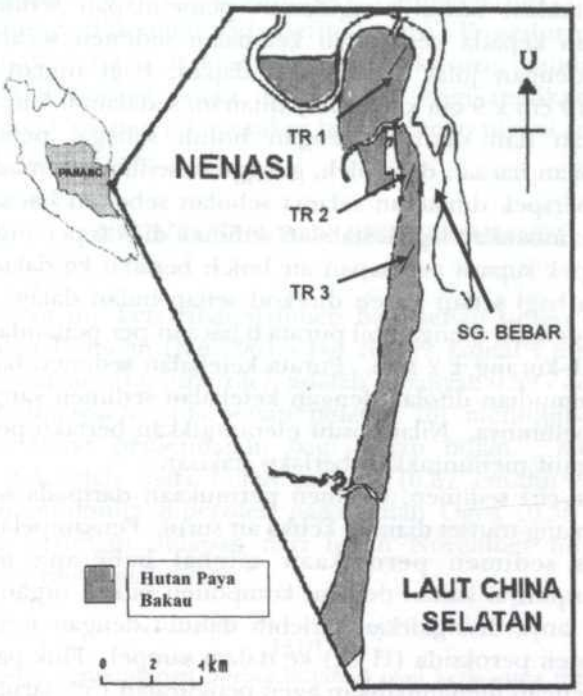

Rajah 1: Lokasi kedudukan transet (TR1, TR2 dan TR3) di hutan paya bakau Bebar, Pahang, Malaysia

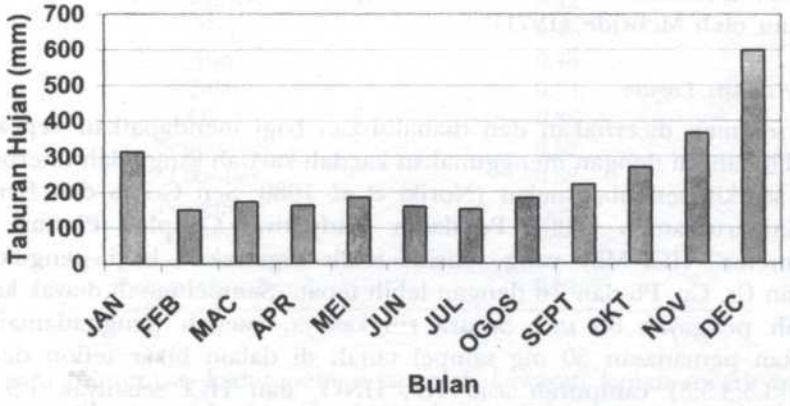

Rajah 2: Purata taburan hujan bulanan tahun 2001 di daerah Kuantan
Sumber: Jabatan Meteorologi Malaysia

Kaedah Penanda Tiruan bagi Mengukur Pemendapan Sedimen

Kaedah yang digunakan untuk pengukuran pemendapan sedimen adalah dengan berdasarkan kepada penentuan ketebalan sedimen secara menegak dan dibahagikan dengan julat masa pemendapan. Bagi tujuan kajian ini, kepingan perspek (9 cm x 9 cm x 1.5 mm) ditanam sedalam 0.5 m pada setiap stesen pensampelan dan ditanda dengan buluh sebagai penanda. Bagi memastikan kestabilan bacaan diperoleh, gangguan sedimen semasa peringkat awal penanaman perspek dibiarkan selama sebulan sebelum bacaan pertama direkod. Bagi menambahkan lagi kestabilan sedimen di atas penanda, 5 lubang ditebuk pada perspek supaya peresapan air boleh berlaku ke dalam sedimen. Ketebalan sedimen bagi setiap stesen direkod setiap bulan dalam tempoh 12 bulan yang diukur dengan mengambil purata 6 bacaan per penanda. Ketepatan bacaan adalah lebih-kurang ± 2 mm. Purata ketebalan sedimen bagi sebulan dalam kajian ini kemudian ditolak dengan ketebalan sedimen yang diperoleh daripada bulan sebelumnya. Nilai positif menunjukkan berlaku pemendapan, manakala nilai negatif menunjukkan berlaku hakisan.

Bagi analisis ciri-ciri sedimen, sedimen permukaan daripada setiap stesen pensampelan sepanjang transet diambil ketika air surut. Pensampelan dilakukan dengan mengikis sedimen permukaan setebal beberapa mm. Corak sedimentologi mempunyai kaitan dengan komponen bukan organik di dalam sedimen di mana ianya disingkirkan terlebih dahulu dengan menambahkan larutan 20% hidrogen peroksida (H_2O_2) ke dalam sampel. Fluk partikel halus pula dihapuskan dengan menambahkan agen penguraian (5% larutan kalgon). Sedimen yang telah dipungut kebanyakannya (80% berat) sedimen halus dan masih berada dalam julat pengesanan mesin penyerakan laser. Jadi saiz butiran sedimen telah dianalisis hanya dengan menggunakan kaedah penyerakan laser sahaja. Saiz butiran dijelaskan dalam unit phi (ϕ), iaitu $\phi = - \log_2 d$ dan d merupakan diameter butiran dalam mm. Min, sisihan piawai, skewness setiap sampel dikira melalui kaedah momen dengan menggunakan persamaan yang ditakrifkan oleh McBride (1971).

Kaedah Analisis Logam

Sampel sedimen dicernakan dan dianalisiskan bagi mendapatkan kepekatan Cr, Cu, Pb dan Zn dengan menggunakan kaedah-kaedah yang telah diterbitkan dengan sedikit pengubahsuaian (Noriki *et al.* 1980; Sen Gupta dan Bertand 1995; Kamaruzzaman 1999). Peralatan "Inductively-Coupled Plasma Mass Spectrometer" (ICP-MS) yang sensitif telah digunakan bagi pengukuran kepekatan Cr, Cu, Pb dan Zn dengan lebih tepat. Sampel tanah diayak kering di bawah pengayak 63 μm. Secara ringkasnya, kaedah penghadaman ini melibatkan pemanasan 50 mg sampel tanah di dalam bikar teflon dengan nisbah (3.5:3.5:3) campuran asid HF, HNO_3 dan HCl sebanyak 1.5 mL. Campuran tadi dimasukkan ke dalam jaket keluli dan dipanaskan pada suhu 150°C selama 5 jam. Selepas penyejukan, larutan campuran asid borik dan EDTA (3 mL) dimasukkan, dan dipanaskan semula pada suhu 150°C selama 5 jam. Setelah penyejukan pada suhu bilik, larutan jernih yang diperoleh dalam

bikar teflon ini akan dimasukkan ke dalam tabung uji polipropilena sebelum dicairkan kepada 10 mL dengan air mili-Q. Larutan jernih yang tidak berkeladak adalah sepatutnya diperoleh pada peringkat ini. Prosedur penghadaman bagi sedimen piawai paya bakau serta pengkosong adalah sama seperti menghadamkan sampel tanah. Nilai relatif bagi replikasi sampel didapati kurang daripada 3% dan nilai terakru bagi sedimen piawai adalah juga didapati dalam lingkungan ± 3%.

KEPUTUSAN DAN PERBINCANGAN

Kadar Pemendapan

Di dalam kajian ini, ketebalan sedimen bagi setiap stesen direkodkan dalam tempoh selama 12 bulan (Jan 2001 – Jan 2002). Jadual 1 menunjukkan purata kadar pemendapan yang diperoleh adalah sebanyak 0.52 cm.thn^{-1} dengan nilai yang positif diperoleh pada setiap bulan. Ini menunjukkan ada terdapat peningkatan kadar pemendapan bagi setiap bulan. Kadar pemendapan maksimum diperoleh pada bulan Januari (0.67 cm.thn^{-1}), manakala kadar pemendapan minimum diperoleh pada bulan Ogos (0.38 cm.thn^{-1}). Kadar pemendapan tertinggi didapati dari bulan November hingga Januari iaitu semasa musim monsun berlaku.

JADUAL 1
Kadar pemendapan purata bulanan bagi ketiga-tiga transet dan kadar pemendapan purata tahunan sebayak 0.52 cm.tahun^{-1}

Bulan	Kadar pemendapan (cm.bulan^{-1})
Januari	0.67
Februari	0.62
Mac	0.56
April	0.42
Mei	0.46
Jun	0.48
Julai	0.54
Ogos	0.38
September	0.55
Oktober	0.58
November	0.45
Disember	0.56
Purata cm tahun^{-1}	0.52

Secara umumnya, kadar pemendapan di kawasan kajian secara relatifnya didapati sedikit tinggi berbanding kajian-kajian di kawasan tanah lembap yang lain (Spenceley 1982; Shahbudin *et al.* 1998). Kadar pemendapan yang tinggi itu adalah disebabkan oleh lokasinya yang terletak berhampiran dengan kawasan muara dan dipengaruhi oleh dua sumber kemasukan sedimen dari sungai dan

lautan. Kadar kemasukan air sungai yang tinggi turut membawa banyak sedimen terampai ke dalam kawasan paya bakau dan terperangkap pada akar pokok bakau. Selain itu faktor ketidakmatangan pokok bakau yang mempunyai pneumatofor yang banyak turut menyumbang kepada kadar pemendapan yang tinggi yang berperanan memerangkap sedimen dalam kuantiti yang besar. Dengan anggaran jangka masa 158 tahun bagi enapan 100 cm sedimen secara menegak, nilai kadar pemendapan yang diperoleh boleh diandaikan tepat. Purata kadar pemendapan yang tinggi menunjukkan hutan paya bakau di Bebar masih berada dalam peringkat belum matang. Selain daripada itu, penemuan ini juga mengesyorkan bahawa hutan paya bakau bukan sahaja dilihat sebagai penghuni pasif dataran lumpur tetapi bertindak sebagai perangkap sedimen yang aktif. Oleh itu, hutan bakau adalah penting dan berperanan bagi memerangkap sedimen halus daripada sumber sungai dan laut.

Ciri-ciri Sedimen Permukaan

Min saiz partikel sedimen permukaan berjulat antara kelodak sederhana (5.15ϕ) hingga kelodak halus (6.91ϕ) semasa musim bukan monsun, dan berubah menjadi pasir halus (3.27ϕ) hingga kelodak sederhana (6.00ϕ) semasa musim monsun. Ciri-ciri sedimen didapati menunjukkan hubungan yang signifikan ($P<0.05$) terhadap perubahan musim dengan penurunan min saiz partikel semasa musim monsun. Sedimen yang lebih kasar didapati lebih dominan semasa musim monsun dan sebaliknya menjadi lebih halus semasa musim bukan monsun (*Rajah 3*). Fenomena ini adalah berkemungkinan disebabkan oleh pergerakan arus sungai yang kuat semasa musim monsun dan mengangkut sedimen-sedimen yang lebih halus keluar ke lautan.

Bagi sisihan piawai pula didapati tidak menunjukkan perhubungan yang signifikan terhadap perubahan monsun. Secara umumnya, sisihan piawai didapati menunjukkan penyisihan sedimen yang tidak sempurna dalam sepanjang tahun

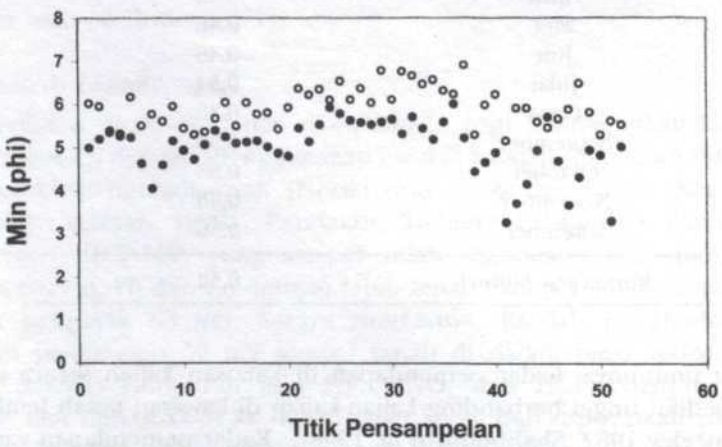

Rajah 3: Taburan min saiz sedimen (ϕ) melawan stesen pensampelan semasa musim monsun (●) dan musim bukan monsun (○)

dengan julat nilai antara 1.46 hingga 2.57. Kepencongan pula didapati menunjukkan hubungan yang signifikan terhadap perubahan musim ($P<0.05$) dan berjulat di antara -0.38 hingga 1.31. Purata nilai kepencongan adalah negatif semasa musim bukan monsun dan menjadi positif semasa musim monsun. Nilai-nilai kepencongan tadi memberikan gambaran bahawa sedimen di kawasan kajian didapati mengalami proses hakisan semasa musim monsun.

Taburan Logam Terpilih secara Mendatar

Taburan mendatar purata kepekatan Cr, Cu, Pb dan Zn bagi ketiga-tiga transet ditunjukkan dalam bentuk graf palang pada *Rajah 4a* dan *4b*. Perbandingan logam kajian terhadap kepekatan purata di dalam batuan dan kerak bumi adalah seperti pada Jadual 2. Kepekatan kuprum (Cu) berada di antara 29.7 mg/kg berat kering hingga 86.2 mg/kg berat kering dengan purata 58.5 mg/kg berat kering (*Rajah 4a*). Purata kepekatan Cu didapati lebih tinggi berbanding kepekatan Cu di dalam batuan dan kerak bumi (Bowen 1979; Mason dan Moore 1982). Sumber utama Cu adalah dipercayai berasal daripada pembuangan

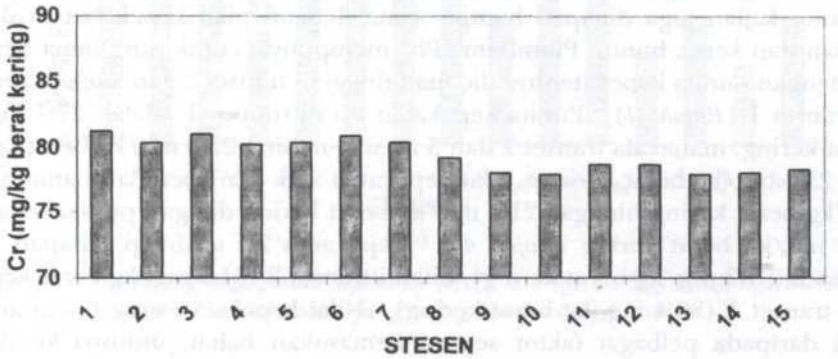

(a)

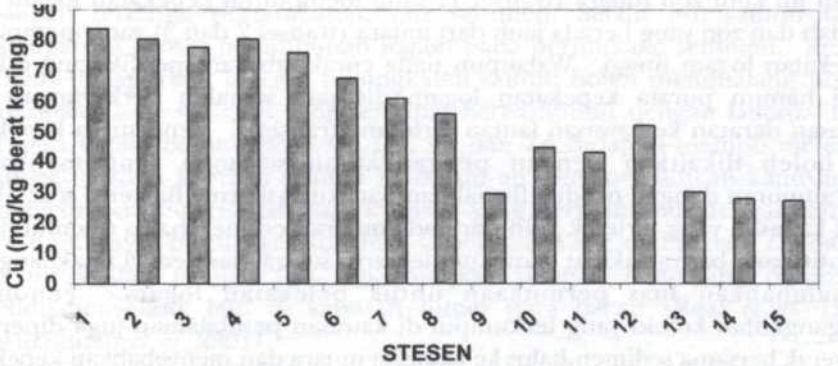

(b)

Rajah 4a: Graf palang bagi purata kepekatan (a) Cr dan (b) Cu bagi ketiga-tiga transet. Stesen 1 adalah stesen yang paling hampir dengan sungai

JADUAL 2
Perbandingan purata kepekatan Cr, Cu, Pb dan Zn pada permukaan sedimen di kawasan kajian terhadap purata kepekatan logam di dalam batuan dan kerak bumi yang dianggarkan oleh Bowen (1979) dan Mason & Moore (1982)

Logam Kajian	Purata kepekatan	Bowen 1979	Mason & Moore 1982
Cr	88	89	90
Cu	58.5	50	55
Pb	16	14	13
Zn	82.9	75	70

sisa kumbahan dari kawasan bandar dan sisa-sisa industri terutamanya berhampiran kawasan pendaratan ikan (berhampiran transet 2 dan 3), di mana masing-masing dengan purata kepekatan sebanyak 63.4 mg/kg berat kering dan 72.9 mg/kg berat kering. Sementara itu bagi kepekatan Cr, ianya didapati hampir malar di antara transet dan berada di dalam julat antara 49.7 mg/kg berat kering hingga 85.2 mg/kg berat kering (*Rajah 4a*). Purata kepekatan di kawasan kajian juga didapati hampir sama dengan nilai kepekatan di dalam batuan dan kerak bumi. Plumbum (Pb) mempunyai corak yang sama dengan Cu dengan purata kepekatannya didapati tinggi di transet 2 dan 3 tetapi rendah di transet 1 (*Rajah 4b*). Purata kepekatan Pb di transet 1 adalah 27.7 mg/kg berat kering, manakala transet 2 dan 3 masing-masing 22.8 mg/kg berat kering dan 23.9 mg/kg berat kering. Julat kepekatan zink (Zn) berada di antara 42.5 mg/kg berat kering hingga 121.6 mg/kg berat kering dengan purata sebanyak 82.9 mg/kg berat kering (*Rajah 4b*). Kepekatan Zn tertinggi didapati pada stesen 2 (87.3 mg/kg berat kering), diikuti transet 3 (81.2 mg/kg berat kering) dan transet 1 (80.4 mg/kg berat kering). Nilai kepekatan yang tinggi adalah hasil daripada pelbagai faktor seperti kemasukan bahan industri ke dalam sungai, luluhawa dan kesan aktiviti setempat berhampiran Sungai Bebar.

Secara umumnya, terdapat dua zon taburan logam yang dikenal pasti dalam kajian ini iaitu zon muara (transet 1) yang mempunyai kepekatan logam yang rendah dan zon yang berada jauh dari muara (transet 2 dan 3) yang mempunyai kepekatan logam tinggi. Walaupun tiada corak taburan spesifik yang dikenal pasti namun purata kepekatan logam didapati semakin berkurangan dari kawasan daratan ke kawasan lautan terutama transet 1. Penurunan kepekatan ini boleh dikaitkan dengan pengangkutan sedimen yang mengalami percampuran dengan produk fluvial dan partikulat marin (Barreiro *et al.* 1994). Bagi kawasan yang terletak jauh daripada muara, sedimen halus ditemui dalam kuantiti yang banyak akibat diangkut oleh arus sungai dan secara tidak langsung menambahkan luas permukaan untuk pelekatan logam. Fenomena pengangkutan koloid yang terkumpul di kawasan pendalaman juga dipercayai bergerak bersama sedimen halus ke kawasan muara dan menyebabkan kepekatan logam didapati lebih tinggi. Seperti yang dilaporkan oleh Jamil (2002), terdapat hubungan korelasi yang positif di antara saiz butiran dengan kepekatan logam Cr, Cu, Pb dan Zn. Sedimen di transet 2 dan 3 yang mempunyai peratusan

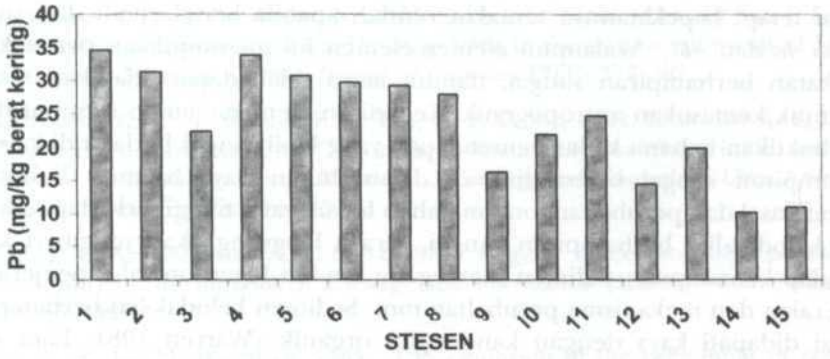

(a)

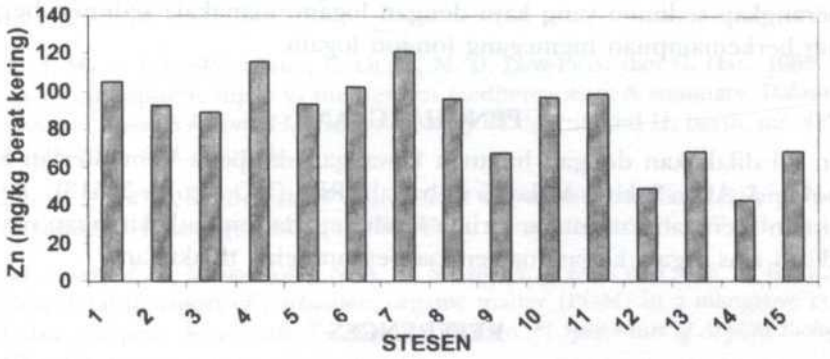

(b)

Rajah 4b: Graf palang bagi purata kepekatan (c) Pb dan (d) Zn bagi ketiga-tiga transet. Stesen 1 adalah stesen yang paling hampir dengan sungai

kelodak dan liat yang tinggi (>75%) menunjukkan hubungan yang baik terhadap kepekatan logam. Bagi transet 1, kepekatan logam yang rendah adalah disebabkan terdapat pertambahan saiz sedimen. Selain itu, saliniti turut mempengaruhi proses penimbunan logam pada permukaan sedimen. Real *et al.* (1993) melaporkan bahawa peningkatan saliniti boleh menghalang proses pengoksidaan bagi sedimen yang terdapat berhampiran dengan lautan. Bagi sesetengah logam berat seperti Cr, Cu, Pb dan Zn didapati mampu melepasi lapisan oksida dan kembali semula ke dalam air dan menjadikan kandungan logam-logam tersebut rendah bagi kawasan yang berhampiran dengan lautan. Secara umumnya, purata keseluruhan kepekatan Cr, Cu, Pb dan Zn dalam kajian ini adalah rendah jika dibandingkan dengan nilai yang diperoleh penyelidik-penyelidik lain di kawasan hutan paya bakau (Real *et al.* 1993; Kamaruzzaman *et al.* 2001).

Perbezaan jumlah kepekatan Cr, Cu, Pb dan Zn di antara stesen bagi setiap transet didapati mempunyai perbezaan yang signifikan ($P<0.05$). Ini menunjukkan kepekatan Cr, Cu, Pb dan Zn tinggi di stesen berhampiran

sungai tetapi kepekatannya semakin rendah apabila berada jauh dari sungai (*Rajah 4a* dan *4b*). Walaupun elemen-elemen ini menunjukkan peningkatan kepekatan berhampiran sungai, namun ianya tidak dapat dijadikan sebagai penunjuk kemasukan antropogenik. Kehadiran elemen-elemen tersebut dapat membuktikan bahawa kadar pemendapan yang lebih tinggi berlaku di kawasan berhampiran sungai berbanding di dalam hutan paya bakau. Kehadiran sedimen asal dan perubahan ion-ion bahan logam yang tinggi terhadap sedimen jenis kelodak-liat berhampiran sungai, secara langsung akan memberi kesan terhadap kemampuan sedimen memegang ion-ion logam melalui penjerapan, pemeraian dan mekanisme perubahan ion. Sedimen kelodak-liat berhampiran sungai didapati kaya dengan kandungan organik (Warren 1981; Lara *et al.* 1985) mempunyai kapasiti pertukaran kation yang tinggi. Sedimen halus mempunyai permukaan yang lebih besar (Horowitz 1985) dan memudahkannya memerangkap sedimen yang kaya dengan logam, manakala sedimen berpasir kurang berkemampuan memegang ion-ion logam.

PENGHARGAAN

Kajian ini dilakukan dengan bantuan kewangan daripada Kementerian Sains, Teknologi & Alam Sekitar Malaysia di bawah IRPA (NO. Projek 51513). Penulis juga ingin merakamkan jutaan terima kasih kepada semua kakitangan makmal MARU di atas segala kerjasama semasa pensampelan dilakukan.

REFERENCES

Barreiro, R., C. Real dan A. Carballeira. 1994. Heavy metal horizontal distribution in surface sediments from a small estuary. *Sci. Total Envinron.* **154**: 87–100.

Bowen, H. J. M. 1979. *Environmental Chemistry of Elements.* ms. 333 London: Academic Press.

Eisma, D., G. W. Berger, C. Wei Yue dan S. Jian. 1989. Pb-210 as a tracer for sediment transport and deposition in the Dutch-German Waddensea. Dalam *Proceedings KNGMFG Symposium Coastal Lowland, Geology and Geotechnology,* ms. 237–253. Dordrecht, Netherlands: Kluwer Academic Publishers.

Gong, W. K. dan J. E. Ong. 1990. Plant biomass and nutrient flux in a managed mangrove forest in Malaysia. *Estuarine and Coastal Shelf Science* **11**: 331–345.

Hatcher, B. G., R. E. Johannes dan A. I. Robertson. 1989. Review of research relevant to conservation of shallow tropical marine ecosystem. *Oceanography and Marine Biology: An Annual Review* **27**: 337–414.

Horowitz, A. J. 1985. *Sediment-trace Element Chemistry.* Edisi kedua. MI, USA: Lewis Publisher.

Jamil, B. T. 2002. Chemical elements in surface sediment of Kuantan mangrove forest, Pahang. Final year report, Bachelor Science (Marine Science), Faculty of Applied Science and Technology, Universiti Putra Malaysia Terengganu.

Kamaruzzaman, B. Y. 1999. Geochemistry of the marine sediments: its paleoceanographic significance. Ph.D Dissertation, Hokkaido University, Japan.

KAMARUZZAMAN, B. Y., I. RAZARUDIN, N. A. M. SHAZILI, H. MOHD LOKMAN dan I. SULONG. 2001. The geochemistry of Ba, U, Cd and Mn in the surface sediments of Matang Mangrove, Malaysia. *Oriental Journal of Chemistry* **17(3):** 377–382.

KAMARUZZAMAN, K. Y., H. SUHAIMI, E. K. TEH, H. F. LEONG, K. H. SOON dan K. Y. CHONG. 2000. The determination of ^{230}Th in the sediments: sedimentation in the mangrove Forests of Pulau Sekeping, Kemaman, Terengganu. *Journal of Ultra Scientist of Physical Sciences* **13(2):** 239–245.

LARA, R. J., E. A. GOMEZ dan A. E. PUCCI. 1985. Organic matter, sediment particle size and nutrient distributions in a sewage affected shallow channel. *Mar. Pollut. Bull.* **16**: 360–364.

MARTIN, J. M. dan M. WHITFIELD. 1983. The significant of the river input of chemical elements to the ocean. Dalam *Trace Metals in Sea Water,* disunting oleh C. C. Wong, E. A. Boyle, K. W. Bruland, J. D. Burton dan E. D. Goldberg, ms. 265–296. New York: Plenum.

MARTIN, J. M., F. ELBAZ-POULICHET, C. GUIEU, M. D. LOYE-PILOT dan G. HAN. 1989. River versus atmospheric input to the western meditereanean: A summary. Dalam *Water Pollution Research Reports 13,* disunting oleh J. M. Martin and H. Barth, ms. 423–434. EROS 2000. CEC Brussels.

MCBRIDE, E. F. 1971. Mathematical treatment of size distribution data. Dalam *Procedures in Sedimentary Petrology,* disunting oleh R. E. Carver. New York: Wiley Interscience.

MOHD LOKMAN, H., S. MEREHOJONO, N. A. M. SHAZILI, Y. ROSNAN dan A. R. K. KAMIL. 1994. Neap tidal transport of particulate organic matter (POM) in a mangrove creek at Pulau Sekeping, Kemaman, Terengganu. Dalam *3rd Symposium of Applied Biology,* ms. 106–109.

MASON, B. dan C. B. MOORE. 1982. *Principles of Geochemistry.* Edisi keempat ms. 344. New York: J. Wiley and Sons.

NOLTING, R. F. dan W. HELDER. 1991. Lead and zinc as indicators for atmospheric and riverine particle transport to sediments in the Gulf of Lions. *Oceanologica Acta* **14(4):** 357–367.

NORIKI, S., K., T. NAKANISHI, M. FUKAWA, T. UEMATSU, H. UCHIDA dan S. TSUNOGAI. 1980. Use of a teflon vessel for the decomposition followed by the determination of chemical contituents of various marine samples. *Bull. Fac. Fish, Hokkaido Univ.* **31**: 354–465.

REAL, C., R. BARREIRO dan A. CARBALLEIRA. 1993. Heavy metal mixing behaviour in estuarine sediments in the Ria de Arousa (NW Spain). *Sci. Total Envinron.* **128**: 51–67.

SEN GUPTA, J. G. dan N. B. BERTRAND. 1995. Direct ICP-MS determination of trace and ultratrace elements in geological materials after decomposition in a microwave oven, Quantitation of Y, Th, U and the lanthanides. *Talanta.* **42**: 1595–1607.

SHAHBUDDIN, S., H. MOHD LOKMAN, Y. ROSNAN dan T. ASANO. 1998. Sediment accretion and variability of sedimentological characteristics of a tropical estuarine mangrove: Kemaman, Terengganu, Malaysia. *Mangroves and Salt Marshes* **55**: 1–8.

SPENCELEY, A. P. 1982. Sedimentation patterns in a mangal on Magnetic Island near Townville, North Queensland, Australia. *Singapore Journal of Tropical Geography* **3**: 100-107.

THONG, K. L. dan A. SASEKUMAR. 1984. The trophic relationships of the fish community of the Ansa Bank, Selangor, Malaysia. Dalam *Proceedings of the UNESCO Asian Symposium on "Mangrove Environment: Research and Management*, disunting oleh E. Soepadmo, A. N. Rao dan D. J. MacIntosh, ms. 385–399. Universiti Malaya.

WAREN, L. J. 1981. Contamination od sediments by lead, zinc and cadmium – A review. *Environ. Pollut.* **2**: 401–436.

YEATS, P. A. dan J. M. BEWERS. 1983. Potential anthropogenic influences on trace metals distribution in the North Atlantic. *Canadian Journal of Fisheries and Aquatic Sciences* **40**: 124 – 131.

ISSN: 0128-7680
Pertanika J. Sci. & Technol. 12(1): 93 - 101 (2004) © Universiti Putra Malaysia Press

Determination of Greenhouse Time Constant Using Steady-state Assumption

Rimfiel B. Janius & [1]Bryan M. Jenkins
Department of Biological and Agricultural Engineering
Faculty of Engineering, Universiti Putra Malaysia
43400 UPM, Serdang, Selangor, Malaysia
[1]Department of Biological and Agricultural Engineering
University of California Davis
California 95616, USA

Received: 22 August 2002

ABSTRAK

Satu kajian dijalankan untuk menentukan kebolehgunaan penyelesaian keadaan mantap untuk meramal perubahan suhu udara dalaman dan jisim terma sebuah rumah kaca berbangku panas sebagai respons kepada satu perubahan tetap pada suhu luaran. Ini adalah kerana analisis keadaan mantap adalah lebih mudah daripada analisis fana. Walau bagaimanapun, penyelesaian keadaan mantap hanya sesuai jika pemalar masa rumah kaca pendek berbanding jumlah masa pada mana keadaan luaran rumah kaca dikira lebih kurang tetap. Satu kaedah berparameter tergumpal berdasarkan Albright *et al.* (1985) digunakan untuk menganggar pemalar masa bagi rumah kaca berbangku panas. Pemalar masa ini didapati amat sensitif kepada pekali pemindahan haba, h_m, di antara jisim terma dan udara dalaman. Nilai h_m yang tinggi menghasilkan pemalar masa yang lebih panjang. Bagi sifat-sifat jisim terma yang dianggarkan, nilai h_m bagi keadaan luaran yang lebih kurang mantap secara sementara ialah 0.23 $Wm^{-2} K^{-1}$ dengan pemalar masa lebih kurang 0.75 jam. Jangka masa ini dikira pendek berbanding tempoh ujian selama 6 jam. Oleh itu analisis keadaan tetap adalah sesuai.

ABSTRACT

A study was conducted to determine the applicability of a steady-state solution in predicting the changes in temperatures of the inside air and thermal mass of a bench-top-heated greenhouse in response to a step change in outside temperature. The steady-state analysis is simpler than that of the transient. However, a steady-state solution would only be appropriate if the time constant of the greenhouse is short compared to the total time under which the conditions outside the greenhouse are considered to be approximately constant. A lumped parameter method based on Albright *et al.* (1985) was used to estimate the time constant of the bench-top-heated greenhouse. The time constant was found to be very sensitive to the heat transfer coefficient, h_m, between the thermal mass and inside air. A high value of h_m results in a longer time constant. For the estimated thermal mass properties, the value of h_m for the temporarily approximately constant outside conditions was calculated to be 0.23 $Wm^{-2} K^{-1}$ for which the estimated time constant was about 0.75 hour. This time was reasonably short compared to the six-hour experimental period; thus the steady-state analysis was appropriate.

Keywords: Bench-top heating, greenhouse time constant, greenhouse thermal mass

INTRODUCTION

As the outside temperature changes, the greenhouse interior air temperature will be forced to change accordingly if there is no control system in the house. If the outside temperature reaches a steady state, the interior air temperature will also eventually come to a steady state. The time constant of a greenhouse is the time taken for the greenhouse to reach 63% of its steady-state value in response to a step change in the corresponding outside condition. If the time constant is very long, say in the order of days, then a steady-state numerical solution would be meaningless as the greenhouse would never achieve steady state before the outside temperature changes again. If the time constant is short, the inside temperature would tend to rapidly follow the outside condition.

In practice, the outside air temperature continually changes and the greenhouse may never achieve a truly steady-state condition even if the time constant were short. A steady-state value obtained by simulation would be that which the house was supposed to have reached had the outside temperature not changed. However, if the outside conditions become relatively stable, then at least a pseudo steady-state inside condition will be observed (assuming the control state is constant), which is the case for the experimental data reported.

Greenhouse temperature can be presented either as single average temperature of the inside air or as a temperature distribution throughout the greenhouse space. The ever changing outside environmental factors influence environmental conditions inside the greenhouse. A number of techniques exist for predicting the interior response for steady or transient outside conditions. Steady-state analyses have been done by many researchers including Walker (1965), Short and Breuer (1985) and Jolliet *et al.* (1991). Many others have used transient analyses, including Takakura *et al.* (1971), Deltour *et al.* (1985) and Garzoli (1985). In these analyses the greenhouse is generally divided into four basic elements making up the greenhouse system, i.e., the floor, the plant, the inside air and the cover. On each of these systems heat balance equations are established and the resulting set of equations solved simultaneously to obtain the desired quantities such as temperature and humidity. The intent is typically to obtain an estimate of the bulk air, soil or crop temperature and air humidity.

The thermal parameters of the greenhouse are usually described in terms of the overall heat transfer coefficient and a number of other factors such as the solar transmission of the greenhouse cover, solar heating efficiency or absorbency, and heat capacity of the soil. Depending upon the individual situation faced, the overall heat transfer coefficient may or may not include the convective, radiative and ventilation losses, and condensation. Since each coefficient is usually calculated for a specific greenhouse with specific geometry and specific nature of heat requirement the values of the overall heat transfer coefficients reported are quite variable.

The objectives of this study are to calculate the overall heat transfer coefficient (h_m) and time constant of the bench-top-heated greenhouse and to observe the effect of a step change in outside temperature on the temperatures of the inside air and thermal mass.

METHODS

Experimental data used in the analysis were those of the works of Jenkins *et al.* (1988 and 1989). Jenkins *et al.* (1989) experimentally examined the two-dimensional overall heat transfer of a bench-top-heated greenhouse. In the bench-top heating system, heat is applied to areas where it is needed most, i.e., the plant canopy, by circulating hot water through tubing running through or on the bench. A gable-roof greenhouse with a floor area of 217 m^2 and longitudinally oriented in the east-west direction, was gutter-connected to identical houses on the north and south sides. It was clad with 3 mm thick glass. The benches were 0.69 m above the floor. Each bench carried a bench-top heat exchanger consisting of 8 mm diameter plastic tubes (wall thickness 1.5 mm) which made four passes up and down the length of the bench. To improve the uniformity of the canopy heating and reduce heating of the pots and soil, an expanded steel mesh was mounted 25 mm above the top bench surface and above the heater tubing. Potted plants were placed on this mesh. The greenhouse was not ventilated and all opening and fan shutters were covered with plastic sheet to reduce infiltration losses. To check for heat transfer across the connecting sidewalls and roof, thermocouples were fixed on the inside and outside surfaces of each wall and ceiling. A detailed description of the bench-top heating system and its instrumentation is described in Jenkins *et al.* (1988 and 1989).

Only night time data from 0000 hours to 0600 hours (both inclusive) were used in the analysis because the outside temperature during this period was reasonably constant at somewhat below 0°C. As shown in the data of Table 1, the outside temperatures during this period were also fairly constant ranging from –0.2°C to –1.5°C with an average of –0.8°C. This condition enabled the actual bench-top heating system to work continuously and steadily at full capacity. The various temperatures inside the greenhouse were also fairly constant at each hour in the period. Thus the greenhouse was essentially already at steady state at 0000 hours. According to Jenkins *et al.* (1989), the temperature distributions in the greenhouse remained nearly steady from midnight to 0600 hours. Therefore the average condition of the greenhouse was calculated to steady state.

TABLE 1
Hourly average outside temperature and wind speed for the experimental greenhouse during the period studied

Hours of night	0000	0100	0200	0300	0400	0500	0600
Outside temp., °C	-0.2	-0.4	-0.7	-1.5	-1.1	-1.5	-0.6
Wind speed, m/s	2.797	3.134	3.202	3.167	3.472	3.399	3.087

A constant temperature boundary condition was assumed for all walls, floor and ceiling. Air temperature at the lower boundary (the bench surface) was approximately constant at 30°C. Boundary temperatures at the top, left and

right were 6.5°C, 16°C and 15°C, respectively. These values were obtained by taking the average of the seven hourly values (from 0000 to 0600 hours, both inclusive) of the air at the inside surfaces of the ceiling, left wall and right wall, respectively.

A lumped parameter representation of the greenhouse based on Albright *et al.* (1985) was used to estimate the time constant of the greenhouse. The greenhouse was divided into two subsystems, namely a) the interior air and b) the thermal mass, which included the crop mass, structural mass, floor mass and all other non-air elements in the greenhouse. Energy balances were carried out on each subsystem by considering each as a control volume. Since the greenhouse was analyzed for the nighttime condition only, no solar radiation was involved.

RESULTS AND DISCUSSION

Symbols:

m_a – mass of air in greenhouse, kg
c_a – heat capacity of inside air, J kg^{-1} K^{-1}
T_i – mean temperature of inside air, °C
t – time, s
h_m – heat transfer coefficient between thermal mass and inside air, $W\ m^{-2}\ K^{-1}$ of floor area
A – greenhouse floor area, 217 m^2
T_m – mean temperature of thermal mass, °C
U – overall heat transfer coefficient between inside air and outside air, $W\ m^{-2}\ K^{-1}$ of floor area
T_o – outside air temperature, °C
k_a – thermal conductivity of air at 1 atm and 15°C = 0.0253 $W\ m^{-1}\ K^{-1}$ (Incropera and De Witt 1985)
m_m – thermal mass, kg
c_m – heat capacity of the thermal mass, J kg^{-1} K^{-1}
m_c – mass of concrete, kg
m_s – mass of soil, kg

A transient energy balance on the interior air gives the following equation:

$$\frac{dT_i}{dt} = \frac{A}{m_a c_a}\{h_m(T_m - T_i) + U(T_o - T_i)\} \quad (1)$$

Air properties inside the greenhouse were taken at one atmospheric pressure and 15°C. The overall heat transfer coefficient of the greenhouse per unit floor area is U=5+1.2v (Jenkins *et al.* 1989), where v is the outside wind speed in m s^{-1}. Average wind speed for the six-hour period under study was 3.18 m s^{-1} giving U = 8.82 $W\ m^{-2}\ K^{-1}$.

According to Albright *et al.* (1985), the thermal mass of a greenhouse is comprised, to a large extent, of the greenhouse floor. In the present study, the heat transfer coefficient between the floor and the inside air was assumed to be the coefficient between the thermal mass and the inside air. Further, the greenhouse floor was assumed to be similar to a heated horizontal plate. Incropera and De Witt (1985) gave the Nusselt number correlation for a heated horizontal plate as: $Nu = 0.54Ra_L^{0.25}$, where Ra_L is the Rayleigh number. Computing for the Pr and the highest Gr used by Janius (1996) in a numerical study of the same greenhouse:

$$Nu \equiv \frac{h_m L}{K_a}$$
$$= 0.54(\mathrm{Pr}*\mathrm{Gr})^{0.25}$$
$$= 0.54(0.715*10^9)^{0.25}$$
$$= 88.3$$

Thus, $h_m = 0.23\ W\ m^{-2}\ K^{-1}$.

A transient energy balance on the thermal mass at night yields:

$$\frac{dT_m}{dt} = -\frac{A}{m_m c_m}\{h_m(T_m - T_i)\} \qquad (2)$$

The 217 m^2 floor area is made up 67% of 0.1 m deep concrete and 33% soil (for thermal mass purposes a depth of 1 m is assumed). Taking the density of concrete to be 2300 kg m^{-3} and that of soil to be 2050 kg m^{-3}, the estimated thermal mass, m_m, is 180,240 kg. The value of c_m is taken to be the average of the specific heat capacities of concrete and soil whose values are 880 J kg^{-1} K^{-1} and 1840 J kg^{-1} K^{-1}, respectively. Thus c_m = 1360 J kg^{-1} K^{-1}.

A numerical integration scheme employing a simple Euler predictor-corrector method was used to solve both equations (1) and (2) simultaneously. Step changes in the outside air temperature were imposed and the response of the interior air was obtained. The time taken for the interior temperature to reach 63% of its steady-state value after imposition of the step change in outside temperature was the time constant, t, of the greenhouse.

The estimated time constant for the greenhouse air under nighttime condition is 0.75 hour. Simulation results, at various values of h_m, of the response of the greenhouse to a step change in outside temperature, are shown in *Figs. 1a-1e.* A plot of the various time constants obtained against their respective heat transfer coefficients, h_m, shows the greenhouse response to outside forcing temperature to be very sensitive to the value of h_m (*Fig. 2*). For the lower time constants and a relatively constant outside temperature, an assumption of steady state is probably reasonable. At larger time constants,

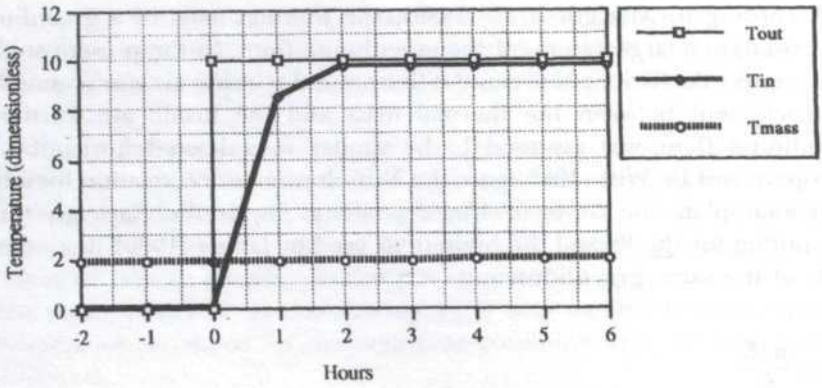

Fig. 1a: Greenhouse response to step change in outside temperature
h_{in}=0.23 W m^{-2} K^{-1}, U=8.8 W m^{-2} K^{-1}

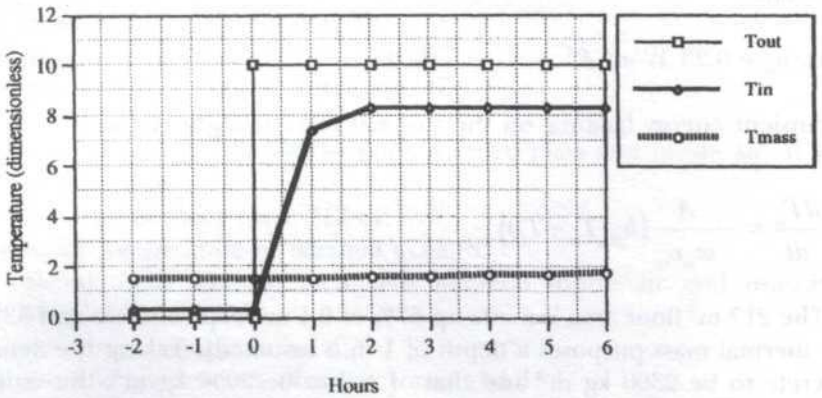

Fig. 1b: Greenhouse response to step change in outside temperature
h_{in}=2.3 W m^{-2} K^{-1}, U=8.8 W m^{-2} K^{-1}

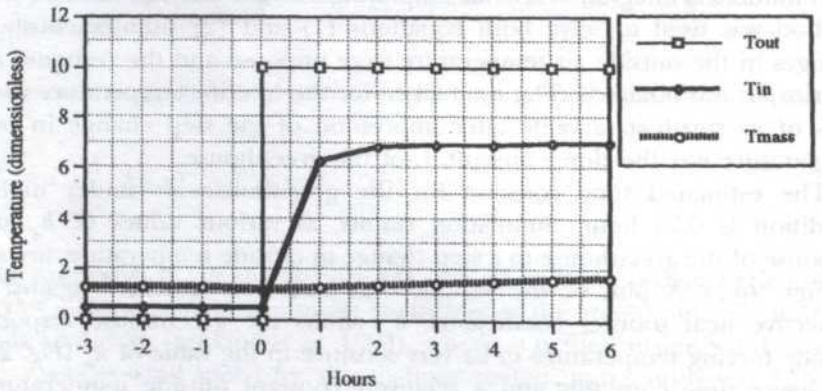

Fig. 1c: Greenhouse response to step change in outside temperature
h_{in}=5 W m^{-2} K^{-1}, U=8.8 W m^{-2} K^{-1}

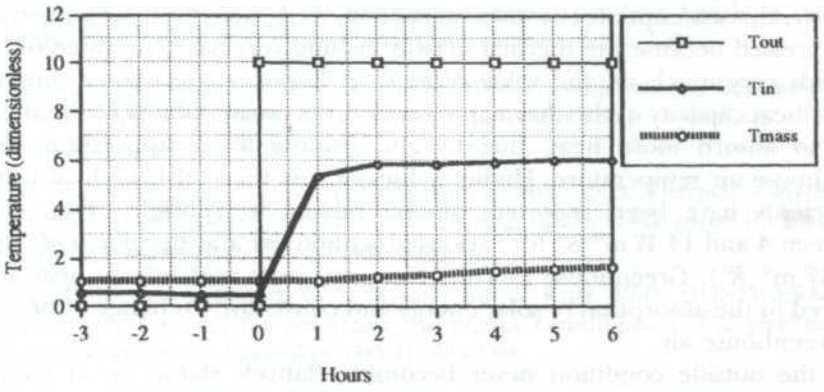

Fig. 1d: Greenhouse response to step change in outside temperature h_m=8 W m^{-2} K^{-1}, U=8.8 W m^{-2} K^{-1}

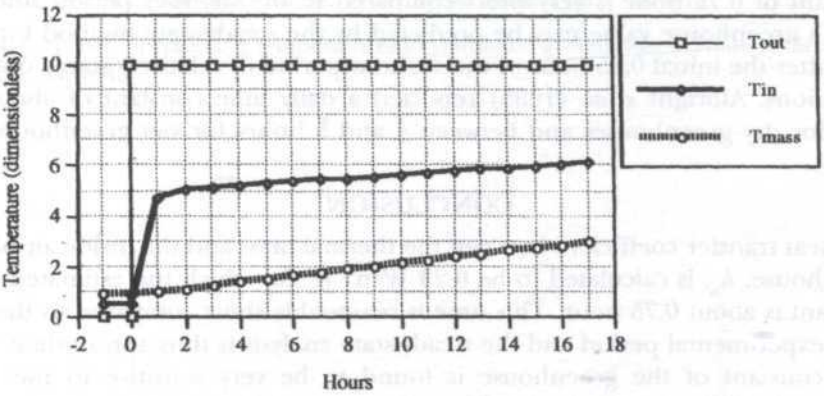

Fig. 1e: Greenhouse response to step change in outside temperature h_m=11 W m^{-2} K^{-1}, U=8.8 W m^{-2} K^{-1}

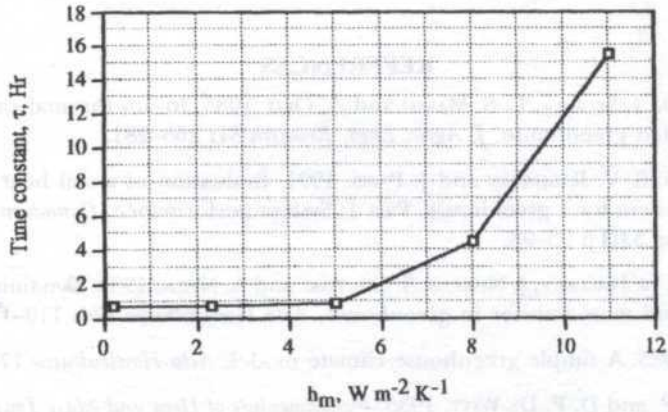

Fig. 2: Sensitivity of the greenhouse time constant to the heat transfer coefficient between the thermal mass and inside air

however, this assumption becomes unjustified. As h_m increases, air temperature is suppressed because the thermal mass is heating very fast. The value of t also depends very much on the value of $m_m c_m$. A higher value of $m_m c_m$ implies a higher heat capacity of the thermal mass, hence a greater ability of the thermal mass to absorb more heat, thereby also leading to a suppression of the greenhouse air temperature. Higher values of soil/thermal mass heat transfer coefficients have been reported, among others, by Albright *et al.* (1985) (between 4 and 14 $W\,m^{-2}\,K^{-1}$ for various greenhouses) and Bernier *et al.* (1991) (5.4 $W\,m^{-2}\,K^{-1}$). Greenhouse thermal mass can store and release heat and is involved in the absorption of solar energy and convective exchange of heat with the greenhouse air.

If the outside condition never becomes relatively stable for at least the length of the time constant, then, no matter how short the time constant is, the steady-state assumption would be invalid. At the estimated h_m, the steady-state assumption for the greenhouse under study is appropriate because the time constant of 0.75 hour is very short compared to the six-hour period studied. Thus a greenhouse value may be predicted by the steady-state method for any time after the initial 0.75 hour of the six-hour period of relatively stable outside conditions. Albright *et al.* (1985) reported a daily time constant of about 40 min. for dry greenhouses and between 4 and 5 hours for wet greenhouses.

CONCLUSION

The heat transfer coefficient between the thermal mass and the inside air of the greenhouse, h_m, is calculated to be 0.23 $W\,m^{-2}\,K^{-1}$ for which the estimated time constant is about 0.75 hour. This time is reasonably short compared to the six-hour experimental period and the steady-state analysis is thus appropriate. The time constant of the greenhouse is found to be very sensitive to the heat transfer coefficient between the thermal mass and the inside air, h_m. For the estimated thermal mass properties, if h_m is low then a steady-state assumption for the analysis is more readily established for temporarily constant outside conditions.

REFERENCES

ALBRIGHT, L. D., I. SEGINER, L. S. MARSH and A. OKO. 1985. In-situ thermal calibration of unventilated greenhouse. *J. Agric. Engr. Research* **31:** 265–281.

BERNIER, H., G. S. V. RAGHAVAN and J. PARIS. 1991. Evaluation of a soil heat exchanger-storage system for a greenhouse. Part 1: System performance. *Canadian Agricultural Engineering* **33(1):** 93–98.

DELTOUR, J., D. DE HALLEUX, J. NISKENS, S. COUTISSE and A. NISEN. 1985. Dynamic modelling of heat and mass transfer in greenhouse. *Acta Horticulturae* **174:** 119–126.

GARZOLI, G. 1985. A simple greenhouse climate model. *Acta Horticulturae* **174:** 393–400.

INCROPERA, F. P. and D. P. DE WITT. 1985. *Fundamentals of Heat and Mass Transfer.* 2nd ed. New York: John Wiley and Sons.

JANIUS, R. B. 1996. A simulation of the laminar convection in a bench-top heated greenhouse. Unpublished Ph.D. thesis, Univ. of Calif. Davis, USA.

JENKINS, B. M., R. M. SACHS and G. W. FORRISTER. 1988. A comparison of bench-top and perimeter heating of greenhouses. *California Agriculture* **42(1):** 13–15. Univ. of Calif. Div. of Agric. and Nat. Resources.

JENKINS, B. M., R. M. SACHS, G. W. FORRISTER and I. SISTO. 1989. Thermal response of greenhouses under bench and perimeter heating, ASAE/CSAE paper no.89–4038. *International Summer Meeting*, Quebec, Canada.

JOLLIET, O., L. DANLOY, J. B. GAY, G. L. MUNDAY and A. REIST. 1991. HORTICERN: An improved static model for predicting the energy consumption of a greenhouse. *Agricultural and Forest Meteorology* **55(3-4):** 265–294.

SHORT, T. H. and J. J. G. BREUER. 1985. Greenhouse energy demand comparisons for the Netherlands and Ohio, USA. *Acta Horticulturae* **174:** 145–153.

TAKAKURA, T., K. A. JORDAN and L. L. BOYD. 1971. Dynamic simulation of plant growth and environment in the greenhouse. *Trans. of the ASAE* **14(5):** 964–971.

WALKER, J. N. 1965. Predicting temperatures in ventilated greenhouses. *Trans. of the ASAE* **8(3):** 445–448.

ISSN: 0128-7680
Pertanika J. Sci. & Technol. 12(1): 103 - 113 (2004) © Universiti Putra Malaysia Press

Structural Response of Initially Loaded RC Beam to Different Retrofitting Techniques

Waleed A. Thanoon, M. S. Jaafar, J. Noorzaei, Mohd Razali Abdul Kadir & Thamer A. Mohamed
Civil Engineering Department, Faculty of Engineering, Universiti Putra Malaysia, 43400 UPM, Serdang, Selangor, Malaysia

Received: 18 November 2002

ABSTRACT

Penambahan bilangan struktur konkrit yang rosak telah menggariskan peri pentingnya memajukan teknik baik pulih yang boleh diterima. Kertas ini membentangkan kajian ke atas kelakuan struktur rasuk konkrit tetulang yang dibaik pulih dengan dua kaedah yang berbeza. Teknik pertama menggunakan CFRP sebagai pengukuh, sementara sistem prategasan luaran digunakan sebagai teknik kedua. Spesimen dikenakan beban awal sehingga dua pertiga daripada beban muktamad yang dijangka. Beban kemudian dilepaskan dan rasuk-rasuk tersebut dibaik pulih dengan CFRP atau prategasan luaran. Spesimen dikenakan dengan beban sehingga ke tahap gagal. Respons struktur telah ditinjau berkenaan kelakuan retakan, hubungan beban-pesongan, kemuluran, agihan terikan, beban muktamad dan ragam kegagalan. Keputusan menunjukkan respons yang serupa pada kedua-dua teknik tersebut. Oleh itu, konsep reka bentuk kenyal yang digunakan untuk konkrit prategasan boleh digunakan untuk reka bentuk konkrit dengan CFRP.

ABSTRACT

The increase in the large number of distressed reinforced concrete structure underscores the importance of developing acceptable retrofitting techniques. This study investigates the structural behaviour of full scale reinforced concrete beams strengthened by two different techniques. The first technique used is the strengthening of the beam by CFRP, while the second technique used is the external pre-stressing. The specimens were initially loaded to two-thirds of their predicted ultimate flexural capacity. They were then unloaded and strengthened with either CFRP or external prestressing. The beams were subsequently subjected to incremental loads until failure. The structural response of the tested specimens had been found in terms of their cracking behaviour, load-deflection relationship, ductility, strain, distribution, ultimate load and failure mechanism. The results indicate similar structural response in both retrofitting techniques at the ultimate range. Hence the concept of elastic design used in prestressed concrete members may be used for reinforced concrete members strengthened with CFRP.

Keywords: Loaded RC beam, retrofitting techniques, CFRP, structural response

INTRODUCTION

The repair of structurally deteriorated reinforced concrete structures becomes necessary as the structural element ceases to provide satisfactory strength and

serviceability. Many different types of distress in the reinforced concrete structures have been observed recently. Cracking and spalling are the common distresses in reinforced concrete slabs and beams. To restore the structural capacity of the damaged element in order to resist the stresses developed due to the applied load, repair and/or strengthening techniques are needed. There are different techniques available for repair and strengthening of different reinforced concrete structural elements. With the rapid development in material and polymer technology, more effective and practically convenient material has been introduced in this field.

Carbon Fibre Reinforced Polymer has a high strength to weight ratio, favourable fatigue behaviour and excellent resistance to electrochemical corrosion to make it practically suited for structural application. Clark and Waldron (1996) presented the application of the advance fibre materials in construction. The carbon CFRP bonded externally appears to be the favourite solution for strengthening reinforced and/or pre-stressed concrete structures. Thin FRP laminates, less than 1 mm thick, are currently used in Switzerland, U.K and Japan in bridge strengthening.

Tan and Wong (1997) investigated the behaviour of 3 simply supported prototype beams externally bonded with CFRP plates. The internal longitudinal steel ratios used are 0.57%, 0.86% and 1.29%. Different amounts of CFRP plates had been added to achieve similar replacement ratio of 0.5 in all the beams. It has been found that for the beam reinforced with a steel ratio less than 0.86%, collapse was due to full bond failure of the CFRP plate. However, for the beam with higher steel ratio of 1.29%, the final collapse was due to flexural compression, i.e. crushing of concrete of the top of the beam.

Alfarabi *et al.* (1998) studied the effect of different strengthening configurations of 10 reinforced concrete beams using CFRP plates. The behaviour of the repaired beams is represented by their load-deflection curves and their different modes of failures. The results generally indicate that the flexural strength of the repaired beams is increased. Failure of different strengthened specimens was initiated at the plate curtailment zone at the beam ends.

Khaled *et al.* (1999) tested six reinforced concrete beams; five of the beams were strengthened with one CFRP strip of SikaCarboDurS1012, which was epoxied to the tension side of the beam. The sixth beam had no CFRP strip and was used as a control beam. The study focused on the effect of strengthening beams by CFRP strips externally to the tension face of the beam with varying un-bonded regions. Beams strengthened with CFRP strips had larger flexural capacity over the control beam. The beams with partially bonded CFRP strips exhibited higher ultimate capacity than the beam with fully bonded CFRP strips. Moreover, it was found that the CFRP strips slipped relative to concrete near the ends of the beam during the loading period. The flexural resistance of the strengthened beams increased by about 20% for yield strength and 34% for ultimate strength when compared to the un-strengthened beams.

Toong and Li (2000) investigated the effect of using CFRP plates to strengthen one-way spanning slab to increase the flexural capacity with particular

emphasis on the cracking behaviour at working load. All the CFRP strengthened specimens exhibited large increase in load-carrying capacity ranging from 60% to 140 %.

In the externally post tensioning pre-stressing strengthening technique, a pre-stressing strand or bar is used to apply a predetermined compressive force. To get effective results, the developed cracks are initially treated before applying the pre-stressing force so that there will be minimum loss in energy required to close the cracks (Raina 1994).

Emmons (1994) describes the use of external post-tensioned prestressing methods for increasing the flexural capacity of reinforced concrete members. External post-tensioning prestressing provides for immediate and active participation in both dead and live load distributions

Tan and Ng (1997) investigate the structural response of 6 reinforced concrete T beams strengthened using external prestressing tendons. The study focuses on the effect of tendon configuration and the number and location of the deviators into the structural response. Test results indicate that the provision of a deviator at the section of maximum deflection led to satisfactory service load behaviour and a higher load carrying capacity compared to the case where no deviators were provided. Moreover, the configuration of the tendon has a significant effect on the structural response of the strengthened beams.

According to ACI Committee-224 (1993), the external post-tensioning is a desirable solution when a major portion of a member must be strengthened or when the cracks that have formed must be closed. Adequate anchorage must be provided for the pre-stressing steel, and care is needed so that the problem will not merely migrate to another part of the structure. The effects of the tensioning force (including those of eccentricity) on the stress within the structure should be carefully analysed.

To date, the effect of many parameters on the structural behaviour of the strengthened structural elements using CFRP strips and external pre-stressing is still not clear especially in the absence of codal requirements and clearly defined design specifications. The main goal of this paper is to investigate experimentally the effectiveness of using CFRP strips in strengthening reinforced concrete beams compared to external pre-stressing concrete beams. The study provides insight on the overall structural behaviour and ductility.

EXPERIMENTAL PROGRAM AND STRENGTHENING TECHNIQUE

Three full scale reinforced concrete beams have been cast, cured and tested. The beams have a span of 3.2m with rectangular cross section having dimension of 130mm by 250mm (width x depth). The steel reinforcement in the beam consists of 2Y10 (steel ratio= 0.48%). The steel has characteristic strength of 460 N/mm^2. The 28-day cube compressive strength, f_{cu} of the concrete used is 30 N/mm^2.

All the specimens are tested under two-point load. Initially, two beam specimens are loaded to two-thirds of their predicted ultimate load capacity. Subsequently, the load was released and the specimens were removed from the

testing frame for strengthening. The other specimens (control specimen) are loaded until failure. The specimens are re-tested after allowing a suitable curing period till failure.

The structural response of each specimen in terms of deflection, stiffness, cracking load, ultimate load, and failure patterns are analysed. A 50 mm wide and 12 mm thick carbon fibre strip (CFRP) have been externally bonded to the soffit of the specimen at the tension face of the reinforced concrete beam using Sikadur30 epoxy adhesive (bonding agent). The carbon fibre strip has been placed at the central part of the beam specimens. The tensile strength of the carbon fibre strip is 2800 N/mm^2. Its modulus of elasticity = 165000 N/mm^2 and the density is 1.5 g/cm^3. The main characteristic of the Sikadur30 epoxy is presented in Table 1.

The third beam was strengthened externally by using 7 mm pre-stressing wires at both sides of the beam. To maintain the cable profile during the application of load, two deviators have been fixed at a distance equal to L/3 from each end of the beam using steel angle section fixed using two steel bolts. In addition, two 10 mm steel plates are fixed at the ends of the beam to anchor the pre-stressing wires. Both wires were pre-stressed until 75% of their ultimate strength (f_{pu}=1570 N/mm^2). After initial loading, the developed cracks are treated before applying the pre-stressing force using epoxy to minimize the loss in the pre-stressing force required to close the cracks.

TABLE 1
Characteristic of the sikadur30 epoxy

Characteristics	Guide Values
Sag flow	3 – 5mm at 35°C
Compressive strength	75 – 100 N/mm^2
Tensile strength	20 – 30 N/mm^2
Shear strength	15 – 20 N/mm^2
E-modulus (Static)	8000 – 16000 N/mm^2
Shrinkage	0.04 – 0.08%
Glass transition point	50°C – 70°C

STRUCTURAL RESPONSE

Cracking Load & Patterns

The initial cracking loads for the control specimen and strengthened beam specimens are shown in *Fig. 1.* The strengthening of the beam by bonding Carbon Fibre Strip (CFRP) at its bottom will not alter the cracking load. The number of cracks observed in the strengthened specimen with CFRP is approximately equal to the number of cracks in the control specimen at service load. However, with the increase of the applied load, the number of cracks increased in the strengthened specimens.

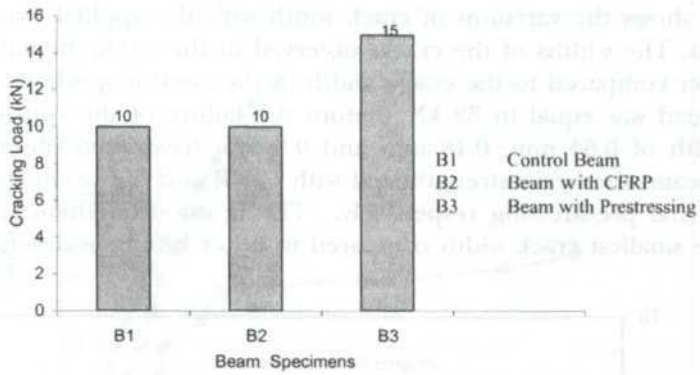

Fig. 1: Cracking load for the tested specimens

Beam specimens strengthened with external pre-stressing wires show the highest cracking load due to the development of compressive stress in concrete because of the external pre-stressing (50% increase in the cracking load has been observed). In the range of service load, the width of the cracks observed in beam B3 are smaller than those observed in B1 and B2. However with further increase in the applied loads, the crack width increases and becomes wider as compared to B1 and B2. The crack patterns for the three beam specimens are shown in *Fig. 2.*

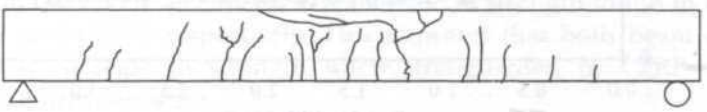

(a) Control Beam, B1

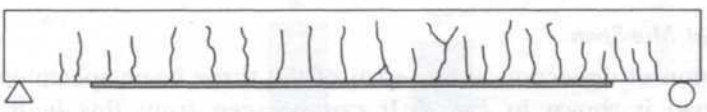

(b) Beam with CFRP, B2

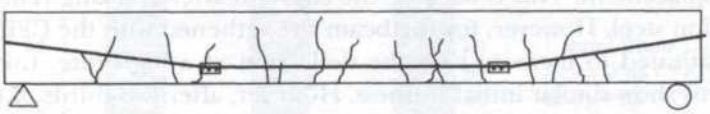

(c) Beam with External Pre-stressing, B3

Fig. 2: Crack patterns for different beam specimens

Fig. 3 shows the variation of crack width with the applied load for beam specimens. The widths of the cracks observed in the strengthened specimens are smaller compared to the cracks width in the control specimen. When the applied load was equal to 32 kN (before the failure of the control beam) a crack width of 0.64 mm, 0.18 mm and 0.8 mm have been observed in the control beam, the beam strengthened with CFRP and the beam strengthened with external pre-stressing respectively. The beam strengthened with CFRP shows the smallest crack width compared to other beam specimens.

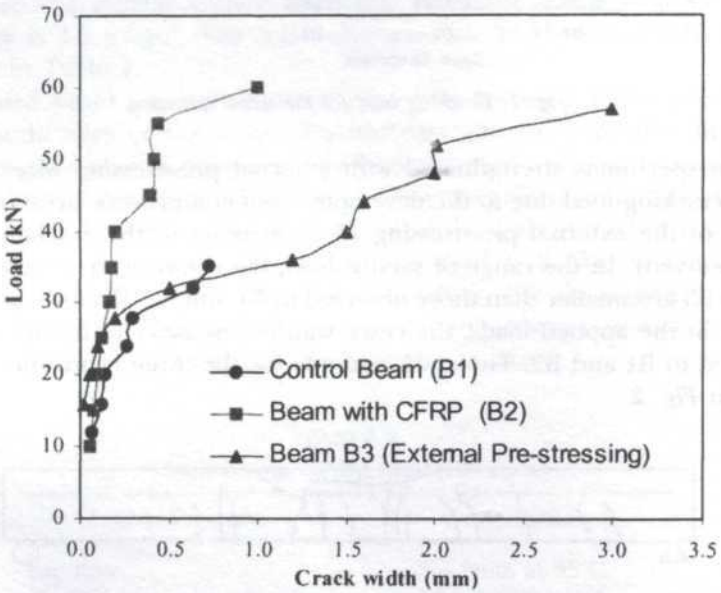

Fig. 3: Variation of crack width with the applied load

Deflection at Mid-Span

The variation of deflection at mid-span of the three beam specimens with the applied load is shown in *Fig. 4*. It can be seen from this figure that the behaviour of the strengthened beams differs from the control specimen. Once the steel yielded in the control specimen, very little additional load caused very large displacement. This is because the strength after cracking relies mainly on the tension steel. However, for the beam strengthened with the CFRP strips, the load continued to increase with the deflection at a high rate. Initially all the specimens show similar initial stiffness. However, after two-thirds of the ultimate load, the strengthened specimens exhibit different levels of ductility pattern compared to the control beam. The deflections decreased for the strengthened beams compared to the control beam by 50% at yielding and 58% at failure load, which indicates less ductile behaviour. The load–deflection curves of the strengthened beams are quite similar.

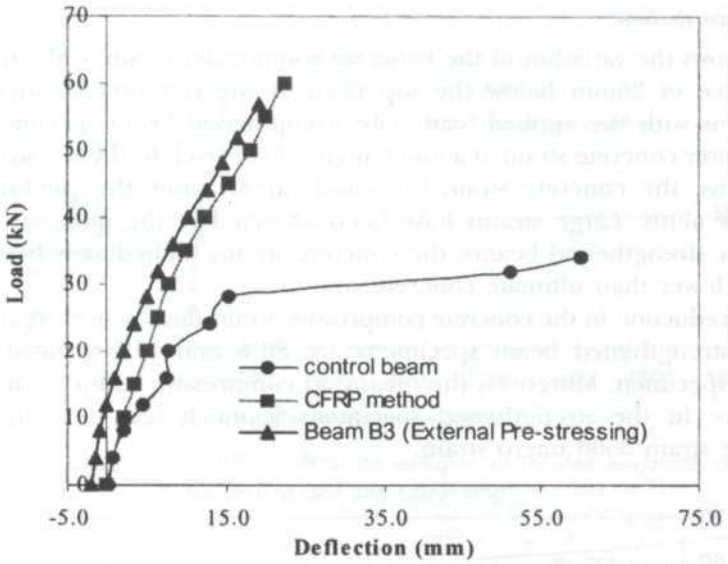

Fig. 4: Load-deformation characteristic for beam specimens

Ultimate Load

The strengthened beam specimens exhibited a significant increase in the flexural capacity over the control specimens. *Fig. 5* shows the ultimate failure loads for all the tested specimens. The increase in strength found in B2 and B3 are 71.5% and 62.8% respectively. This indicates that both beam specimens show similar increase in strength when strengthened by CFRP strips and external pre-stressing wires.

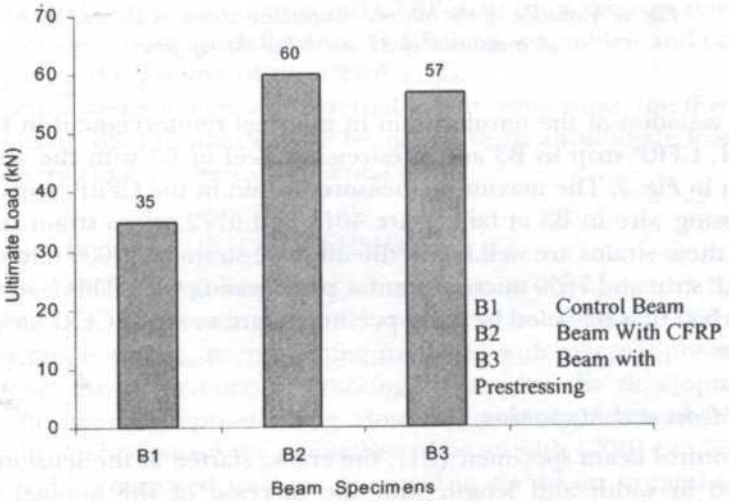

Fig. 5: Ultimate load for the tested specimens

Strain Distribution

Fig. 6 shows the variation of the concrete compressive strain at the mid-span at a distance of 25mm below the top fibre of the reinforced concrete beam specimens with the applied load. The strengthened beam specimens exhibit much lower concrete strain at a much higher load level. In the un- strengthened specimens, the concrete strain increased rapidly after the yielding of steel reinforcements. Large strains have been observed at the moment of failure, while for strengthened beams, the concrete strains immediately before failure are still lower than ultimate concrete strain.

The reduction in the concrete compressive strain (and hence stress) observed in the strengthened beam specimens are 80% and 71% compared to the control specimen. Moreover, the measured compressive strain in the concrete at failure in the strengthened specimens is much less than the ultimate concrete strain 3500 micro strain.

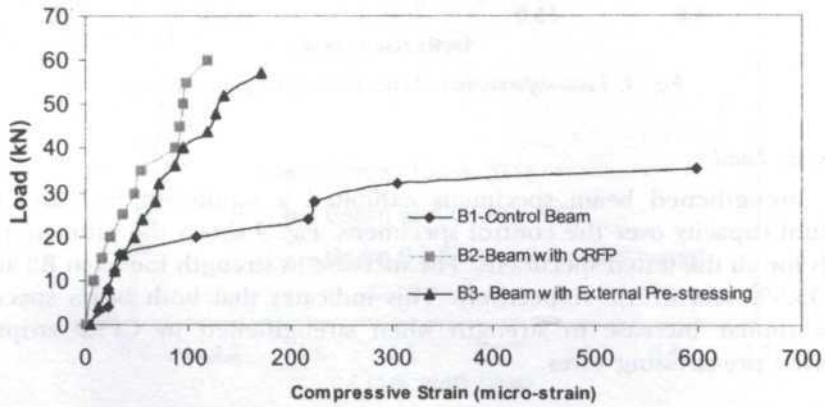

Fig. 6: Variation of the concrete compressive strain at the mid-span at a distance of 25 mm below the top fibre

The variation of the tensile strain in the steel reinforcement in the control beam-B1, CFRP strip in B3 and prestressing steel in B2 with the applied load is shown in *Fig. 7*. The maximum measured strain in the CFRP strips in B2 and pre-stressing wire in B3 at failure are 4011 and 5772 micro strain respectively. Both of these strains are well below the ultimate strain of 17000 micro-strain for the CFRP strip and 7650 micro strain for pre-stressing wire. This is in agreement with the fact that B2 failed by shear peeling failure mode at CFRP strip-concrete interface.

Failure Modes and Mechanism

In the control beam specimen (B1), the cracks started at the tension sides and increased in width and length with the increase of the applied load. The neutral axis location is shifted upwards until the concrete strain reaches its

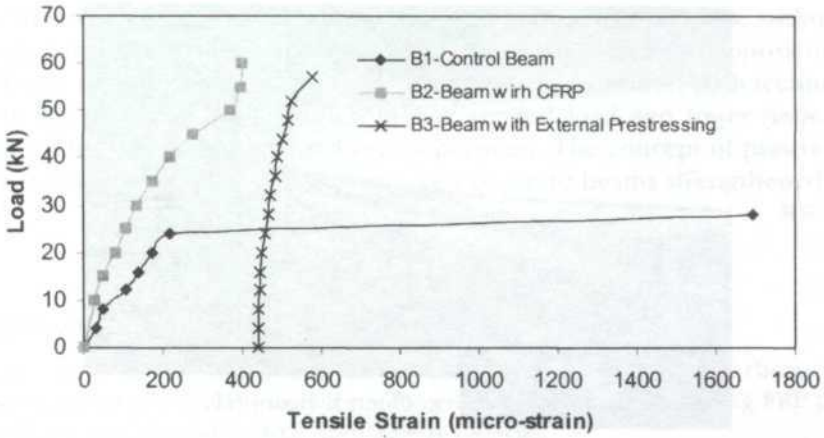

Fig. 7: Variation of the tensile strain at the mid-span in the steel reinforcement, prestressing steel and CRFP strip

ultimate value. At this stage, the steel reinforcement is yielded which quickly led to compressive crushing of concrete. This failure mechanism is a typical ductile failure observed in under-reinforced concrete sections. *Fig. 8* shows the crack pattern of the beam specimens at failure.

For the beam specimen with CRPF, the theoretical analysis using strain compatibility method according to the BS8110 indicates that the beam can resist a total load of 87.2kN before the concrete crushed in the strengthened beam. At this load, both steel and CFRP layers have reached their yielding stresses. The addition of CFRP increases the tensile area of the reinforcement and hence the beam is over-reinforced and fails in compression. However, from the experimental results, the strengthened beam fails at a load of 60 kN due to the separation of both the Sika paste and CFRP strip from the concrete at the strip ends after showing large deflection. The failure was sudden and occurred immediately after the peeling of the CFRP strips.

For the beam strengthened with external pre-stressing wires, the theoretical calculations using BS8110 indicate the beam can resist an ultimate load of 54 kN which is very close to the experimental value.

CONCLUSIONS

The structural behaviour of reinforced concrete beam strengthened by CFRP strip and external pre-stressing wires have been investigated. Within the serviceability range of load, strengthening the beam with external pre-stressing wires will delay the occurrence of cracking because of the development of compressive stresses due to pre-stressing. However, as the applied load increases, the crack width increases and the strengthened beam with CFRP exhibit much lower crack width compared to those observed in the beam strengthened by external pre-stressing wires. Bonding CFRP with the concrete will control and reduce the crack width.

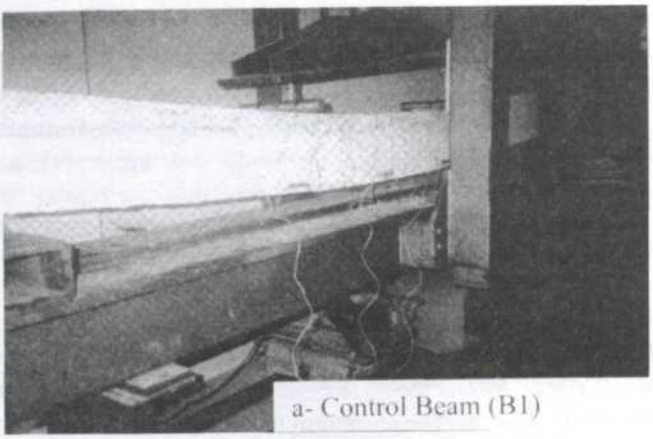

a- Control Beam (B1)

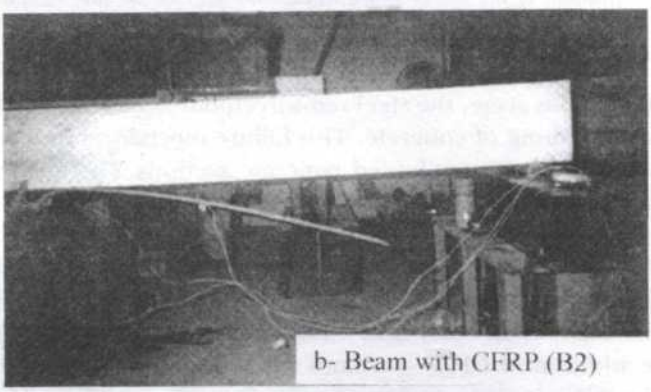

b- Beam with CFRP (B2)

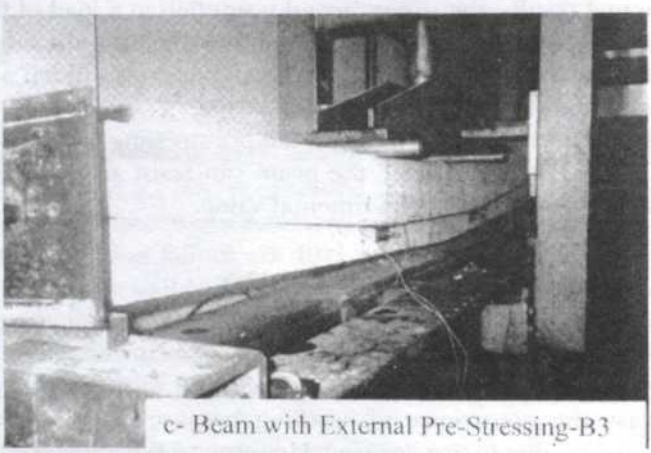

c- Beam with External Pre-Stressing-B3

Fig. 8: Failure mode of tested specimens

Both strengthening techniques show similar structural response within the ultimate range of loading. The ultimate failure load found was approximately double the failure load of the un-strengthened beam. However, both techniques lead to brittle failure under much higher applied load and lower deflection compared to the un-strengthened beam specimen. The concept of prestressing might be used for the design of reinforced concrete beams strengthened with CFRP.

REFERENCES

ACI 224.1R-93. Causes, evaluation & repair of cracks in concrete.

Alfarabi Sharif, G. J. Alsulaimani, I. A. Basunbul, M. H. Bamch and B. N. Ghaeb. 1998. Strengthening of initially loaded reinforced concrete beams with using FRP plates. *ACI Structural Journal* (March-April 1994): 160–168.

Emmons P. H. 1994. *Concrete Repair and Maintenance.* R.S. Means Inc.

J. K. Clarke and P. Waldron. 1996. The reinforcement of concrete structures with advanced composites. *The Structural Engineer* **74(17/3)** Sept.

Khaled A. Soudki and Andrew Lawrence. 1999. Behaviour of R.C. beams strengthened with partially bonded carbon fibre reinforced polymer strip. Research Report, Department of Civil Engineering, University of Waterloo, Canada.

Kiang-Hwee Tan and Chee-Khoon Ng. 1997. Effects of Deviators and Tendon Configuration on Behaviour of Externally Prestressed Beams. *ACI Structural Journal* January-February.

Kiang Hwee Tan and Nam-Yuen Wong. 1994. Behaviour of R.C. beams externally bonded with FRP plates. Research report. Department of Civil Engineering, The National University of Singapore.

Tan, K. H. and N. Y. Wong. 1997. Behaviour of RC beams externally bonded with FRP plate. Report, Dept. of Civil Engineering, National University of Singapore.

Toong K. Chan and Li Xiaoan. 2000. Improving crack behaviour of one-way slabs with carbon fibre plates. In *Proceeding of the 4th Asia-Pacific Structural Engineering and Construction, Conference* **2:** 351–358, Sept 13-15, Kuala Lumpur.

Raina V. K. 1994. *Concrete Bridges.* Tata MacGraw-Hill.

Structural Use of Concrete. 1997. BS8110 British Standard Institution, U.K.

ISSN: 0128-7680
Pertanika J. Sci. & Technol. 12(1): 115 - 128 (2004) © Universiti Putra Malaysia Press

Observational Methods for Predicting Embankment Settlement

Bujang B.K Huat, Ng Chung Hoe & H. A. Munzir
Department of Civil Engineering, Faculty of Engineering,
Universiti Putra Malaysia,
43400 UPM Serdang, Selangor, Malaysia
E-mail: bujang@eng.upm.edu.my

Received: 18 December 2002

ABSTRAK

Kaedah satu-dimensi Terzaghi diguna dengan meluas untuk menganggar enapan. Persamaan kebezaan diselesaikan dengan membuat andaian yang pekali pengukuhan tidak berubah. Dengan itu, persamaan berbentuk linear (lelurus). Akan tetapi dalam realiti persamaan ini bukanlah linear. Ini adalah kerana kebolehmampatan, kebolehtelapan dan pekali pengukuhan tanah berubah dengan enapan. Oleh yang demikian, kita masih tidak begitu mampu untuk menganggar atau meramal kadar enapan dengan baik. Dalam kertas kerja ini beberapa data enapan jangka masa panjang yang berkualiti tinggi diguna untuk menguji kesahihan beberapa kaedah cerapan, seperti kaedah Hiperbolik dan kaedah Asaoka untuk meramal enapan. Data-data lapangan ini diperoleh daripada benteng cubaan di Tangkak (1987-1996) dan Juru (1990-1992). Berdasarkan rekod enapan benteng di atas tanah-tanah lembut ini, ianya dapat dirumuskan yang enapan diramal menggunakan kaedah Hiperbolik dapat diperbaiki dengan banyak sekiranya data enapan semenjak bermulanya pembinaan digunakan, iaitu selepas kira-kira 50% enapan telah berlaku. Enapan jangka masa panjang yang diramal menggunakan data peringkat awal (iaitu kurang daripada 6 bulan) boleh mengelirukan. Kemampuan kaedah ini juga boleh diperhatikan daripada ciri-ciri lengkung yang dilukis. Sebagai contoh, dalam kes kaedah hiperbolik, didapati sekiranya kehubungan antara t/ρ dan ρ menghampiri satu garisan lurus (linear), maka ramalan yang baik akan diperoleh. Ramalan menggunakan kaedah Asaoka juga diperbaiki sekiranya pangkalan data yang besar digunakan.

ABSTRACT

The one dimensional Terzaghi method is still widely used for prediction of settlement. Its differential equation is solved on the assumption that coefficient of consolidation is a constant, in which case the equation becomes linear. But in reality this equation is non linear because compressibility, permeability and coefficient of consolidation changes with settlement. This is why the capability of predicting the rate of settlement or time-settlement relationship remains rather poor. In this paper a number of high quality long-term field settlement data are used to verify the applicability of the observational methods, namely the hyperbolic and the Asaoka method. The field data were from the Tangkak trial embankment (1987-1996) and the Juru trial embankment (1990-1992). Based on the available settlement record for embankment on soft ground, it can be concluded that the prediction of settlement using the hyperbolic method is significantly improved using the start of construction settlement data, notably after more than 50% of the settlements have occurred. Long-term settlement predicting using the early stage data (6 months or less) could be

misleading. The capability of the method can also be diagnosed from the characteristics of the curve plotted. For the case of hyperbolic method, it is evident that if a close linear relation of t/ρ and ρ is obtained, then the prediction is seemingly good. Prediction of settlement using the Asaoka method is also improved using larger settlement database.

Keywords: Asaoka method, hyperbolic method, settlement prediction

INTRODUCTION

The one-dimensional Terzaghi method is still widely used for prediction of settlements. Its differential equation is solved on the assumption that the coefficient of consolidation is a constant, in which case the equation becomes linear. But in reality this equation is non linear because compressibility, permeability and coefficient of consolidation changes with settlement. This is why the capability of predicting the rate of settlement or time-settlement relationship remains rather poor.

Numerous attempts to improve the capability of predicting the magnitude and rate of settlement and excess pore water pressure dissipation by introducing more refined soil models and less restricted assumptions on the parameters describing these models have taken place. These improvements have been proposed by various authors to take into account some of the real conditions that Terzaghi idealised. For example, time dependent loading, variation of soil parameters with change in effective stress, finite (large) strain, submergence of fill and layered systems can be taken into account (Brand and Brenner 1981). However, despite these refinements, predictions of the development of settlement with time using laboratory-derived parameters, for example, coefficient of consolidation, remain speculative. This leads to an interest in studying other methods such as those based on field observations.

A few observational methods based on settlement records are available to predict future settlement behaviour, namely the hyperbolic (Tan 1971; Chin 1975), Velocity (Parkin 1978), and Asaoka (Asaoka 1978) method. Theoretically by extrapolating from observed settlement behaviour, many uncertainties regarding the variability of soil, magnitude and distribution of load can be overcome (Aboshi and Inoue 1986). This new category of settlement analyses is the subject of interest as settlement plates are cheap and can be easily installed.

In this paper a number of high quality long-term field settlement data are used to verify the applicability of the observational methods, namely the Hyperbolic and the Asaoka method. The field data were from the Tangkak trial embankment (1987-1996) and the Juru trial embankment (1990-1992).

THE OBSERVATIONAL METHODS

The Hyperbolic Method

The usefulness of the hyperbolic approach has long been recognised in analysing experimental observations. Tan (1971) made use of the hyperbolic

dependence on time of clay undergoing secondary compression and proposed the following relationship:

$$t/\rho = M\,t + C \tag{1}$$

where ρ is the total settlement at any time, t, after the excess pore water pressure has dissipated. M and C are empirical constants. This equation, when plotted with the ratio of t/ρ on the ordinate and time t on the abscissa will give a straight line, the slope of which, M, and the intercept on the ordinate, C. Tan (1971) found the significance of M by writing the equation as follows:

$$1/\rho = M + C/t \tag{2}$$

When t becomes very large, i.e. $t \to \infty$, then $1/t \to 0$ and hence $1/\rho = M$. which means the ultimate settlement, $\rho_{ult} = 1/M$.

Chin (1975) also made use of the hyperbolic dependence on time of settlement, and in his case for both the primary and secondary compression. In fact Chin (1978) also used this approach to diagnose the condition of driven piles.

Huat (1996) examined the applicability of the hyperbolic method for predicting embankment settlement using end of construction settlement data and found that the accuracy of the prediction is limited to 1 to 2 years. In this paper, the capability of the method is once again examined but by using settlement data from start of construction.

The Asaoka Method

According to Asaoka (1978), settlement at time, t, (ρ_i) can be expressed as:

$$\rho_i = \beta_o + \beta_1\,\rho_{i-1} \tag{3}$$

This is a time-settlement relationship, which is a linear equation, where β_o is an intercept on the vertical axis, and β_1 is a gradient. As predicted final settlement (ρ_f) is reached, the equation is shown to be equal to:

$$\rho_i = \rho_{i+1} = \rho_f \tag{4}$$

The settlements plotted (ρ_i, ρ_{i+1}) are for selected time intervals, Δt, which usually ranges between 30-100 days.

THE TRIAL EMBANKMENT

Field data from two trial embankments were considered in this paper. They were Tangkak and Juru trial embankments. Details of these embankments were presented in the symposium organised by the Malaysia Highway Authority in 1989, and in the paper by Huat (1996).

Tangkak Trial Embankment

The Tangkak trial embankment is located at Tangkak in the valley of the Muar rivers, Johor (*Fig. 1*). The subsoil profile beneath the trial is generalised as follows. The upper 17 m consist of soft to very soft silty clay with natural water content 50-120%, liquid limit (w_l) of 40-80% and plastic limit (w_p) of 20-40%. Traces of seashells indicate a marine origin. Underlying this layer is a layer of peat of about 0.5 m thick, followed by some 2 m of sandy clay, which is underlain in turn by a thick deposit of medium to coarse sand with SPT values ranging from 6-50. The undrained strengths obtained from the vane tests showed an almost linear increase of strength below a surface crust, with strength of 9 kPa at 1 m increasing to 36 kPa at 17 m. Results obtained from the odometer tests indicate that the clays are slightly over-consolidated but highly compressible. Values of coefficient of consolidation (c_v) range from 1-10 m²/yr.

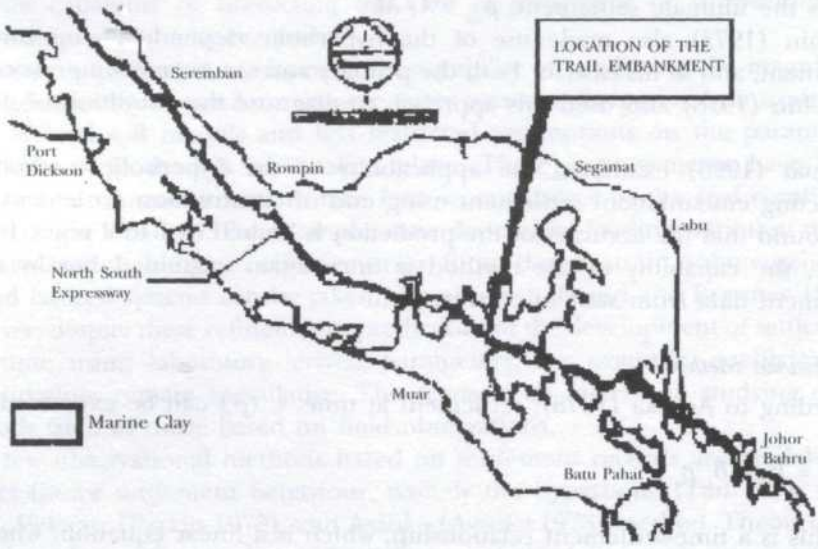

Fig 1: Location of Tangkak trial embankment

Construction of the embankments commenced in early 1987, and the whole project was the subject of a symposium sponsored by the Highway Authority in 1989. One of the embankments, i.e. the 3 m high control embankment, is analysed in this paper.

Juru Trial Embankment

The Juru trial embankment is located some 10 km south of Butterworth, in the northern part of Peninsular Malaysia, about 600 km north of the Tangkak trial (*Fig. 2*). The site of the trial embankment is between km 4.9 to km 5.2 of the Butterworth-Jawi route of the North-South expressway. The area is low-lying with original ground level varying from 0.2 m to 0.7 m above mean sea level.

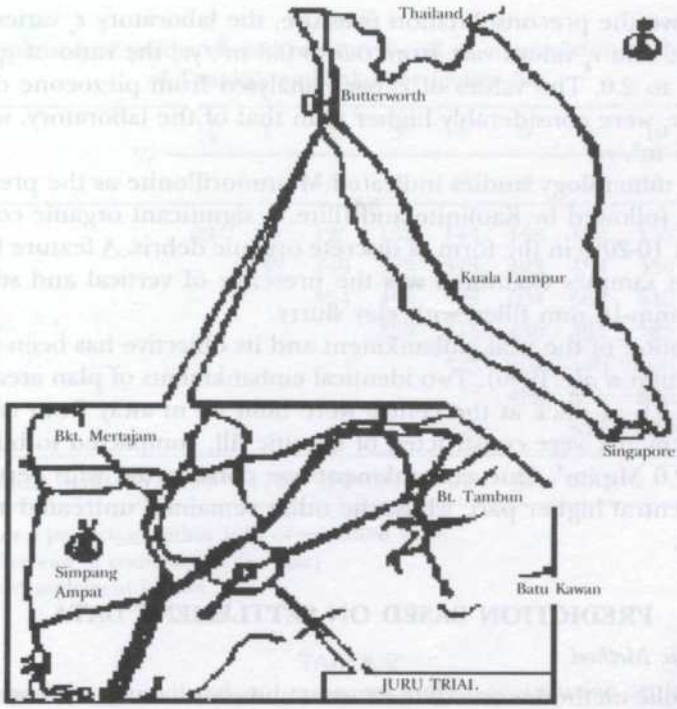

Fig. 2: Location of Juru trial embankment

A comprehensive site investigation was carried out in 1990 to determine the subsoil profile and properties of the trial site. The investigation revealed the presence of a desiccated upper crust of about 1.5 m thick. Beneath the upper crust is a layer of very soft silty clay of about 12.5 m thick. The clay has been identified as part of the Holocene marine deposits formed after the last period of low sea level between 15,000 to 18,000 years ago. Below the clay stratum is a layer of loose to medium dense sand of about 2 m thick, which is underlain in-turn with residual soil deposit. The clay is of high plasticity with liquid limit in the range of 80-120%, plasticity index of 40-80%, and with moisture content close to the liquid limit. The densities of the clay are typically low of the order of 1.35 – 1.40 Mg/m^3.

Field vane measurements show an almost linear increase in undrained strength (S_u) from about 10 kPa below the surface crust to about 30 kPa at depth 12 m. The vane strength-effective vertical stress (S_u / s'_v) ratio being around 0.6 except for isolated higher values in the crust. Sensitivity of the clay is modest, ranging from 3.5 to 5.0. From the odometer tests, the clay is shown to be lightly over-consolidated but highly compressible.

The initial void ratio (e_o) is high, typically 3.0 to 3.5. The compression ratio, ($c_c/1 + e_o$) is in the region of 0.4 to 0.6 for most of the deposit except in and just below the upper crust. Tests were carried out to establish the coefficient of consolidation in both the vertical (c_v) and horizontal (c_h) directions. For

pressure above the preconsolidation pressure, the laboratory c_v varies from 0.3 to 0.4 m^2/yr. The c_h values vary from 0.5 to 0.8 m^2/yr, the ratio of c_h/c_v ranges between 1.7 to 2.0. The values of c_h back analysed from piezocone dissipation test, however, were considerably higher than that of the laboratory, with values of 3.5 to 4.5 m^2/yr.

The clay mineralogy studies indicated Montmorillonite as the predominant clay mineral followed by Kaolinite and Illite. A significant organic content was noted, about 10-20% in the form of discrete organic debris. A feature frequently seen in most samples examined was the presence of vertical and sub vertical holes of 10 mm-15 mm filled with clay slurry.

A description of the trial embankment and its objective has been presented by Wan Hashimi *et al.* (1990). Two identical embankments of plan area of 100 m x 56 m and 3.6 m thick at the centre were built 60 m away from each other. The embankments were constructed of lateritic fill, compacted to bulk density of around 2.0 Mg/m^3. One embankment was constructed with vertical drain under the central higher part, whilst the other remained untreated and served as a control.

PREDICTION BASED ON SETTLEMENT DATA

The Hyperbolic Method

The Hyperbolic method is one of the easiest and most commonly used methods for predicting future performance based on available settlement data. The availability of an eight year settlement record as in the case of the Tangkak trial embankment offers a rare opportunity to examine the accuracy of the hyperbolic method of prediction. While the Juru trial, which is on a completely different test site, provides a basis for comparison, it also offers an opportunity to test whether the same observational method can be used to predict settlements for the case of vertical-drains-treated embankment.

Tables 1, 2 and 3 summarise comparisons of the predicted and measured end of construction settlement of the Tangkak embankment. Note that settlement gauges S2, S5 and S8 were all centre line settlement gauges. Predictions are made based on end of construction settlement data of 3 months, 6 months, and 1, 2, 3, 4 and 5 years. As concluded by Huat (1996), a reasonable prediction (but not necessarily 'good') can only be made based on the 2 year data. A good prediction is arbitrarily defined as that with a discrepancy of within 10% of the measured values. Predictions made using the early stage data (< 3 months), however, consistently under-predict the settlements. A similar trend of behaviour is also observed by Hudson (1991).

Tables 4, 5 and 6 summarise comparisons of the predicted and measured settlements of the same embankment but using settlement data from start of construction. As shown in the table below, the prediction capability is significantly enhanced by using data from start of construction, especially based on the 2 year data onward. However, the predictions of future settlements using early stage data (< 6 months) can be misleading.

TABLE 1
Comparison of predicted and measured end of construction settlement of Tangkak embankment (gauge S2)

t_r	1/4	1/2	1	2	3	4	5	6	10	20	30
	ρ	ρ	ρ	ρ	ρ	ρ	ρ	ρ	ρ	ρ	ρ
1/4		69	99	125	137	144	148	152	158	164	166
1/2			148	249	323	378	423	458	550	646	686
1				324	436	528	604	668	849	965	1163
2					357	415	458	494	583	675	718
3						423	469	506	600	690	740
4							469	505	600	690	740
5								513	610	710	754
Actual settlement (mm)	45	90	170	290	370	435	485	500			

Indicates a prediction within 10% of measured value
t_r = time after end of construction (in year)
ρ = predicted settlement in mm

TABLE 2
Comparison of predicted and measured end of construction settlement of Tangkak embankment (gauge S5)

t_r	1/4	1/2	1	2	3	4	5	6	10	20	30
	ρ	ρ	ρ	ρ	ρ	ρ	ρ	ρ	ρ	ρ	ρ
1/4		56	68	77	81	83	84	85	86	87	88
1/2			160	265	377	390	430	460	547	630	665
1				227	273	303	325	341	378	410	424
2					320	365	398	425	480	550	573
3						394	434	466	540	623	655
4							443	476	559	643	677
5								492	583	676	714
Actual settlement (mm)	50	95	160	270	350	416	470	488			

Indicates a prediction within 10% of measured value
t_r = time after end of construction (in year)
ρ = predicted settlement in mm

Based on the degree of consolidation, it appears from examining the data presented that some 50% of consolidation must occur before the predictions become more reliable. In another words, one to two years must be given in order to harvest good results (Huat 2002).

TABLE 3
Comparison of predicted and measured end of construction settlement of Tangkak embankment (gauge S8)

t_c	1/4	1/2	1	2	3	4	5	6	10	20	30
		ρ	ρ	ρ	ρ	ρ	ρ	ρ	ρ	ρ	ρ
1/4		53	59	64	65	66	67	67	68	68	69
1/2			123	161	179	190	197	202	213	220	230
1				174	194	205	214	219	230	240	250
2					293	326	349	367	408	445	459
3						378	432	440	501	561	585
4							440	456	525	593	619
5								483	564	645	677
Actual settlement (mm)	50	100	160	280	360	415	480	490			

Indicates a prediction within 10% of measured value
t_c = time after end of construction (in year)
ρ = predicted settlement in mm

TABLE 4
Comparison of predicted and measured start of construction settlement of Tangkak trial embankment (gauge S2)

t_o	1/4	1/2	1	2	3	4	5	6	7	8	10	20	30
		ρ	ρ	ρ	ρ	ρ	ρ	ρ	ρ	ρ	ρ	ρ	ρ
1/4		744	918	1041	1089	1115	1131	1142	1150	1156	1165	1182	1188
1/2			820	901	932	948	958	965	969	973	978	986	992
1				1092	1185	1238	1272	1296	1313	1326	1346	1386	1400
2					1089	1158	1204	1236	1261	1379	1306	1365	1385
3						1192	1233	1262	1283	1299	1324	1374	1392
4							1267	1306	1335	1357	1389	1460	1485
5								1228	1259	1283	1318	1395	1423
6									1350	1386	1434	1542	1581
Actual settlement (mm)	550	670	835	1010	1150	1230	1300	1350	1390	1400			

Indicates a prediction within 10% of measured value
t_c = time after end of construction (in year)
ρ = predicted settlement in mm

TABLE 5
Comparison of predicted and measured start of construction settlement of Tangkak trial embankment (gauge S5)

t_o	¼	½	1	2	3	4	5	6	7	8	10	20	30
	ρ	ρ	ρ	ρ	ρ	ρ	ρ	ρ	ρ	ρ	ρ	ρ	ρ
¼	781	952	1069	1115	1139	1155	1165	1173	1178	1186	1203	1208	
½		837	911	939	954	963	969	973	976	984	990	993	
1			1027	1108	1153	1183	1203	1218	1229	1245	1279	1292	
2				1117	1178	1218	1246	1267	1283	1306	1355	1373	
3					1202	1238	1263	1282	1297	1317	1362	1377	
4						1267	1302	1329	1349	1379	1444	1467	
5							1335	1370	1400	1442	1534	1568	
6								1431	1467	1521	1643	1688	
Actual settlement (mm)	550	700	850	1040	1167	1239	1316	1381	1394	1413			

Indicates a prediction within 10% of measured value
t_o = time after end of construction (in year)
ρ = predicted settlement in mm

TABLE 6
Comparison of predicted and measured start of construction settlement of Tangkak trial embankment (gauge S8)

t_o	¼	½	1	2	3	4	5	6	7	8	10	20	30
	ρ	ρ	ρ	ρ	ρ	ρ	ρ	ρ	ρ	ρ	ρ	ρ	ρ
¼	766	924	1029	1071	1092	1106	1115	1121	1126	1134	1148	1153	
½		837	911	939	953	962	968	973	976	981	991	994	
1			979	1044	1079	1101	1116	1128	1136	1148	1174	1182	
2				1197	1267	1314	1346	1371	1389	1417	1475	1496	
3					1252	1297	1328	1353	1371	1397	1454	1474	
4						1252	1289	1317	1339	1371	1439	1464	
5							1254	1282	1303	1335	1402	1426	
6								1338	1353	1375	1421	1437	
Actual settlement (mm)	550	700	850	1040	1170	1250	1320	1390	1400	1420			

Indicates a prediction within 10% of measured value
t_o = time after end of construction (in year)
ρ = predicted settlement in mm

Tables 7 and 8 summarise the comparisons of predicted and measured end of construction settlement of the Juru embankments. The measured settlements were taken at the centre of the embankment. As noted by Huat (1996), the observation in this case is only limited to $1^1/_2$ years, but the trend of behaviour is nevertheless quite similar to the above. Long-term settlement predicted based on the early stage data is small compared with that over a larger base.

TABLE 7
Comparison of predicted and measured end of construction settlement of Juru embankment - control section

t_r	¼	½	1	1½	10	20	30
		ρ	ρ	ρ	ρ	ρ	ρ
¼		450	550	600	700	715	720
½			600	665	820	840	845
1				715	970	1000	1010
Actual settlement (mm)	201	490	625	750			

Indicates a prediction within 10% of measured value
t_r = time after end of construction (in year)
ρ = predicted settlement in mm

TABLE 8
Comparison of predicted and measured end of construction settlement of Juru embankment – treated section

t_r	¼	½	1	1½	10	20	30
		ρ	ρ	ρ	ρ	ρ	ρ
¼		620	830	930	1180	1205	1215
½			840	950	1205	1235	1245
1				1005	1330	1370	1380
Actual settlement (mm)	369	640	890	1020			

Indicates a prediction within 10% of measured value
t_r = time after end of construction (in year)
ρ = predicted settlement in mm

Tables 9 and 10 show comparisons of the predicted and measured settlement of the Juru embankment using the start of construction settlement data. It is of interest to note that the early stage data (both 3 and 6 months in this case) gave negative time – settlement relationship because of the large increment of cumulative settlements, while the rest appears to be good to the limit of the available data, i.e. for the next year in this case. Having examined all the cases

presented, it appears that the capability of the hyperbolic method to predict future settlement is highly dependent on the characteristics of the graph plotted. A good prediction is only possible if the curve of the plotted graph is very close to a linear relationship.

TABLE 9
Comparison of predicted and measured start of construction settlement of Juru embankment – control section

t_o	¼	½	1	1½	2	10	20	30
				ρ	ρ	ρ	ρ	ρ
¼								
½								
1				1099	1198	1485	1532	1549
1½					1203	1499	1548	1565
Actual settlement (mm)	420	659	953	1101	1234			

Indicates a prediction within 10% of measured value
t_o = time after end of construction (in year)
ρ = predicted settlement in mm

TABLE 10
Comparison of predicted and measured start of construction settlement of Juru embankment – treated section

t_o	¼	½	1	1½	2	10	20	30
				ρ	ρ	ρ	ρ	ρ
¼								
½								
1				1938	2200	3008	3162	3217
1½					1937	2356	2426	2405
Actual settlement (mm)	425	962	1602	1848	1991			

Indicates a prediction within 10% of measured value
t_o = time after end of construction (in year)
ρ = predicted settlement in mm

The Asoaka Method

Tables 11, 12 and 13 summarise comparisons of the predicted and measured settlement of the Tangkak embankment. Predictions were made based on settlement data of 1, 2, 3, 4 and 5 years and time interval Δt of 60 days. A good prediction, as in the above, is arbitrarily defined as that of within 10% of the

measured values. As shown in the tables below, predictions made based on 1 year or so data are good at least for the next 5 years. Using a larger database significantly enhances the prediction capability.

TABLE 11
Comparison of predicted and measured settlement of Tangkak trial embankment (gauge S2)

t_c	1	2	3	4	5	6
		ρ	ρ	ρ	ρ	ρ
1		303	376	421	450	467
2			377	424	453	472
3				440	475	498
4					488	515
5						541
6						
Actual settlement (mm)	170	290	370	435	485	500

Indicates a prediction within 10% of measured value
t_c = time after end of construction (in year)
ρ = predicted settlement in mm
Time interval, Dt = 60 days

TABLE 12
Comparison of predicted and measured settlement of Tangkak trial embankment (gauge S5)

t_c	1	2	3	4	5	6
		ρ	ρ	ρ	ρ	ρ
1		287	362	412	445	466
2			377	435	475	503
3				422	458	482
4					482	514
5						519
6						
Actual settlement (mm)	160	270	350	416	470	488

Indicates a prediction within 10% of measured value
t_c = time after end of construction (in year)
ρ = predicted settlement in mm
Time interval, Dt = 60 days

TABLE 13
Comparison of predicted and measured settlement of Tangkak trial embankment (gauge S8)

t_i	1	2	3	4	5	6
		ρ	ρ	ρ	ρ	ρ
1		293	379	441	484	515
2			377	434	473	500
3				437	477	505
4					515	555
5						537
6						
Actual settlement (mm)	160	280	360	415	480	490

Indicates a prediction within 10% of measured value
t_i = time after end of construction (in year)
ρ = predicted settlement in mm
Time interval, Dt = 60 days

CONCLUSION

Based on the available settlement record for embankment on soft ground, it can be concluded that the prediction of settlement using the hyperbolic method is improved by using the start of construction settlement data, notably after more than 50% of the settlements have occurred. Long-term settlement predicted using the early stage data (<6 months) could be misleading. The capability of the method can also be diagnosed from the characteristic of the curve plotted. For the case of hyperbolic method, it is evident that if a close linear relation of t/ρ and ρ is obtained, then the prediction is seemingly good.

Prediction of settlement made using the Asaoka method is also improved using a larger settlement database.

Using the hyperbolic method, the advantage is that it can use the start of construction settlement data. Prediction can therefore be made after 1 year or so from start of construction. The Asaoka method uses the end of construction settlement data and prediction can only be made after the end of construction, which usually takes between 1-2 years. In this respect, the hyperbolic method holds an advantage of being able to predict future settlement at an earlier time.

REFERENCES

ABOSHI, H. and T. INOUE. 1986. Prediction of consolidation settlement of clay layers especially in case of soil stabilisation by vertical drains. In *Proceedings of IEM-JSSMFE Symposium on Geotechnical Problems*, p. 31–40. Kuala Lumpur.

ASAOKA, A. 1978. Observational procedure of settlement prediction. Soils and foundations. *JSSMFE* **18(4):** 87-101.

BRAND, E. W. and R. P. BRENNERS. 1981. *Soft Clay Engineering.* Amsterdam: Elsevier Scientific Publishing Co.

CHIN, F. K. 1975. The seepage theory of primary and secondary consolidation. In *Proceedings of 4th Southeast Asian Conference on Soil Engineering,* p. 21–28. Kuala Lumpur.

CHIN, F. K. 1978. Diagnosis of pile condition. *Geotechnical Engineering* **9(2)**: 1–21.

HUDSON, R. R. 1991. Low embankment on soft ground. *Proceedings of Seminar on Geotechnical Aspects of the North South Expressway,* p. 109–118. Kuala Lumpur.

HUAT, B. B. K. 1996. Observational method of predicting settlements. In *Proceedings of Twelfth Southeast Asian Geotechnical Conference* **1:** 191–196. Kuala Lumpur.

HUAT, B. B. K. 2002. Hyperbolic method for predicting embankment settlement. In *Proceedings of 2nd World Engineering Congress – Geotechnical Engineering and Transportation,* p. 228–234, 22-25 July, Kuching, Sarawak.

Malaysian Highway Authority 1989. In *Proceedings of International Symposium on Trial Embankments on Malaysian Marine Clays.* Kuala Lumpur.

PARKIN, A. K. 1978. Coefficient of consolidation by velocity method. *Geotechnique* **28(4)**: 472–474.

TAN, S. B. 1971. Empirical method for estimating secondary and total settlement. In *Proceedings of 4th Asian Regional Conference on Soil Mechanics and Foundation Engineering,* **(2):** 147–151. Bangkok.

WAN HASHIMI, A., H. K. OTHMAN, H. K. THAI and C. P. CHIN. 1991. Vertical drain embankment trial at Sungai Juru. In *Proceedings of Seminar on Geotechnical Aspects of the North South Expressway,* p. 195–205. Kuala Lumpur.

ISSN: 0128-7680
Pertanika J. Sci. & Technol. 12(1): 129 - 135 (2004) © Universiti Putra Malaysia Press

Thermal Diffusivity Measurement of BSCCO Superconductor (85 to 300 K) Using PVDF Transducer

M. Haydari, M. M. Moksin, W. M. M. Yunus, V. I. Grozescu, I. Hamadneh & S. A. Halim

Department of Physics, Faculty of Science and Environmental Studies
Universiti Putra Malaysia, 43400 UPM, Serdang, Selangor, Malaysia
E-mail: mehdi@fsas.upm.edu.my

Received: 19 December 2002

ABSTRAK

Dilaporkan pengukuran peresapan terma untuk sampel seramik superkonduktor Bi-Pb-Sr-Ca-Cu-O. Dalam kerja ini 'camera flash' dan filem polyvinylidene difluoride (PVDF) adalah masing-masing digunakan sebagai sumber pemanas dan pengesan pyroelektrik. Pengiraan secara teori ke atas isyarat dilakukan dengan menggunakan penghampiran berdasarkan fungsi Dirac-g untuk profil tempohan cahaya kilat daripaa camera flash dalam menentukan pemalar peresapan terma. Pengukuran ini dijalankan dari suhu 85 K hingga suhu bilik. Lengkungan peresapan terma mempamerkan suatu gaung pada peralihan kerintangan pada suhu mula dan suatu puncak/bpnggol pada suhu akhir peralihan kerintangan sifar. Oleh itu, kami mendapati bahawa transducer PVDF adalah sangat berkesan dalam mengesan fenomena peralihan dari keadaan normal kepada keadaan superkonduktor dan juga dalam ukuran pemalar peresapan terma untuk bahan superkonduktor pada suhu rendah

ABSTRACT

Thermal diffusivity measurement of the Bi-Pb-Sr-Ca-Cu-O superconducting ceramic sample is reported. In this work camera flash and polyvinylidene difluoride (PVDF) film were respectively used as heating source and pyroelectric detector. The theoretical signal calculation based on Dirac- function approximation for camera flash temporal profile was used to deduce the thermal diffusivity. The measurement was done from 85 K to room temperature. The thermal diffusivity curve shows a dip at the resistive transition onset temperature and a cusp at the zero-resistance temperature. Thus, we found that the PVDF transducer is very effective in determining the normal-to-superconductor transition phenomena and also for the measurement of the thermal diffusivity of the superconducting samples at low temperatures.

Keywords: PVDF, thermal diffusivity, BSCCO, flash technique

INTRODUCTION

The thermal properties of high-T_c superconductor have been measured by various photoacoustic methods, such as the two-beam phase lag (Aravind *et al.* 1996), photothermal method (Bertolotti *et al.* 1995), thermocouple detection (Armstrong *et al.* 1991), photoacoustice technique (Yunus *et al.* 2002) and photopyroelectric method (Aravind and Fung 1999; Peralta *et al.* 1991). Photothermal technique, of which photopyroelectric detection forms a subset,

has been widely applied in the measurement of thermal parameters as the thermal diffusivity for solids. Among the various photothermal detection schemes, however, photopyroelectric methods combine extreme sensitivity with high temporal resolution, as well as low cost. The photopyroelectirc method can be based on two different methods which depend on the sample heating source, i.e. modulated CW (Aravind and Fung 1999) and pulsed radiation (Peralta *et al.* 1991). In this paper we describe a method, based on photopyroelecric detection of the sample response to camera flash excitation, which allows measurement of the thermal diffusivity. For this work we chose polyvinylidene difluoride (PVDF) as the transducer, which demonstrates pyroelectrics properties, and camera flash was used as the heating source. The theoretical model is based on the Dirac- function heating source which was introduced before by Power and Mandelis (1987).

THEORY

For one-dimensional heating propagation in a system consisting of four layers: gas, sample, PVDF sensor and backing, assuming that the sample is optically opaque and the backing has similar thermal properties to the PVDF sensor (i.e. effusivity ratio = 1), the average temperature T_p, in the sensor has a simplified expression (Frandas 1995):

$$\left\langle T_p(x,t)\right\rangle = (-1)\frac{\left(\alpha_s\alpha_p\right)^{1/2}}{\alpha_s\left(b_{ps}+1\right)}\sum_{n=0}^{\infty}(-1)^n\gamma^n\left[erfc\left(\frac{(2n+1)\ell}{2\sqrt{a_s t}}+\frac{d}{2\sqrt{a_p t}}\right)-erfc\left(\frac{(2n+1)\ell}{2\sqrt{a_s t}}\right)\right] \quad (1)$$

where $\gamma=\dfrac{b_{ps}-1}{b_{ps}+1}$ the thermal reflectance, $b_{ps}=\dfrac{e_p}{e_s}$ the effusivity ratio pyroelectric material/sample, $e_p=\dfrac{k_p}{\sqrt{\alpha_p}}$, $e_s=\dfrac{k_s}{\sqrt{\alpha_s}}$, $k_{p,s}$ the thermal conductivity for the pyroelectric film and sample, α_p and α_s are the thermal diffusivity for the pyroelectric film and sample respectively, ℓ, d are the thickness of the sample and pyroelectric film, respectively. The current response $I(t)$ of the pyroelectric sensor is proportional to derivative of the average temperature profile i.e.

$$I(t)=\frac{pd}{\varepsilon}\frac{\partial\left\langle T_p(x,t)\right\rangle}{\partial t} \quad (2)$$

where p, ε are the pyroelectric coefficient and dielectric constant of the sensor, respectively.

The pyroelectric impulse response $I(t)$ can be extracted from Eq (1) and Eq (2) as

$$I(t) = \frac{KA}{t^{3/2}} \sum_{n=0}^{\infty} (-1)^n \gamma^n \left(\tau_{1n}^{1/2} e^{-\frac{\tau_{1n}}{4t}} - \tau_{2n}^{1/2} e^{-\frac{\tau_{2n}}{4t}} \right) \quad (3)$$

where $\tau_{1n}^{1/2} = \frac{(2n+1)\ell}{\sqrt{\alpha_s}}$, $\tau_{2n}^{1/2} = \frac{(2n+1)\ell}{\sqrt{\alpha_s}} + \frac{d}{\sqrt{\alpha_p}}$, $A = \frac{\sqrt{\alpha_s \alpha_p}}{\alpha_s (b_{ps}+1)} \frac{1}{\sqrt{\pi}}$ and K is a constant, which incorporates the electrical properties of the pyroelectric film. The factor A is a constant, which incorporates the static thermal properties of the sample/pyroelectric system. Because the absolute intensity of the recovered signal is a function of instrumental factors such as irradiation power, amplifier gain, and excitation geometry that has no bearing on the thermal diffusivity, the impulse response was conveniently normalized to give $I(t)$ at the peak of the time-delay response.

EXPERIMENT

The bulk sample used was BSCCO with nominal composition $Bi_{1.6}Pb_{0.4}Sr_2Ca_2Cu_3O_\delta$, which was fabricated by coprecipitation technique (Hamadneh 2002). The metal acetates compounds of bismuth, strontium, lead, calcium and copper (purity ≥ 99.99 %), were weighed and dissolved with glacial acetic acid to form a clear blue solution. The oxalic acid solution was prepared and added to the blue solution and a uniform, stable blue suspension was obtained. The slurry was filtered and dried and subjected to the heat treatment which was carried out by heating the powders to 730 °C in air for 12 hours, calcined at 845 °C in air for 24 hours followed by cooling at 2 °C /minute. The powders were reground and pressed into pellets of 12.5 mm in diameter and 2 mm in thickness. The pellets were sintered at 850 °C for 24 hours and slowly cooled down to room temperature at 120 °C/ hour.

The experimental setup is schematically depicted in *Fig.1*. The sensor was a 52 μm thick, PVDF film where the thermal properties from low temperature to room temperature have been determined by Bonno *et al.* (2001). The excitation source was a flash camera (Minolta 5200i) with 5 *ms* pulse duration. The signal from the sensor was monitored by a digital oscilloscope (LeCroy 9310 A – 400 MHz) and fitting the theory to experimental data was done using Origin (Version 6). A vulcanized rubber was used as backing in four-layer setup and the sample thickness 0.875 mm was attached to the PVDF transducer with a thin layer of vacuum grease. The transducer was rigidly clamped to the glass holder inside the liquid nitrogen cryostat, which was equipped with a heater for temperature variation. The temperature was varied from 85 K up to room temperature and the value was measured by a calibrated platinum resistance thermometer with a resolution of 0.1 K.

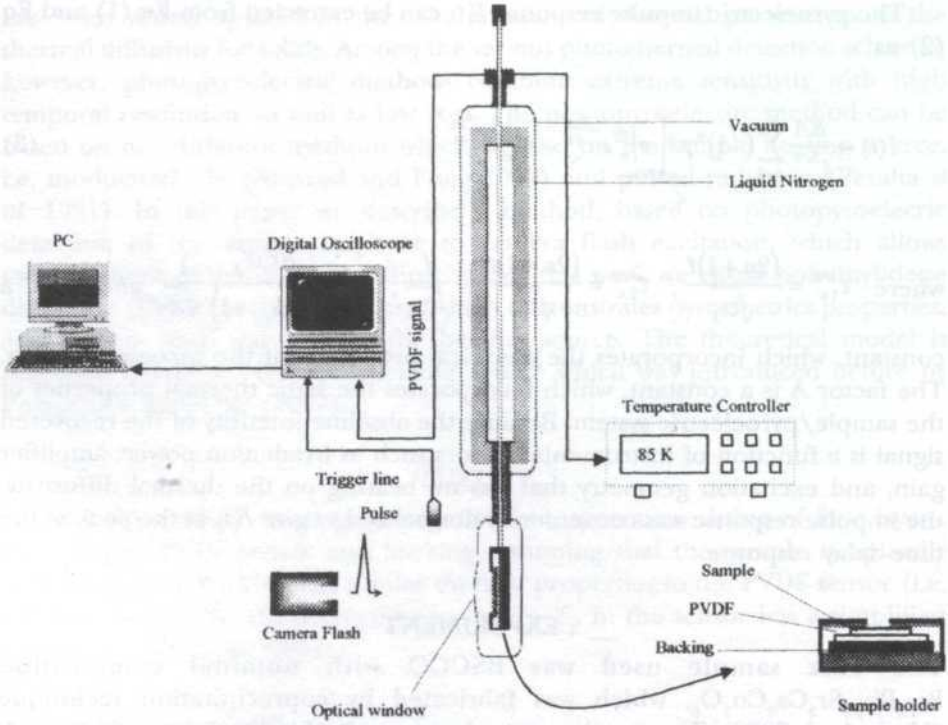

Fig. 1: The experimental setup

RESULTS AND DISCUSSION

Fig. 2 shows normalized impulse responses for the BSCCO sample at 85,102,110, 200 and 300 K.

It is observed that, the impulse response at low temperature is narrower than at higher temperature, which is due to the higher thermal diffusivity at low temperature. The initial normally present PVDF spike is negligible in our analysis, since the fastest thermal transit time through the sample is in the order of tens of milliseconds. The solid curves are the theoretical impulse response from Eq (3), using thermal diffusivity and thermal conductivity values for PVDF in different temperatures, from other works (Bonno *et al.* 2001). The fit of the theoretical expression to the experimentally obtained data is excellent, except the lingering tail that is almost of no effect on the fitted value of thermal diffusivity. This is a consequence of the fact that the signal response at earlier times is a strong function of the thermal diffusivity, while at long times at the tail is only very weakly dependent on the sample thermal diffusivity. The temperature dependence of the thermal diffusivity is shown in *Fig. 3.*

The curve exhibits that the minor dip at 110 K and a local CUSP at 102 K which correspond to resistive transition onset and resistive transition offset respectively. We believe that the minor dip in thermal diffusivity at the resistive transition onset temperature is a result of the abrupt increase in the electron

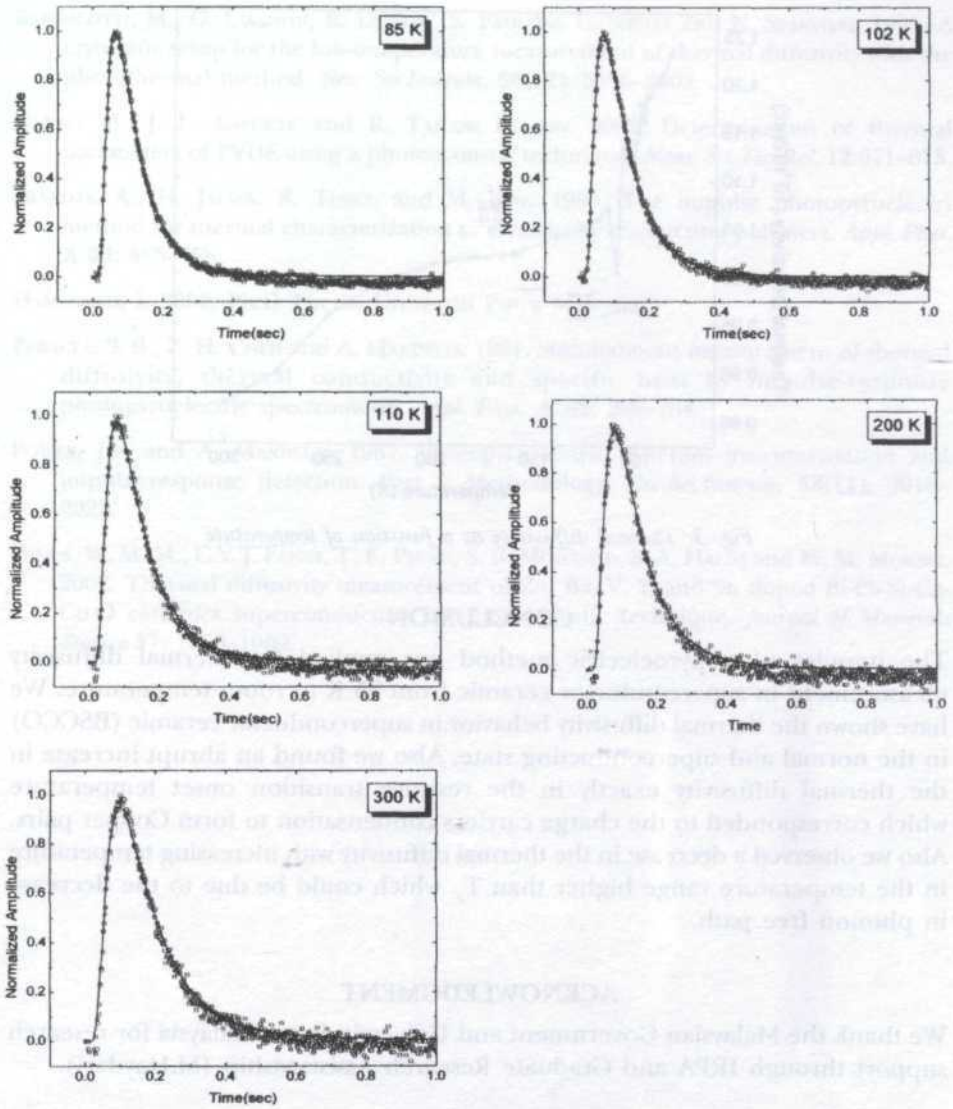

Fig. 2: Photophyroelectric response for $Bi_{1.6}Pb_{0.4}Sr_2Ca_2Cu_3O_d$ (BSCCO) at 85, 102, 110, 200 and 300 K. Similar responses were observed at different temperatures. Solid curves correspond to the theoretical model

specific heat (Aravind and Fung 1999). Furthermore, the increase in the thermal diffusivity below T_c could be due to the increase in the mean free path of phonon. Below T_c the charge carriers condense to form Cooper pairs which do not scatter phonons and as a result the mean free path of phonon increases. Also we can see a decrease in the thermal diffusivity with increasing temperature in the temperatures higher than T_c which could be due to a decrease in phonon free path due to the lattice vibration.

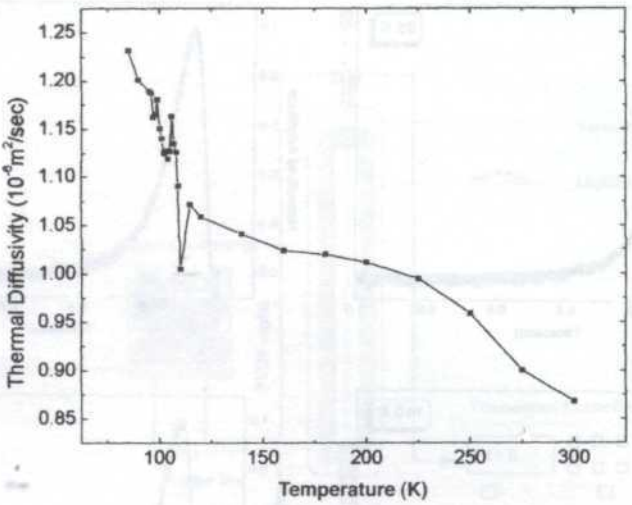

Fig. 3: Thermal diffusivity as a function of temperature

CONCLUSION

The impulse photopyroelectric method was applied for thermal diffusivity measurement in superconductor ceramic from 85 K to room temperature. We have shown the thermal diffusivity behavior in superconductor ceramic (BSCCO) in the normal and superconducting state. Also we found an abrupt increase in the thermal diffusivity exactly in the resistive transition onset temperature which corresponded to the charge carriers condensation to form Cooper pairs. Also we observed a decrease in the thermal diffusivity with increasing temperature in the temperature range higher than T_c which could be due to the decrease in phonon free path.

ACKNOWLEDGMENT

We thank the Malaysian Government and Universiti Putra Malaysia for research support through IRPA and Graduate Research Assistantship (M.Haydari).

REFERENCES

ARAVIND, M. and P. C. FUNG. 1999. Thermal parameter measurements of bulk YBCO superconductor using PVDF transducer. *Meas.Sci.Technol.* **10**: 979–985.

ARAVIND, M., P. C. FUNG, S.Y. TANG and H.L. TAM. 1996. Two-beam photoacoustic phase measurement of the thermal diffusivity of a Gd-doped bulk YBCO. *Rev Sci.Instrum.* **67(4)**: 1564–1569.

ARMESTRONG, J. V., M. MCLOUGHLIN, J. C. LUNNEY and M. D. COEY. 1991. Thermal diffusivity and laser melting of $YBa_2Cu_3O_7$ superconductor. *Supercond.Sci.Technol.* **4**: 89–92.

BERTOLOTTI, M., G. LIAKHOU, R. LI VOTI, S. PAOLONI, C. SIBILIA and N. SPARVIERI. 1995. A cryostatic setup for the low-temperature measurement of thermal diffusivity with the photothermal method. *Rev. Sci.Instrum.* **66(12)**: 5598–5602.

BONNO, B., J. L. LAPORTE and R. TASCON D'LEON. 2001. Determination of thermal parameters of PVDF using a photoacoustic technique. *Meas. Sci.Technol.* **12**:671–675.

FRANDAS, A., H. JALINK, R. TURCU and M. BRIE. 1995. The impulse photopyroelectri method for thermal characterization of electrically conducting polymers. *Appl. Phys. A* **60**: 455–458.

HAMADNEH, I. 2002. Ph.D Thesis, Universiti Putra Malaysia.

PERALTA, S. B., Z. H. CHEN and A. MANDELIS. 1991. Simultaneous measurement of thermal diffusivity, thermal conductivity and specific heat by impulse-response photopyroelectric spectrometry. *Appl. Phys. A.* **52**: 289–294.

POWER, J.F. and A. MANDELIS. 1987. Photopyroelectric thin-film instrumentation and impulse-response detection. Part I: Methodology. *Rev.Sci.Instrum.* **58(11)**: 2018–2023.

YUNUS, W. M. M., C.Y. J. FANNY, T. E. PHING, S. B. MOHAMED, S. A. HALIM and M. M. MOKSIN. 2002. Thermal diffusivity measurement of Zn, Ba, V, Y, and Sn doped Bi-Pb-Sr-Ca-Cu-O ceramics superconductors by photoacoustic technique. *Journal of Materials Science* **37**: 1055–1060.

ISSN: 0128-7680
Pertanika J. Sci. & Technol. 12(1): 137 - 147 (2004) © Universiti Putra Malaysia Press

Stochastic Rainfall Model for Irrigation Projects

Lee Teang Shui & Aminul Haque
Department of Biological and Agricultural Engineering
Universiti Putra Malaysia, 43400 UPM, Serdang, Selangor, Malaysia
E-mail: tslee@eng.upm.edu.my

Received: 19 December 2002

ABSTRAK

Model hujan stokastik adalah berkenaan dengan waktu berlaku dan jumlah ukuran hujan turun. Wujudnya beberapa model hujan berdasarkan skala masa berbeza-beza. Model hujan harian yang telah digunakan dengan luasnya, didapati sesuai diperguna di dalam model-model berkeadaan seimbang air terperinci, pertanian dan persekitaran. Dalam kajian ini, satu model penjanaan hujan stokastik disuaikan untuk Projek Pengairan Besut yang terletak di Terengganu, Malaysia. Model ini menyelaku jujukan kejadian hujan dengan kaedah matrik kebarangkalian alihan, sementara jumlah hujan harian dijanakan dengan menggunakan taburan normal pencong. Data-data hujan daripada enam stesen meteorologi yang terletak dalam Projek Pengairan Besut digunakan dalam model ini. Parameter-parameter model dianggar daripada rekod sejarah hujan. Pengesahan model dengan satu set data berasingan dibuat kemudian. Keputusan yang dihasilkan menunjukkan bahawa model ini boleh diperguna untuk menjanakan data hujan dengan sempurna.

ABSTRACT

Stochastic rainfall models are concerned with the time of occurrence and depth of rainfall. Various rainfall models have been using different time scales. Daily rainfall models have gained wide applicability as being appropriate for use in detailed water balance and agricultural and environmental models. In this study a stochastic daily rainfall generation model was adapted for the Besut Irrigation Scheme located in Terengganu, Malaysia. The model simulates the sequence of rainfall occurrence using the method of transitional probability matrices, while daily rainfall amount was generated using a skewed normal distribution. Rainfall data from six meteorological stations located at the Besut Irrigation Scheme were used for this model. The model parameters were estimated from historical rainfall records. The model validation was then performed with a separate set of data. Results obtained showed that the model could be used to generate rainfall data satisfactorily.

Keywords: Stochastic model, rainfall occurrence, rainfall generation, transitional probability

INTRODUCTION

Stochastic rainfall models are designed as a one-part or two-part model depending on whether time of occurrence and depth are generated simultaneously or separately. For the one-part models, the transition probability matrix, and the modified transition probability are the most popular. In the case of two-part

models, the two states Markov chain for simulating the occurrence of rainfall coupled with a statistical distribution for simulating rainfall depth is of interest (Chin 1977; Carey and Haan 1978; Mimikou 1983; Srikanthan and McMahon 1983; Efremides and Tsakiris 1994).

The amount and pattern of rainfall are among the most important weather characteristics and they affect agriculture profoundly. In addition to their direct effects on water balance in soil, they are strongly related to other weather variables such as solar radiation, temperature, and humidity, which are also important factors affecting the growth and development of crops, pests, diseases and weeds. However, rainfall data form an essential input into many climatologic studies for agriculture, wherein considerable research focused on rainfall analysis and modeling (Austine 2001). For instance, in rain-fed agriculture, information on total amount, as well as expected rainfall, is useful in planning agricultural policies. Monthly and seasonal rainfall data are used in determining supplemental irrigation, water requirements, and in engineering studies related to storage analysis and reservoir management.

In recent years, agricultural scientists have shown considerable interest in modeling and simulation of rainfall as new ways of analyzing rainfall data and assessing its impact on agriculture. Among the proposed methods, a combination of Markov chain and a skewed normal distribution is recognized as a simple approach and is demonstrated to be effective in generating daily rainfall for many environments (Hanson *et al.* 1980; Garbutt *et al.* 1981; Stern and Coe 1982; Hanson 1982, 1984; French 1983; Tung 1983; Osborn 1984, 1987; Geng *et al.* 1986; Jimoh and Webster 1996, 1999). In this approach, a Markov chain is used to describe the occurrence of daily rainfall, and skewed normal distribution is applied to fit the amount of rainfall for a rainy day. A first-order Markov chain is generally recognized as a simple and effective description of the rainfall occurrence. This research, while recognizing the difficult task of accurately predicting rainfall, adapted a model for forecasting daily rainfall in the Besut Irrigation Scheme, Terengganu, Malaysia.

Study Area

Irrigation in Malaysia is almost entirely devoted to rice cultivation. Eight designated granaries totaling 217,000 ha are located for rice cultivation in Malaysia. The Besut Irrigation Scheme was completed in 1977 and is one of the eight designated granary areas in Malaysia. The Besut Irrigation Scheme is located at the northeastern corner of Peninsular Malaysia in the state of Terengganu. The project area encompasses 5,164 ha of land with climatic conditions favorable for rice production. The Besut river, one of the two water sources in the scheme, runs northwards towards the South China Sea along the west boundary of the scheme. The Angga river is another water source for the scheme, converges to Besut river towards the south of the scheme area. One important aspect of the scheme is that the production cycle is based primarily on the annual rainfall pattern and distribution. The total mean annual rainfall is about 2900 mm, with extreme rain intensity reaching 400 mm over a 24hr

period. Heavier rainfalls (average) occur in October, November, December and January with 280, 590, 550 and 180 mm of rainfall respectively (JICA 1998). Significantly dry periods with low monthly averages are outside the main monsoon season in the months from March to August. During the November-January period, 40% of the total annual rains generally fall. Therefore, rainfall plays a very significant role for rice production in this scheme.

Data

A first-order Markov chain and skewed normal distribution method requires daily weather records for many years in order to estimate the model parameters. Thus the availability of the weather data limits the applicability of the simulation method. Daily rainfall data for six stations in Besut Irrigation Scheme were obtainable from the Data Information Section, Hydrological branch, Department of Irrigation and Drainage, Ampang, Malaysia. The stations were chosen due to their spatial representations as well as availability of adequate data for the study. The information for the six rainfall stations is given in Table 1.

METHODS

A first order Markov chain was used to simulate the occurrence of rainfall. Two states were used in the Markov chain, and they are the wet and dry states. A wet day is defined as one where a trace or larger amount of rainfall is recorded. Dry days, on the contrary, are days that are not wet. The decision to include trace amounts in the wet category arose primarily from solar radiation simulation considerations. Two assumptions made underlying the first-order Markov chain are namely, (1) the probability that the current day is in a particular state (i.e. wet or dry) depends only on the state of the previous day; and (2) for a given season within the year, the stochastic structure of daily rainfall is the same for each day and does not change from year to year. It has been further assumed that these so-called transition probabilities are independent of the particular day within individual months. The probability of a wet day can be calculated directly from the number of wet days by using this equation.

$$PW = NWD / ND \quad (1)$$

TABLE 1
Location of stations where daily rainfall records were collected for this study

Station	Latitude	Longitude	Period of records
Ibu Bekalan Angga	5°36'00" N	102°30'55" E	1951-1998
Sek Keb Kg Jabi	5°40'45" N	102°33'50" E	1980-1998
Sek Keb Keruk	5°29'00" N	102°29'30" E	1980-1999
Sek Keb Kg Tambila	5°44'25" N	102°36'30" E	1980-1999
Rumah Merinyu Tali air	5°44'15" N	102°30'15" E	1948-1991
Pasir Akar	5°38'25" N	102°30'15" E	1980-1990

where, PW = the probability of a wet day, or % of wet days, in a month
NWD = the number of rainy days in a month
ND = the number of days in a month

The probability of occurrence of daily rainfall consists of two transition probabilities. These are the transition probability of a wet day, given that the previous day was a wet day P (W/W), and the transition probability P (W/D) for the state of a wet day following a given dry day. Therefore from statistical data, the probability of a wet day after a dry day P (W/D) and the probability of a wet day following a wet day P (W/W) can be calculated directly using the following relationship:

$$P\ (W/D) = a + b\ f \quad (2)$$

$$P\ (W/W) = (1\text{-}b) + P\ (W/D) \quad (3)$$

where f is the perennial mean monthly precipitation frequency, being the ratio of the number of perennial monthly rainfall days and number of days of the month, while a, b are regression coefficients.

Input for the model must include monthly probabilities of receiving rainfall. On any given day, the input must include information as to whether the previous day was dry or wet. The probability for the particular day in that month is calculated with either Equation (2) or Equation (3) depending on the known wet-dry condition of the previous day. Then it is input into the random number generation form. The random number generation is obtained from a Visual Basic program written for this purpose. A random uniform number between 0 and 1 is obtained by clicking a button. If the random number is less than or equal to the wet-dry probability entered, rain is predicted to occur for that day and a wet day is expected to follow. On the contrary, when the random number generated is greater than the wet-dry probability, no rain is predicted for that day and a dry day is expected to follow. Since the wet or dry state of the first day can be established, the process can be repeated for the next day and so on throughout the simulation period.

When a rain event is predicted to occur, the rainfall amount to be expected can be generated from a skewed normal daily precipitation distribution (Nicks 1974).

$$R_i = \left(\frac{\left(\left(SND_i - \frac{SCF_k}{6} \right) \left(\frac{SCF_k}{6} \right) + 1 \right)^3 - 1}{SCF_k} \right) RSDV_k + \overline{R}_k \quad (4)$$

where R_i is the amount of rainfall in mm and SND_i is the standard normal deviate for day i respectively, while SCF_k is the skew coefficient, $RSDV_k$ is the

standard deviation of daily rainfall, and $\bar{R}_k$ is the mean daily rainfall, for the month *k*. For each month, the total number of wet days and the total sum of rainfall for these days can then be predicted.

RESULTS AND DISCUSSION

Daily rainfall records for the Besut area were used to run the model. The period of rainfall record has permitted the investigation of trends in the annual number of wet days. The time plots of the annual number of wet days at the six stations are presented in *Fig. (1). Fig. (1[a, c, e, f])* shows persistent decline in the annual number of wet days from the 1990s onwards. A simple linear regression analysis was performed for each location separately and for the combined data. Results presented in Table 2 showed that none of the intercepts (a values) is significantly different from zero and none of the slope coefficients (b values) is significantly different from any other slope coefficient among the locations. The combined regression line with a zero intercept and slope 0.75 explains 96% of the total variation that existed among the transitional probabilities across time and space. Monthly transitional probabilities were then calculated with the fractions of wet days, and these are shown in *Fig. 2.* To validate the stochastic rainfall model, which could be used for generating rainfall occurrence and rainfall amount, historical data from one rainfall station, the Angga Station, was selected for evaluation. *Fig. 3* shows the Visual Basic screen where the wet-dry probability calculated is then entered for the month and a random number is generated, after which the condition for the next day is given upon clicking the start button to initiate comparison of numbers. Table 3 shows an example calculation for the case of January 1st to 31st 2001. Table 4 shows a summary of the comparison between the historical and simulated data for frequency of wet days for Angga Station for the years 2000 and 2001. As far as the rainy days are concerned, there was no case in which the generated monthly values were different from the actually observed

TABLE 2
Regression coefficients a and b of regressing the transitional probabilities of a wet day to a dry day for the data of six rainfall stations

Location	a	(s.e)*	b	(s.e)	r^2 **
Ibu Bekalan Angga	0.002	0.006	0.725	0.028	0.980
Sek Keb Kg Jabi	0.008	0.041	0.810	0.029	0.975
Sek Keb Keruk	-0.015	0.012	0.856	0.041	0.970
Sek Keb Kg Tambila	0.021	0.004	0.721	0.035	0.969
Rumah Merinyu Tali air	-0.004	0.015	0.645	0.046	0.965
Pasir Akar	0.006	0.005	0.768	0.015	0.890
Combined	0.003	0.014	0.754	0.032	0.958

* s.e is the standard error ** r^2 is the correlation coefficient

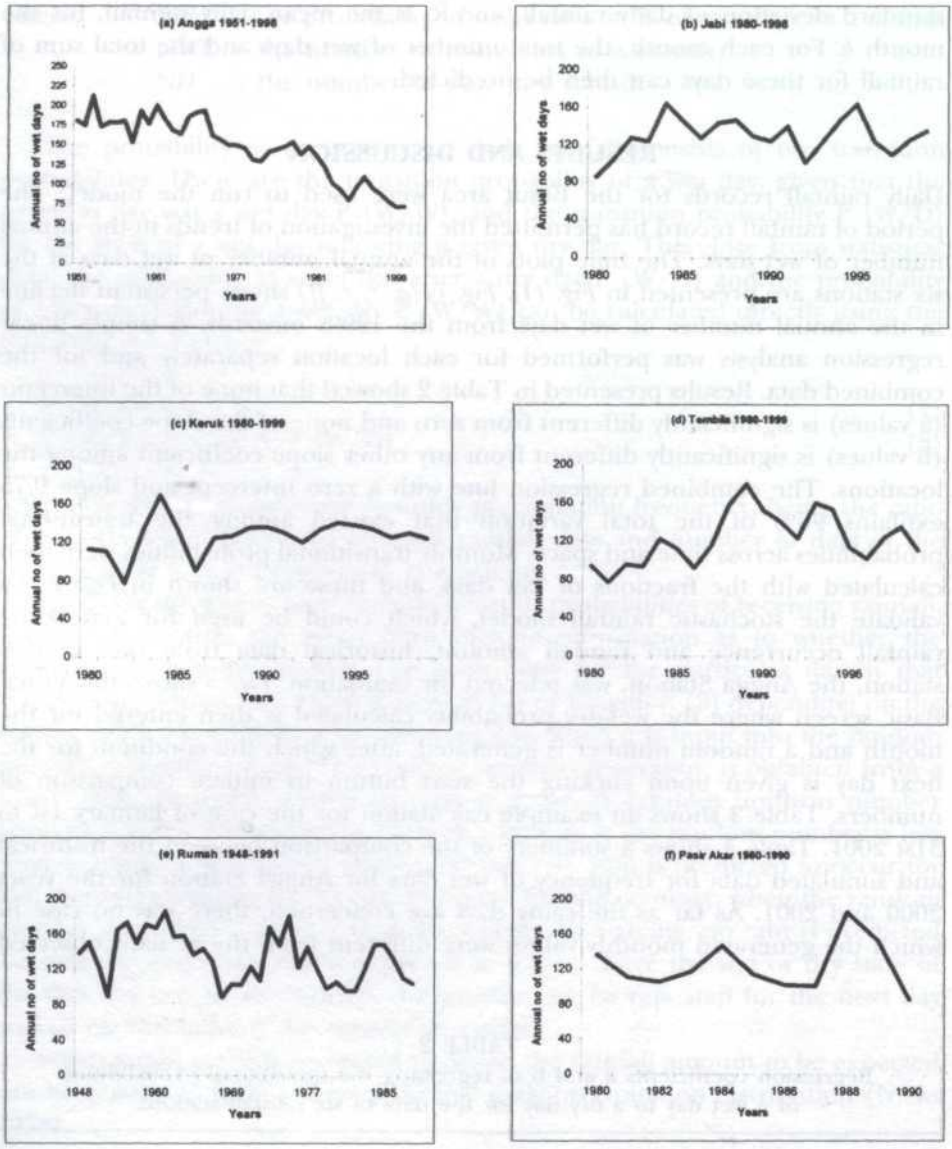

Fig. 1: Time plot of annual number of wet days of six rainfall stations

monthly values by more than two days. In terms of amount of rainfall, simulated results were again very close to the observed values, with a slight overestimation in a few months. The amount overestimated was less than 5% of the observations in all cases. The model thus allows for satisfactory rainfall simulation and can be used for water management of irrigation practices.

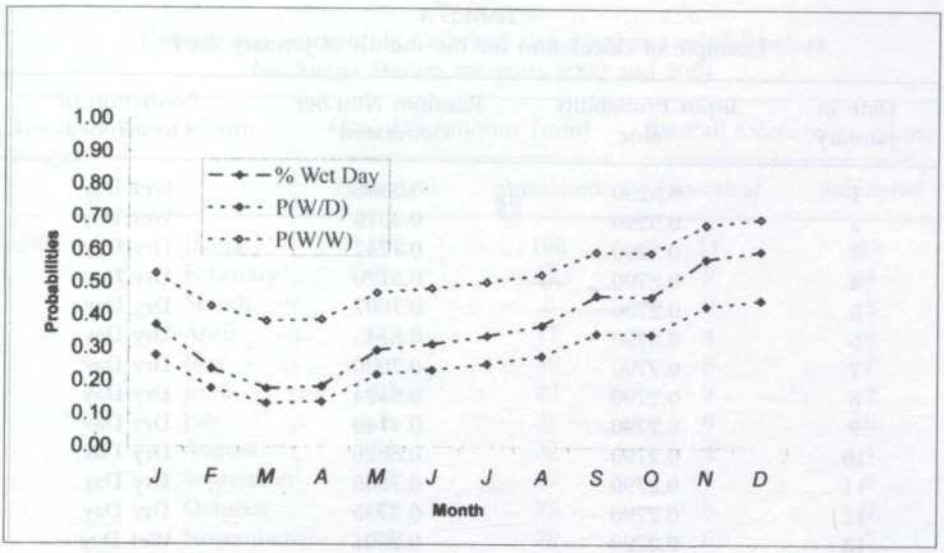

Fig. 2: Transitional probabilities and fractions of wet days for each month

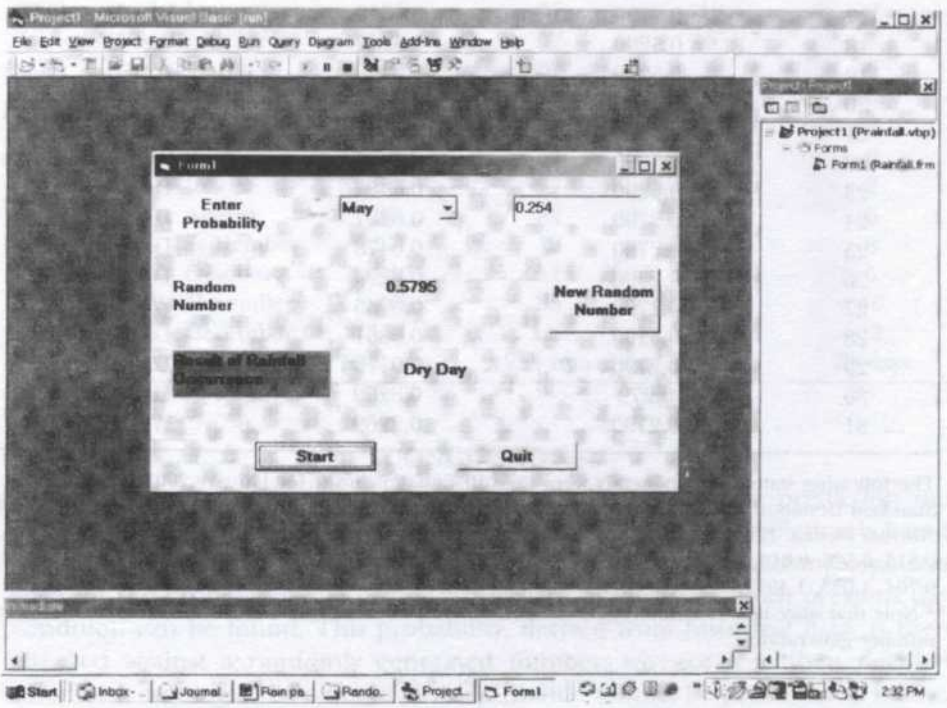

Fig. 3: Visual basic screen showing the random number generation result

TABLE 3
Example of calculation for the month of January 2001

Date in January	Input Probability Value	Random Number Generated*	Prediction of Occurrence
1	0.5290	0.2896	Wet Day
2	0.5290	0.3019	Wet Day
3	0.5290	0.7747	Dry Day
4	0.2790	0.5120	Dry Day
5	0.2790	0.7607	Dry Day
6	0.2790	0.8145	Dry Day
7	0.2790	0.7090	Dry Day
8	0.2790	0.6124	Dry Day
9	0.2790	0.4140	Dry Day
10	0.2790	0.8626	Dry Day
11	0.2790	0.7905	Dry Day
12	0.2790	0.3735	Dry Day
13	0.2790	0.2501	Wet Day
14	0.5290	0.0214	Wet Day
15	0.5290	0.0562	Wet Day
16	0.5290	0.9496	Dry Day
17	0.2790	0.1512	Wet Day
18	0.5290	0.5249	Wet Day
19	0.5290	0.5150	Wet Day
20	0.5290	0.0535	Wet Day
21	0.5290	0.0712	Wet Day
22	0.5290	0.4687	Wet Day
23	0.5290	0.6587	Dry Day
24	0.2790	0.6227	Dry Day
25	0.2790	0.6478	Dry Day
26	0.2790	0.8294	Dry Day
27	0.2790	0.0235	Wet Day
28	0.5290	0.9861	Dry Day
29	0.2790	0.9110	Dry Day
30	0.279	0.8280	Dry Day
31	0.2790	0.2269	Wet Day

The following statistical parameters were used in Equation no.4, for January 2001
Standard Deviation = 31.360, Skew Coefficient = 5.945, Mean Daily Rainfall = 12.074 mm, Standard Normal Deviate (SND) daily (1st - 31st January) = 0.594, 0.673, 0.501, 0.381, 0.375, 0.439, 0.434, 0.816, 0.586, 0.619, 0.632, 0.422, 0.539, 0.740, 0.579, 0.828, 0.790, 0.875, 0.930, 0.551, 1.120, 1.205, 0.704, 1.033, 1.453, 0.858, 1.606, 1.419, 1.080, 0.985, 1.492.

* Note that since it is a randomly generated number, it will change. Numbers shown are a first time number generation.

TABLE 4
Comparison of monthly historical and simulated rainfall values for Angga Station for years 2000 and 2001

Location/Year Angga	Month	Rainfall Amount (mm)		Rainfall Occurrence (days)	
		Historical	Simulated	Historical	Simulated
2001	January	162	166	11	13
	February	85	82	5	4
	March	10	8	2	3
	April	23	17	4	6
	May	55	49	8	7
	June	25	24	2	2
	July	0	0	0	0
	August	30	32	4	4
	September	50	47	7	6
	October	73	75	8	9
	November	85	72	8	7
	December	375	393	16	18
	Total	973 mm	965 mm	75 days	79 days
2000	January	105	97	10	9
	February	45	37	6	5
	March	70	67	6	6
	April	35	29	4	4
	May	27	28	3	4
	June	62	60	6	8
	July	25	27	3	2
	August	95	82	7	6
	September	57	49	7	8
	October	65	52	4	5
	November	90	88	9	10
	December	152	140	11	12
	Total	828 mm	756 mm	76 days	79 days

CONCLUSIONS

A study was carried out to adapt a mathematical model for predicting the probability of rainfall, given a previous day's condition. This prediction is based on a first-order Markov chain process and its accompanying assumptions and wherein the probability of a wet or a dry day's to follow a known previous day condition can be found. This probability, derived from historical data, is then checked against a randomly generated number, whence it is then decided whether it is going to be a wet or dry day. Should rainfall be predicted to follow, then the expected amount of rainfall is evaluated by a method in which its parameters were predetermined from a statistical analysis of past long term historical daily and monthly data. The total predicted number of rainy days for

the month, and the total monthly rainfall can be tallied up. In the year 2000, the actual number of days with rainfall recorded was 76 and the total amount of annual rainfall was 828 mm. The number of wet days predicted was 79 with a total annual rainfall of 756 mm. This gave a percentage difference between observed and predicted days of rainfall and amount of rainfall as +4% and -8.6% respectively. Similarly, the total number of wet days and total rainfall was observed to be 75 and 973 mm respectively in 2001. The predicted number of wet days for 2001 is 79 days while the annual rainfall predicted is 965 mm giving a +5.3% more number of wet days and -0.01% less rainfall amount. Hence the model hence can generate satisfactory results.

ACKNOWLEDGEMENTS

The authors wish to express their sincere gratitude to the staff of the Besut Irrigation Scheme, the Drainage and Irrigation Department and the Malaysian Meteorological Service. The authors would also like to thank The Ministry of Science, Technology and the Environment for the funding of the Project IRPA 01-02-04-0422.

REFERENCES

NNAJI, A. O. 2001. Forecasting seasonal rainfall for agricultural decision-making in northern Nigeria. *J. of Agricultural and Forest Meteorology* **107**: 193–205.

CAREY, D. I. and C. T. HAAN. 1978. Markov processes for simulating daily point rainfall. *Journal of Irrigation and Drainage Division ASCE* **104 (IRI):** 111–125.

CHIN, E. H. 1977. Modelling daily precipitation occurrence process with Markov chain. *Water Resources Research* **13(6):** 949–956.

EFREMIDES D. and G. TSAKIRIS. 1994. Stochastic modelling of point rainfall in a Mediterranean Island environment. *Water Resources Management* **8:** 171–182.

FRENCH, R. H. 1983. Precipitation in southern Nevada. *J. of Hydraulics Division ASCE* **10** (HY 7): 1023–1036.

GARBUTT, D. J., R. D. STERN, M. D. DENNETT and J. ELSTON. 1981. A comparison of the rainfall climate of eleven places in West Africa using a two-part model for daily rainfall. *Arch. Met. Geophy. Biokl. Ser. B.* **29:** 137–155.

GENG, S., F. W. T. PENNING DE VRIES and I. SUPIT. 1986. A simple method for generating daily rainfall data. *J. Agricultural and Forestry Meteorology* **36:** 363–376.

HANSON, C. L. 1982. Distribution and stochastic generation of annual and monthly precipitation on a mountainous watershed in southwest Idaho. *Water Resources Bulletin AWRA* **18(5):** 875–883.

HANSON, C. L. 1984. Annual and monthly precipitation generation in Idaho. *Transactions of the ASCE* **27(6)**: 1792–1797.

HANSON, C. L., R. P. MORRIS, R. L. ENGLEMAN, D. C. COON and C. W. JHONSON. 1980. Spatial and seasonal precipitation distribution in southwest Idaho. USDA, ARS Agricultural Research Mannual. ARMW-13.

JICA. 1998. The study on modernization of irrigation water management system in the granary area of Peninsular Malaysia. Draft Final Report, Volume -II, Annexes, March.

JIMOH, O. D. and P. WEBSTER. 1996. Optimum order of Markov chain for daily rainfall in Nigeria. *Journal of Hydrology* **185:** 45–69.

JIMOH, O. D. and P. WEBSTER. 1999. Stochastic modeling of daily rainfall in Nigeria: intra-annual variation of model parameters. *Journal of Hydrology* **222:** 1–17.

MIMIKOU, M. 1983. Daily occurrence modeling with Markov chain of seasonal order. *Hydrology Science Journal* **28(2):** 221–223.

NICKS, A. D. 1974. Stochastic generation of the occurrence, pattern, and location of maximum amount of daily rainfall. In *Proc. Symp. Statistical Hydrology*, p.154–171, Aug.-Sept. 1971, Tucson, AZ.U.S. Dept. Agric., Misc. Publ. No. 1275.

OSBORN, H. B. 1984. Estimating precipitation in mountainous regions. *J. of Hydraulics Div. ASCE* **110(HY 12):** 1859–1863.

OSBORN, H. B. 1987. Closure: estimating precipitation in mountainous regions. *J. of Hydraulics Division ASCE* **113(HY 4):** 549–550.

SRIKANTHAN, R. and T. A. MCMAHON. 1983. Stochastic generation of daily rainfall for Australian stations. *Trans. ASCE*: 754–766.

STERN, R. D. and R. COE. 1982. The use of rainfall models in agricultural planning. *J. of Agric. Meteorology* **26:** 35–50.

TUNG, YEOU-KOUNG. 1983. Point rainfall estimation for a mountainous region. *J. of Hydraulics Division ASCE* **109 (HY 10):** 1386–1393.

Pertanika J. Sci. & Technol. 12(1): 149 - 172 (2004)
ISSN: 0128-7680
© Universiti Putra Malaysia Press

Exchange Rates Forecasting Model: An Alternative Estimation Procedure

Ahmad Zubaidi Baharumshah,[a]* Liew Khim Sen & Lim Kian Ping[b]
[a]Department of Economics, Faculty of Economics and Management, Universiti Putra Malaysia, 43400 UPM Serdang, Selangor, Malaysia
[b]Labuan School of International Business and Finance, Universiti Malaysia Sabah, P.O.Box 80594, 87015 W.P. Labuan, Malaysia

Received: 9 January 2003

ABSTRAK

Kajian ini mengesyorkan suatu prosedur alternatif untuk memodel kelakuan pertukaran asing, melalui gabungan linear fungsi jangka masa panjang dan pendek. Di antara segala kombinasi kaedah-kaedah permodelan yang mungkin, kami mengesyorkan kombinasi yang paling ringkas, iaitu membentuk model jangka masa panjang berasaskan model Pariti Kuasa Beli (PPP) yang terkenal, diikuti dengan pembentukan model untuk fungsi jangka masa pendek berasaskan sifat-sifat siri masanya. Keputusan-keputusan yang diperolehi dalam kajian ini mencadangkan bahawa prosedur kami dapat menghasilkan model-model peramalan yang unggul kerana mereka meramal dengan lebih tepat lagi jika dibandingkan dengan model pergerakan rawak mudah (SRW) yang jarang diatasi secara keseluruhan oleh model-model peramalan pertukaran asing sebelum ini, dari segi peramalan luar sampel. Kajian ini memberikan kita suatu harapan yang cerah dalam penghasilan ramalan pertukaran asing negara-negara ASEAN dengan menggunakan model berasaskan kewangan dengan sedikit perubahan yang mudah.

ABSTRACT

This study proposes an alternative procedure for modelling exchange rates behaviour, which is a linear combination of a long-run function and a short-run function. Our procedure involves modelling of the long-run relationship and this is followed by the short-run function. Among all the possible combinations of modelling techniques, we proposed the simplest form, namely modelling the long-run function by the well established purchasing power parity (PPP) based model and setting up the short-run function based on its time series properties. Results of this study suggest that our procedure yields powerful forecasting models as they easily outperform the simple random walk model-which is rarely defeated in the literature of exchange rate forecasting-in terms of out-of-sample forecasting, for all the forecast horizons ranging from one to fourteen quarters. This study provides us with some hope of achieving a reasonable forecast for the ASEAN currencies using the fundamental monetary model just by a simple adaptation.

Keywords: Forecasting, exchange rate, purchasing power parity, interest rate differential, mean deviation, mean percentage error, Fisher's sign test

*Correspondence author

INTRODUCTION

Most exchange rate markets in the floating exchange rate regime have experienced continuous and sometimes dramatic fluctuations and volatility. Mussa (1996) has summarized the broad features of exchange rate behaviour. Mussa noted that (i) exchange rates are extremely volatile, with deviation of about 3 percent per month for the US dollar-Japanese yen and US dollar-Deutschmark rates; (ii) changes in exchange rates are very persistent, and the exchange rate closely approximates a random walk; (iii) there is correlation of almost unity between real and nominal exchange rates on high frequency data; and (iv) the variability of real exchange rates increases dramatically when a country moves from fixed to floating exchange rates. All these suggest that exchange rates can be much more volatile than the apparent fundamentals, and in practice deviation from equilibrium value can be persistent. Thus, the researches of exchange rate behaviour and exchange rate forecasting have become perennial topics in international finance since the floating exchange rate regime was established in March 1973. As a result, many theories and models were developed.

The existing models of foreign exchange rates were developed using the linear and non-linear frameworks. Models based on the linear framework include the simple efficiency market approach (Fama 1965; Cornell 1977; Hsieh 1984), simple random walk approach (Giddy and Duffey 1975; Hakkio and Rush 1986), the linear fundamentals approach (for example, Dornbusch 1976; Frankel 1979; Meese and Rogoff 1983; Mark 1995; Clark and MacDonald 1998), the time series approach (for instance, Keller 1989; Cheung 1993; Palma and Chan 1997; Brooks 1997; Parikh and Williams 1998; Baharumshah and Liew 2003), the conditional heteroscedasticity approach (Engle 1982; Bollerslev 1986), among others.

There is a growing consensus among researchers that exchange rates and other financial variables are non-linear in nature (Brooks 1996; Taylor and Peel 2000; Liew *et al.* 2002) and so they are linearly unpredictable (Boothe and Glassman 1987; Plasmans *et al.* 1998). Hence the non-linear structural models are regarded more relevant in modelling these variables. Models in conjunction with this more recent view are commonly estimated through the non-linear fundamentals approach (see for example, Meese and Rose 1991; Lin and Chen 1998; Ma and Kanas 2000; Coakley and Fuertes 2001), the Exponential GARCH approach (Nelson 1991), the SETAR approach (Krāger and Kugler 1993), and the neural networks approach (Franses and Homelen 1998; Plasmans *et al.* 1998), among others.

Nevertheless, after three decades of research, exchange rate theory that provides a satisfactory and empirically consistent theory of the exchange rate remains to be uncovered (Hallwood and MacDonald 1994: p. 22). Like any other financial variables, exchange rates are difficult to forecast with any precision. The bulk of evidence has so far been proven illusive (Berkowitz and Giorgianni 1997; Lin and Chen 1998). In their survey on empirical work of exchange rate, Frankel and Rose (1995) make the following remark: We, like

much of the profession, are doubtful of the value of further time series modelling of exchange rates at high or medium frequencies using macroeconomic models.' This observation has motivated us to search for an alternative approach to model exchange rates.

This study attempts to model exchange rates and the focus is on the ability of the model to yield reliable forecast in the short and intermediate run. The main focus is to construct a model that can capture the dynamics of exchange rates in the emerging economies. The model that we consider is a linear combination of long and short run functions. The long run component of the model is set to represent the relationship between any exchange rate and its fundamental variables (e.g. relative price, interest differential and money supply), whereas the short-run equation is based on time series model and is used to capture the deviations of the exchange rate from its long-run path[1]. Thus, the estimation procedure involves two stages: first, the long-run model is fitted to the data, and this is followed by the short-run function. To this end, we relied on the widely used linear structural model (purchasing power parity, PPP) hypothesis to trace the long-run relationship between exchange rate and its determinant[2]. To account for the inadequacy of the pure PPP model, we augmented the short-run component of the model based on statistical properties of the data[3]. In this article, our focus is on the PPP and interest differential models (IRD). We have no intention to identify a set of fundamental variables that is most appropriate to tract the movements of the exchange rates but simply to show that information contained in both domestic and foreign macroeconomic variables (prices and term structures of interest rates) may not be sufficient to tract the movement of exchanges rates. Intuitively, one may expect to gain efficiency in the forecasts, by adding more information to the

---

[1] Many theoretical models suggest that exchange rates should be jointly determined with macroeconomic variables such as foreign ad domestic money supplies, real growth rates, interest rates, price levels, and balance of payments. However, as mentioned earlier the empirical performance of these models has been very poor. In fact, Meese (1990) concludes that '*the proportions of (monthly or quarterly) exchange rate changes that current models can explain is essentially zero.*"

[2] A hallmark of the conventional model of real exchange rate is that it follows a PPP benchmark in the long run. Briefly, the PPP doctrine states that the price of a basket of goods should equate across countries when evaluated in common currency. For the empirical work on PPP, see Nagayasu (1998), Coakley and Fuertes (1997), and M-Azali et al. (2001), to name a few. The work by Nagayasu found support for a "semi-strong' version of the long-run PPP hypothesis in a sample of 16 African countries. M-Azali et al. also found evidence that PPP holds between the developing Asian countries and Japan.

[3] This is in line with the view that PPP is a long run relationship and overtime prices adjust and PPP is re-established.

model. For this purpose, we compare the performance of the simple PPP model with that of the interest rate differential (IRD) model[4].

The rest of this paper is organized as follows: In the section that follows, we construct the proposed model. Section 3 describes the method used in the analysis and Section 4 interprets the results of the empirical investigation. The last section concludes this paper.

Derivation of the Model

The estimation of model is based on a two-step procedure. First, the long-run component of the model is considered and second, the deviation of the actual observations from its long-run equilibrium path is considered to model the short-run component of the model. In this way, our forecasting model will not only trace the long-run movement, but is also capable of capturing misalignment in the exchange rate series that may occur in the short-run. This strategy is also in line with the argument that exchange rates can be more volatile than the fundamentals; in our case it is the relative price and/or interest rate differential. Consider the model

$$X_t = f_t(l_1,l_2,...,l_l) + g_t(s_1,s_2,...,s_s) \quad (1)$$

where X_t is exchange rate defined as domestic currency, per unit foreign currency; $f_t(l_1,l_2,...,l_l)$ is a set of long-run determinants $\{l_1,l_2,...,l_l\}$ that explained the long-run movement of the exchange rate; and $g_t(s_1,s_2,...,s_s)$ is a function of a set of short-run determinants $\{s_1,s_2,...,s_s\}$ that may cause exchange rate to deviate from its long-run equilibrium path.

Let the expected value of f_t be given by $\hat{X}_t$, which is determined by the fundamental variables. By subtracting the value of $\hat{X}_t$ on both sides of (1) we obtained

$$X_t - \hat{X}_t = f_t - \hat{X}_t + g_t \quad (2)$$

If $\hat{X}_t$ is an unbiased predictor of f_t, then the term $(f_t - \hat{X}_t)$ on the RHS of (2) vanishes to random error term, ε_t with mean zero and variance σ_ε^2. Thus, we have

$$X_t - \hat{X}_t = \varepsilon_t + g_t \qquad \text{where } \varepsilon_t \sim \text{WN } (0, \sigma_\varepsilon^2) \quad (3)$$

---

[4] The literature has not provided conclusive evidence on the long-run determinants of exchange rate. Frankel (1979) sets the long-run determinants as the relative interest rates. Dornbusch (1976) and Chin dan Meese (1995) identify the long-run determinants based on the standard monetary model (money supply, income and inflation rate). Clark and MacDonald (1998) include interest rates, government debt ratio, terms of trade, price levels and net foreign assets to model the exchange rates.

or equivalently

$$X_t = \hat{X}_t + g_t + \varepsilon_t \quad (4)$$

Modelling short-run function g_t is even more complicated as the subsets of short-run determinants may change over time due to either internal or external events (e.g. policy change, capital reversal and regional financial crises). One way out of this dilemma is to think of g_t as generated by time series mechanism, whatever the underlying macroeconomic determinants may be. For instance, one may think of g_t as represented by the ARIMA, ARFIMA or GARCH processes. It is worth noting that the GARCH process involves modelling the square of residuals, and in our case, g_t. However, authors like McKenzie (1999) have pointed out that by squaring the residuals, one effectively imposes a structure on the data, which has the potential of reducing the forecasting performance of the model. In the present study, we assume that g_t as proportionate to its most recent available value, g_{t-1}, to avoid the problem of complexity, i.e.

$$g_t = \alpha\, g_{t-1} + v_t \text{ where } v_t \sim \text{WN } (0, \sigma_v^2) \quad (5)$$

with $\alpha < 1$ if g_t is stationary and $\alpha \geq 1$ if g_t is non-stationary.

By simply substituting (5) into (4) and upon simplification, we obtained the final model that is

$$X_t = \hat{X}_t + \alpha\,(X_{t-1} - \hat{X}_{t-1}) + \mu_t \quad \text{where } \mu_t = \varepsilon_t + v_t \quad (6)$$

Clearly, the estimation of Equation (6) also involves procedures to solve for $\hat{X}_t$ and searching for optimal value of α.

METHODOLOGY

In this study we attempt to model the Malaysia ringgit (MYR), the Singapore dollar (SGD), and Thailand baht (THB) against the US dollar (USD) and Japanese yen (JPY), all of which have received little attention in the exchange rate literature. The base currencies chosen are based on the importance of trade to these ASEAN countries. According to the International Monetary Fund (IMF)'s classification, these countries pegged their currency to a basket of currencies (the US dollar received that highest weight). Our sample period covers the first quarter of the year 1980 to the fourth quarter of the year 2000 (1980:1 to 2000:4). Bilateral rates used in the analysis are the end of period market rate specified as line ae in *International Financial Statistics* published by the IMF, except for the MYR/USD rate. For the case of MYR/USD rate, we choose the series from line aa, which is calculated on the basis of SDR rate. This is to avoid the problem of zero denominators that may arise during the assessment of the performance of the forecasting exercises.

Besides the bilateral exchange rate series, data on relative price and interest differential are also utilized in this study. The price variable is constructed as the ratio of domestic price to foreign price. We use consumer price indices (CPI 1995 = 100) as the proxy for prices. Interest rate differential is computed by dividing the domestic market rate over the foreign market rate. All the data series are taken from various monthly issues of IMF/IFS. The full sample period is divided into two periods. The first sub-period that begins in 1980:1 and ends in 1997:2 is used for the purpose of estimation and the remaining observations (1997:2-2000:4) are kept for assessing the out-of-sample forecast performance of the model. Following the work of García-Ferrer *et al.* (1997), our data are purposely treated in such a way that they showed a break in the trend (due to the 1997 Asian financial crisis) during the forecasting period, making the prediction exercise more difficult. Specifically, the large depreciation in the post currency crisis period makes the post-sample prediction more stringent [5].

For each country, we first examine the time series properties of three variables used in the analysis. We applied the augmented Dickey Fuller (ADF) and the Philips-Perron (PP) unit root tests to the level and first differences of the data. Results of unit root test are summarized in Table 1.

Overwhelmingly, the results of the unit root tests suggest that we cannot reject the hypothesis of nonstationarity in levels and reject it in first differences in all the series, except in one case (SGD/JPY)[6]. Since exchange rates, relative price and interest rate differential exhibit the same order of integration, this allows us to proceed with the co-integration test. To this end we utilise the Johansen and Juselius (1990) multivariate cointegration test that is based on statistics: trace test and the maximum eigenvalue tests.

For each country we ran the vector autoregressive (VAR) system in levels with one to five lags. The primary goal was to eliminate serial correlation while avoiding power-draining due to the presence of too many lags. We also check for serial correlation using the Bruesch-Godfrey asymptotic test before deciding on the optimal lag for the VAR model. The results of the Johansen-Juselius co-integration test are tabulated in Table 2. Table 2 reveals that all the exchange rates (except THB/USD) are co-integrated with their corresponding relative prices at the 5% significance level or better. This finding suggests that long-run relationship between exchange rate and relative price exists in the studied countries. Hence, the co-integration test results are consistent with the PPP hypothesis at least for the five exchange rates (MYR/USD, SGD/USD, MYR/JPY, THB/JPY and SGD/JPY).

Similarly, we found that for all the countries exchange rates, relative price and interest differential variables for all cases (except SGD/JPY and THB/

---

[5] Visual inspection of the data reveals that up to the middle of 1997 volatility is less pronounced, whilst thereafter it rises substantially.

[6] Because of the low power of the classical unit root tests, we continue with the analysis by assuming that all the exchange rate series are I(1) variable.

TABLE 1
Results unit root tests

Countries	Intercept Without Trend						Intercept With Trend					
	X	ΔX	P	ΔP	I	ΔI	X	ΔX	P	ΔP	I	ΔI
Augmented Dickey - Fuller Test												
Malaysia - US	-0.658	-5.079*	-1.445	-5.170*	-2.001	-3.923*	-2.763	-5.088*	-0.780	-5.434*	-1.980	-4.043*
Thailand - US	-0.562	-5.377*	-0.479	-3.866*	-2.131	-4.801*	-1.691	-5.377*	-1.482	-3.971*	-2.782	-4.802*
Singapore - US	-1.000	-5.114*	-2.492	-6.148*	-3.104#	-4.768*	-0.544	-5.131*	-1.729	-6.583*	-3.142	-4.738*
Malaysia - Japan	-0.362	-4.958*	1.989	-5.537*	-2.148	-4.815*	-2.696	-4.953*	-0.040	-6.260*	-2.802	-4.657*
Thailand - Japan	0.179	-6.336*	1.237	-3.541*	-1.758	-5.566*	-2.489	-6.482*	-0.985	-3.920*	-2.494	-5.533*
Singapore - Japan	-0.211	-3.712*	0.054	-5.551*	-3.633#	-3.076*	-0.575	-3.989*	-1.172	-5.744*	-4.066#	-2.721
Philips - Perron Test												
Malaysia - US	-0.661	-10.70*	-1.948	-10.83*	-2.448	-7.097*	-2.973	-10.09*	-1.152	-11.19*	-2.251	-7.106*
Thailand - US	-0.731	-9.827*	-0.414	-7.479*	-2.084	-7.227*	-2.161	-9.828*	-1.351	-7.572*	-2.354	-7.171*
Singapore - US	-1.370	-9.930*	-3.626#	-8.823*	-3.072#	-6.957*	-0.987	-9.930*	-1.817	-9.906*	-3.117	-6.903*
Malaysia - Japan	-0.528	-8.653*	3.726	-11.67*	-2.998	-11.54*	-2.987	-8.653*	0.233	-12.86*	-3.726#	-11.44*
Thailand - Japan	-0.576	-11.10*	-1.360	-9.811*	-1.787	-7.014*	-3.107	-11.10*	-0.757	-10.13*	-2.541	-6.948*
Singapore - Japan	0.240	-5.811*	0.991	-11.18*	-3.439#	-10.79*	-0.832	-5.811*	-0.842	-11.43*	-4.042#	-10.70*

Notes:X, P and I denote exchange rate, relative price and interest differential respectively. Δ denotes first difference. Optimum lag length is automatically given by E-views based on Newey and West (1987).
Critical values are given by McKinnon (1991). Test-statistics with * and # denote reject null hypothesis of unit-root at 1% and 5% level respectively.

TABLE 2
Co-integration test results

Pairwise Variables	Exchange Rate and Relative Price			Exchange Rate, Relative Price and Interest Differential[a]			
	Likelihood Ratio[b]			Likelihood Ratio[b]			
Countries	Lag[c]	r = 0	r ≤ 1	Lag[c]	r = 0	r ≤ 1	r ≤ 2
Based Country: United States							
Malaysia	8	21.646#	8.189	6	33.576#	11.412	1.363
Thailand	10	12.573	4.765	3	28.346	13.435	4.066
Singapore	12	38.982*	8.871	2	33.610#	10.058	0.568
Based Country: Japan							
Malaysia	10	24.369#	5 061	12	89.299*	21.391*	1.359
Thailand	11	23.884#	9.080	12	36.579*	13.122	2.106
Singapore	12	24.559#	2.817	—	—	—	—
Critical Values							
5%		19.90	9.24		29.68	15.41	3.76
1%		24.60	12.97		36.65	20.04	6.65

Note. [a]For SGD/JPY, the three variables are not integrated of the same order, hence cointegration does not exist by definition.
[b] r denotes the hypothesized number of co-integrating equation.
[c] Optimum lag-length is determined by the AIC statistics.
* and # denote rejection of hypothesis at 1% and 5% significance level respectively.

USD) are co-integrated (see Table 2). All in all, there exists at least one co-integrating vector in the exchange rates based on conventional significance levels.

Our next task is to proceed with the forecasting model as given in Equation (6). The estimation involves two steps. In step one, we estimate the PPP model by regressing the exchange rate (X_t) on CPI (or IPI) ratios (P_t). For the case of SGD/USD, for instance, the PPP model is estimated by running SGD/USD on PS/PU, where PS and PU are CPI (1995=100) of Singapore and CPI (1995=100) of US respectively. Then we compute the values of $\hat{X}_t$, which is the predictor of the spot exchange rate, g_t. The deviation from the long-run model, g_t is obtained as

$$g_t = \text{Xt} - \hat{X}_t \tag{7}$$

In step two, we estimate the function as suggested in Equation (5). In this study, we employ a search algorithm to determine the optimum value of α such that the in-sample forecasting error is the minimum with respect to the selected criteria (e.g. Mean Square Forecast Error (MSE) and the Mean Square Percentage

Error (MSPE), Mean Absolute Percentage Error (MAPE) and Theils' *U*). We chose to minimise the MAPE of the in-sample forecasts as we found that it is more reliable in the sense that the selected optimum for the in-sample period is a better estimator for the optimum value of the out-of-sample period (results not shown here but are available upon request).

The optimum model is then subjected to a battery of diagnostic tests. We emphasized two important aspects, namely the efficiency of the forecasts and the stationarity of the residuals, μ_t. If the model is capable of capturing the long run and short run movements of the actual exchange rate behaviour, the residuals must be random errors and hence stationary. Besides that, since we utilize time series data it is important that we eliminate serial correlation. We checked for serial correlation by using the standard Durbin-Watson (*d*) and Bruesch-Godfey Lagrange Multiplier (LM) test for autocorrelation.

To sum up, the selection process for the "optimum" model can be summarized by the follow steps:

Step One: (1) Regress sample exchange rate, X_t on sample relative price, P_t; (2) Obtain $\hat{X}_t$ from the regression; and (3) Compute $g_t = X_t - \hat{X}_t$.

Step Two: (1) Search for optimum with based on selected criteria; (2) Check for serial correlation on the residuals and efficiency of model; and (3) proceed with forecasting.

In order to forecast X_{t+n} where the number of quarter, $n = 1, ..., 14$ for the out-of-sample period (1997:3 to 2000:4), we need to have the values of P_{t+n}. As P_{t+n} is also not available, the fastest way of obtaining reliable estimator for it is to do forecasting using the ARIMA methodology. The reason why we chose not to forecast directly using the ARIMA methodology is that although this method could provide better forecasts (see for examples, Montogomery *et al.* 1990; Lupoletti and Webb 1986 and Litterman 1986), it is not capable of significantly outperforming the simple naïve model for the case of ASEAN currencies; see Baharumshah and Liew (2003).

The performance of our forecasting models over the forecast horizon of $n = 1$, then $n = 2$ and so forth until $n = 14$ quarters are evaluated by taking the naïve models of predicting no change as the benchmark. The criteria involved are the minimum of the Mean Square Forecast Error (*MSE*) and the Mean Square Percentage Error (*MSPE*) and the Mean Absolute Percentage Error (*MAPE*) ratios of the two competing models, with the appropriate error criterion of the naïve model as denominator. If the ratio is greater than one, it implies the naïve model is better. If the ratio is less than one, it means the forecasting model has defeated the naïve model and the researchers' effort is at least paid-off. It is worth noting that the closer the ratio to zero, the better is the forecast. We also provide the statistical significance of the MSE ratio using Meese and Rogoff (1988) (MR) test statistics defined as:

$$MR = \frac{\bar{s}_{UV}}{\sqrt{\frac{1}{n^2}\sum_{j=1}^{n} u_j^2 v_j^2}} \underset{\sim}{asy} N(0,1) \qquad (8)$$

where $\bar{s}_{UV}$ is the sample covariance of means of U and V (transformed functions of forecast errors of two rival models) and is approximated by $\frac{1}{n}\sum_{j=1}^{n}\left(u_j-\bar{u}\right)\left(v_j-\bar{v}\right)$ where $\bar{u}=\frac{1}{n}\sum_{j=1}^{n}u_j$ and $\bar{v}=\frac{1}{n}\sum_{j=1}^{n}v_j$ with $u_j = e_{1j} - e_{2j}$ and $u_j = e_{1j} + e_{2j}$ in which e_{ij}, $i = 1, 2$ is the j^{th} forecast error of model i; and n is the number of forecasts.

Following Wu and Chen (2001), we also applied the Fisher's sign test (FS). Briefly, the FS test compares the forecast accuracy of two competing models term by term on the basis of loss differential, whereby the accuracy criterion could be based on MSE, MSPE, MAPE, among others. The Fisher's sign test is the total number of negative loss differential (d_j) observations in a sample size n. Under the null hypothesis of "equal accuracy of two competing forecasts", FS has a binomial distribution with parameter n and 0.5. The significance of test is assessed using a table of the cumulative binomial distribution.

In this study we also estimated our model by using the same procedure as described above but a different long-run fundamental model that is the interest rate differential (IRD) model. This is achieved by adding the interest rate differential to the pure PPP model as an additional explanatory variable. The purpose is to study whether by adding extra information, the forecasting performance of the model could be improved or not.

RESULTS AND INTERPRETATION

The empirical results from the estimated PPP model and its adapted form are summarized in Table 3. As expected, the true PPP model only managed to capture the long-run movement of the actual exchange rate, but the adapted model has been adapted (or trained) to trace the short-run deviation of the actual exchange rate from its long-run course (*Fig.* 1). The R^2 suggests that relative price, P_t could account for 58.52 to 68.35% of the variation in bilateral rates of the ASEAN currencies (Table 3). The adapted model for the five ASEAN currencies tabulated is selected based on MAPE criterion. Notice that the R^2 value for the Singapore-yen rate (SGD/JPY) rate is unacceptably low (17.96)! Because of the poor performance base on the R^2, we did not pursue further and dropped it from the analysis[7].

[7] We found that the optimum model selected through this criterion (and in fact, other criteria e.g. MSE and Theil-U) may not necessary pass all the diagnostic tests. These results based on other criteria are not shown here but are available upon request from the authors.

TABLE 3
Estimated models

Exchange Rates	Estimated Coefficients[a]				
	Intercept	Relative Price	Interest Differential	R^2 Values	Optimal α Values[b]
			PPP Model[c]		
MYR/USD	12.283 (13.54)*	-8.881 (-9.94)*	—	0.585	0.929
SGD/USD	-0.529 (-2.62)#	2.177 (11.96)*	—	0.678	0.900
MYR/JPY	-0.010 (-3.12)*	0.028 (7.467)*	—	0.451	0.935
THB/JPY	-0.178 (-6.14)*	0.448 (12.12)*	—	0.684	0.940
SGD/JPY	0.020 (6.97)*	-0.011 (3.564)*	—	0.180	—
			IRD Model		
MYR/USD	12.030 (11.17)*	-8.669 (8.51)*	0.038 (0.44)	0.352	0.929
SGD/USD	-1.468 (-5.52)*	3.113 (13.24)*	-0.048 (-0.40)	0.755	0.900
MYR/JPY	-0.029 (-5.55)*	0.054 (8.38)*	-0.001 (-4.66)*	0.549	0.995
THB/JPY	-0.295 (-6.69)*	0.659 (9.12)*	-0.022 (-3.35)*	0.729	0.700

Notes: [a] t-statistics are given in parenthesis. * and # stand for significantly different from zero at 1% and 5% level respectively.

[b] The adapted model is of the form $\hat{\hat{X}} = \hat{X}_t + \alpha (X_{t-1} - \hat{X}_{t-1})$ where $\hat{\hat{X}}$ and $\hat{X}_t$ denote exchange rate (X_t) predicted by the adapted model and PPP Model or IRD Model respectively, and the optimal value for each adapted model is obtained by a computer search algorithm.

[c] Estimated PPP Model for SGD/JPY has very low R^2 value and hence we do not attempt to adapt it.

We subjected the selected model to a battery of diagnostic checking before the model is used to generate the in-sample and post-sample forecasts. Results of diagnostic tests performed on both the pure and adapted models' are depicted in Table 4. A striking feature of the results shown in Table 4 is that the pure PPP model proved incapable of completely attaining the serial correlation standard. The PPP model is contaminated with series correlation problem (positively correlated) as it has low Durbin-Watson *d* statistic[8]. This finding is further supported by the large values of Breusch-Godfrey Lagrange Multiplier (*LM*) statistics, which indicate that there exists serial correlation up to 12-lag length. On the other hand, the adapted PPP model easily passed the serial correlation tests. We consider these results as indication that the standard

[8] In our study, we have 70 in-sample observations and hence the actual decision region for the Durbin-Watson autocorrelation test of no autocorrelation in our model is $1.485 \leq d \leq 2.571$, at 1% significance level.

TABLE 4
Diagnostic test for PPP model and the adapted form

PPP Model		Adapted PPP Model	
1. MYR/USD			
$X_t = -0.163 + 1.032\ \hat{X}_t + \varepsilon_t$		$X_t = 0.039 + 0.987\ \hat{\hat{X}} + \mu_t$	
(0.217) (0.064)		(0.108) (0.033)	
$R^2 = 0.793$	$\varepsilon_t \sim I(1)$	$R^2 = 0.932$	$\mu_t \sim I(0)$
$d = 0.361$	$LM\ (12) = 48.226$	$d = 2.385$	$LM\ (12) = 11.839$
$\chi^2_2 = 4.039$	$\chi^2_1 = 0.250$	$\chi^2_2 = 0.200$	$\chi^2_1 = 0.154$
2. SGD/USD			
$X_t = -0.761 + 1.446\ \hat{X}_t + \varepsilon_t$		$X_t = -0.204 + 1.115\ \hat{\hat{X}}_t + \mu_t$	
(0.200) (0.116)		(0.047) (0.026)	
$R^2 = 0.752$	$\varepsilon_t \sim I(1)$	$R^2 = 0.971$	$\mu_t \sim I(0)$
$d = 0.141$	$LM\ (12) = 60.232$	$d = 2.23$	$LM\ (12) = 11.655$
$\chi^2_2 = 0.951$	$\chi^2_1 = 0.358$	$\chi^2_2 = 4.389$	$\chi^2_1 = 3.402$
3. MYR/JPY			
$X_t = 0.000 + 0.977\ \hat{X}_t + \varepsilon_t$		$X_t = 0.001 + 0.933\ \hat{\hat{X}}_t + \mu_t$	
(0.001) (0.144)		(0.006) (0.037)	
$R^2 = 0.423$	$\varepsilon_t \sim I(1)$	$R^2 = 0.905$	$\mu_t \sim I(0)$
$d = 0.145$	$LM\ (12) = 0.767$	$d = 1.728$	$LM\ (12) = 13.821$
$\chi^2_2 = 5.516$	$\chi^2_1 = 5.160$	$\chi^2_2 = 3.913$	$\chi^2_1 = 3.242$
4. THB/JPY			
$X_t = 0.002 + 0.989\ \hat{X}_t + \varepsilon_t$		$X_t = 0.006 + 0.959\ \hat{\hat{X}}_t + \mu_t$	
(0.013) (0.085)		(0.005) (0.026)	
$R^2 = 0.664$	$\varepsilon_t \sim I(1)$	$R^2 = 0.953$	$\mu_t \sim I(0)$
$d = 0.145$	$LM\ (12) = 60.414$	$d = 1.706$	$LM\ (12) = 13.965$
$\chi^2_2 = 0.023$	$\chi^2_1 = 2.868$	$\chi^2_2 = 2.877$	$\chi^2_1 = 2.528$

Notes: X_t is the actual exchange rate, $\hat{X}_t$ and $\hat{\hat{X}}$ are the predictors of X_t with the former from the PPP model and the latter from the adapted model. The standard error for each estimated coefficient is given in parenthesis. The Wald tests for the null hypotheses of strong (β=0 and β_1=1) and weak (β_1=1) form efficiency of the predictors are reported as χ^2_2 and χ^2_1 respectively. The 5% critical values for the chi-square concerned are in that order, 5.99 and 3.84. Both *d* and *LM*(12) are the Durbin-Watson statistic and Lagrange Multiplier statistic for serial correlation. The 5% critical value for *LM*(12) statistic (chi-squared distributed) is 21.03.

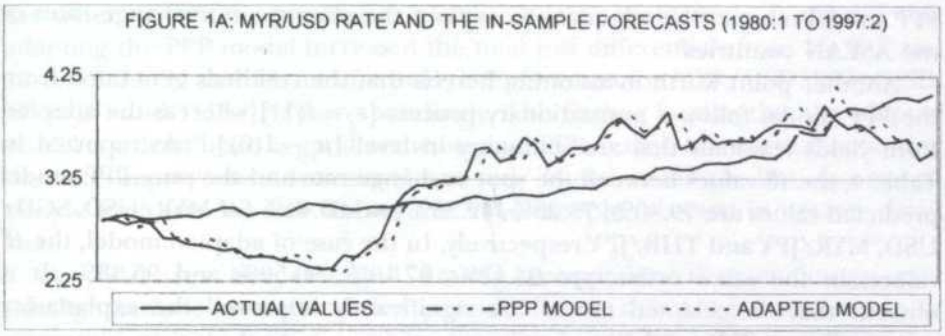

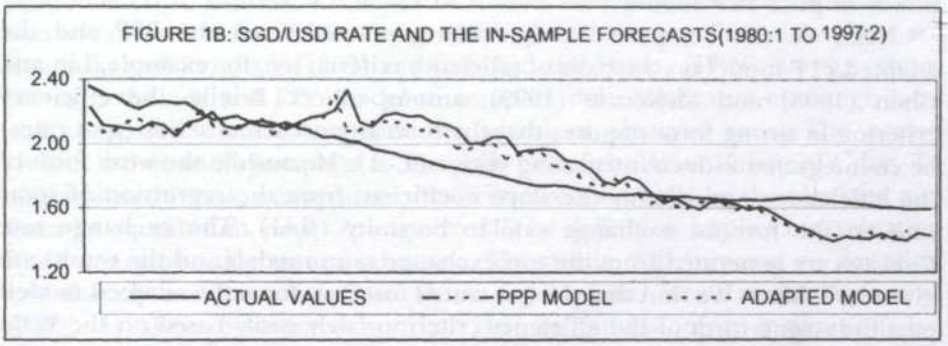

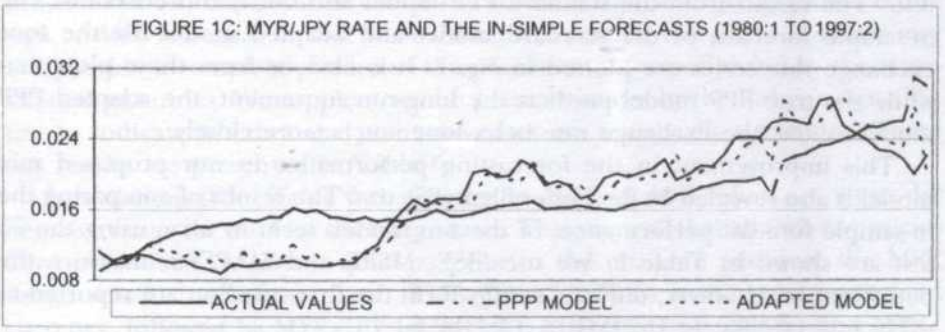

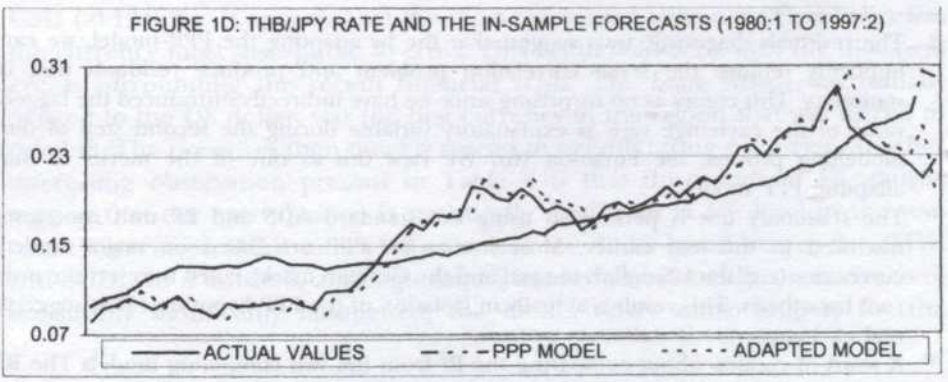

Fig. 1: Graphs of in-sample forecasts

PPP model may not be adequate to explain the changes in exchange rates of the ASEAN countries[9].

Another point worth mentioning here is that the residuals generated from the PPP model follow a nonstationary process [$\varepsilon_t \sim I(1)$] whereas the adapted form yields residuals that are stationary in level [$\mu_t \sim I(0)$].[10] As reported in Table 4, the R^2 values between the spot exchange rate and the pure PPP model predicted values are 79.30%, 75.23%, 42.33% and 66.44% for MYR/USD, SGD/USD, MYR/JPY and THB/JPY respectively. In the case of adapted model, the R^2 values, in the same order, are 93.17%, 97.10%, 90.50% and 95.33%. It is obvious that the adapted model has significantly improved the explanatory power of pure PPP model[11].

Next, we can compare the forecasts generated from the PPP and the adapted PPP model on the basis of efficiency criteria; see, for example, Lin and Chen (1998) and McKenzie (1999), among others. Briefly, the efficiency criterion in strong form requires that the forecast and actual series (spot rates) be co-integrated with co-integrating vector (1, -1). Meanwhile the weak form of the efficiency requires only the slope coefficient from the regression of sport rate on the forecast exchange rate to be unity (β_1=1). The exchange rate forecasts are generated from the two exchange rates models and the results are given in Table 4. We find that the generated forecasts form the adapted models pass the strong form of the efficiency criterion fairly easily based on the Wald test. The results from the standard PPP model also satisfy this criterion. The in-sample forecasts of the standard model and adapted model for the four exchange rate series are plotted in *Fig.* 1. It is obvious from these plots that while the true PPP model predicts the long-run movement, the adapted PPP model follows the exchange rate behaviour much more closely.

This improvement in the forecasting performance in our proposed mix model is also revealed by the Fisher Sign (FS) test. The results of comparing the in-sample forecast performances of the two models term by term using the FS test are shown in Table 5. We use MSE, MSPE and MAPE to measure the performance. However, only the results form the first criterion are reported as

---

[9] The residuals diagnostic tests suggest that the by adapting the PPP model, we can implicitly remove the serial correlation problem and produce residuals that is stationary. This comes as no surprising since we have indirectly introduced the lagged value of the exchange rate as explanatory variable during the second step of our modelling process; see Equation (6). We view this as one of the merits of our adapting PPP model.

[10] The stationary test is performed using the standard ADF and PP unit root tests discussed in the text earlier. Most studies on PPP are based on major traded currencies (e.g. the US dollar, the yen and the German mark) failed to reject the unit root hypothesis. This result is actually in violation of the PPP hypothesis that suggests real exchange rate is stationary process.

[11] A word of caution about comparing the R^2 from the two competing models The R^2 from the standard PPP model should be interpreted with care because of the problem of autocorrelation (the R^2 values would be smaller; see Gujarati 1995, p. 411).

the other two criteria produce the same outcome qualitatively. It appears that adapting the PPP model increased the total loss differentials from 15, 9, 7 and 10 to 32, 24, 24 and 33 out of a total of 65 forecasts for MYR/USD, SGD/USD, MYR/JPY and THB/JPY correspondingly. This finding implies that the adapted model is at least twice as good as the original PPP model. It is worth mentioning that the improvement is realised not only in the in-sample but also out-of-sample forecasts. We will discuss the out-of-sample forecasts in greater detail later.

A consensus has emerged among economists that exchange rate misalignments over an extended period of time may trigger a currency or economic crisis. Indeed, a number of studies have provided the evidence that overvaluation is a key factor in predicting forthcoming financial crises; see Kaminsky and Reinhart (1999) and Goldfajn and Valdes (1999), among others. We used the adapted PPP model to compute the equilibrium exchange rates and compared these values with the actual or observed rates. The period chosen is 8 quarters just prior to the outbreak of the Asian Financial Crisis. To accomplish this task, we calculate the mean deviation (*MD*) of the observed rate from its equilibrium value. A negative *MD* by definition implies overvaluation while a positive value means otherwise. Meanwhile, *MD*=0 means no deviation and the observed rate is effectively in equilibrium. Mean percentage error (*MPE*) is also constructed so that the magnitude of overvaluation (or undervaluation) can easily be compared across currencies. Interpretation of the sign of *MPE* is similar to that of *MD*. Simply reporting the point estimates may not provide a complete picture of the misalignment experienced by the crisis-affected countries. We supplement the point estimates by the Fisher's sign (FS) test to indicate whether the point estimates are statistically significant. These test results are presented in Table 6.

It is obvious from Table 6 that both the *MD* and *MPE* values are all in the negative range for the four exchange rates. This suggests that all four currencies were overvalued in several quarters prior to the crisis. In addition, the MPE values reveal that baht-yen rate (THB/JPY, -7.6889%) is the most overvalued currency, followed by MYR/JPY (-4.9811%), SGD/USD (-0.6966%) and MYR/USD (-0.1348%). It appears that the most overvalued currency (Thai baht) was the currency most susceptible to crisis. This result coincided with the historical events surrounding the recent financial crisis. The baht, which was initially pegged to the US dollar, was the first currency in the region that was forced to devalue. The pressures then quickly spread to neighbouring countries. Another interesting observation present in Table 6 is that the values of FS statistic suggest that the overvaluation is statistically significant at 5% level in the yen-based currencies (MYR and THB) but not for dollar-based currencies (MYR and SGD). In a nutshell, although the *FS* test indicates not all currencies were statistically significanly misaligned, the model offers some support for the

TABLE 5
Forecasting performance of PPP models and adapted PPP models by Fisher's sign (FS) test[a]

PPP Model Vs. Random Walk[b]				Adapted PPP Model Vs. Random Walk[c]			
MYR/USD	SGD/USD	MYR/JPY	THB/JPY	MYR/USD	SGD/USD	MYR/JPY	THB/JPY
In-sample (Forecast Horizon = 65 Quarters)							
15 (0.000)	9 (0.000)	7 (0.000)	10 (0.000)	32 (0.098)	24 (0.011)	24 (0.010)	33 (0.098)
Out-of-sample (Forecast Horizon = 14 Quarters)							
0 (0.000)	3 (0.022)	4 (0.061)	5 (0.122)	8 (0.183)	10 (0.061)	8 (0.183)	6 (0.183)

Notes: [a] Total numbers of negative loss differential are reported with marginal significance value (msv) given in parenthesis. The null hypothesis of FS test is 2 forecasting models have equal accuracy.

[b] Loss differential = $SE_{PPP,j} - SE_{RW,j}$; $j = 1, ..., n$, where n is the forecast horizon. SE_{PPP} and SE_{RW} stand for Square Error of PPP model and Random Walk model respectively.

[c] Loss differential = $SE_{ADPPP,j} - SE_{RW,j}$; j = 1, ..., n, where n is the forecast horizon. SE_{ADPPP} and SE_{RW} stand for Square Error of Adapted PPP model and Random Walk model respectively.

TABLE 6
Evaluation of the position of exchange rates before Asian crisis

For 8 Quarterly Forecasted Values				
CRITERIA	MYR/USD	SGD/USD	MYR/JPY	THB/JPY
MD[a]	-0.0079	-0.0097	-0.0008	-0.0177
MPE[b]	-0.1348	-0.6966	-4.9811	-7.6889
FS[c]	5 (0.2188)	5(0.2188)	7 (0.0313)	7 (0.0313)

Notes: [a]*MD* = Mean deviation. Negative value implies overvaluation is detected.
[b]*MPE* = Mean percentage error. Negative value implies overvaluation is detected.
[c]*FS* = Fisher's sign test. Total numbers of overvaluation are reported with marginal significance value (msv) given in parenthesis. The null hypothesis of FS test is the exchange rate is in equilibrium before crisis.

notion that the Asian Financial Crisis may be due to overvaluation of the some of the regional currencies[12].

The estimated IRD models together with their adapted versions are tabulated in Table 3, and the related diagnostic test results are given in Table 7. Several interesting observations emerged from these tables. The Wald (χ^2_2) statistics in Table 7 suggest that both models meet the strongly efficient criteria, since β_0 and β_1 are not significantly different from zero and one respectively for each model. As previously observed in the PPP models, the standard IRD model is contaminated with autocorrelation problem as indicated by both the Durbin-Watson and Lagrange Multiplier test results. The problem, however, disappeared in the adapted IRD models. Notice that the R^2 values of the adapted IRD models are generally lower than the corresponding adapted PPP models (Table 3). This comes as a surprise since we expect the adapted IRD models to have higher explanatory power given that we have added interest rate differential to adapted PPP models[13].

Both the adapted PPP and IRD models are used to generate the forecasted values of the exchange rate in the out-of-sample period. The out-of-sample forecasts form these models are compared with the simple random walk model based on *MSE*, *MSPE* and *MAPE* ratios. Our preliminary results showed that all

[12] Alternatively, one may interpret that overvaluation is necessary but not sufficient condition for a currency crisis.

[13] In this study, we find that interest rates do not enter in the long-run relationship for ringgit-US dollar and Singapore dollar-US dollar rates. They may suggest that exchange rate dynamics are affected by other factors that are not in the interest rate dynamics. We are also aware that short-term interests (Treasury bills of 3-month rate) may not be appropriate to the model. Some authors have used long-term rates and obtained more favourable results. With the usual caveat, we are in debted to one of the referees for pointing this out.

TABLE 7
Diagnostic test for IRD model and the adapted form

IRD Model		Adapted IRD Model	
1. MYR/USD			
$X_t = 0.038 + 0.987\ \hat{X}_t + \varepsilon_t$		$X_t = 0.035 + 0.988\ \hat{\hat{X}}_t + \mu_t$	
(0.106) (0.033)		(0.109) (0.033)	
$R^2 = 0.790$	$\varepsilon_t \sim I(1)$	$R^2 = 0.933$	$\varepsilon_t \sim I(0)$
$d = 0.350$	$LM\ (12) = 49.290$	$d = 2.370$	$LM\ (12) = 13.036$
$\chi^2_2 = 3.975$	$\chi^2_1 = 0.223$	$\chi^2_2 = 0.189$	$\chi^2_1 = 0.132$
2. SGD/USD			
$X_t = -0.019 + 1.009\ \hat{X}_t + \varepsilon_t$		$X_t = -0.050 + 1.027\ \hat{\hat{X}}_t + \mu_t$	
(0.146) (0.075)		(0.051) (0.028)	
$R^2 = 0.754$	$\varepsilon_t \sim I(1)$	$R^2 = 0.961$	$\varepsilon_t \sim I(0)$
$d = 0.150$	$LM\ (12) = 47.362$	$d = 2.142$	$LM\ (12) = 10.623$
$\chi^2_2 = 1.558$	$\chi^2_1 = 1.426$	$\chi^2_2 = 3.117$	$\chi^2_1 = 3.053$
3. MYR/JPY			
$X_t = 0.0003 + 0.977\ \hat{X}_t + \varepsilon_t$		$X_t = 0.001 + 0.960\ \hat{\hat{X}}_t + \mu_t$	
(0.002) (0.144)		(0.001) (0.025)	
$R^2 = 0.564$	$\varepsilon_t \sim I(1)$	$R^2 = 0.837$	$\varepsilon_t \sim I(0)$
$d = 0.434$	$LM\ (12) = 48.831$	$d = 1.924$	$LM\ (12) = 22.484$
$\chi^2_2 = 0.026$	$\chi^2_1 = 0.245$	$\chi^2_2 = 2.249$	$\chi^2_1 = 2.186$
4. THB/JPY			
$X_t = -0.001 + 1.003\ \hat{X}_t + \varepsilon_t$		$X_t = 0.004 + 0.973\ \hat{\hat{X}}_t + \mu_t$	
(0.020) (0.060)		(0.006) (0.033)	
$R^2 = 0.712$	$\varepsilon_t \sim I(1)$	$R^2 = 0.931$	$\varepsilon_t \sim I(0)$
$d = 0.248$	$LM\ (12) = 56.423$	$d = 1.820$	$LM\ (12) = 17.596$
$\chi^2_2 = 0.002$	$\chi^2_1 = 0.016$	$\chi^2_2 = 1.816$	$\chi^2_1 = 1.547$

Notes: X_t is the actual exchange rate, $\hat{X}_t$ and $\hat{\hat{X}}_t$ are the predictors of with the former from the IRD model and the latter from the adapted model. The standard error for each estimated coefficient is given in parenthesis. The Wald tests for the null hypotheses of strong (β_0=0 and β_1=1) and weak (β_1=1) form efficiency of the predictors are reported as χ^2_2 and χ^2_1 respectively. The 5% critical values for the chi-square concerned are in that order, 5.99 and 3.84. Both *d* and *LM*(12) are the Durbin-Watson statistic and Lagrange Multiplier statistic for serial correlation. The 5% critical value for *LM*(12) statistic (chi-squared distributed) is 21.03.

the three criteria yield almost the same conclusion. Given the unanimity of the results across the three criteria and to conserve space, we only report the result based on *MSE* criterion in Table 8. For the adapted PPP model, all the MSE ratios are found to be less than unity (Table 8A), implying that all the forecasting models estimated based on the adapted PPP model outperformed the random walk, for the entire forecast horizon ranging from one to fourteen

TABLE 8
Out-of-sample forecasting performances of the adapted PPP and IRD models as measured by MSE ratio

n[c]	(A) Adapted PPP Model Vs Random Walk[a]				(B) Adapted IRD Model Vs Random Walk[a]				(C) Adapted PPP Model Vs Adapted IRD Model[b]			
	MYR/USD	SGD/USD	MYR/USD	THB/JPY	MYR/JPY	THB/JPY	MYR/JPY	THB/JPY	MYR/USD	SGD/USD	MYR/JPY	THB/JPY
1	0.878***	0.709***	0.799***	0.246***	0.890***	0.761***	0.962	0.451***	0.986***	0.932**	0.831***	0.546***
2	0.982**	0.872***	0.861***	0.456***	0.987***	0.924***	1.022**	0.541***	0.996***	0.944***	0.842***	0.844***
3	0.935***	0.863***	0.890***	0.708***	0.939***	0.899***	1.026	0.609***	0.996***	0.959	0.868***	1.163***
4	0.974	0.895***	0.887**	0.711***	0.977	0.957***	1.017	0.629***	0.997***	0.958	0.873***	1.131***
5	0.955**	0.890***	0.912**	0.729***	0.958**	0.928**	1.023	0.650***	0.997***	0.959	0.892***	1.121***
6	0.966**	0.887***	0.913	0.714***	0.968*	0.924*	1.005	0.624***	0.997***	0.959	0.909*	1.144***
7	0.957***	0.895***	0.914	0.723***	0.960*	0.932*	1.006	0.635***	0.997***	0.960	0.909	1.140***
8	0.955***	0.898***	0.913	0.728***	0.958**	0.936	1.005	0.678***	0.997***	0.959	0.909	1.089***
9	0.967	0.895***	0.915	0.754***	0.970**	0.933	0.999	0.670***	0.997***	0.960	0.916	1.125***
10	0.967	0.895***	0.915	0.764***	0.969	0.933	0.997	0.664***	0.997***	0.960	0.918	1.150***
11	0.964	0.895***	0.916	0.770***	0.966	0.931	0.997	0.668***	0.997***	0.961	0.919	1.153***
12	0.964*	0.895***	0.916	0.767***	0.966	0.929	0.997	0.669***	0.997***	0.964	0.919	1.145***
13	0.959*	0.895***	0.916	0.763***	0.961	0.928	0.997	0.669***	0.997***	0.965	0.919	1.141***
14	0.961	0.895***	0.948	0.948***	0.963	0.928	0.995	0.665***	0.997***	0.965	0.953	1.169***

Notes: *a* MSE ratio = MSE of estimated model ÷ MSE of random walk model.
b MSE ratio = MSE of Adapted PPP model ÷ MSE of Adapted IRD model.
c n denotes number of quarters forecasted.
*, ** and *** denotes statistically significant at 10%, 5% and 1% level as suggested by Meese-Rogoff (MR) statistics.

quarters. In particular, the forecasting models for SGD/USD and THB/JPY rates statistically outperformed the random walk model at 1% significance level regardless of wheter we are comparing on the basis of one forecast value, two forecast values or more. Meanwhile, the ratio for the MYR/USD and MYR/JPY rates are statistically significant at 10% or better up to at least 6 quarters. It is interesting to note that our forecasting models have defeated the random walk model, even in the presence of more stringent forecasting period and also over the short forecasting horizon.

Turning to the adapted IRD model, all the MSE ratios for the MYR/USD (significant up to 9 quarters), SGD/USD (significant up to 7 quarters) and THB/JPY (significant for all 14 quarters) rates are less than one (Table 8B). Hence, the adapted IRD model could also outperform the random walk for these three rates. The ratio for MYR/JPY rate shows mixed results but the MR statistics suggest that adapted IRD is only comparable with the random walk with a minor exception that the former is significantly beaten.

The forecast accuracy of the adapted PPP and IRD models are compared and the results are also depicted in Table 8C. Overall, the weight of the evidence is against the adapted RID model. The adapted PPP models have smaller MSE values when compared to the adapted IRD models. As shown in the table, the ratios are smaller than one for the MYR/USD, SGD/USD and MYR/JPY rates across all forecasting horizons. Statistically, the adapted PPP model is better than the adapted IRD up to all the 14 quarters in MYR/USD, 2 quarters in SGD/USD and 6 quarters in MYR/JPY. However, the adapted PPP model for SGD/USD rate is statistically better than the adapted IRD model only for forecast up to 2 quarters ahead and for the rest of the forecasting horizon, the latter is statistically better. Generally, these results suggest that the adapted IRD model, which is incorporated with more information, does not necessarily out-perform the adapted PPP model. Thus, we have shown that the simple PPP model can adequately represent the movements in exchange rate series by adapting the model to include information from the deviation form equilibrium value.

CONCLUSION

Numerous studies have compared the forecasting performance of the exchange rate models against the random walk model. The consensus that emerged from these studies is that it is extremely difficult to out-predict a random walk using structural or non-structural models. In this article, we consider alternative procedures to model exchange rates in the ASEAN countries. Specifically, the proposed model is a linear combination of long run and short-run functions. We exploit the long-run information from the well-known PPP hypothesis in estimating the model, whereas the time series properties of the temporary deviations from equilibrium PPP is incorporated in our estimating procedure to capture the unusual feature of the data generating process. Our results show that even if the model includes the right set of fundamentals, they still could

not explain movements of exchange rates well. Meese (1990) and Frankel and Rose (1995), among others have highlighted this point.

Our forecasting models are purposely set to allow the model to forecast in the post-crisis period, to make the task much more difficult. The empirical results based on the bilateral exchange rates of three ASEAN countries suggest that our approach has improved significantly the explanatory power of the pure PPP model. In other words, we found that the adapted model is capable of capturing the salient features of currencies that experienced speculative attacks and severe deprecation. Furthermore, the out-of-sample forecasts of our model out-predict the simple random walk, even during the post-crisis period. The adapted PPP model outperformed the rarely beaten naïve model, for the forecast horizons ranging from one to fourteen quarters.

Giddy and Duffey (1975) pointed out that successful forecasting has its premise in the satisfaction of at least one of the following criteria: (a) has used a superior forecasting model; (b) has consistent access to information; (c) is able to exploit small, temporary deviations from equilibrium; and (d) can predict the nature of government intervention in the foreign exchange market. Based on our empirical results, we showed that our procedure is capable of producing models that satisfy the above criteria. Specifically, the model is able to incorporate the long-run information based on macroeconomic theory, and our procedure is able to exploit small and temporary deviations from equilibrium and thereby yield a forecasting model much superior to the naïve model. Therefore, a reasonable conclusion that can be drawn from this study is that it provides some hope of achieving a reasonable forecast for the ASEAN currencies. Finally, the model could easily include other determinants as suggested by monetary models and may be used to forecast other financial variables and we reserve this for future research.

ACKNOWLEDGEMENT

The first author would like to acknowledge the financial support from IRPA 2000 (Project No: 05-02-04-0046). The authors would like to thank the anonymous reviewers for their helpful comments and suggestions on the earlier versions of this paper. All remaining errors are solely our responsibility, of course.

REFERENCES

Baharumshah, A. Z. and K. S. Liew. 2003. The predictability of ASEAN-5 exchange rates in the post-crisis era. *Pertanika Journal of Social Science and Humanities* (Forthcoming).

Berkowitz, J. and L. Giogianni. 1997. Long–horizon exchange rate predictability? Working Paper, WP/97/6. Washington: International Monetary Fund.

Bollerslev, T. 1986. Generalised autoregressive conditional heteroscedasticity. *Journal of Econometrics* **51**: 307–327.

Boothe, P. and D. Glassman. 1987. Comparing exchange rate forecasting models. *International Journal of Forecasting* **3**: 65–79.

Brooks, C. 1996. Testing for non-linearity in daily sterling exchange rates. *Applied Financial Economics* **6**: 307–317.

Brooks, C. 1997. Linear and non-linear non- forcastability of high-frequency exchange rates. *Journal of Forecasting* **16**: 125–145.

Cheung, Y. W. 1993. Long memory in foreign-exchange rates. *Journal of Business and Economics Studies* **11**: 93–101.

Chinn, M. and R. Meese. 1995. Banking on currency forecasts: how predictable is change in money. *Journal of International Economics* **38**: 161–178.

Clark, P. B. and R. Macdonald. 1998. Exchange rates and economics fundamentals: a methodological comparison of BEERs and FEERs. Working Paper, WP/98/67. Washington: International Monetary Fund.

Coakley, J. and A. Fuertes. 1997. New panel unit root tests of PPP. *Economics Letters* **57**: 17–22.

Coakley, J. and A. Fuertes. 2001. Nonparametric co-integration analysis of real exchange rates. *Applied Financial Economics* **11**: 1–8.

Cornell, B. 1977. Spot rates, forward rates and exchange market efficiency. *Journal of Financial Economics* **5**: 55–65.

Dornbusch, R. 1976. Expectations and exchange rate dynamics. *Journal of Political Economy* **84**: 116–1176.

Engle, R. F. 1982. Autoregressive Conditional Heteroscedasticity, with estimation of the variance of United Kingdom inflation. *Econometrica* **50**: 987–1007.

Engle, R. F. and W. J. Granger. 1986. Co-integration and error correction representation, estimation, and testing. *Econometrica* **55**: 251–276.

Fama, E. F. 1965. The behaviour of stock market prices. *Journal of Business* **38**: 24–105.

Frankel, J. 1979. On the Mark: a theory of floating exchange rates based on real interest differentials. *American Economic Review* **69(4)**: 610–622.

Frankel, J. and A. K. Rose. 1995. A survey of empirical research on nominal exchange rates. In *Handbook of International Economics*, ed. G. Grossman and K. Rogoff. Amsterdam: North-Holland.

Franses, P. H. and P. V. Homelen. 1998. On forecasting exchange rates using Neural Networks. *Applied Financial Economics* **8**: 589–596.

García-ferrer, A., J. Del Hoyo and A. S. Martín-arroyo. 1997. Univariate forecasting comparisons: the case of the Spanish automobile industry. *Journal of Forecasting* **16**: 1–17.

Giddy, I. H. and G. Duffey. 1975. The random behaviour of flexible exchange rates: implication for forecasting. *Journal of International Business Studies* **6**: 1–33.

Goldfajn, I. and R. Valdes. 1999. The aftermath of appreciation. *Quarterly Journal of Economics* **114**: 229–262.

Gujarati, D. N. 1995. *Basic Econometrics*. 3rd edition. US: McGraw-Hill Inc.

HAKKIO, C. S. and M. RUSH. 1986. Market efficiency and cointegration: an application to the Sterling and Deutschemark exchange markets. *Journal of International Money and Finance* **5**: 221–230.

HALLWOOD, C. and R. MACDONALD. 1994. *International Money and Finance.* Oxford: Blackwell.

JOHENSEN, S. and K. JUSELIUS. 1990. Maximum likelihood estimation and inference on cointegration – with application to the demand for money. *Oxford Bulletin of Economics and Statistics* **52**: 169–210.

KAMINSKY, S. and C. REINHART. 1999. Currency and banking crises: the early warnings of distress. *American Economic Review* **89**: 473–500.

KELLER, A. 1989. Advanced time-series analysis. In *Exchange Rate Forecasting*, ed. C. Dunis and M. Feeny, p. 206–299. England: Woodhead-Faulkner.

KRÄGER, H. and P. KUGLER. 1993. Non-linearities in foreign exchange markets, a different perspective. *Journal of International Money and Finance* **12**: 195–208.

LIEW, K. S., A. Z. BAHARUMSHAH and E. LAU. 2002. Nonlinear adjustment to purchasing power parity: empirical evidence from Asian exchange rates. In *Proceedings of Asian Pacific Economics and Business Conference* 2002, ed. M-Azali, M.Yusoff, M. S. Habibullah, S. A. Mansor, R. Mustafa, S. Mohamad, Z. Yusop, A. Radam, A. Hassan and S. Pilai, p. 902-910. Malaysia: Universiti Putra Malaysia Press.

LIN, W. T. and Y. H. CHEN. 1998. Forecasting foreign exchange rates with an intrinsically nonlinear dynamic speed of adjustment model. *Applied Economics* **30**: 295–312.

LITTERMAN, R. B. 1986. Forecasting with Bayesian vector autoregressive – five years of experience. *Journal Business & Economic Statistics* **4** : 25–38.

LUPOLETTI, W. M. and R. H. WEBB. 1986. Defining and improving the accuracy of the macroeconomics forecasts: contribution of a VAR model. *Journal of Business.* **59**: 263 – 284.

M-AZALI, M. S. HABIBULLAH and A. Z. BAHARUMSHAH. 2001. Does PPP hold between Asian and Japanese economies? Evidence using panel unit root and panel co-integration. *Japan and the World Economy* **13**: 35–50.

MA, Y. and A. KANAS. 2000. Testing for a nonlinear relationship among fundamentals and exchange rates in ERM. *Journal of International Money and Finance* **19**: 135–152.

MACKINNON, R. 1991. The rules of economic game: international money in historical perspective. *Journal of Economic Literature:* 15–32.

MARK, N. 1995. Exchange rates and fundamentals: evidence on long-run horizon predictability. *America Economic Review* **85**: 201–218.

MCKENZIE, M. D. 1999. Power transformation and forecasting the magnitude of exchange rate changes. *International Journal of Forecasting* **15**: 49–55.

MEESE, R. A. and K. ROGOFF. 1983. Empirical exchange rate models of the seventies: do they fit out of sample. *Journal of International Economics* **14**: 3–24.

MEESE, R. and K. ROGOFF. 1988. Was it real? The exchange rate-interest differential relation over the modern floating rate period. *Journal of Finance* **43**: 933–948.

MEESE, R. A. 1990. Currency fluctuations in the post-Bretton Woods era. *The Journal of Economic Perspectives* **4**: 117–134.

MEESE, R. A. and A. K. ROSE. 1991. An empirical assessment of non-linearities in models of exchange rate determination. *Review of Economics Studies* **58**: 603–619.

MONTOGOMERY, D. C., L. A. JOHNSON and J. S. GARDINER. 1990. *Forecasting and Time Series Analysis*. 2nd edition. US: McGraw-Hill Inc.

MUSSA, M. 1996. Nominal exchange rate regimes and behaviour of real exchange rates: evidence and implications. *Carnegie-Rochester Series on Public Policy* **25**: 117-214.

NAGAYASU, J. 1998. Does the long-run PPP hypothesis hold for Africa?: evidence from panel co-integration study. Working Paper, 98/123. Washington: International Monetary Fund.

NELSON, D. B. 1991. Conditional heteroskedasticity in asset returns: a new approach. *Econometrica* **59**: 347–370.

PALMA, W. and N. H. CHAN. 1997. Estimation and forecasting of long-memory processes with missing values. *Journal of Forecasting* **16**: 395–410.

PARIKH, A. and G. WILLIAMS. 1998. Modelling real exchange rate behaviour: a cross-country study. *Applied Financial Economics* **8**: 577–587.

PLASMANS, J., W. VERKOOIJEN and H. DANIELS. 1998. Estimating structural exchange rate models by Artificial Neural Networks. *Applied Financial Economics* **8**: 541–551.

TAYLOR, M. P. and D. A. PEEL. 2000. Nonlinear adjustment, long-run equilibrium and exchange rate fundamentals. *Journal of International Money and Finance* **19**: 33–53.

WU, J. L. and S. L. CHEN. 2001. Nonlinear exchange-rate prediction: evidence from a nonlinear approach. *Journal of International Money and Finance* **20**: 521–532.

Preparation of Manuscript

General
The manuscript, including footnotes, tables, and captions for illustrations, should be typewritten double spaced on paper 210 x 297 mm in size, with margins of 40 mm on all sides. Three clear copies are required. Typing should be on one side of the paper only. Each page of the manuscript should be numbered, beginning with the title page.

Title page
The title of the paper, name of author and full address of the institution where the work was carried out should appear on this page. A short title not exceeding 60 characters should be provided for the running headline.

Abstract
Abstracts in Bahasa Melayu and English of not more than 200 words each are required for full articles and communications. No abbreviation should appear in the abstract. Manuscripts from outside of Malaysian may be submitted with an English abstract only.

Keywords
Up to a maximum of ten keywords are required and they should be placed directly below the abstract.

Footnotes
Footnotes to material in the text should not be used unless they are unavoidable. Where used in the text, footnotes should be designated by superscript Arabic numerals in serial order throughout the manuscript. Each footnote should be placed at the bottom of the manuscript page where reference to it is made.

Equations
These must be clearly typed, triple-spaced and should be identified by numbers in square brackets placed flush with the right margin. In numbering, no distinction is made between mathematical and chemical equations. routine structural formulae can be typeset and need not be submitted as figures for direct reproduction but they must be clearly depicted.

Tables
Tables should be numbered with Arabic numerals, have a brief title, and be referred to in the text. Columns headings and descriptive matter in tables should be brief. Vertical rules should not be used. Footnotes in tables should be designated by symbols or superscripts small italic letters. Descriptive materials not designated by a footnote may be placed under a table as a *note.*

Illustrations & Photographs
Illustration including diagrams and graphs are to be referred to in the text as 'figures' and photographs as 'plates' and numbered consecutively in Arabic numerals. All photographs (gloosy black and white prints) should be supplied with appropriate scales.

Illustrations should be of print quality; outputs from dotmatrix printers are not acceptable, Illustrations should be on separate sheets, about twice the size of the finished size in print. All letters, numbers and legends must be included on the illustration with the author's name, short title of the paper, and figure number written on the vereso. A list of captions should be provided on a separate sheet.

Unit of Measure
Metric units must be used for all measurements.

Citations and References
Items in the reference list should be referred to in the text by inserting, within parentheses, the year of publication after the author's name. If there are more than two authors, the first author should be cited followed by '*et al*'. The names of all authors, however, will appear in the reference list.

In the case of citing an author who has published more than one paper in the same year, the papers should be distinguished by addition of a small letter, e.g. Choa (1979a); Choa (1979b); Choa (1979c).

In the reference list, the names should be arranged alphabetically according to the name of the first author. Serials are to be abbreviated as in the *World List of Scientific Periodicals.*

The abbreviation for Pertanika Journal of Science and Technology is *Pertanika J. Sci. Technol.*

The following reference style is to be observed:

Monograph
Alefed, G. and J. Herzberger. 1983. *Introduction to Interval Computations.* New York: Academic Press.

Chapter in Edited Book
Muzzarell, R.A.A. 1980. Chitin. In *Polymers in Nature,* ed. E.A. MacGregor and C.T. Greenwood, p. 417-449. New York: John Wiley.

Serials
Kamaruzaman Ampon. 1991. The effect of attachment of hydrophobic imidoesters on the catalytic activity of trypsin. *Pertanika* **14(2)**: 18-185.

Proceedings
Mokhtaruddin, A.M. and L.M. Maene. 1981. Soil erosion under different crops and management practices. In *Agricultural Engineering in National Development,* ed. S.L. Choa, Mohd Zohdie Bardaie, N.C. Saxena and Van Vi Tran, p. 245-249. Serdang, Malaysia: Universiti Pertanian Malaysia Press.

Unpublished Materials (e.g. theses, reports & documents)

Sakri, I. 1990. Proper construction set-up of Malaysian Fish Aggregating Devices (Unjam). Ph.D. Thesis, Universiti Pertanian Malaysia, Serdang, Selangor.